UNIVERSAL
LIBRARY

OU_160141

UNIVERSAL
LIBRARY

ELEMENTARY FLUID MECHANICS

BY

JOHN K. VENNARD

Assistant Professor of Fluid Mechanics

New York University

NEW YORK

JOHN WILEY & SONS, INC.

LONDON: CHAPMAN & HALL, LIMITED

1940

COPYRIGHT, 1940, BY
JOHN K. VENNARD

All Rights Reserved

This book or any part thereof must not be reproduced in any form without the written permission of the publisher.

PRINTED IN U. S. A.

PRESS OF
BRAUNWORTH & CO., INC.
BUILDERS OF BOOKS
BRIDGEPORT, CONN.

ELEMENTARY FLUID MECHANICS

PREFACE

Fluid mechanics is the study of all fluids under all possible conditions of rest and motion. Its approach is analytical, rational, and mathematical rather than empirical; it concerns itself with those basic principles which lead to the solution of numerous diversified problems, and it seeks results which are widely applicable to similar fluid situations and not limited to isolated special cases. Fluid mechanics recognizes no arbitrary boundaries between fields of engineering knowledge but attempts to solve all fluid problems, irrespective of their occurrence or of the characteristics of the fluids involved.

This textbook is intended primarily for the beginner who knows the principles of mathematics and mechanics but has had no previous experience with fluid phenomena. The abilities of the average beginner and the tremendous scope of fluid mechanics appear to be in conflict, and the former obviously determine limits beyond which it is not feasible to go; these practical limits represent the boundaries of the subject which I have chosen to call *elementary fluid mechanics.* The apparent conflict between scope of subject and beginner's ability is only along mathematical lines, however, and the *physical ideas* of fluid mechanics are well within the reach of the beginner in the field. Holding to the belief that physical concepts are the *sine qua non* of mechanics, I have sacrificed mathematical rigor and detail in developing physical pictures and in many cases have stated general laws only (without numerous exceptions and limitations) in order to convey basic ideas; such oversimplification is necessary in introducing a new subject to the beginner.

Like other courses in mechanics, fluid mechanics must include disciplinary features as well as factual information—the beginner must follow theoretical developments, develop imagination in visualizing physical phenomena, and be forced to think his way through problems of theory and application. The text attempts to attain these objectives in the following ways: omission of subsidiary conclusions is designed to encourage the student to come to some conclusions by himself; application of bare principles to specific problems should develop ingenuity; illustrative problems are included to assist in overcoming numerical difficulties; and many numerical problems for

the student to solve are intended not only to develop ingenuity but to show practical applications as well.

Presentation of the subject begins with a discussion of fundamentals, physical properties and fluid statics. Frictionless flow is then discussed to bring out the applications of the principles of conservation of mass and energy, and of impulse-momentum law, to fluid motion. The principles of similarity and dimensional analysis are next taken up so that these principles may be used as tools in later developments. Frictional processes are discussed in a semi-quantitative fashion, and the text proceeds to pipe and open-channel flow. A chapter is devoted to the principles and apparatus for fluid measurements, and the text ends with an elementary treatment of flow about immersed objects. Throughout the text, the foot-pound-second system of dimensions has been used, and problems of conversion from the metric system, which so frequently divert the beginner's attention from the physical ideas, have been avoided; justifications for experimental results and empirical formulas have been presented except at points where the student should discover them for himself; bibliographies have been included to guide the inquiring reader to more exhaustive treatments of the subject.

For criticism of my *Notes on Elementary Fluid Mechanics* which have been expanded into the present text, I wish to extend my appreciation to many of my colleagues at New York University, Professor Boris A. Bakhmeteff of Columbia University, and Professor William Allan of the College of the City of New York.

I am deeply indebted to Mr. William H. Peters of the Curtiss-Wright Corporation for carefully reviewing the first eight chapters of the manuscript, and to Professor Frederick K. Teichmann of New York University for critical comments on the last chapter. I also wish to thank Mr. J. Charles Morgan for general comments and assistance in reading proof and Miss Katherine Williams for her care and patience in typing the manuscript.

JOHN K. VENNARD

NEW YORK, N.Y.
May, 1940

CONTENTS

CHAPTER PAGE

I. FUNDAMENTALS 1

Art. 1—Development of Fluid Mechanics. 2. Physical Characteristics of the Fluid State. 3. Density, Specific Weight, Specific Volume, and Specific Gravity. 4. Compressibility, Elasticity. 5. Viscosity. 6. Surface Tension, Capillarity. 7. Vapor Pressure.

II. FLUID STATICS 22

Art. 8—Pressure-Density-Height Relationships. 9. Absolute and Gage Pressures. 10. Manometry. 11. Forces on Submerged Plane Surfaces. 12. Forces on Submerged Curved Surfaces. 13. Buoyancy and Flotation. 14. Stresses in Circular Pipes and Tanks. 15. Fluid Masses Subjected to Acceleration.

III. THE FLOW OF AN IDEAL FLUID 55

Art. 16—Definitions. 17. Equation of Continuity. 18. Euler's Equation. 19. Bernoulli's Equation. 20. Energy Relationships. 21. Flow of an Incompressible Fluid. 22. Flow of a Compressible Fluid. 23. Impulse-Momentum Relationships. 24. Flow Curvatures, Types of Vortices, Circulation.

IV. THE FLOW OF A REAL FLUID 106

Art. 25—Laminar and Turbulent Flow. 26. Fluid Flow Past Solid Boundaries. 27. Fluid Flow between Parallel Plates. 28. Flow about Immersed Objects. 29. Stability—Secondary Flows.

V. SIMILARITY AND DIMENSIONAL ANALYSIS 125

Art. 30—Similarity and Models. 31. Dimensional Analysis.

VI. FLUID FLOW IN PIPES 139

Art. 32—Energy Relationships. 33. General Mechanics of Fluid Flow in Pipe Lines. 34. Laminar Flow. 35. Dimensional Analysis of the Pipe-Friction Problem. 36. Results of Pipe-Friction Experiments. 37. Velocity Distribution in Circular Pipes—The Pipe Coefficient. 38. Approximate Thickness of the Laminar Film. 39. Pipe Friction for Compressible Fluids. 40. Pipe Friction in Non-Circular Pipes. 41. Pipe-Friction Calculations by the Hazen-Williams Method. 42. Minor Losses in Pipe Lines. 43. The Pressure Grade Line and Its Use. 44. Branching Pipes.

CHAPTER PAGE

VII. FLUID FLOW IN OPEN CHANNELS 196

Art. 45—Fundamentals. 46. Uniform Flow—The Chezy Equation. 47. The Chezy Coefficient. 48. Best Hydraulic Cross Section. 49. Variation of Velocity and Rate of Flow with Depth in Closed Conduits. 50. Specific Energy. 51. Critical Depth Relationships. 52. Occurrence of Critical Depth. 53. Varied Flow. 54. The Hydraulic Jump.

VIII. FLUID MEASUREMENTS 229

Art. 55—Measurement of Fluid Properties. 56. Measurement of Static Pressure. 57. Measurement of Surface Elevation. 58. Measurement of Stagnation Pressure. 59. The Pitot (Pitot-Static) Tube. 60. The Venturi Tube. 61. The Pitot-Venturi. 62. Anemometers and Current Meters. 63. Total Quantity Methods. 64. Venturi Meters. 65. Nozzles. 66. Orifices. 67. Flow Bends. 68. Pitot-Tube Methods. 69. Dilution and Thermal Methods. 70. Salt-Velocity Method. 71. Weirs. 72. Current-Meter Measurements. 73. Float Measurements.

IX. FLOW ABOUT IMMERSED OBJECTS 294

Art. 74—Fundamentals and Definitions. 75. Dimensional Analysis of the Drag Problem. 76. Frictional Drag. 77. Profile Drag. 78. Drag at High Velocities. 79. Lift by Change of Momentum. 80. Circulation Theory of Lift. 81. Origin of Circulation. 82. Foils of Finite Length. 83. Lift and Drag Diagrams.

APPENDICES 335

I. Description and Dimensions of Symbols. II. Specific Weight and Density of Water. III. Velocity of a Pressure Wave through a Fluid. IV. Viscosities of Liquids and Gases. V. Cavitation.

INDEX 347

ELEMENTARY FLUID MECHANICS

CHAPTER I

FUNDAMENTALS

1. Development of Fluid Mechanics. Man's desire for knowledge of fluid phenomena began with his problems of water supply and disposal and the use of water for obtaining power. With only a rudimentary appreciation for the physics of fluid flow he dug wells, operated crude water wheels and pumping devices, and, as his cities increased in size, constructed ever larger aqueducts, which reached their greatest size and grandeur in those of the City of Rome. However, with the exception of the thoughts of Archimedes (250 B.C.) on the principles of buoyancy little of the scant knowledge of the ancients appears in modern fluid mechanics. After the fall of the Roman Empire (A.D. 476) no progress was made in fluid mechanics until the time of Leonardo Da Vinci (1452–1519). This great genius designed and built the first chambered canal lock near Milan and ushered in a new era in hydraulic engineering; he also studied the flight of birds and developed some ideas on the origin of the forces which support them.

After the time of Da Vinci, the accumulation of hydraulic knowledge rapidly gained momentum, the contributions of Galileo, Torricelli, Newton, Pitot, D. Bernoulli, and D'Alembert to the fundamentals of the science being outstanding. Although the theories proposed by these scientists were in general confirmed by crude experiments, divergences between theory and fact led D'Alembert to observe in 1744 that, "The theory of fluids must necessarily be based upon experiment." D'Alembert showed that there is no resistance to motion when a body moves through an ideal (non-viscous) fluid, yet obviously this conclusion is not valid for bodies moving through real fluid. This discrepancy between theory and practice is called the "D'Alembert paradox" and serves to demonstrate the limitations of theory alone in solving fluid problems.

Because of the conflict between theory and practice, two schools of thought arose in the treatment of fluid problems, one dealing with

the theoretical and the other with the practical aspects of fluid flow, and in a sense these two schools of thought have persisted down to the present day, resulting in the theoretical field of "hydrodynamics" and the practical one of "hydraulics." Notable contributions to theoretical hydrodynamics have been made by Euler, La Grange, Helmholtz, Kirchhoff, Lord Rayleigh, Rankine, Lord Kelvin, and Lamb. In a broad sense, experimental hydraulics became a study of the laws of fluid resistance, mainly in pipes and open channels. Among the many scientists who devoted their energies to this field were Brahms, Bossut, Chezy, Dubuat, Fabre, Coulomb, Eytelwein, Belanger, Dupuit, d'Aubisson, Hagen, and Poisseuille.

Toward the middle of the last century, Navier and Stokes succeeded in modifying the general equations for ideal fluid motion to fit that of a viscous fluid and in so doing showed the possibilities of adjusting the differences between hydraulics and hydrodynamics. At about the same time, theoretical and experimental work on vortex motion by Helmholtz was aiding in explaining away many of the divergent results of theory and practice.

Meanwhile, hydraulic research went on apace, and large quantities of excellent data were collected or formulas proposed for fluid resistance, notably by Darcy, Bazin, Weisbach, Fanning, Ganguillet, Kutter, and Manning; among researchers on other hydraulic problems were Thomson, Fteley, Stearns, and H. Smith. Unfortunately, researches led frequently to empirical formulas obtained by fitting curves to experimental data or merely presenting the results in tabular form, and in many cases the relationship between the physical facts and the resulting formula was not apparent.

Toward the end of the last century, new industries arose which demanded data on the flow of fluids other than water; this fact and many significant advances in knowledge tended to arrest the increasing empiricism of hydraulics. These advances were: (1) the theoretical and experimental researches of Reynolds; (2) the development of dimensional analysis by Lord Rayleigh; (3) the use of models by Froude, Reynolds, Fargue, and Engels in the solution of fluid problems; and (4) the rapid progress of theoretical and experimental aeronautics in the work of Lanchester, Lilienthal, Kutta, Joukowski, and Prandtl. These advances allowed new tools to be applied to the solution of fluid problems and gave birth to modern fluid mechanics.

Since the beginning of the present century, empiricism has waned and fluid problems have been solved by increasingly rational methods; these methods have produced so many fruitful results and have aided

so materially in increasing our knowledge of the details of fluid phenomena that the trend appears likely to continue into the future. Among the foremost contributors to modern fluid mechanics are Prandtl, Blasius, Karman, Stanton, Nikuradse, Bakhmeteff, Koch, Buckingham, Gibson, Rehbock, Durand, and Taylor.

2. Physical Characteristics of the Fluid State. Matter exists in two states—the solid and the fluid, the fluid state being commonly divided into the liquid and gaseous states.

Solids differ from liquids and liquids from gases in the spacing and latitude of motion of their molecules, these variables being large in a gas, smaller in a liquid, and extremely small in a solid. It follows that intermolecular cohesive forces are large in a solid, smaller in a liquid, and extremely small in a gas. These fundamental facts account for the familiar compactness and rigidity of form possessed by solids, the ability of liquid molecules to move freely within a liquid mass, and the capacity of gases to fill completely the containers in which they are placed.

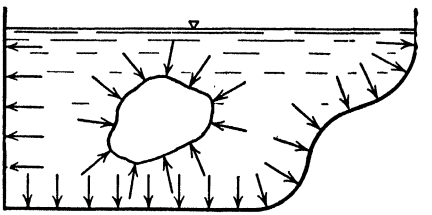


FIG. 1.

A more fruitful and rigorous mechanical definition of the solid and fluid states may be made on the basis of their actions under the various types of stress. Application of tension, compression, or shear stresses to a solid results first in elastic deformation, and later, if these stresses exceed the elastic limits, in permanent distortion of the material. Fluids, however, possess elastic properties under compression stress, but application of infinitesimal shear stress results in continual and permanent distortion. This inability to resist shear stress gives fluids their characteristic ability to "flow". Fluids will support tension stress to the extent of the cohesive forces between their molecules. Since such forces are extremely small, it is customary in engineering problems to assume that fluid can support no tension stress.

Since shear stress applied to fluids always results in distortion or "flow," it is evident that in fluids at rest no shear stresses can exist and compression stress, or "pressure," becomes the only stress to be considered.

Fluids being continuous media, it follows that pressures occurring or imposed at a point in a fluid will be *transmitted undiminished* to all other points in the fluid (neglecting the weight of the fluid).

Before examining the methods of dimensional analysis, recall that there are two different systems by which the dimensions of physical quantities may be expressed. These systems are the force-length-time system and the mass-length-time system. The former system, generally preferred by engineers, becomes the familiar "foot-pound-second" system when expressed in English dimensions; the latter system in English dimensions becomes the "foot-slug-second" system. The latter system is generally preferred in dimensional analysis, and, since the student is familiar with the former system, the use of the latter will serve to develop versatility in the use of dimensions.

A summary of the fundamental quantities of fluid mechanics and their dimensions in the various systems is given in Table VI, the conventional system of capital letters being followed to indicate the dimensions of quantities. The basic relation between the force-length-time and mass-length-time systems of dimensions is given by the Newtonian law, force or weight = (Mass) × (Acceleration) and, therefore, dimensionally,

$$F = M\frac{L}{T^2}$$

from which the dimensions of any quantity may be converted from one system to the other.

To illustrate the mathematical steps in a simple dimensional problem, consider the familiar equation of fluid statics

$$p = wh$$

but assume that the dimensions of w and h are known and those of p unknown. The dimensions of p can be only some combination of M, L, and T, and this combination may be discovered by writing the equation dimensionally as

Unknown dimensions of p = (Dimensions of w) × (Dimensions of h)

or

$$M^aL^bT^c = \left(\frac{M}{L^2T^2}\right) \times (L)$$

in which a, b, and c are unknowns. The principle of dimensional homogeneity being applied, the exponents of *each* of the quantities is the same on each side of the equation, giving

$$a = 1, \quad b = -2 + 1 = -1, \quad c = -2$$

TABLE VI

DIMENSIONS OF FUNDAMENTAL QUANTITIES USED IN FLUID MECHANICS

Quantity	Symbol	English Engineering Dimensions	Force-Length-Time Dimensions	Mass-Length-Time Dimensions
Acceleration	a	ft/sec^2	L/T^2	L/T^2
Acceleration due to gravity	g	ft/sec^2	L/T^2	L/T^2
Area	A	ft^2	L^2	L^2
Density	ρ	lb sec^2/ft^4	FT^2/L^4	M/L^3
Force	F	lb	F	ML/T^2
Kinematic viscosity	ν	ft^2/sec	L^2/T^2	L^2/T
Length	l	ft	L	L
Mass	M	lb sec^2/ft	FT^2/L	M
Power	P	ft lb/sec	FL/T	ML^2/T^3
Pressure	p	lb/ft^2	F/L^2	M/LT^2
Rate of flow	Q	ft^3/sec	L^3/T	L^3/T
Specific weight	w	lb/ft^3	F/L^3	M/L^2T^2
Time	t	sec	T	T
Velocity	V	ft/sec	L/T	L/T
Viscosity	μ	lb sec/ft^2	FT/L^2	M/LT
Weight	W	lb	F	ML/T^2
Weight rate of flow	G	lb/sec	F/T	ML/T^3

whence

$$\text{Dimensions of } p = ML^{-1}T^{-2} = \frac{M}{LT^2}$$

It is obvious, of course, that this result might have been obtained more directly by cancellation of L on the right-hand side of the equation, for this has been, and will continue to be, the usual method of obtaining the unknown dimensions of a quantity. It is of utmost importance, however, to note the mathematical steps which lie unrevealed in this hasty cancellation, if the basis of dimensional analysis is to be understood.

The above methods may now be used in quite another and more important way. To illustrate by another familiar example, suppose that it is known that the power P, which can be derived from a hydraulic motor, is dependent upon the rate of flow through the motor Q, the specific weight of the fluid flowing w, and the unit energy E which is given up by every pound of fluid as it passes through the

Since pressure is compression stress, the equilibrium of a mass of fluid at rest occurs from pressure acting *inward upon* its boundary surface as shown in Fig. 1. If this mass of fluid is reduced to infinitesimal size, it becomes evident that at a point in a fluid the pressure is the *same in all directions*. Since fluids are unable to support tangential (shear) stresses, no component of force can exist *along* the solid boundary of Fig. 1, and thus pressure must be transmitted from a fluid to a solid boundary *normal* to the boundary at every point.

PHYSICAL PROPERTIES OF FLUIDS

3. Density, Specific Weight, Specific Volume, and Specific Gravity. Density [1] is the mass of fluid contained in a unit of volume; specific weight,[1] the weight of fluid contained in a unit of volume. Both these terms are fundamentally measures of the number of molecules per unit of volume. Since molecular activity and spacing increase with temperature fewer molecules will exist in a given unit volume as temperature rises, thus causing density and specific weight to decrease with increasing temperature.[2] Since a larger number of molecules can be forced into a given volume by application of pressure, it will be found that density and specific weight will increase with increasing pressure.

Density, ρ (rho), will be expressed in the mass-length-time system of dimensions and will have the dimensions of mass units (slugs) per cubic foot (slugs/ft^3).

Specific weight, w, will be expressed in the force-length-time system of dimensions and will have the dimensions of pounds per cubic foot (lb/ft^3).

Since a mass, M, is related to its weight, W, by the equation

$$M = \frac{W}{g}$$

in which g is the acceleration due to gravity, density and specific weight (the mass and weight of a unit volume of fluid) will be related by a similar equation

$$\rho = \frac{w}{g} \quad \text{or} \quad w = \rho g$$

[1] In American engineering practice, specific weight is frequently termed "density" and density "mass density."

[2] A variation in temperature from 32° F to 212° F will decrease the specific weight of water 4 per cent (Appendix II) and will decrease the density of gases 37 per cent (assuming no pressure variation).

Using the fact that physical equations are dimensionally homogeneous, the foot-pound-second dimensions of ρ (which are equivalent to slugs per cubic foot) may be calculated as follows:

$$\text{Dimensions of } \rho = \frac{\text{Dimensions of } w}{\text{Dimensions of } g} = \frac{\dfrac{\text{lb}}{\text{ft}^3}}{\dfrac{\text{ft}}{\text{sec}^2}} = \frac{\text{lb sec}^2}{\text{ft}^4}$$

This algebraic use of the dimensions of quantities in the equation expressing physical relationship will be employed extensively and will prove to be an invaluable check on engineering calculations.[3]

The specific volume, v, defined as volume per unit of weight, will have dimensions of cubic feet per pound (ft^3/lb). This definition identifies specific volume as the reciprocal of specific weight and introduces the equations

$$v = \frac{1}{w} \quad \text{or} \quad w = \frac{1}{v}$$

Specific gravity, S, is the ratio of specific weight or density of a substance to the specific weight or density of pure water. Since all these items vary with temperature, temperatures must be quoted when specific gravity is used in precise calculations of specific weight or density. Specific gravities of a few common liquids at 68° F. (except as noted), are presented in Table I, from which the specific weights of liquids

TABLE I *

SPECIFIC GRAVITIES, S, OF VARIOUS LIQUIDS AT 68° F †
(Referred to water at 39.2° F)

Ethyl alcohol	0.789	
Turpentine (*d*-pinene)	0.862	
Benzene	0.888	
Linseed oil	0.934	(59.9° F)
Castor oil	0.960	
Water	0.998	
Glycerine	1.264	(57° F)
Carbon tetrachloride	1.594	
Mercury	13.546	

* *Smithsonian Physical Tables*, Eighth Ed., 1933, Smithsonian Institution.
† Except as noted.

[3] A summary of quantities and their dimensions is given in Appendix I.

may be readily calculated by

$$w = S \times 62.45 \text{ lb/ft}^3$$

The specific weight of gases may be calculated by means of Boyle's law and Charles' law. Using the specific volume of a gas, Boyle's law may be stated as [4]

$$pv = \text{Constant}$$

which expresses the law of compression or expansion of a gas at constant temperature. Charles' law, expressing the variation of pressure with temperature in a constant volume of gas, is [4]

$$\frac{p}{T} = \text{Constant}$$

Obviously the only combination of variables which will satisfy both Boyle's and Charles' laws simultaneously is

$$\frac{pv}{T} = R$$

which is called the "equation of state" of the gas in which the constant, R, is called the "gas constant" and has dimensions of feet/degree Fahrenheit absolute. Since $w = 1/v$, the above equation may be transformed into

$$w = \frac{p}{RT}$$

from which specific weights of gases may be readily calculated.

Application of Avogadro's law, that "all gases at the same pressures and temperatures have the same number of molecules per unit of volume," allows the calculation of a "universal gas constant." Consider two gases having constants R_1 and R_2, specific weights w_1 and w_2, and existing at the same pressure and temperature, p and T. Dividing their equations of state

$$\frac{\dfrac{p}{w_1 T} = R_1}{\dfrac{p}{w_2 T} = R_2}$$

[4] p is the absolute pressure in pounds per square foot, T is the temperature in degrees F absolute (degrees F + 459.6), and the above "constants" are constant if the gas is "perfect." Common gases in the ordinary engineering range of pressures and temperatures may be considered to be "perfect" for most engineering calculations.

results in

$$\frac{w_2}{w_1} = \frac{R_1}{R_2}$$

but, according to Avogadro's principle, the specific weight of a gas must be proportional to its molecular weight, giving $w_2/w_1 = m_2/m_1$, in which m_1 and m_2 are the respective molecular weights of the gases. Combining this equation with the preceding one gives $m_2/m_1 = R_1/R_2$, or

$$m_1R_1 = m_2R_2$$

In other words, the product of molecular weight and gas constant is the same[5] for all gases. This product mR is called the "universal gas constant" and is preferred for general use by many engineers. Values of these gas constants are given in Table II.

TABLE II

GAS CONSTANTS FOR COMMON GASES *

	R, ft/°F abs	mR
Sulphur dioxide	23.6	1512
Carbon dioxide	34.9	1536
Oxygen	48.3	1546
Air	53.3	1545
Nitrogen	55.1	1543
Ammonia	89.5	1516
Hydrogen	767.0	1546

* O. W. Eshbach, *Handbook of Engineering Fundamentals*, p. 7–16, John Wiley & Sons, 1936.

ILLUSTRATIVE PROBLEM

Calculate the density of carbon dioxide at a temperature of 80° F and absolute pressure of 100 lb/in.^{2}

$$m = 12 + 2(16) = 44, \qquad R = \frac{1536}{44} = 34.9$$

$$w = \frac{p}{RT} = \frac{100 \times 144}{34.9 \times (80 + 460)} = 0.793 \frac{\text{lb}}{\text{ft}^3}$$

$$\rho = \frac{0.793}{32.2} = 0.0246 \text{ slugs/ft}^3$$

[5] The constancy of mR is particularly true for the monatomic and diatomic gases. Gases having more than two atoms per molecule tend to deviate from the law mR = Constant. See Table II.

4. Compressibility, Elasticity. All fluids may be compressed with consequent increase in density, the process of compression taking place at the expense of the space between molecules. Therefore, as fluids are compressed the molecular spacing is diminished and the fluids become increasingly difficult to compress further. Fluids also become more difficult to compress as temperature increases because of increased molecular activity reducing the molecular spacing available for compression. Owing to these facts, it is obviously an approximation to express elastic compression of fluids by Hooke's law

$$E = \frac{\text{Stress}}{\text{Strain}}$$

because E is not a constant but increases with increased temperature or pressure. Such an approximation, however, is justified for ordinary engineering calculations since the range of pressure encountered in engineering is comparatively small and the change in E over this pressure range is usually negligible.[6] The above equation then becomes

$$E = -\frac{\Delta p}{\frac{\Delta V}{V}}$$

the strain $(-\Delta V/V)$ being the *decrease* in volume (ΔV) per original volume (V) obtained by an increment of pressure (Δp).

Compression of gases may take place according to various laws of thermodynamics. The isothermal compression of a volume of perfect gas, V_1, existing at an absolute pressure, p_1, to a volume V_2 at a pressure p_2 will be accomplished according to Boyle's law.

$$p_1 V_1 = p_2 V_2 \quad \text{or} \quad pV = \text{Constant}$$

Using the specific volume, v, in this equation there results

$$pv = \text{Constant} \quad \text{or} \quad \frac{p}{w} = \text{Constant}$$

Frequently expansion of gases occurs so rapidly that there is no opportunity for flow of heat during the process. Such an expansion follows the *adiabatic* law

$$p_1 V_1^k = p_2 V_2^k \quad \text{or} \quad pV^k = \text{Constant}$$

[6] E for water is commonly taken as a constant, 300,000 lb/in.^{2}

which, written in terms of specific volume and specific weight, becomes

$$pv^k = \text{Constant} \quad \text{or} \quad \frac{p}{w^k} = \text{Constant}$$

in which k, called the "adiabatic constant," is the ratio of the two specific heats of the gas, that at constant pressure, c_p, to that at constant volume, c_v. Values of k for common gases are given in Table III.

TABLE III

ADIABATIC CONSTANTS, k, FOR COMMON GASES *

Sulphur dioxide	1.26
Carbon dioxide	1.30
Oxygen	1.40
Air	1.40
Nitrogen	1.40
Ammonia	1.32
Hydrogen	1.40

* O. W. Eshbach, *Handbook of Engineering Fundamentals*, p. 7–17, John Wiley & Sons, 1936.

Values of modulus of elasticity of gases, E, may be derived for isothermal and adiabatic processes for use in subsequent developments. Writing the law of elastic compression in differential form

$$E = -\frac{dp}{\frac{dV}{V}} = -V\frac{dp}{dV}$$

For isothermal compression

$$pV = \text{Constant}$$

Differentiating this equation in respect to V results in

$$V\frac{dp}{dV} + p = 0$$

whence

$$\frac{dp}{dV} = -\frac{p}{V}$$

and substituting this in the first expression

$$E = p$$

for an isothermal process.

By a similar analysis E for an adiabatic process may be shown to be given by

$$E = kp$$

Imposed pressures or pressure disturbances are not transmitted instantaneously from point to point in a fluid, but move in waves at finite velocity. The velocity or celerity of propagation of such waves is dependent upon the elastic properties of the fluid; fluids which are more easily compressible (having low values of E) transmit pressures with smaller velocity than those which are difficult to compress. A pressure disturbance is transmitted in a fluid with a celerity, c, which is given by the equation [7]

$$c = \sqrt{\frac{E}{\rho}}$$

in which c is frequently termed the "sonic" or "acoustic" velocity since it is the velocity with which sound, a pressure disturbance, travels. In a gas, sound moves by a series of *adiabatic* compressions and rarefactions. Thus the sonic velocity in a gas may be calculated from

$$c = \sqrt{\frac{kp}{\rho}}$$

an equation which is accurately confirmed by experiment.

Illustrative Problems

Ten cubic feet of water exist at atmospheric pressure. When a pressure of 2000 lb/in.^{2} is applied, what reduction in volume results?

$$E = -\frac{\Delta p}{\frac{\Delta V}{V}} = 300{,}000 = -\frac{2000}{\frac{\Delta V}{10}}$$

$$-\Delta V = 0.0667 \text{ ft}^3$$

Calculate the velocity with which sound travels in water.

$$c = \sqrt{\frac{E}{\rho}} = \sqrt{\frac{300{,}000 \times 144}{\frac{62.4}{32.2}}} = 4720 \text{ ft/sec}$$

[7] For derivation see Appendix III.

5. Viscosity. The property of viscosity, which is exhibited by all fluids, is due fundamentally to the existence of cohesion and interaction between fluid molecules. As fluids flow these cohesions and interactions result in tangential or shear stresses between the moving fluid layers. Consider the thin viscous fluid layers shown in relative motion in Fig. 2. Let them have a thickness, dy, and areas of contact, A, the lower layer moving with velocity, v, the upper one with velocity $v + dv$. To maintain this velocity difference a force F must be continually exerted on the upper layer as indicated, which results in a shear or friction stress, τ (tau), between the layers, given by

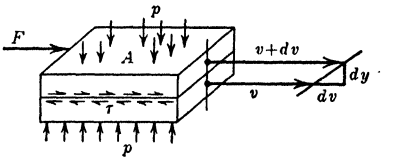


FIG. 2.

$$\tau = \frac{F}{A} ,$$

For viscous fluid motion the shear stress, τ, has been found to be porportional to the *rate of change of velocity* along y or

$$\tau \propto \frac{dv}{dy}$$

and the "coefficient of viscosity," μ (mu),[8] is defined as the constant of proportionality in the above equation, or

$$\tau = \mu \frac{dv}{dy}$$

in which the pressure does not appear, indicating that the shear stress, τ, and thus the coefficient of viscosity, μ, are independent[9] of pressure.

Viscosity varies widely with temperature, but temperature variation has an opposite effect upon the viscosities of liquids and gases due to their fundamentally different intermolecular characteristics. In *gases*, where intermolecular cohesion is negligible, the shear stress, τ,

[8] The dimensions of μ may be obtained by writing

$$\text{Dimensions of } \mu = \frac{\text{Dimensions of } \tau}{\text{Dimensions of } \dfrac{dv}{dy}} = \frac{\text{lb/ft}^2}{\dfrac{\text{ft/sec}}{\text{ft}}} = \text{lb sec/ft}^2$$

[9] Viscosity actually increases slightly with pressure, but this variation is negligible in most engineering problems. Oils manifest the greatest increase of viscosity with pressure.

between moving layers of fluid results from an exchange of momentum between these layers brought about by molecular agitation normal to

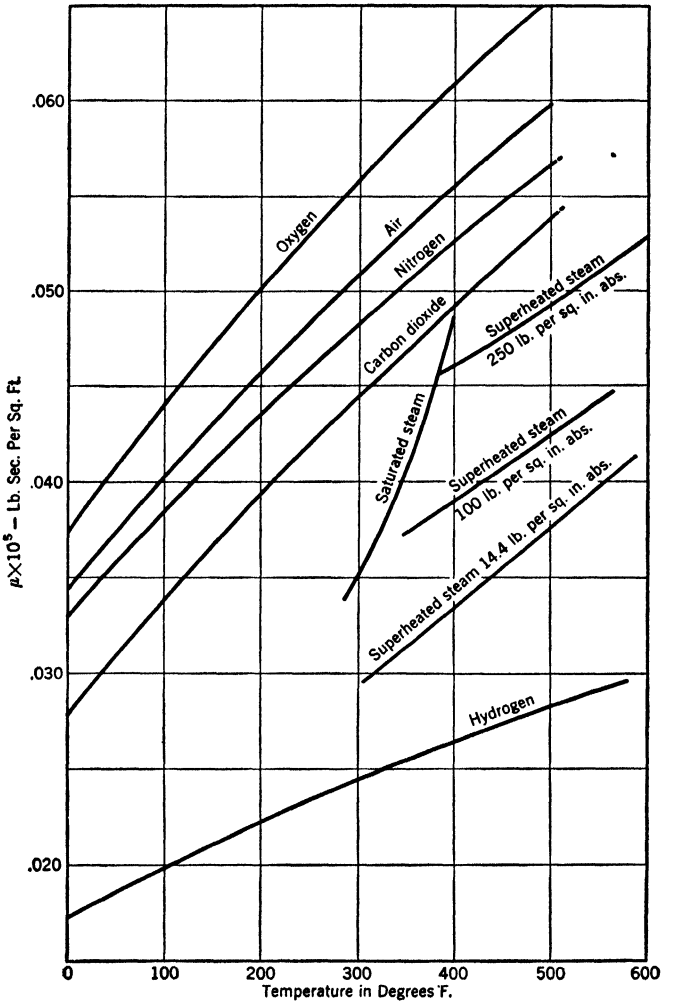


FIG. 3. Viscosities of Gases.[10]

the general direction of motion. Since this molecular activity is known to increase with temperature, the shear stress, and thus the viscosity

[10] Data on viscosities from *Smithsonian Physical Tables*, Eighth Edition, 1933, Smithsonian Institution. (For original data see Appendix IV.) Data on viscosity of steam from *Fluid Meters, Their Theory and Application*, Fourth Edition, 1937, A.S.M.E.

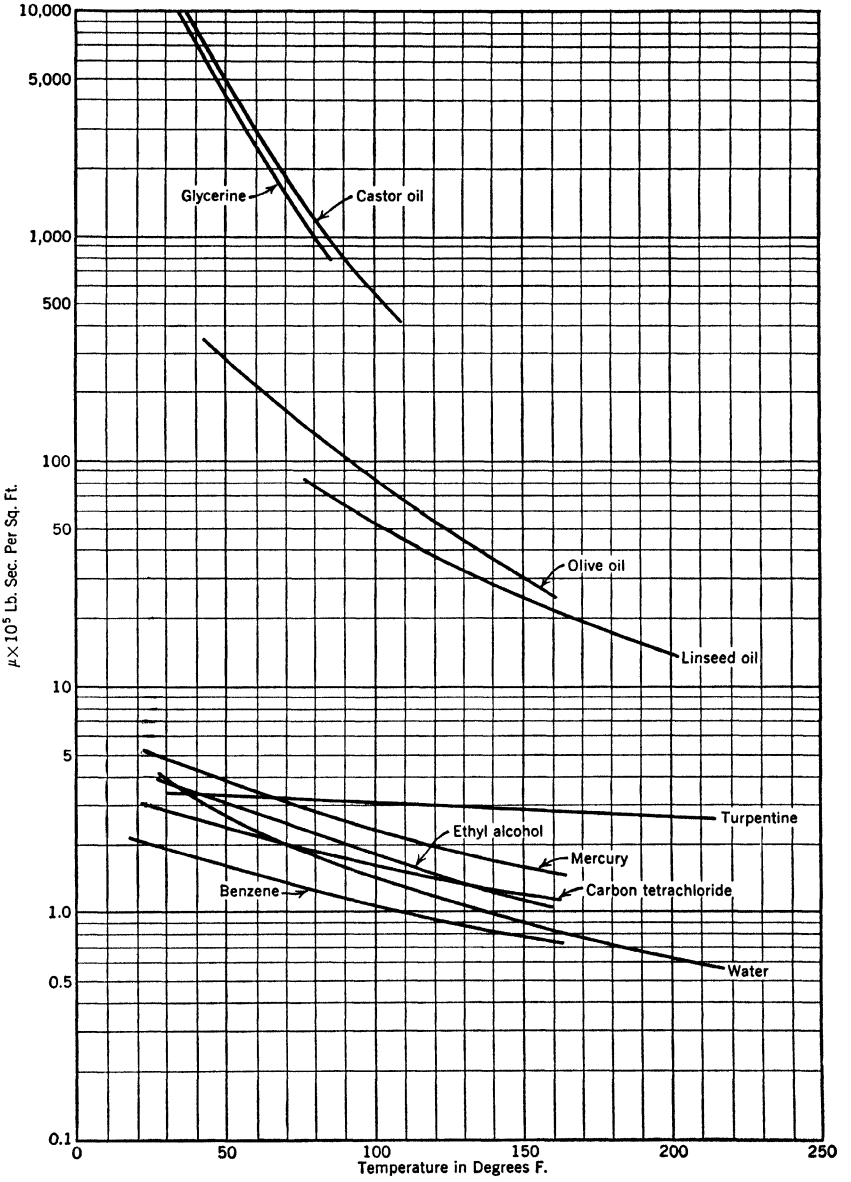


FIG. 4. Viscosities of Liquids.[10]

[10] Data on viscosities from *Smithsonian Physical Tables*, Eighth Edition, 1933, Smithsonian Institution. (For original data, see Appendix IV.) Data on viscosity of steam from *Fluid Meters, Their Theory and Application*, Fourth Edition, 1937, A.S.M.E.

of gases, will increase with temperature (Fig. 3). This reasoning is borne out by tests and by considerations of the kinetic theory of gases which indicate that gas viscosities vary directly with the square root of the absolute temperature.

In a viscous liquid, momentum exchange due to molecular agitation is small compared to the cohesive forces between the molecules, and thus shear stress, τ, and viscosity, μ, are primarily dependent on the magnitude of these cohesive forces. Since these forces decrease rapidly with increases of temperature, liquid viscosities decrease as temperature increases (Fig. 4).

Owing to the continual appearance of the ratio $\frac{\mu}{\rho}$ in subsequent developments, this term has been defined by

$$\nu(\text{nu}) = \frac{\mu}{\rho}$$

in which ν is called the "kinematic viscosity." The kinematic viscosity embraces both the viscosity and density properties of a fluid. Dimensional consideration of the above equation shows the dimensions of ν to be square feet per second, a combination of kinematic terms, which explains the name "kinematic" viscosity.

ILLUSTRATIVE PROBLEM

Calculate the kinematic viscosity of glycerine at 80° F.
From Fig. 4, $\mu = 0.0103$ lb sec/ft.^{2}
From Table I, $S = 1.26$

$$\nu = \frac{\mu}{\rho} = \frac{0.0103}{\frac{62.4 \times 1.26}{32.2}} = 0.00423 \text{ ft}^2/\text{sec}$$

6. Surface Tension, Capillarity. The apparent tension effects, which occur on the free surfaces of liquids, where the surfaces are in contact with another fluid or a solid, depend fundamentally upon the relative sizes of intermolecular cohesive and adhesive forces. On a free liquid surface in contact with the atmosphere, surface tension manifests itself as an apparent "skin" over the surface which will support small loads.[11] The magnitude of surface tension, T, is the force in the surface and normal to a line of unit length drawn in the

[11] A small needle placed gently upon a water surface will not sink but will be supported by the tension in the liquid surface.

liquid surface; thus it will have dimensions of pounds per foot. Since surface tension is directly dependent upon intermolecular cohesive forces, its magnitude will decrease as temperature increases.[12] Surface tension is also dependent upon the gas in contact with the liquid surface, thus surface tensions are usually quoted "in contact with air" as indicated in Table IV.

TABLE IV

SURFACE TENSION, T, OF COMMON LIQUIDS *

(At 68° F in contact with air)

	lb/ft
Ethyl alcohol	0.001527
Carbon tetrachloride	0 001832
Turpentine	0.001857
Benzene	0.001980
Olive oil	0 002295
Water	0.004985
Mercury	0.03562

* *International Critical Tables*, First Edition, 1926–1933, McGraw-Hill Book Company.

Surface tension in the surface of a droplet of liquid causes the pressure inside of the droplet to be greater than that outside. The relation of this excess pressure to the surface tension can be found by a simple mechanical analysis as follows. Consider the droplet of diam-

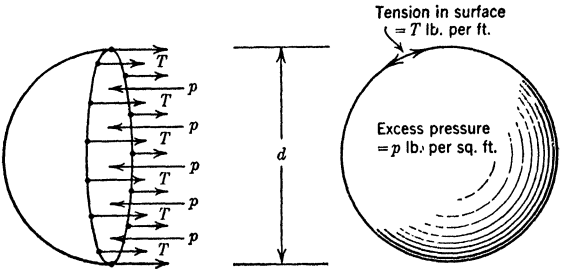


FIG. 5.

eter d, indicated in Fig. 5. If the droplet is halved the forces on one half are seen to be (1) the force due to surface tension, T, existing around the circumference of the droplet and acting to the right, and

[12] For example, the surface tension of water decreases from 0.00498 lb/ft at 68° F to 0.00421 lb/ft at 212° F.

(2) the force due to the excess pressure, p, acting to the left. These forces are in equilibrium resulting in

$$\text{Surface tension force} - \text{Pressure force} = 0$$

or

$$\pi dT - p\frac{\pi d^2}{4} = 0$$

giving

$$p = \frac{4T}{d}$$

thus relating excess pressure to surface tension and indicating that these pressures increase as the size of droplet decreases.

The angle of contact made by a liquid on a horizontal surface illustrates another surface-tension phenomenon of more complex nature. Consider the mercury and water on a glass surface illustrated by Fig. 6.

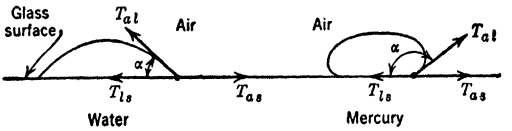


FIG. 6.

The familiar large angle of contact assumed by the mercury indicates a comparatively large affinity of mercury molecules for each other (cohesion) and small affinity of these molecules for those of the glass (adhesion). The opposite effect is exhibited by the water. The water is said to "wet" the glass since its angle of contact is less than 90 degrees. The stability of these liquids on a solid surface may be characterized by the equilibrium of assumed surface tensions [18] at their points of contact. Thus the following equation may be written

$$T_{ls} + T_{al}\cos\alpha = T_{as}$$

Frequently equilibrium does not exist between these tensions, and the following inequality results

$$T_{as} > T_{ls} + T_{al}\cos\alpha$$

[18] T_{al} = surface tension between liquid and air.
T_{ls} = surface tension between liquid and solid.
T_{as} = surface tension between air and solid.

causing the liquid to spread over the surface on which it is placed. Such a condition exists when certain types of oil are placed on a water surface.

Surface-tension effects like the above, existing when surfaces of liquids come in contact with vertical solid surfaces, result in the phenomenon known as "capillarity." Water and mercury in contact with a vertical clean glass plate are illustrated in Fig. 7. Here again are demonstrated the results of attractions and repulsions, cohesions and adhesions, between the molecules of liquid and solid.

When a vertical tube is placed in a liquid as in Fig. 8, these surface phenomena form a "meniscus," or curved surface, in the tube, and the liquid in the tube stands above or below that outside, depending upon the size of the angle of contact. The "capillary rise," h, in such a tube may be calculated approximately by considering the equilibrium of the vertical forces on the mass of fluid $ABCD$. Neglecting the fluid above the low point of the meniscus the weight of $ABCD$ is given by

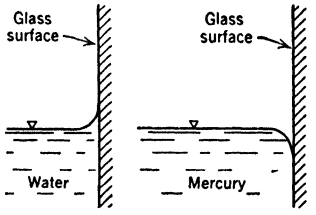


FIG. 7.

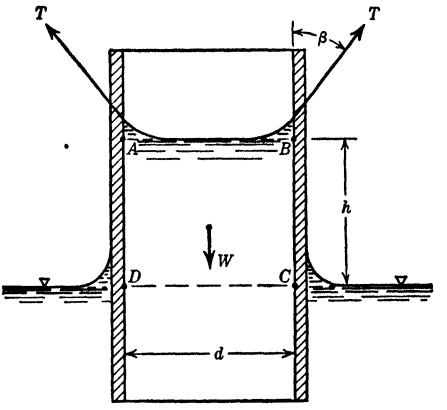


FIG. 8.

$$W = wh\frac{\pi d^2}{4}$$

which acts downward. The vertical component, F_T, of the force due to surface tension is given by

$$F_T = \pi dT \cos \beta$$

which acts upward and is in equilibrium with the downward force, thus

$$wh\frac{\pi d^2}{4} = \pi dT \cos \beta$$

giving

$$h = \frac{4T \cos \beta}{wd}$$

allowing the capillary rise to be calculated approximately and confirming the familiar fact that capillary rise becomes greater as tube diameter is decreased.

Similarly it may be shown that the capillary rise between vertical parallel plates is given by

$$h = \frac{2T \cos \beta}{wd}$$

where d is the distance between the plates.

ILLUSTRATIVE PROBLEM

Of what diameter must a droplet of water be to have the pressure within it 0.1 lb/in.^{2} greater than that outside?

From Table IV, $T = 0.004985$ lb/ft.

$$p = \frac{4T}{d}, \quad d = \frac{4 \times 0.004985}{0.1 \times 144} = 0.001385 \text{ ft} = 0.0166 \text{ in.}$$

7. Vapor Pressure. All liquids possess a tendency to vaporize, i.e., to change from the liquid state into the gaseous state. Such vaporization occurs because molecules are continually projected through the free liquid surface and lost from the body of liquid. Such molecules, being gaseous, are capable of exerting a partial pressure, the "vapor pressure" of the liquid, and since this pressure is dependent primarily upon molecular activity it will increase with increasing temperature. The variation of the vapor pressure of water with temperature is indicated in Fig. 9.

For boiling to occur a liquid's temperature must be raised sufficiently for the vapor pressure to become equal to the pressure imposed on the liquid. This means that the boiling point of a liquid is dependent upon its pressure as well as its temperature.[14]

Table V offers a comparison of the vapor pressures of a few common liquids at the same temperature. The low vapor pressure of mercury along with its high density makes this liquid well suited for use in barometers and other pressure-measuring devices.

[14] For instance, water boils at 212° F when exposed to an atmospheric pressure of 14.7 lb/sq in., but will boil at 200° F if the imposed pressure is reduced to 11.4 lb/sq in.

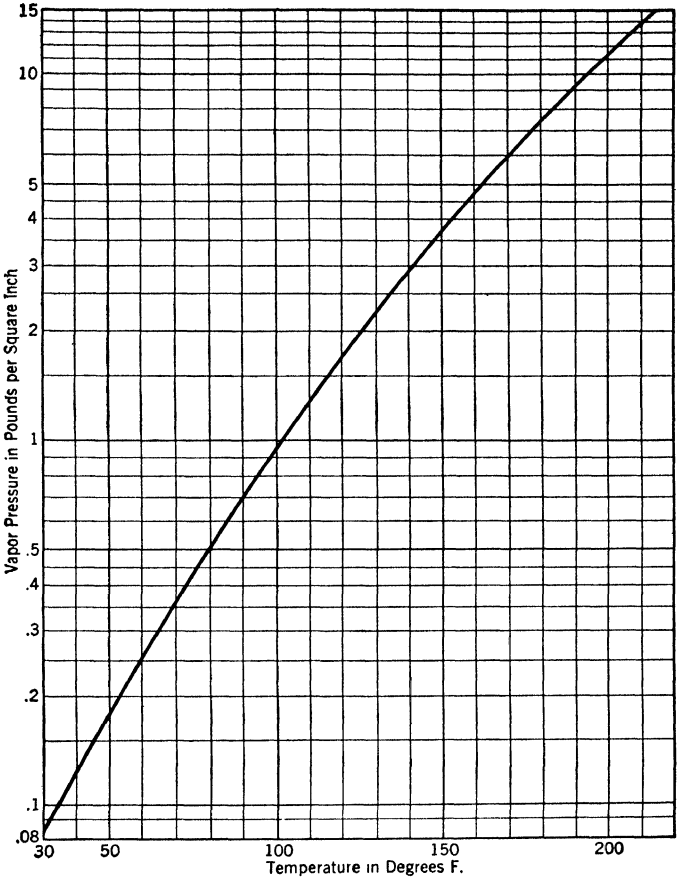


FIG. 9. Vapor Pressure of Water.

TABLE V *

VAPOR PRESSURE, p_v, OF COMMON LIQUIDS AT 68° F

	lb/ft^2	lb/in.^{2}
Ether	1231.	8.55
Carbon tetrachloride	250.	1.738
Benzene	208.	1.448
Ethyl alcohol	122.4	0.850
Water	48.9	0.339
Turpentine	1.115	0.00773
Mercury	0.00362	0.0000251

* *Smithsonian Physical Tables*, Eighth Edition, 1933, Smithsonian Institution.

BIBLIOGRAPHY

Historical

W. F. Durand, "The Development of Our Knowledge of the Laws of Fluid Mechanics," *Science*, Vol. 78, No. 2025, p. 343, October 20, 1933.

R. Giacomelli and E. Pistolesi. *Historical Sketch, Aerodynamic Theory*, Vol. I, p. 305, Julius Springer, Berlin, 1934.

C. E. Bardsley, "Historical Résumé of the Development of the Science of Hydraulics," *Pub.* 39, Engineering Experiment Station of Oklahoma Agricultural and Mechanical College, April, 1939.

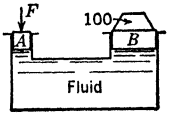
Viscosity

E. C. Bingham, *Fluidity and Plasticity*, McGraw-Hill Book Co., 1922.

E. Hatschek, *The Viscosity of Liquids*, Van Nostrand, 1928.

PROBLEMS

1. The two pistons A and B have respectively cross-sectional areas of 2 in.^{2} and 50 in.^{2} What force, F, must be applied to piston A to support a weight of 100 lb on B?



2. If 186 ft^3 of a certain oil weigh 9860 lb, calculate the specific weight, density, and specific gravity of this oil.

3. Calculate the specific weight and density of mercury at 68° F.

4. Calculate the specific weight and density of glycerine at 57° F.

5. The density of alcohol is 1.53 slugs/ft^3. Calculate its specific weight, specific gravity, and specific volume.

6. A cubic foot of air at 14.7 lb/in.^{2} and 59° F weighs 0.0765 lb/ft^3. What is its specific volume?

7. Calculate the specific weight, specific volume, and density of air at 40° F and 50 lb/in.^{2} absolute.

8. Calculate the density, specific weight, and specific volume of carbon dioxide at 100 lb/in.^{2} absolute and 200° F.

9. Calculate the density, specific weight, and specific volume of chlorine gas at 50 lb/in.^{2} absolute and 100° F.

10. Calculate the density of carbon monoxide at 20 lb/in.^{2} absolute and 50° F.

11. The specific volume of a certain perfect gas at 30 lb/in.^{2} absolute and 100° F is 10 ft.^{3} Calculate its gas constant and molecular weight.

12. If $h = \dfrac{p}{w}$, what are the dimensions of h?

13. If $V = \sqrt{2gh}$, calculate the dimensions of V.

14. If $F = QwV/g$, what are the dimensions of F?

15. Twelve cubic feet of water are placed under a pressure of 1000 lb/in.^{2}. Calculate the volume at this pressure.

16. If the volume of a liquid is reduced 0.035 per cent by application of a pressure of 100 lb/in.^{2}, what is its modulus of elasticity?

17. What pressure must be applied to water to reduce its volume 1 per cent?

18. Ten cubic feet of air at 100° F and 50 lb/in.^{2} absolute are compressed isother-

mally to 2 cu ft. What is the pressure when the air is reduced to this volume? What is the modulus of elasticity at the beginning and end of the compression?

19. If the air in the preceding problem is compressed adiabatically to 2 cu ft, calculate the final pressure and temperature and the modulus of elasticity at beginning and end of the compression.

20. Calculate the velocity of sound in air of standard conditions (32° F and 14.7 lb/in.^{2} absolute).

21. Calculate the velocity of sound in fresh water.

22. Calculate the kinematic viscosity of turpentine at 68° F.

23. Calculate the kinematic viscosity of castor oil at 68° F.

24. Calculate the kinematic viscosity of nitrogen at 100° F and 80 lb/in.^{2} absolute.

25. What is the ratio between the viscosities of air and water at 50° F? What is the ratio between their kinematic viscosities at this temperature and standard barometric pressure?

26. A space of 1-in. width between two large plane surfaces is filled with glycerine at 68.5° F. What force is required to drag a very thin plate of 5 ft^2 area between the surfaces at a speed of 0.5 ft/sec if this plate remains equidistant from the two surfaces? If it is at a distance of 0.25 in. from one of the surfaces?

27. Castor oil at 68° F fills the space between two concentric cylinders of 10-in. height and 6-in. and 6.25-in. diameters. What torque is required to rotate the inner cylinder at 12 rpm, the outer cylinder remaining stationary?

28. What force is necessary to overcome viscous action when removing the above inner cylinder from the outer one at a speed of 1 ft/sec?

29. A circular disk of diameter d is rotated in a liquid of viscosity μ at a small distance Δh from a fixed surface. Derive an expression for the torque T, necessary to maintain an angular velocity ω. Neglect centrifugal effects.

30. Calculate the excess pressure within a droplet of water at 68° F if the droplet has a diameter of 0.01 in.

31. What excess pressure may be caused within a 0.20-in.-diameter cylindrical jet of water by surface tension?

32. Calculate the capillary rise of water in a glass tube of 1-mm diameter at 68° F. ($\beta = 0°$.)

33. Calculate the capillary rise of water (68° F) between two vertical, clean glass plates spaced 1 mm apart. ($\beta = 0°$.)

34. Develop the equation for theoretical capillary rise between parallel plates.

35. Calculate the capillary depression of mercury in a glass tube of 1-mm diameter at 68° F. ($\beta = 140°$.)

36. A soap bubble 2 in. in diameter contains a pressure (in excess of atmospheric) of 0.003 lb/in.^{2} Calculate the surface tension of the soap film.

37. What force is necessary to lift a thin wire ring of 1-in. diameter from a water surface at 68° F? Neglect weight of ring.

38. What is the minimum absolute pressure which may be maintained in the space above the liquid, in a can of ether at 68° F?

39. To what value must the absolute pressure over carbon tetrachloride be reduced to make it boil at 68° F?

40. What reduction below standard atmospheric pressure must occur to cause water to boil at 150° F?

41. A 6-in.-diameter cylinder containing a tight-fitting piston is completely filled with water at 150° F. What force is necessary to withdraw the piston if atmospheric pressure is 14.70 lb/in.^{2}?

CHAPTER II

FLUID STATICS

The subject of fluid statics involves fluid problems in which there is no relative motion between fluid particles. If no relative motion exists between particles of a fluid, viscosity can have no effect, and the fluids involved may be treated as if they were completely devoid of viscosity. With the effects of viscosity excluded from fluid statics exact solutions of problems may be obtained by analytical methods without the aid of experiment.

8. Pressure-Density-Height Relationships. The fundamental equation of fluid statics is that relating pressure, density, and vertical distance in a fluid. This equation may be derived readily by considering the vertical equilibrium of an element of fluid such as the small cube of Fig. 10. Let this cube be differentially small and have dimensions dx, dy, and dz, and assume that the density of the fluid in the cube is uniform. If the pressure upward on the bottom face of this cube is p, the force due to this pressure will be given by $p\,dx\,dy$. Assuming an increase of pressure in the positive direction of z, the pressure downward on the top face of the cube will be $p + \frac{dp}{dz}\,dz$, and the force due to this pressure will be $\left(p + \frac{dp}{dz}\,dz\right) dx\,dy$. The other vertical force involved is the weight, dW, of the cube, given by

$$dW = w\,dx\,dy\,dz$$

The vertical equilibrium of the cube will be expressed by

$$\left(p + \frac{dp}{dz}\,dz\right) dx\,dy + w\,dx\,dy\,dz - p\,dx\,dy = 0$$

giving

$$\frac{dp}{dz} = -w$$

the fundamental equation of fluid statics, which must be integrated for the solution of engineering problems. Such integration may be accomplished by transposing the terms w and dz, resulting in

$$\frac{dp}{w} = - dz$$

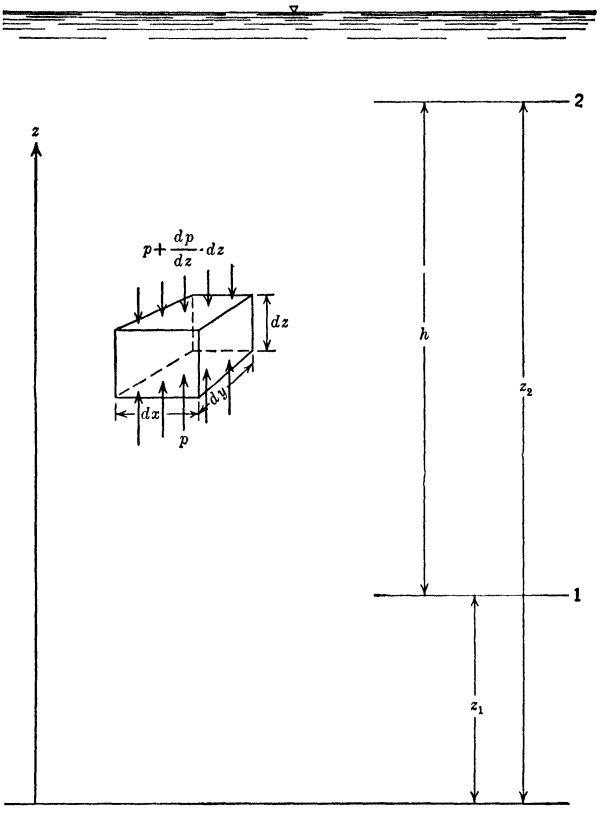


FIG. 10.

which may be integrated as follows:

$$\int_{p_2}^{p_1} \frac{dp}{w} = - \int_{z_2}^{z_1} dz = z_2 - z_1$$

giving

$$\int_{p_2}^{p_1} \frac{dp}{w} = h$$

in which p_1 is the greater pressure existing at the lower point 1, p_2 the lesser pressure existing at the upper point 2, and h the vertical distance between these points. The integration of the left-hand side of the equation cannot be carried out until $w = f(p)$ is known. For gases this relationship may be obtained from certain laws of thermodynamics. For liquids the specific weight, w, is sensibly constant allowing integration of the equation to

$$\frac{p_1 - p_2}{w} = h \quad \text{or} \quad p_1 - p_2 = wh \tag{1}$$

permitting ready calculation of the increase in pressure in a liquid as depth is gained. It should be noted that equation 1 embodies certain basic and familiar facts concerning fluids at rest. It shows that, if $h = 0$, the pressure difference is zero and thus pressure is constant over horizontal planes in a fluid. Conversely, if the pressure is constant over a horizontal plane the height of fluid above that plane is constant, resulting in the tendency of liquids to "seek their own levels."

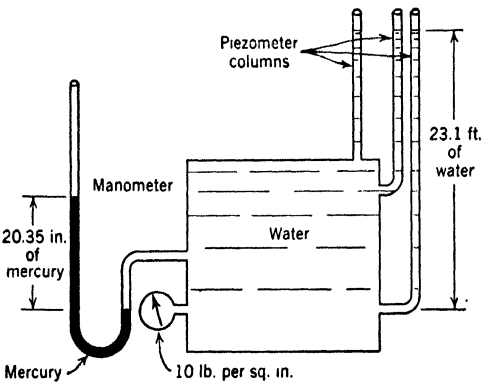


FIG. 11.

Equation 1 also indicates the fact that pressure at a point in a liquid of given density is dependent solely upon the height of the liquid above the point, allowing this vertical height, or "head," of liquid to be used as an indication of pressure. Thus pressures may be quoted in "inches of mercury," "feet of water," etc. The relation of pressure and head [1] is illustrated numerically by the "manometer" and "piezometer columns" of Fig. 11.

[1] For use in problem solutions it is advisable to keep in mind certain pressure and head equivalents for common liquids. The use of "conversion factors," whose physical significance is rapidly lost, may be avoided by remembering that standard atmospheric pressure is 14.70 lb/in.^{2}, 29.92 in. of mercury (32° F), or 33.9 ft of water (60° F).

ILLUSTRATIVE PROBLEMS

A closed tank is partially filled with carbon tetrachloride. The pressure on the surface of the liquid is 10 lb/in.^{2}. Calculate the pressure 15 ft below the surface.

$$w = 1.59 \times 62.4 = 99.1 \text{ lb/ft}^3$$

$$p_1 - p_2 = wh, \quad p_1 - 10 \times 144 = 99.1 \times 15$$

$$p_1 = 2927 \text{ lb/ft}^2 = 20.3 \text{ lb/in.}^2$$

If the atmospheric pressure at the earth is 14.70 lb/in.^{2} and the air temperature there 60° F, calculate the pressure 1000 ft above the earth, assuming that the air temperature does not vary between the earth's surface and this elevation.

Isothermal condition, therefore, $p_1/w_1 = p_2/w_2 = p/w$.

$$w_1 = \frac{14.70 \times 144}{53.3(60 + 460)} = 0.0763 \text{ lb/ft}^3$$

$$\frac{p}{w} = \frac{p_1}{w_1} = \frac{14.70 \times 144}{0.0763} = 27{,}750 \text{ ft}$$

$$h = \int_{p_2}^{p_1} \frac{dp}{w} = 1000 = 27{,}750 \int_{p_2}^{p_1} \frac{dp}{p}$$

$$\frac{1000}{27{,}750} = 0.0361 = \ln \frac{p_1}{p_2} = \ln \frac{14.70}{p_2}$$

$$\log \frac{14.70}{p_2} = 0.0361 \times 2.303 = 0.083$$

Therefore

$$\frac{14.70}{p_2} = 1.21, \quad p_2 = 12.15 \text{ lb/in.}^2$$

9. Absolute and Gage Pressures. Although pressures are measured and quoted by two different systems, one relative, the other absolute, no confusion will result if the relation between these systems is completely understood.

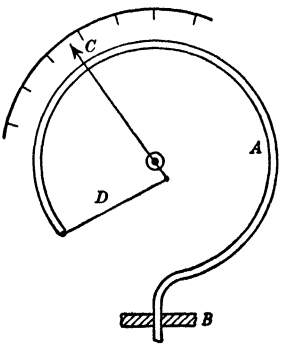


FIG. 12.

"Gage pressures" may be best understood by examination of the common Bourdon pressure gage, a diagrammatic sketch of which is shown in Fig. 12. A bent tube (A) is held rigidly at B and its free end connected to a pointer (C) by means of the link (D). When pressure is admitted to the tube at B, the tube tends to straighten, thus actuating the lever system which moves the pointer over a graduated

scale. When the gage is in proper adjustment the pointer rests at zero on the scale when the gage is disconnected, and in this condition the pressure inside and outside of the tube will be the same, thus giving the tube no tendency to deform. Since atmospheric pressure usually exists outside of the tube, it is apparent that pressure gages are actuated by the *difference* between the pressure inside and that outside of the tube. Thus, in the gage, or relative, system of pressure measurement, the atmospheric pressure becomes the zero of pressure. For pressure greater than atmospheric the pointer will move to the right; for pressure less than atmospheric the tube will tend to contract, moving the pointer to the left. The reading in the first case is positive and is called "gage pressure" or simply "pressure," [2] and is usually measured in pounds per square inch; the reading in the second case is negative, is designated as "vacuum," and is usually measured in inches of mercury.

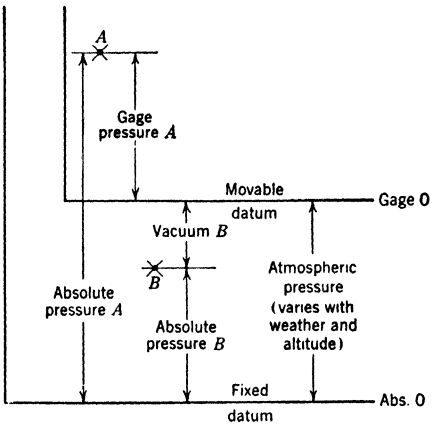


FIG. 13.

The absolute zero of pressure will exist only in a completely evacuated space (perfect vacuum). Atmospheric pressure as measured by a barometer will be seen to be pressure in excess of this absolute zero and is, therefore, an "absolute pressure." [2] The magnitudes of the atmospheric pressure in both the absolute and gage system, being known, the following equation may be written

$$\text{Absolute pressure} = \text{Atmospheric pressure} \begin{matrix} - \text{ Vacuum} \\ + \text{ Gage pressure} \end{matrix}$$

which allows easy conversion from one system to the other. Possibly a better picture of these relationships can be gained from a diagram such as that of Fig. 13 in which are shown two typical pressures, A and B, one above, the other below, atmospheric pressure, with all the relationships indicated graphically.

[2] Throughout the remainder of the book "pressure" should be understood to mean "gage pressure"; when "absolute pressure" is meant, it will be designated as such.

ILLUSTRATIVE PROBLEM

A Bourdon gage registers a vacuum of 12.5 in. of mercury when the barometric pressure is 14.50 lb/in.^{2} Calculate the corresponding absolute pressure.

$$\text{Vacuum} = 12.5 \times \frac{14.70}{29.92} = 6.15 \text{ lb/in.}^2$$

$$\text{Absolute pressure} = 14.50 - 6.15 = 8.35 \text{ lb/in.}^2$$

10. Manometry. Bourdon pressure gages, owing to their inevitable mechanical limitations, are not in general satisfactory for precise measurements of pressure; when greater precision is required, measurements of the height of liquid columns of known density are commonly used. Such measurements may be accomplished by means of "manometers" like those of Fig. 14, pressures being obtained by the application of the pressure-density-height relationships.

Consider the elementary manometer of Fig. 14*a*, consisting of a glass tube connected to a reservoir of liquid. With both the reservoir and the tube open to the atmosphere the liquid surfaces will stand on the horizontal line *O–O*. If the reservoir is now connected to a volume of gas having an unknown pressure, p_x, the surface of the reservoir liquid will drop to the line 1–1 and that in the tube will rise to the point 2. Since pressures over horizontal planes in a fluid are constant, the pressure p_x existing on the reservoir surface will also exist as indicated in the tube. Applying equation 1

$$p_x - p_2 = wh$$

and with the tube open to the atmosphere, $p_2 = 0$ and

$$p_x = wh$$

thus p_x may be obtained by measurement of the distance h.

Figure 14*b* illustrates the measurement of a pressure less than atmospheric with the same type of manometer. Here the reservoir is open to the atmosphere and the unknown pressure, p_x, admitted to the tube. Applying the same principles to the liquid column of height h,

$$p_1 - p_x = wh$$

in which

$$p_1 = 0$$

giving

$$p_x = -wh$$

the negative sign indicating the pressure to be less than the atmospheric pressure.

The familiar mercury barometer is shown in Fig. 14*c*. Such a barometer is constructed by filling a glass tube, closed at one end, with

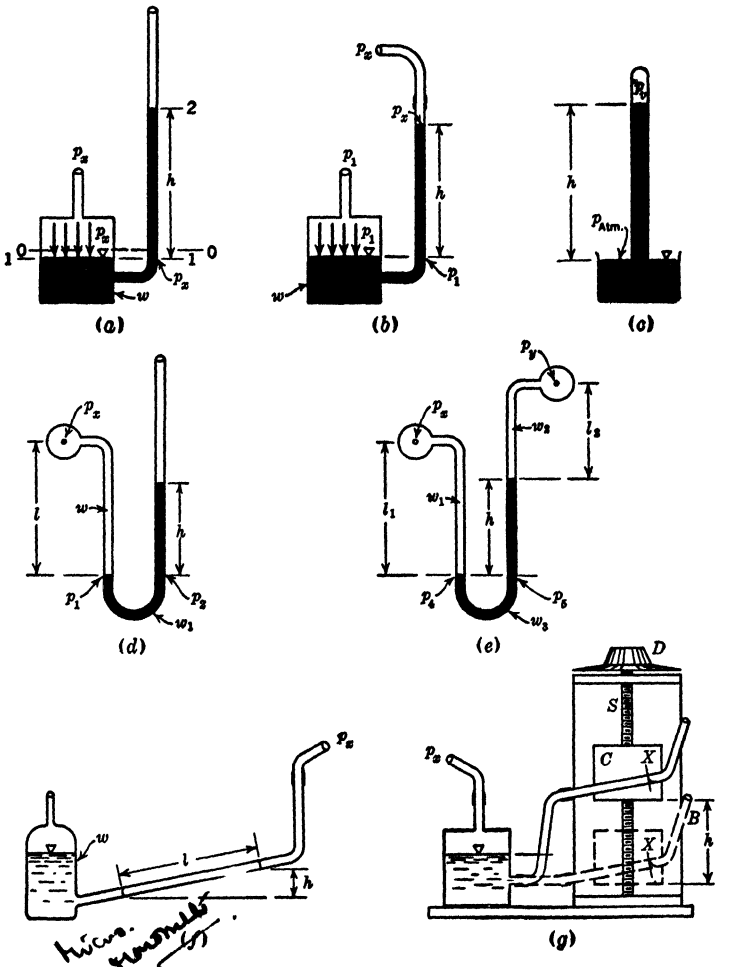


FIG. 14. Manometers.

mercury and inverting the tube, keeping its open end below the surface of the mercury in a reservoir. The mercury column, h, will be supported by the atmospheric pressure, leaving an evacuated space, containing only mercury vapor, in the top of the tube. Using the absolute

system of pressures, equilibrium of the mercury column, h, will be expressed by

$$P_{\text{atm.}} - p_v = wh$$

in which p_v for mercury has been seen to be negligible at ordinary temperatures (Table V) resulting in

$$P_{\text{atm.}} = wh$$

thus allowing atmospheric pressure to be easily obtained by measurement of the height of the mercury column.

Calculation of the pressure, p_x, measured by the U-tube manometer of Fig. 14*d* may be obtained easily by noting that

$$p_1 = p_2$$

and that

$$p_1 = p_x + wl$$

$$p_2 = 0 + w_1h$$

giving

$$p_x + wl = 0 + w_1h$$

resulting in

$$p_x = w_1h - wl$$

allowing p_x to be calculated.[3]

U-tube manometers are frequently used to measure the difference between two unknown pressures p_x and p_y, as in Fig. 14*e*. Here, as before,

$$p_4 = p_5$$

and

$$p_4 = p_x + w_1l_1$$

$$p_5 = py + w_2l_2 + w_3h$$

giving

$$p_x + w_1l = p_y + w_2l_2 + w_3h$$

and

$$p_x - p_y = w_2l_2 + w_3h - w_1l$$

thus allowing direct calculation of the pressure difference, $p_x - p_y$. "Differential manometers" of the above type are frequently made with the U-tube inverted, a liquid of small density existing in the top of the inverted U; the pressure difference measured by manometers of this

[3] The use of formulas for manometer solutions is not recommended until experience has been gained in their limitations.

type may be readily calculated by application of the foregoing principles.

When large pressures or pressure differences are to be measured a number of U-tube manometers may be connected in series. Several applications of the above principles will allow solution for the unknown pressure or pressure difference.

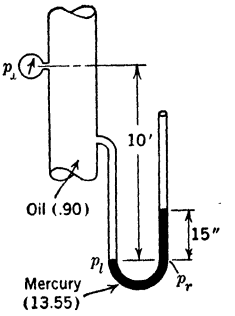
There are many forms of precise manometers, two of the most common of which are shown in Figs. 14*f* and 14*g*. The former is the ordinary "draft gage" used in measuring the comparatively small pressures in drafts of all types. Its equilibrium position is shown at A, and when it is submitted to a pressure, p_x, a vertical deflection, h, is obtained in which $p_x = wh$. In this case, however, the liquid is forced down a gently inclined tube so that the manometer "deflection," l, is much greater than h and, therefore, more accurately read. The draft gage is usually calibrated to read directly in inches of water.

The principle of the sloping tube is also employed in the alcohol micromanometer of Fig. 14*g*, used in aeronautical research work. Here the gently sloping glass tube is mounted on a carriage, C, which is moved vertically by turning the dial, D, which actuates the screw, S. When p_x is zero the carriage is adjusted so that the liquid in the tube is brought to the hair line, X, and the reading on the dial recorded. When the unknown pressure, p_x, is admitted to the reservoir the alcohol runs upward in the tube toward B and the carriage is then raised until the liquid surface in the tube rests again at the hair line, X. The difference between the dial reading at this point and the original one gives the vertical travel of the carriage, h, which is the head of alcohol equivalent to the pressure p_x.

Along with the above principles of manometry the following practical considerations should be appreciated: (1) manometer liquids, in changing their specific gravities with temperature, will induce errors in pressure measurements if this factor is overlooked; (2) errors due to capillarity may usually be canceled by selecting manometer tubes of uniform size; (3) although some liquids appear excellent (from density considerations) for use in manometers, their surface-tension effects may give poor menisci and thus inaccurate readings; (4) fluctuations of the manometer liquids will reduce accuracy of pressure measurement, but these fluctuations may be reduced by a throttling device in the manometer line, a short length of small tube proving excellent for this purpose; (5) when fluctuations are negligible refined optical devices and verniers may be used for extremely precise readings of the liquid surfaces.

ILLUSTRATIVE PROBLEM

This vertical pipe line with attached gage and manometer contains oil and mercury as shown. The manometer is open to the atmosphere. What will be the gage reading, p_x?



$$p_l = p_x + (0.90 \times 62.4)10$$

$$p_r = (13.55 \times 62.4)\tfrac{15}{12}$$

Since

$$p_l = p_r$$

$$p_x = 505 \text{ lb/ft}^2 = 3.51 \text{ lb/in.}^2$$

11. Forces on Submerged Plane Surfaces. The calculation of the magnitude, direction, and location of the total forces on surfaces submerged in a liquid is essential in the design of dams, bulkheads, gates, tanks, etc.

For a submerged, plane, *horizontal* area the calculation of these force properties is simple, because the pressure does not vary over the

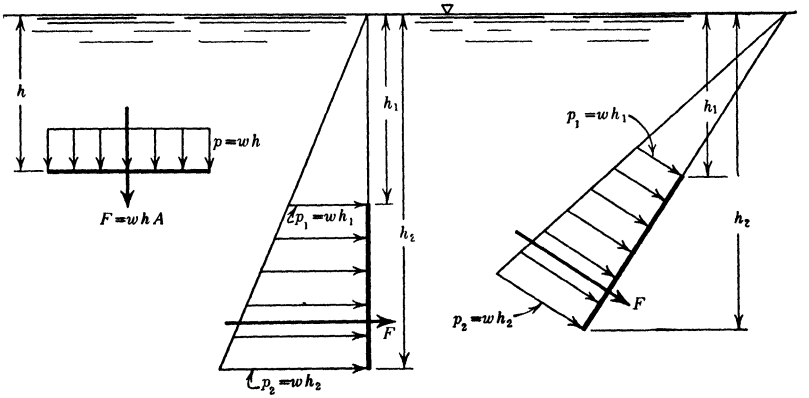


FIG. 15.

area; for non-horizontal planes the problem is complicated by pressure variation. Pressure in liquids, however, has been shown to vary linearly with depth (equation 1), resulting in the typical pressure diagrams and resultant forces of Fig. 15.

Now consider the general case[4] of a plane submerged area AB, such as that of Fig. 16, located in any inclined plane X–X. Let the center of

[4] A general solution for the magnitude, direction, and location of the resultant force on this area will allow easy calculation of the forces on areas of more regular shape.

gravity of this area be located as shown, at a depth h_g and at a distance l_g from the line of intersection, O–O, of plane X–X and the liquid surface. Calculating the force, dF, on the small area, dA,

$$dF = pdA = whdA$$

but $h = l \sin \alpha$, and substituting this value for h

$$dF = wl \sin \alpha \, dA$$

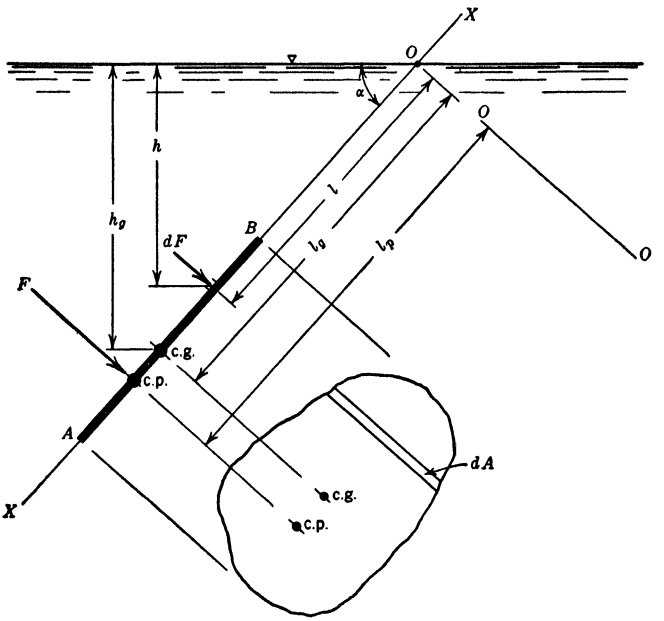


FIG. 16.

and the total force on the area AB will result from the integration of this expression, giving

$$F = w \sin \alpha \int^{A} ldA \tag{2}$$

but $\int^{A} ldA$ is recognized as the statical moment of the area AB, about the line O–O which is also given by the product of the area, A, and the perpendicular distance, l_g, from O–O to the center of gravity of the area. Thus

$$\int^{A} ldA = l_g A$$

and substituting this in equation 2

$$F = wAl_g \sin \alpha$$

but $h_g = l_g \sin \alpha$, giving

$$F = wh_gA \tag{3}$$

indicating that the magnitude of the resultant force on a submerged plane area may be calculated by multiplying the area, A, by the pressure at its center of gravity, wh_g.

The magnitude of the resultant force having been calculated, its direction and location must be considered. Its direction, because of the inability of liquids to support shear stress, is necessarily normal to the plane, and its point of application may be found if the moment of the force can be calculated and divided by the magnitude of the force.

Referring again to Fig. 16, the moment, dM, of the force, dF, about the line O–O is given by

$$dM = ldF$$

in which

$$dF = wl \sin \alpha \, dA$$

Therefore, by substitution,

$$dM = wl^2 \sin \alpha \, dA$$

and integrating to obtain the total moment, M,

$$M = w \sin \alpha \int^A l^2 dA$$

in which $\int^A l^2 dA$ is the moment of inertia of the area A, about the line O–O, thus

$$I_{O-O} = \int^A l^2 dA$$

and

$$M = wI_{O-O} \sin \alpha$$

Designating the point of intersection of the resultant force and the plane as the "center of pressure" and its distance from O–O as l_p, l_p will be given by

$$l_p = \frac{M}{F}$$

in which

$$M = wI_{O-O} \sin \alpha$$

and

$$F = wl_gA \sin \alpha$$

Substituting these values above gives

$$l_p = \frac{wI_{O-O} \sin \alpha}{wl_gA \sin \alpha} = \frac{I_{O-O}}{l_gA}$$

thus locating the resultant force in respect to the line O–O, and completing the solution of the general problem.

The above equation may be made more usable by placing it in terms of the moment of inertia, I_g, about an axis parallel to O–O through the center of gravity of the area. Using the equation for transferring moment of inertia of an area from one axis to another,

$$I_{O-O} = I_g + l_g^2 A$$

and substituting in the equation for l_p

$$l_p = \frac{I_g + l_g^2 A}{l_g A}$$

which may be written as

$$l_p = \frac{I_g}{l_g A} + l_g$$

or

$$l_p - l_g = \frac{I_g}{l_g A} \tag{4}$$

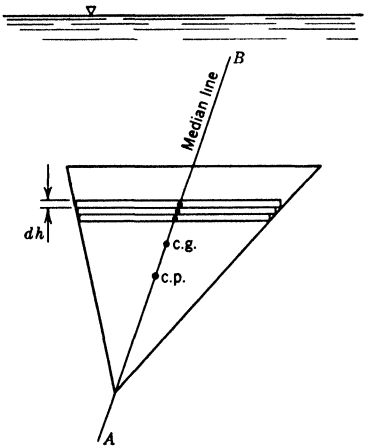


FIG. 17.

allowing direct calculation of the distance along the X–X plane between center of gravity and center of pressure. This equation also indicates that center of pressure is always *below* center of gravity except for a horizontal area, but that the distance between center of pressure and center of gravity diminishes as the depth of submergence of the area is increased.[5]

The lateral location of the center of pressure for regular plane areas, such as that of Fig. 17, is readily calculated by considering the area to be composed of a large number of rec-

[5] This fact allows the approximation made for small areas under great submergence, or pressure, that the resultant force acts at their centers of gravity.

tangles of differentially small height, dh. The center of gravity and center of pressure of each of these small rectangles will be coincident and at the center of the rectangle, and, therefore, all the forces on these rectangles will act on the median line AB. The resultant of these forces must also act on the median line. The vertical and lateral location of the center of pressure of areas of more irregular form may be obtained by dividing the area into regular areas, locating the forces on these, and finding the location of the resultant of these forces by taking moments about any convenient axis. The point where the line of action of the resultant force pierces the area is the center of pressure of the whole area.

ILLUSTRATIVE PROBLEM

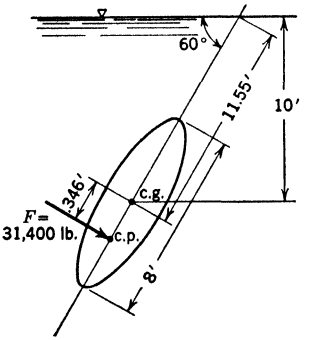
A circular gate 8 ft in diameter lies in a plane sloping 60° with the horizontal. If water stands above the center of the gate to a depth of 10 ft, calculate the magnitude, direction, and location of the total force exerted by water on gate.

Direction: normal to gate

Magnitude:

$$F = wh_gA$$

$$F = 62.4 \times 10 \times \frac{\pi}{4}(8)^2 = 31{,}400 \text{ lb}$$



Location:

$$I_g = \frac{\pi}{64}(8)^4 = 64\pi \text{ ft}^4$$

$$l_g = \frac{10}{0.866} = 11.55 \text{ ft}$$

$$A = \frac{\pi}{4}(8)^2 = 50.3 \text{ ft}^2$$

$$l_p - l_g = \frac{I_g}{l_gA} = \frac{64\pi}{11.55 \times 50.3} = 0.346 \text{ ft}$$

Therefore force passes through a point (c.p.) located 0.346 ft below the center of gravity measured down the plane.

12. Forces on Submerged Curved Surfaces. The total forces on submerged curved areas cannot be calculated by the foregoing methods. These forces may be readily obtained, however, by calculating the horizontal and vertical components of the forces as indicated below.

The curved area, AB, of Fig. 18a is exposed to liquid pressure on its upper and lower surfaces. Obviously, the vertical component of

the pressure force is downward on the upper surface, upward on the lower surface, and these two force components have the same line of action and the same magnitude. If the liquid vertically above the area AB is isolated by drawing the lines BC and AD, it becomes apparent that no vertical force can be transmitted across these lines because of the inability of the liquid to support shear stress. Hence, the vertical component of force on the area AB is simply the weight of liquid, $ABCD$, thus

$$F_V = W_{ABCD}$$

and the line of action of this force will pass through the center of gravity of $ABCD$.

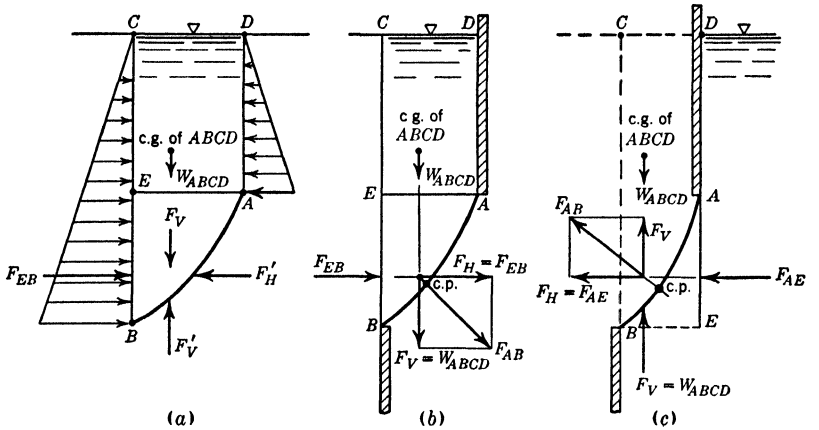


FIG. 18.

The horizontal component of force may be readily established by considering the horizontal equilibrium of the mass of liquid ABE, EB being the projection of AB on a vertical plane. If F_H is the horizontal component of force exerted by the area *on* the liquid ABE horizontal equilibrium is expressed by

$$F'_H = F_{EB}$$

in which the magnitude, direction, and location of F_{EB} may be calculated by the methods of Art. 11. The horizontal component of force exerted *by* the liquid *on* the area AB will have the direction, magnitude, and line of action of F_{EB}, and the resultant force, F, may be obtained by composition of the horizontal and vertical components as indicated in the two typical cases of Figs. 18*b* and 18*c*.

Illustrative Problem

Calculate magnitude, direction, and location of the total force exerted by the water on the area AB which is a quarter of a circular cylinder and is 8 ft long (normal to plane of paper).

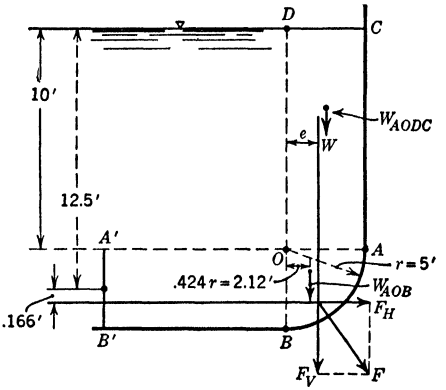
Horizontal component, F_H

Direction: Horizontal to right

Magnitude:

$$F_H = (Awh_g)_{A'B'}$$

$$F_H = 8 \times 5 \times 62.4 \times 12.5 = 31{,}200 \text{ lb}$$



Location:

$$A_{A'B'} = 8 \times 5 = 40 \text{ ft}^2$$

$$I_{A'B'} = \frac{8 \times 5^3}{12} = 83.2 \text{ ft}^4$$

$$(l_p - l_g)_{A'B'} = \frac{83.2}{12.5 \times 40} = 0.166 \text{ ft}$$

Vertical component, F_V

Direction: Vertically downward

Magnitude:

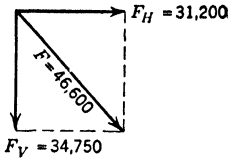
$$F_V = W_{AODC} + W_{AOB}$$

$$F_V = 10 \times 5 \times 8 \times 62.4 + \frac{\pi(5)^2}{4} \times 8 \times 62.4 = 34{,}750 \text{ lb}$$

Location: e = distance between F_V and line DB, and taking moments about point B

$$34{,}750 \times e = 24{,}950 \times 2.5 + 9800 \times 2.12$$

$$e = 2.40 \text{ ft.}$$



Total force F:
Direction: Downward to right
48° with horizontal

Magnitude: $F = 1000\sqrt{31.2^2 + 34.75^2} = 46{,}600$ lb
Location: Through a point located 2.334 ft above B and 2.40 ft to the right of B

13. Buoyancy and Flotation. The familiar principles of buoyancy (Archimedes' principle) and flotation are usually stated respectively: (1) A body immersed in a fluid is buoyed up by a force equal to the weight of fluid displaced by the body; and (2) a floating body displaces its own weight of the fluid in which it floats. These principles may be easily proved by the methods of Art. 12.

A body, $ABCD$, suspended in a liquid of specific weight, w, is illustrated on Fig. 19. After the vertical lines AE and CF are drawn, it is obvious that the force F_1, acting vertically downward on the upper surface ADC, is given by

$$F_1 = w(\text{Volume } ADCFE)$$

and F_2, the force upward on the lower surface ABC, by

$$F_2 = w(\text{Volume } ABCFE)$$

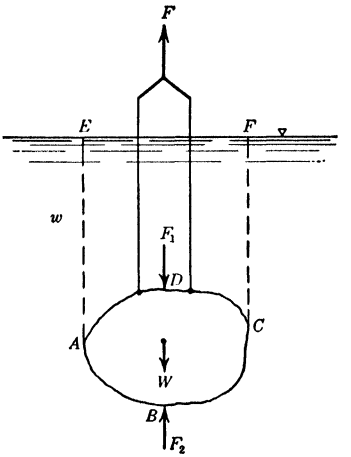


FIG. 19.

The net vertical force, F_B, exerted by the liquid on the body is upward and given by

$$F_B = F_2 - F_1$$

or

$$F_B = w(\text{Volume } ABCFE - \text{Volume } ADCFE)$$

Performing the indicated subtraction results in

$$F_B = w(\text{Volume } ABCD) = w(\text{Volume of body})$$

thus "the buoyant force is equal to the weight of fluid displaced by the body." The vertical equilibrium of the body is expressed by

$$F + F_B - W = 0$$

For a floating body (Fig. 20) vertical equilibrium is expressed by

$$F_B - W = 0$$

and the vertical component of force on the immersed area, $ABCD$, will (Art. 12) be given by

$$F_B = w(\text{Volume } ABCD)$$

thus

$$W = w(\text{Volume } ABCD)$$

and the body "displaces its own weight of the fluid in which it floats." The above principles find many applications in engineering, such as calculations: of the draft of surface vessels; of the weight of a ship's cargo from the increment in depth of flotation; of the lift of balloons; etc.

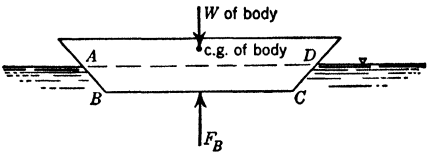


FIG. 20.

The stability of submerged or floating bodies is dependent upon the relative location of the buoyant force and the weight of the body. The buoyant force acts upward through the center of gravity of the displaced volume; the weight acts downward at the center of gravity

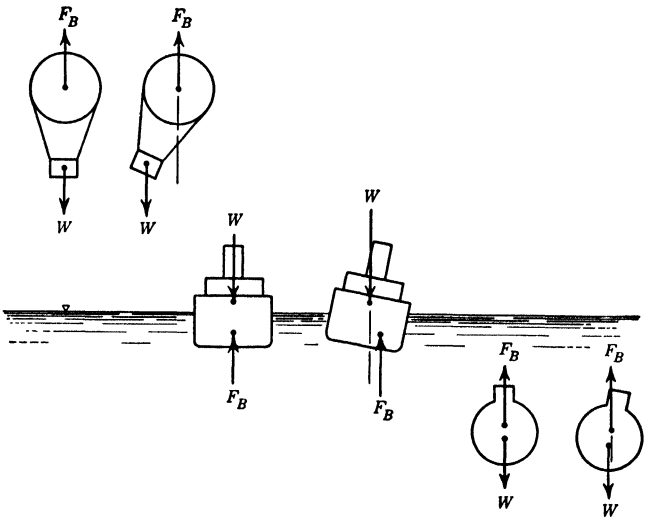


FIG. 21.

of the body. Stability or instability will be determined by whether a righting or overturning moment is developed when the center of gravity and center of buoyancy move out of vertical alignment. Obviously, for the submerged bodies, such as the balloon and submarine of Fig. 21, stability requires the center of buoyancy to be above the

center of gravity. In surface vessels, however, the center of gravity is usually above the center of buoyancy, and stability exists because of movement of the center of buoyancy to a position outboard of the center of gravity as the ship "heels over," thus producing a righting moment. An overturning moment, resulting in capsizing, occurs if the center of gravity moves outboard of the center of buoyancy.

Illustrative Problem

A ship has a cross-sectional area of 4000 ft^2 at the water line when the draft is 10 ft. How many pounds of cargo will increase the draft 2 in.? Assume salt water.

Since the ship floats, the weight of water displaced by the cargo equals the weight of the cargo. Therefore

$$\text{Weight of cargo} = 4000 \times \tfrac{2}{12} \times 64.0 = 42{,}700 \text{ lb}$$

14. Stresses in Circular Pipes and Tanks. The circumferential tension stresses in pipes and tanks under pressure may be readily calculated if pressure variation is neglected and if the thickness of the pipe or tank is small compared to the diameter.

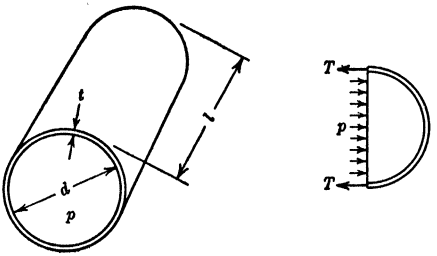


FIG. 22.

A section of pipe of length l, having an internal diameter d, is shown in Fig. 22. This pipe contains a fluid whose pressure is p; the circumferential tension stress in the walls is s_t. Pass a vertical plane through the center of the pipe and consider the horizontal equilibrium of the forces acting on the section of pipe to the right of this plane. This equilibrium is expressed by

$$2T - pdl = 0$$

in which T is the total tension force in the wall of length l and thickness t due to the stress s_t, and therefore is given by

$$T = s_t tl$$

Substituting this in the equation above

$$2s_t tl = pdl$$

$$s_t = \frac{1}{2}\frac{pd}{t}$$

thus allowing the wall stress to be calculated when the internal pressure and the dimensions of the pipe or tank are known. The final equation also indicates that the stress caused by a given pressure may be reduced by decreasing the diameter d, or increasing the wall thickness t. Since increasing the wall thickness increases the cost it becomes evident why small-bore tubing is in general use in high-pressure work.

A mechanical analysis similar to the above may be applied in the design of wooden tanks or pipes where the tension is carried by external circumferential hoops, and in the design of concrete structures of this type where the tension stress is carried by circumferential reinforcing rods.

15. Fluid Masses Subjected to Acceleration. Fluid masses may be subjected to various types of acceleration without relative motion occurring between fluid particles or between fluid particles and boundaries. Such fluid masses will be found to conform to the laws of fluid statics, modified to account for the inevitable inertia forces which exist when acceleration occurs.

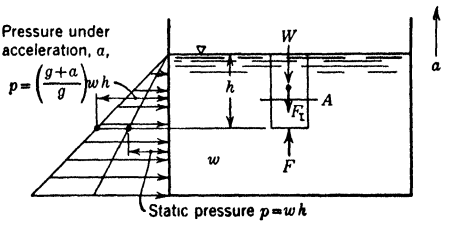


FIG. 23.

An open container of liquid subjected to a vertical upward acceleration, a (Fig. 23), will contain greater pressures than if the liquid is at rest, owing to the forces of inertia which act in the opposite direction to that of acceleration. The general relationships for this type of accelerated motion may be obtained by considering the vertical equilibrium of a cylinder of fluid, of height h, cross-sectional area A, and having its upper base in the liquid surface.

The force F, upward on the bottom of the cylinder due to pressure, will balance the forces of inertia F_I and weight W, acting downward. Therefore,

$$F = W + F_I$$

in which

$$F = pA$$

$$W = Mg$$

$$F_I = Ma$$

in which M, the mass of the liquid cylinder, is expressed by

$$M = \rho hA = \frac{w}{g} hA$$

and substituting these values in the first equation

$$pA = \frac{w}{g} hAg + \frac{w}{g} hAa$$

and solving for p

$$p = \left(\frac{g + a}{g}\right) wh$$

indicating that pressure variation with depth is linear and that the pressure at any point will be given by the product of $\left(\frac{g + a}{g}\right)$ and the static pressure, wh, at the point. These facts are indicated graphically in Fig. 23.

Similarly it may be shown that, for a fluid mass undergoing a vertical downward acceleration a, pressure p, at a depth h, will be given by

$$p = \left(\frac{g - a}{g}\right) wh$$

If $a = g$ in this equation, the pressure becomes zero, showing that a freely falling unconfined fluid mass exerts no pressure, a fact which will have many applications in subsequent problems.

Horizontal acceleration of a liquid mass in an open container is indicated in Fig. 24, acceleration of this kind causing the liquid surface to drop at the front of the tank and to rise at the rear. The forces which a liquid particle at the surface will exert on its neighboring particles will be its weight, W, acting downward, and its inertia force, F_I, acting horizontally and in a direction opposite to that of acceleration. However, for a liquid surface to be stable the resultant of these forces must act normal to the liquid surface; thus, referring to Fig. 24, the liquid surface will stand at an angle, θ, with the horizontal, and

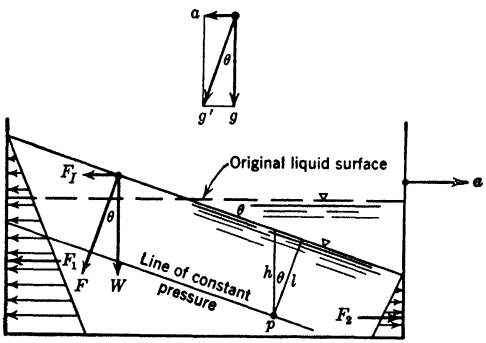


FIG. 24.

$$\tan \theta = \frac{F_I}{W} = \frac{Ma}{Mg} = \frac{a}{g}$$

proving that the liquid surface and other lines of constant pressure are straight lines having a slope a/g.

A fruitful means of examining this problem further is to imagine the magnitude and direction of the acceleration due to gravity, g, to be changed to those of g'. When this is done the pressure-variation problem may be analyzed as one of simple fluid statics in which the relation of pressure, p, to depth, l, along the direction of g' will be given by

$$p = w'l$$

in which w' is the apparent specific weight of the liquid in a system where acceleration due to gravity is g' instead of g. The density of the liquid, ρ, is the same in both systems and, therefore,

$$\frac{w}{g} = \rho = \frac{w'}{g'}$$

from which

$$w' = \left(\frac{g'}{g}\right) w$$

Substituting above

$$p = \left(\frac{g'}{g}\right) wl \tag{5}$$

but from similar triangles

$$\frac{g'}{g} = \frac{h}{l}$$

and substitution of this relation in equation 5 gives the familiar equation

$$p = wh$$

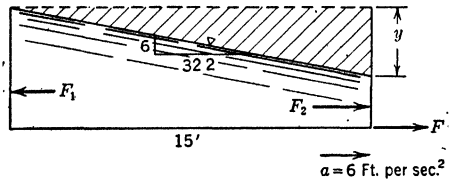
The fact that this equation applies to fluid masses while they are being accelerated horizontally means that the total forces on vertical areas, such as the ends of the container of Fig. 24, may be calculated by the principles of Art. 11. These forces are indicated as F_1 and F_2, and if the mass of fluid in the container is designated by M, it will be found that

$$F_1 - F_2 = Ma$$

the unbalanced force, $F_1 - F_2$, being equal to the product of mass and acceleration, thus checking the Newtonian relationship, $F = Ma$.

Illustrative Problem

A rectangular tank 15 ft long, 5 ft high, and 8 ft wide is filled with water and accelerated along the direction of its length, at 6 ft/sec^2. Calculate the volume of water spilled, and check the equality of force to accelerate the final mass and the force exerted by liquid on the ends of the tank.



$$y = \frac{6}{32.2} \times 15 = 2.80 \text{ ft}$$

Volume spilled $= \frac{1}{2} \times 2.80 \times 15 \times 8 = 168 \text{ ft}^3$

Force, F, for acceleration $= Ma$

$$F = (5 \times 15 \times 8 - 168) \frac{62.4}{32.2} \times 6 = 5020 \text{ lb}$$

$$F_1 = 5 \times 8 \times 2.5 \times 62.4 = 6230 \text{ lb}$$

$$F_2 = \frac{2.2}{2} \times 2.2 \times 8 \times 62.4 = 1210 \text{ lb}$$

$$F_1 - F_2 = 6230 - 1210 = 5020 \text{ lb } (\textit{Check})$$

Fluid masses subjected to rotation at constant angular velocity will contain pressure variations unlike those in fluids at rest, because of the centrifugal forces exerted by fluid particles. The centrifugal force exerted by a mass M, rotating about an axis with circumferential velocity V, at a radius r, is given by

$$F = \frac{MV^2}{r} \tag{6}$$

in which V^2/r is termed the "centrifugal acceleration."

The simple case of fluid rotation about a vertical axis is indicated

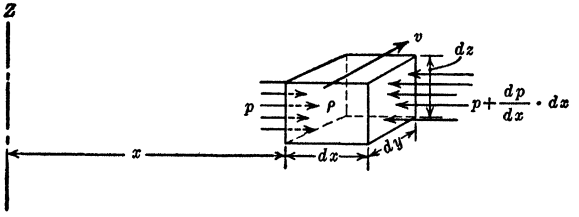


Fig. 25.

in Fig. 25 where the forces on a small element of fluid are considered. Let this element have dimensions dx, dy, and dz and rotate with the circumferential velocity, v, at a distance x from the axis of rotation Z.

Since the mass of fluid does not move in the radial direction an equilibrium of forces exists in this direction which may be stated as

$$\text{Centrifugal force} = \text{Centripetal force}$$

in which the centripetal force can result only from pressure variation along x. Taking the pressure on the inner vertical face of the element to be p and assuming the pressure to increase with x, the pressure on the outer face will be

$$p + dp \quad \text{or} \quad p + \frac{dp}{dx}\,dx$$

thus

$$\text{Centripetal force} = \left(p + \frac{dp}{dx}\,dx\right) dy\,dz - p\,dy\,dz$$

$$= \frac{dp}{dx}\,dx\,dy\,dz$$

The centrifugal force may be calculated from equation 6 in which, for the fluid element,

$$M = \rho\,dx\,dy\,dz = \frac{w}{g}\,dx\,dy\,dz$$

$$V = v = \omega x$$

$$r = x$$

ω being the angular velocity of rotation. Therefore

$$\text{Centrifugal force} = \frac{w}{g}\,dx\,dy\,dz\,\frac{(\omega x)^2}{x}$$

Equating centrifugal and centripetal forces,

$$\frac{dp}{dx}\,dx\,dy\,dz = \frac{w}{g}\,dx\,dy\,dz\,\frac{(\omega x)^2}{x}$$

results in

$$\frac{dp}{dx} = \frac{w}{g}\,\omega^2 x$$

a differential equation expressing the variation of pressure in the radial direction for fluid masses subjected to constant angular velocity. Since dp/dx is a positive quantity it may be concluded directly that pressure will increase as radius increases. This equation may be integrated for practical use between the axis of rotation where $x = 0$ and $p = p_c$

and any point, x, where a pressure, p, exists. Separating the variables and integrating,

$$\int_{p_c}^{p} \frac{dp}{w} = \int_{0}^{x} \frac{\omega^2 x\, dx}{g}$$

gives

$$\frac{p}{w} - \frac{p_c}{w} = \frac{\omega^2 x^2}{2g} \tag{7}$$

the physical meaning of which is given on Fig. 26.

Figure 26*a* shows an open cylindrical container being rotated about a central vertical axis. The terms p/w and p_c/w are recognized

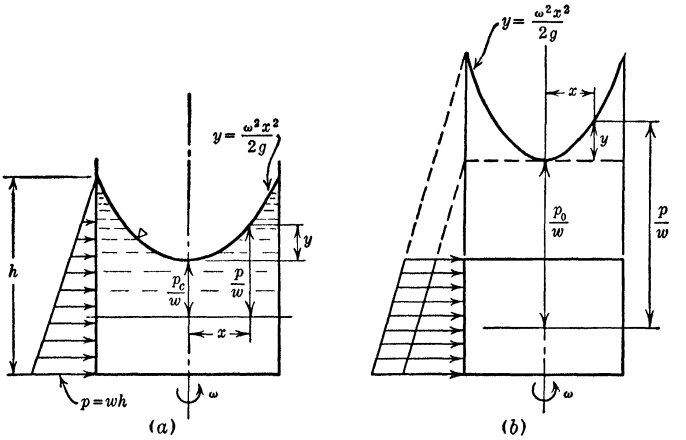


FIG. 26.

as the "heads" of liquid corresponding respectively to the pressures p and p_c. The equation

$$y = \frac{p}{w} - \frac{p_c}{w}$$

is obvious from the figure and hence equation 7 becomes

$$y = \frac{\omega^2}{2g} x^2$$

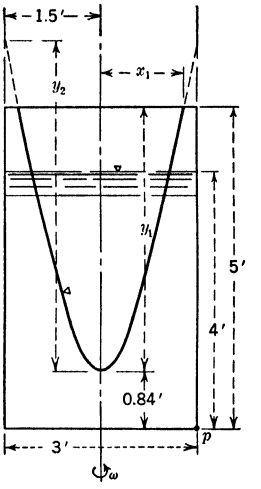
indicating the liquid surface to be of paraboloidal form. Since no acceleration exists in a vertical direction the variation of pressure with depth (as for horizontal linear acceleration) will follow the static law

$$p = wh$$

which is indicated on the figure.

Figure 26*b* illustrates a closed container filled with liquid having an initial pressure before rotation begins. This initial pressure, p_0, at some point in the liquid is represented by the corresponding head of liquid p_0/w. Since there is no velocity *on* the axis of rotation, no increase in pressure will exist here and the parabolic curve of pressure variation becomes as indicated on the figure.

The foregoing analysis indicates that pressure may be created by the rotation of a fluid mass. This principle is utilized in centrifugal pumps and blowers to create pressure in order to cause fluids to flow.



Illustrative Problem

A vertical cylindrical tank 5 ft high and 3 ft in diameter is filled with water to a depth of 4 ft. The tank is then closed and the pressure in the space above the water surface raised to 10 lb/in.^{2} What pressure will exist at the intersection of wall and tank bottom when the tank is rotated about a central vertical axis at 150 rpm?

Since no liquid escapes, space above liquid remains same.

$$\text{Volume of this space} = \frac{\pi}{4} \times (3)^2 \times 1 = 7.08 \text{ ft}^3$$

$$\tfrac{1}{2}\pi x_1^2 y_1 = 7.08$$

but

$$y_1 = \frac{\omega^2 x_1^2}{2g}$$

Therefore

$$\tfrac{1}{2}\pi x_1^2 \left(\frac{\omega^2 x_1^2}{2g}\right) = 7.08$$

in which

$$\omega = 150 \times \frac{2\pi}{60} = 15.7 \text{ rad./sec.}$$

Solving,

$$x_1 = 1.044 \text{ ft}, \quad y_1 = 4.16 \text{ ft}$$

$$y_2 = \frac{\overline{15.7}^2 \times \overline{1.5}^2}{2g} = 8.60 \text{ ft}$$

$$p = (8.60 + 0.84)\, 62.4 + 10 \times 144 = 2029 \text{ lb/ft}^2$$

$$p = \frac{2029}{144} = 14.1 \text{ lb/in}^2$$

PROBLEMS

42. Calculate the pressure in an open tank of benzene at a point 8 ft below the surface.

43. If the pressure 10 ft below the free surface of a liquid is 20 lb/in.^{2}, calculate its specific weight and specific gravity.

44. If the pressure at a point in the ocean is 200 lb/in.^{2}, what is the pressure 100 ft below this point? Specific weight of salt water is 64.0 lb/ft^3.

45. An open vessel contains carbon tetrachloride to a depth of 6 ft and water on the CCl_4 to a depth of 5 ft. What is the pressure at the bottom of the vessel?

46. How many inches of mercury are equivalent to a pressure of 20 lb/in.^{2}? How many feet of water?

47. One foot of air at 60° F and 14.7 lb/in.^{2} is equivalent to how many pounds per square inch? inches of mercury? feet of water?

48. The barometric pressure at sea level is 30.00 in. of mercury when that on a mountain top is 29.00 in. If the air temperature is constant at 60° F and the specific weight of air is assumed constant at 0.075 lb/ft^3, calculate the elevation of the mountain top.

49. If atmospheric pressure at the ground is 14.7 lb/in.^{2} and temperature is 60° F, calculate the pressure 10,000 ft above the ground, assuming (*a*) no density variation; (*b*) an isothermal variation of density with pressure; (*c*) an adiabatic variation of density with pressure.

50. Prove that the depth of an assumed isothermal atmosphere is infinitely great.

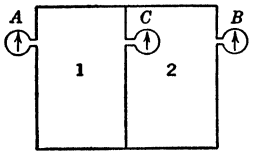
51. Calculate the depth of an adiabatic atmosphere if temperature and pressure at the ground are respectively 60° F and 14.7 lb/in.^{2}

52. With atmospheric pressure at 14.5 lb/in.^{2}, what absolute pressure corresponds to a gage pressure of 20 lb/in.^{2}?

53. When the barometer reads 30 in. of mercury, what absolute pressure corresponds to a vacuum of 12 in. of mercury?

54. If a certain absolute pressure is 12.35 lb/in.^{2}, what is the corresponding vacuum if atmospheric pressure is 29.92 in. of mercury?

55. A Bourdon pressure gage attached to a closed tank of air reads 20.47 lb/in.^{2} with the barometer at 30.50 in. of mercury. If barometric pressure drops to 29.18 in. of mercury, what will the gage read?



56. The compartments of these tanks are closed and filled with air. Gage *A* reads 30 lb/in.^{2} Gage *B* registers a vacuum of 10 in. of mercury. What will gage *C* read if it is connected to compartment 1 but inside of compartment 2? Barometric pressure is 14.6 lb/in.^{2}

57. Assuming the liquid in Fig. 14*a* to be mercury and h to be 16 in., calculate the pressure p_x.

58. Calculate the pressure p_x in Fig. 14*b* if the liquid is carbon tetrachloride and h is 8.0 feet.

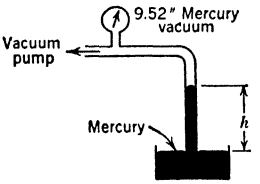
59. If the barometer of Fig. 14*c* is filled with ether ($S = 0.94$) at 68° F, calculate h if the barometric pressure is 14.7 lb/in.^{2}

60. Calculate the height of the column of a water barometer for an atmospheric pressure of 14.7 lb/in.^{2} if the water is at 50° F ($w = 62.42$ lb/ft^3); at 150° F ($w = 61.15$ lb/ft^3); at 212° F ($w = 59.83$ lb/ft^3).

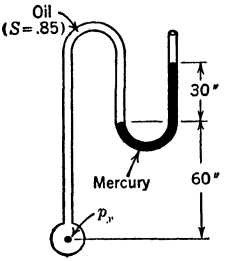
61. Barometric pressure is 29.43 in. of mercury. Calculate h.

62. Calculate the pressure p_x in Fig. 14*d* if $l = 30$ in., $h = 20$ in.; liquid w is water and w_1 mercury.

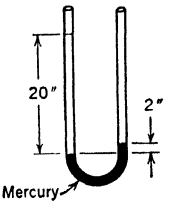
63. With the manometer reading as shown, calculate p_x.



PROBLEM 61.



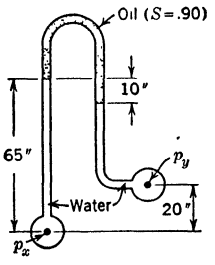
PROBLEM 63.



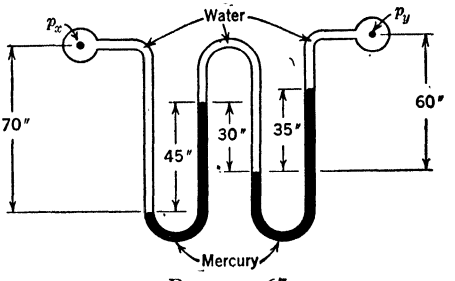
PROBLEM 64.

64. The specific gravity of the liquid in the left side of this open U-tube is unknown. Calculate it.

65. In Fig. 14*e*, $l_1 = 50$ in., $h = 20$ in., $l_2 = 30$ in., liquid w_1 is water, w_2 benzene, w_3 mercury. Calculate $p_x - p_y$.



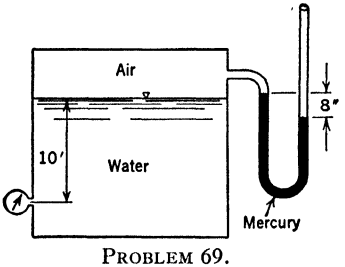
PROBLEM 66.



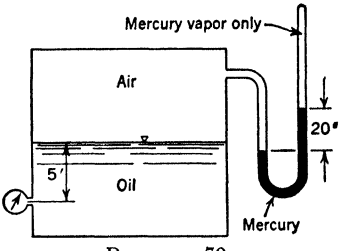
PROBLEM 67.

66. Calculate $p_x - p_y$ for this inverted U-tube manometer.

67. Two manometers as shown are connected in series. Calculate $p_x - p_y$.



PROBLEM 69.



PROBLEM 70.

68. An inclined gage having a tube of 1/8-in. bore laid on a slope of 1 : 20, and reservoir of 1-in. diameter, contains linseed oil. What distance will the oil move along the tube when a pressure of 1 in. of water is connected to the gage?

69. Calculate the gage reading.

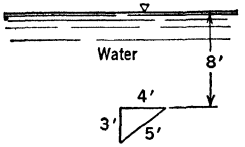
70. Calculate the gage reading. Specific gravity of oil is 0.85. Barometric pressure is 29.75 in. mercury.

71. A rectangular gate 6 ft long and 4 ft high lies in a vertical plane with its center 7 ft below a water surface. Calculate magnitude, direction, and location of the total force on the gate.

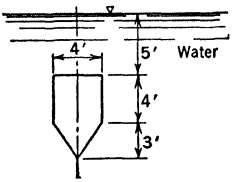
72. A circular gate 10 ft in diameter has its center 8 ft below a water surface and lies in a plane sloping at 60°. Calculate magnitude, direction, and location of total force on this gate.

73. A triangular area of 6-ft base and 5-ft altitude has its base horizontal and lies in a 45° plane with its apex 9 ft below a water surface. Calculate magnitude, direction, and location of total force on this area.

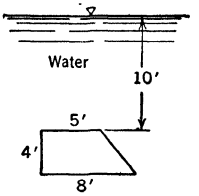
74. A square 9 ft by 9 ft lies in a vertical plane. Calculate the distance between



PROBLEM 75.



PROBLEM 76.



PROBLEM 77.

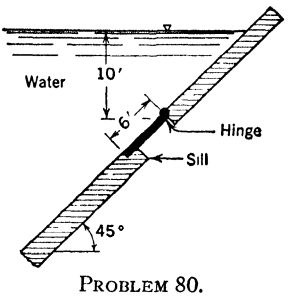
the center of pressure and the center of gravity, and the total force on the square, when its upper edge is (*a*) in the water surface and (*b*) 50 ft below the water surface.

75. Calculate the vertical and lateral location of the center of pressure of this triangle, which is located in a vertical plane.

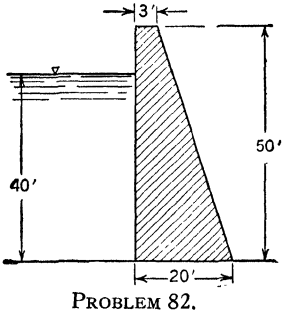
76. Calculate magnitude and location of the total force on this vertical plane area.

77. Calculate magnitude and location of the total force on this vertical plane area.

78. An 8 ft square gate lies in a vertical plane. If one diagonal of this gate is vertical and its center is 10 ft below a water surface, calculate magnitude, direction, and location of the total force on the gate.



PROBLEM 80.



PROBLEM 82.

79. A vertical rectangular gate 10 ft high and 6 ft wide has a depth of water on its upper edge of 15 ft. What is the location of a horizontal line which divides this area (*a*) so that the forces on the upper and lower portions are the same; (*b*) so that the moments of these forces about the line are the same?

80. This rectangular gate is hinged at the upper edge and is 4 ft wide. Calculate the total force on the sill, neglecting weight of the gate.

81. The center of pressure of an isosceles triangle of 9-ft altitude and 6-ft base, lying in a vertical plane, is at a depth of 12 ft. Calculate the depth of water over the apex of the triangle.

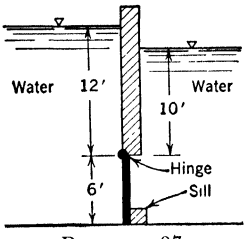
82. Is this concrete dam (w = 150 lb/ft^3) safe against overturning? Neglect uplift.

83. Water will rise behind a 10-ft concrete wall of rectangular cross section to a depth of 6 ft. How thick must the wall be to prevent overturning? w for concrete = 150 lb/ft^3.

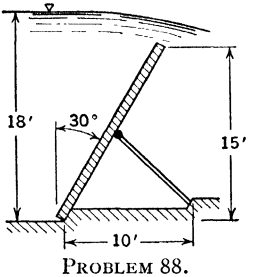
84. A sliding gate 10 ft wide and 5 ft high situated in a vertical plane has a coefficient of friction between itself and guides of 0.20. If the gate weighs 2 tons and if its upper edge is at a depth of 30 ft, what vertical force is required to raise it? Neglect buoyancy of the gate.

85. A butterfly valve, consisting essentially of a circular area pivoted on a horizontal axis through its center, is 7 ft in diameter and lies in a 60° plane with its center 10 ft below a water surface. What torque must be exerted on the valve's axis to just open it?

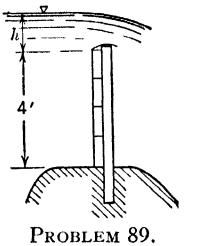
86. A rectangular tank 5 ft wide, 6 ft high, and 10 ft long contains water to a depth of 3 ft and oil (S = 0.85) on the water to a depth of 2 ft. Calculate magnitude and location of the force on one end of this tank.



PROBLEM 87.



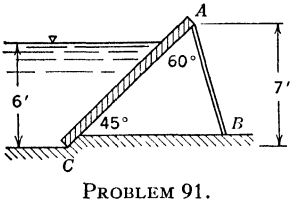
PROBLEM 88.



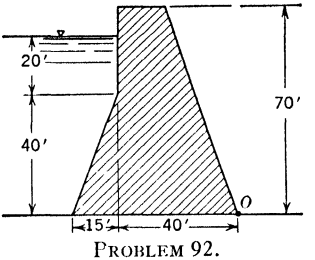
PROBLEM 89.

87. This 6 ft by 6 ft square gate is hinged at the upper edge. Calculate the total force on the sill.

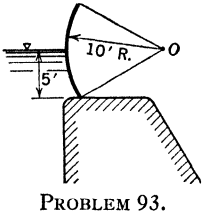
88. This wicket dam is 15 ft high and 4 ft wide and is pivoted at its center. Assume a hydrostatic pressure distribution, and calculate the vertical and horizontal reactions at the two sills. Neglect weight of the dam and consider all joints to be pin connected.



PROBLEM 91.



PROBLEM 92.



PROBLEM 93.

89. The flashboards on a spillway crest are 4 ft high and supported on steel posts spaced 2 ft on centers. The posts are designed to fail under a bending moment of 5000 ft-lb. What depth over the flashboards will cause the posts to fail? Assume hydrostatic pressure distribution.

90. Calculate the horizontal and vertical components of the force on a gate 4 ft square, located in a 60° plane, and having its upper edge 10 ft below a water surface.

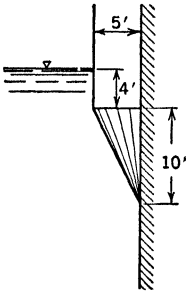
91. Using force components, calculate the load in the strut AB, if these struts have 5-ft spacing along the small dam AC. Consider all joints to be pin connected.

92. Calculate the magnitude, direction, and location of the total force on the upstream face of a section of this dam 1 ft wide. What is the moment of this force about O?

93. This tainter gate is pivoted at O and is 30 ft long. Calculate the horizontal and vertical components of force on the face of the gate.

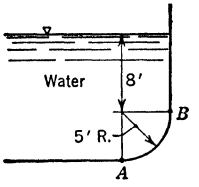
94. A concrete pedestal having the shape of the frustum of a right pyramid of lower base 4 ft square, upper base 2 ft square, and height 3 ft, is to be poured. Taking the specific weight of concrete as 150 lb/ft^3, calculate the vertical force of uplift on the forms.

95. A hemispherical shell 4 ft in diameter is connected to the vertical wall of a tank containing water. If the center of the shell is 6 ft below the water surface, what are the vertical and horizontal force components on the shell?

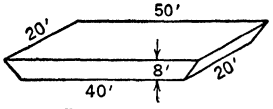


PROBLEM 96.

96. This half conical buttress is used to support a half cylindrical tower on the upstream face of a dam. Calculate the vertical and horizontal components of force exerted by the water on the buttress.



PROBLEM 97.



PROBLEM 103.

97. This rectangular tank 10 ft wide has a quarter cylinder AB joining its end and bottom. Calculate the magnitude, direction, and location of the total force on AB.

98. A 12-in.-diameter hole in a vertical wall between two water tanks is closed by an 18-in.-diameter sphere in the tank of higher water surface elevation. The difference in the water surface elevations in the two tanks is 5 ft. Calculate the force exerted by the water on the sphere. Neglect buoyancy.

99. A stone weighs 60 lb in air and 40 lb in water. Calculate its volume and specific gravity.

100. If the specific gravity of ice is 0.90, what percentage of the volume of an iceberg will remain above sea water ($S = 1.025$)?

101. Six cubic inches of lead ($S = 11.4$) are attached to the apex of a conical can, having an altitude of 12 in. and a base of 6-in. diameter, and weighing 1 lb. When placed in water, to what depth will the can be immersed?

102. A cylindrical can 3 in. in diameter and 7 in. high weighing 4 oz contains water to a depth of 3 in. When this can is placed in water, how deep will it sink?

103. The barge shown weighs 40 tons and carries a cargo of 40 tons. Calculate its draft in fresh water.

104. A barge having water line area of 2000 ft^2 sinks 2 in. when a certain load is added. Calculate the load.

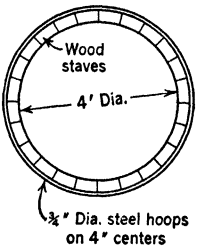
105. A balloon having a total weight of 800 lb contains 15,000 ft^3 of hydrogen. How many pounds of ballast are necessary to keep the balloon on the ground? Barometric pressure = 14.7 lb/in.^{2} Temperature of air and hydrogen, 60° F. Pressure of the hydrogen is the same as that of the atmosphere.

106. A concrete (w = 150 lb/ft^3) slab 2 ft thick and 10 ft square is dragged on rollers up a 30° incline under water, by a force exerted parallel to the incline. Calculate this force if the coefficient of friction between slab and incline may be taken as 0.05.

107. Calculate the tension stress in the $\frac{1}{2}$-in. wall of a 24-in. steel pipe containing fluid under a pressure of 100 lb/in.^{2}

108. What is the minimum thickness allowable for a 5-ft-diameter steel pipe line to carry a fluid at a pressure of 150 lb/in.^{2}? Take allowable tension stress for steel to be 16,000 lb/in.^{2}

109. This wood stave pipe line is to withstand a pressure of 50 lb/in.^{2} Calculate the stress developed in the steel hoops.

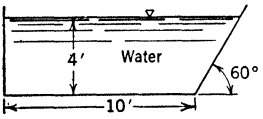


110. A 5-ft-diameter wood stave pipe line is to carry water under a 60-ft head. If allowable steel stress is taken as 16,000 lb/in.^{2}, what spacing of $\frac{3}{4}$-in.-diameter steel hoops will be necessary?

111. A concrete water tank 60 ft high and 20 ft in diameter is reinforced with 1-in.-diameter steel hoops spaced 3 in. on centers. When the tank contains water 50 ft deep, what is the stress in the hoops, assuming that the concrete takes no tension?

112. An open cylindrical container containing 1.0 cu ft of water at a depth of 2 ft is accelerated vertically upward at 20 ft/sec.^{2} Calculate the pressure and total force on the bottom of the container. Calculate this total force by application of Newton's law.

113. The container of the preceding problem is accelerated vertically downward at 20 ft/sec.^{2} Calculate pressure and total force on the bottom of the container.



PROBLEM 114.

114. Calculate the total forces on the ends and bottom of this container when at rest and when being accelerated upward at 10 ft/sec.^{2} Container is 5 ft wide.

115. A closed tank 10 ft high is filled with water, and the pressure at the top of the tank raised to 30 lb/in.^{2} Calculate the pressure at top and bottom of this tank when accelerated vertically downward at 15 ft/sec.^{2}

116. An open conical container 6 ft high is filled with water and moves vertically downward with a deceleration of 10 ft/sec.^{2} Calculate the pressure at the bottom of the container.

117. A rectangular tank 5 ft wide, 10 ft long, and 6 ft deep contains water to a depth of 4 ft. When it is accelerated horizontally at 10 ft/sec.^{2} in the direction of its length, calculate the depth of water at each end of the tank and the total force on each end of the tank. Check the difference between these forces by calculating the inertia force of the accelerated mass.

118. When the tank of the preceding problem is accelerated at 15 ft/sec^2 how much water is spilled? Calculate the forces on the ends of the tank, and check as indicated above.

119. The above tank is accelerated at 20 ft/sec^2. Calculate the water spilled and the forces on the ends, and check as indicated above.

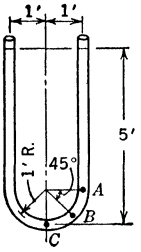
120. The tank of problem 117 contains water to a depth of 2.0 ft and is accelerated horizontally to the right at 15 ft/sec^2. Calculate the depth at the left end of the tank.

121. A closed rectangular tank 4 ft high, 8 ft long, and 5 ft wide is filled with water, and the pressure at the top raised to 20 lb/in.^{2} Calculate the pressures in the corners of this tank when it is accelerated horizontally along the direction of its length at 15 ft/sec^2. Calculate the forces on the ends of the tank, and check their difference by Newton's law.

122. The tank of the preceding problem is $\frac{3}{4}$ full of water, and the pressure in the air space above the water is 20 lb/in.^{2} Calculate the pressures and forces, and check as indicated above for the same acceleration.

123. An open container of liquid accelerates down a 30° inclined plane at 15 ft/sec^2. What is the slope of its free surface?

124. An open container of liquid accelerates up a 30° inclined plane at 10 ft/sec^2. What is the slope of its free surface?



125. When this U-tube containing water is accelerated horizontally to the right at 10 ft/sec^2, what are the pressures at A, B, and C?

126. An open cylindrical tank 3 ft in diameter and 5 ft deep is filled with water and rotated about its axis at 100 rpm. How much liquid is spilled? What are the pressures at the center of the bottom of the tank and at a point on the bottom 1 ft from the center?

127. The above tank contains water to a depth of 3 ft. What will be the depth at the wall of the tank when rotated at 60 rpm?

128. The above tank contains water to a depth of 4 ft and is rotated at 100 rpm. How much water is spilled?

129. The above tank contains water to a depth of 1 ft. At what speed must it be rotated to uncover a bottom area 1 ft in diameter?

130. The above tank is filled with water and closed, the pressure at its top is raised to 20 lb/in.^{2}, and the tank is rotated at 200 rpm. Calculate the pressure on the axis and at the wall on the top and bottom of the tank. If the tank is of steel (allowable tension stress 16,000 lb/in.^{2}) how thick must its walls be?

131. A tube 2 in. in diameter and 4 ft long is filled with water and closed. It is then rotated at 150 rpm in a horizontal plane about one end as a pivot. Calculate the pressure on the outer end of the tube using the equation in the text, and check by calculating the centrifugal force of the rotating mass.

132. The pressure at a point 12 in. from the axis of rotation in a closed filled vessel of mercury is 100 lb/in.^{2} before rotation starts. What will this pressure become when the vessel is rotated at 500 rpm?

133. The impeller of a closed filled centrifugal water pump is rotated at 1750 rpm. If the impeller is 2 ft in diameter, what pressure is developed by rotation?

134. When the U-tube of problem 125 is rotated at 200 rpm about its central axis, what are the pressures at A, B, and C?

CHAPTER III

THE FLOW OF AN IDEAL FLUID

An insight into the basic laws of fluid flow can best be obtained from a study of the flow of a hypothetical "ideal fluid." An ideal or "perfect" fluid is a fluid assumed to have no viscosity. In such a fluid, therefore, there can be no frictional effects between moving fluid layers or between these layers and boundary walls, and, thus, no cause for eddy formation or energy loss due to friction and turbulence. The assumption of an ideal fluid allows a fluid to be treated as an aggregation of small spheres which will support pressure forces normal to their surfaces, but will slide over one another without resistance. Thus, the motion of these ideal fluid particles becomes analogous to the motion of a solid body on a resistanceless plane, and leads to the

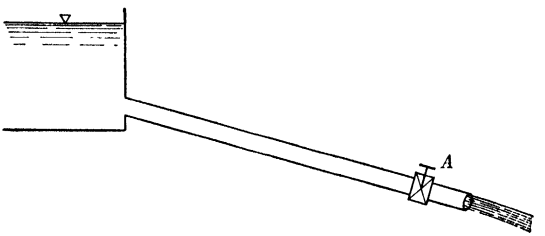


FIG. 27.

conclusion that unbalanced forces existing on particles of an ideal fluid will result in the acceleration of these particles according to Newton's law.

By assuming an ideal fluid, simple equations can be derived based on familiar physical concepts. Later these equations must be modified to suit the flow of real fluids after an understanding of the mechanics of fluid friction is obtained.

16. Definitions. Fluid flow may be *steady* or *unsteady*. Steady flow occurs in a system when none of the variables involved changes with time; if any variable changes with time, the condition of unsteady flow exists. In the pipe of Fig. 27, leading from a large reservoir of fixed surface elevation, unsteady flow exists *while* the valve

A is being adjusted; with the valve opening fixed, steady flow occurs. The problems of steady flow are more elementary than those of unsteady flow and have more general engineering application; therefore, the latter will be omitted from subsequent treatment, with the exception of certain simple principles and examples.

If the paths of ideal fluid particles in steady flow are traced, the result is a series of smooth curves, called "streamlines," and the sketching of such streamlines results in a "streamline picture." In an unsteady flow the picture changes from instant to instant, but smooth curves may be drawn in the flow indicating the instantaneous directions

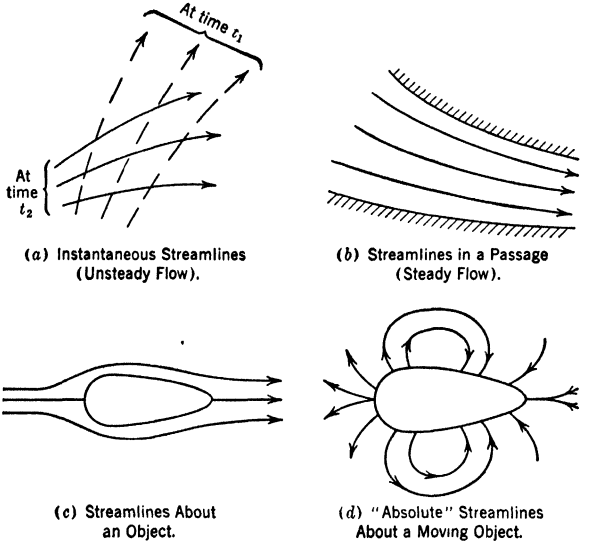


FIG. 28.

of fluid particles; such curves are called "instantaneous streamlines" (Fig. 28*a*).

Streamlines may be relative or absolute, depending upon the motion of the observer. Figures 28*b* and *c* illustrate relative streamlines in a steady flow through a passage and about an object as seen by an observer fixed to the passage or object. Such a streamline picture will remain the same to the observer (1) if the fluid flows through the passage (or about the object) or (2) the passage or object moves in the opposite direction through fluid at rest. Fixed at a point in the fluid as the object passes, the observer sees an unsteady flow picture on which he may note the paths of individual fluid particles. However, an instantaneous observation of fluid motion as the object passes

results in the streamline picture of Fig. 28*d*. The lines occurring thereon are sometimes termed "absolute" streamlines, and move with the moving object.

Generally, streamline pictures are of more qualitative than quantitative value to the engineer; they allow him to visualize fluid flows and (as will be seen directly) to locate regions of high and low velocity, and of high and low pressure.

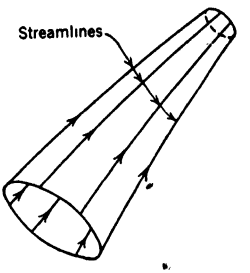


FIG. 29.

When streamlines are drawn through a closed curve in a steady flow, these streamlines form boundaries across which the fluid particles cannot pass. Thus, the space between streamlines becomes a tube, called a "streamtube," and such a tube may be treated as if isolated from the remaining fluid (Fig. 29).

The velocity of a particle moving along a streamline in a fluid flow may be expressed by

$$v = \frac{dl}{dt}$$

in which (Fig. 30) dl is the distance covered by the particle in time dt.

If the velocity changes as the particle covers the distance dl, an acceleration, a, exists which is expressed by

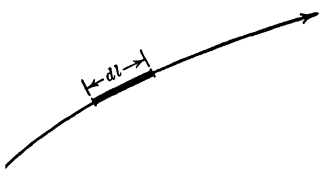


FIG. 30.

$$a = \frac{dv}{dt} = \frac{dl}{dt}\frac{dv}{dl} = v\frac{dv}{dl}$$

for steady motion. In unsteady flow, however, a change of velocity with respect to time occurs, not only because the particle moves from one point to another, but also because the whole flow picture is changing and *at any point* a change of velocity occurs with time. If this latter change of velocity with respect to time is designated by $\partial v/\partial t$, the total acceleration is given by

$$a = v\frac{dv}{dl} + \frac{\partial v}{\partial t} \tag{8}$$

in which the first term is called "convective" acceleration, and the second "local" acceleration. Obviously, local acceleration is a term peculiar to unsteady flow and vanishes from the above equation when it is applied to steady flow.

17. Equation of Continuity. The application of the principle of conservation of mass to fluid flow in a streamtube results in the "equation of continuity," expressing the continuity of the flow from point to point along the streamtube. If the cross-sectional areas and average velocities at sections 1 and 2 in the streamtube of Fig. 31 are designated by A_1, A_2, V_1 and V_2, respectively, the quantity of fluid passing section 1 per unit of time will be expressed by $A_1 V_1$, and the mass of fluid passing section 1 per unit of time will be $A_1 V_1 \rho_1$. Similarly, the mass of fluid passing section 2 will be $A_2 V_2 \rho_2$. Obviously, no fluid mass is being created or destroyed between sections 1 and 2, and therefore

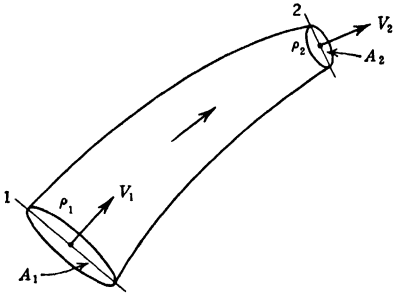


FIG. 31.

$$A_1 V_1 \rho_1 = A_2 V_2 \rho_2$$

Thus the mass of fluid passing any point in a streamtube per unit of time is the same.

If this equation is multiplied by g, the acceleration due to gravity, there results

$$A_1 V_1 w_1 = A_2 V_2 w_2 = G$$

giving the equation of continuity in terms of weight. The product, G, will be found to have dimensions of pounds per second and is termed the "weight rate of flow" or "weight flow." Its calculation will be necessary to express concisely the rate of flow of gases, whose densities may vary during the flow process.

For liquids, and for gases when pressure and temperature changes are negligible, $w_1 = w_2$, resulting in

$$A_1 V_1 = A_2 V_2 = Q$$

indicating that for fluids of constant density the product of cross-sectional area and velocity at any point in a streamtube will be the same. This product Q, is designated as the "rate of flow" or "flow" and will have dimensions of cubic feet per second.

The fact that the product $A\,V$ remains constant along a streamtube allows partial interpretation of the streamline picture. As the distance

between streamlines (A) increases, the velocity must decrease, hence the conclusion: Streamlines widely spaced indicate regions of low velocity; streamlines closely spaced indicate regions of high velocity.

Illustrative Problem

Twelve pounds per minute of air flow through a 6-in. diameter pipe line. If the gage pressure in the line is 30 lb/in.^{2} and the temperature 100° F, calculate the average velocity in the line if the barometric pressure is 15.0 lb/in.^{2}

$$G = \tfrac{12}{60} = 0.20 \text{ lb/sec}$$

$$W = \frac{(30 + 15)\,144}{53.3(100 + 460)} = 0.217 \text{lb}/\text{ft}^3$$

$$A = \frac{\pi}{4}\left(\frac{6}{12}\right)^2 = 0.196 \text{ ft}^2$$

$$G = 0.20 = AwV = 0.196 \times 0.217 \times V$$

$$V = 4.70 \text{ ft/sec}$$

18. Euler's Equation. By applying Newton's law to the motion of fluid masses, Leonhard Euler (1750) laid the groundwork for the study of the dynamics of ideal fluids. Although Euler's original equations were entirely general and written in terms of the components of force and acceleration along the three axes, the mathematics may be simplified considerably by writing the equation in the direction of motion, that is, along a streamtube.

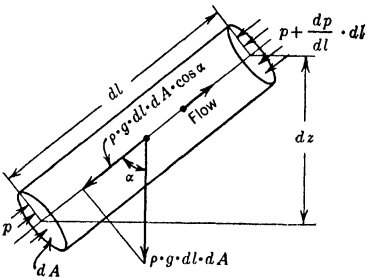


FIG. 32.

Consider a differentially small section of streamtube having the dimensions shown in Fig. 32. The forces tending to accelerate the fluid mass contained therein are: (1) the component of weight in the direction of motion, and (2) the forces on the ends of the element in the direction of motion due to pressure. Assuming that motion is in an upward direction and that pressure and velocity increase in this direction, the force dF_W in the direction of motion due to the weight of the element is given by

$$dF_W = -\rho g\, dl\, dA \cos\alpha = -\rho g\, dl\, dA \frac{dz}{dl}$$

The force dF_P, in the direction of motion, due to the pressure on the ends of the element, is

$$dF_P = p\,dA - \left(p + \frac{dp}{dl}\,dl\right)dA = -\frac{dp}{dl}\,dl\,dA$$

The mass dM of fluid being accelerated is

$$dM = \rho\,dl\,dA$$

and the total acceleration a (equation 8) is

$$a = v\frac{dv}{dl} + \frac{\partial v}{\partial t}$$

Substituting the above values in the Newtonian equation,

$$dF_W + dF_P = (dM)a$$

there results

$$-\rho g\,dl\,dA\frac{dz}{dl} - \frac{dp}{dl}\,dl\,dA = \rho\,dl\,dA\left(v\frac{dv}{dl} + \frac{\partial v}{\partial t}\right)$$

Dividing by $\rho\dfrac{dl}{dl}\,dA$ gives

$$\frac{dp}{\rho} + vdv + gdz + \frac{\partial v}{\partial t}\,dl = 0 \tag{9}$$

which is Euler's differential equation for unsteady fluid motion in a streamtube. For steady motion $\partial v/\partial t = 0$ and the Eulerian equation simplifies to

$$\frac{dp}{\rho} + vdv + gdz = 0 \tag{10}$$

the fundamental equation of steady fluid motion. By dividing this equation by g an alternate form of the equation is obtained

$$\frac{dp}{w} + \frac{vdv}{g} + dz = 0 \tag{10}$$

19. Bernoulli's Equation. Euler's equation may be integrated along the streamtube with the following result

$$\int\frac{dp}{\rho} + \int vdv + \int gdz = \text{Constant}$$

and if the fluid is a liquid, or a gas flowing with negligible change of density, the integrations may be carried out giving

$$\frac{p}{\rho} + \frac{V^2}{2} + gz = \text{Constant}$$

or, multiplying by ρ,

$$p + \rho \frac{V^2}{2} + \rho g z = \text{Constant} \tag{11}$$

or, dividing by w,

$$\frac{p}{w} + \frac{V^2}{2g} + z = \text{Constant} \tag{12}$$

The existence of these equations was first recognized by Bernoulli, and they were first presented in his *Hydrodynamica* (1738), a few years before the development of Euler's equations.

The Bernoulli equations impose another mathematical condition upon flow in a streamtube. It has already been shown that (for an incompressible fluid) the product of area and velocity is everywhere constant along a streamtube. Now from the Bernoulli equation it becomes evident that the sum of three terms involving pressure, velocity, and vertical elevation will also be a constant at every point along the streamtube.

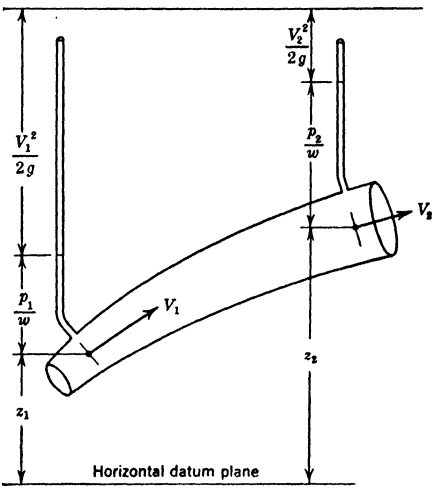


FIG. 33.

Writing equation 12 between two points on the typical streamtube of Fig. 33

$$\frac{p_1}{w} + \frac{V_1^2}{2g} + z_1 = \frac{p_2}{w} + \frac{V_2^2}{2g} + z_2 \tag{12a}$$

it becomes evident that the terms involved are linear distances, allowing a simple graphical interpretation of the equation. The terms p_1/w and p_2/w are the familiar "pressure heads" of fluid statics and may be represented by the piezometer columns; the terms z_1 and z_2, the "potential heads," are the vertical heights of sections 1 and 2 above a horizontal datum plane; the terms $V_1^2/2g$ and $V_2^2/2g$, the "velocity heads," represent the head due to motion of the fluid. The sum of these terms is the same at all points in the streamtube and is equal to the vertical distance between the upper and lower parallel lines. The Bernoulli terms in equation 12 thus are seen to have the dimensions of feet, or,

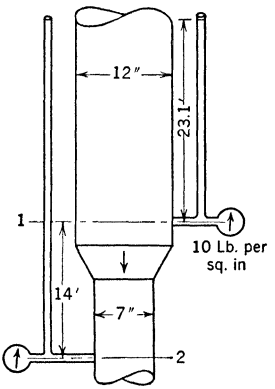
more rigorously, "feet of the fluid flowing," since w, the specific weight of the flowing fluid, appears in one of the terms. The Bernoulli terms in equation 11 will have the dimensions of pressure (pounds per square foot) and are designated respectively as "pressure" or "static pressure," "velocity pressure," and "potential pressure."

Bernoulli's equation gives further aid in the interpretation of streamline pictures, equations 11 and 12 indicating that, when velocity increases, the sum of pressure and potential head must decrease. In the usual streamline picture, the potential head varies little, allowing the general statement: where velocity is high pressure is low. Regions of closely spaced streamlines have been shown to indicate regions of high velocity, and now from the Bernoulli equation these are seen also to be regions of low pressure.

Illustrative Problem

Ten cubic feet of water flow per second downward through this pipe line. When the upper pressure gage reads 10 lb/in.^{2}, calculate the reading of the lower gage and the height to which water will rise in the open piezometer tubes.

$$V_1 = \frac{10.0}{\frac{\pi}{4}\left(\frac{12}{12}\right)^2} = 12.7 \text{ ft/sec}, \quad V_2 = \left(\frac{12}{7}\right)^2 V_1 = 37.5 \text{ ft/sec}$$



Taking datum plane at section 2 and using Bernoulli equation,

$$\frac{p_1}{w} + \frac{V_1^2}{2g} + z_1 = \frac{p_2}{w} + \frac{V_2^2}{2g} + z_2$$

$$\frac{10 \times 144}{62.4} + \frac{(12.7)^2}{2g} + 14 = \frac{p_2}{w} + \frac{(37.5)^2}{2g} + 0$$

$$23.1 + 2.5 + 14 = \frac{p_2}{w} + 21.8 + 0$$

$$\frac{p_2}{w} = 17.8 \text{ ft}, \quad p_2 = \frac{17.8 \times 62.4}{144} = 7.70 \text{ lb/in.}^2$$

Height of column 1 = 23.1 ft
Height of column 2 = 17.8 ft.

At this point it should be noted that with increase of velocity or potential head the pressure within a flowing fluid can drop no farther than to the absolute zero of pressure, thus placing a restriction upon the Bernoulli equation. Such a condition is not possible in gases, however, owing to their expansion with reduction in pressure, but

frequently assumes great importance in the flow of liquids. In liquids the absolute pressure can drop only to the vapor pressure of the liquid, whereupon vaporization takes place and "cavitation"[1] may occur, with accompanying vibration, destructive action, and other deleterious effects.

Before the time of Bernoulli, Torricelli (1643) discovered that the velocity of efflux, V, of a fluid from an orifice under a head h was given theoretically by

$$V = \sqrt{2gh}$$

the velocity being equal to that attained by a solid body falling from rest through a height h. Torricelli's theorem is now recognized as a special case of Bernoulli's theorem involving certain assumptions and conditions which continually appear in engineering problems. The above equation may be derived from Bernoulli's equation by considering steady flow through the reservoir and orifice of Fig. 34. Taking section 1 at the free reservoir surface, section 2 in the jet immediately outside of the orifice, and the datum plane at the center of the orifice, Bernoulli's equation may be written as

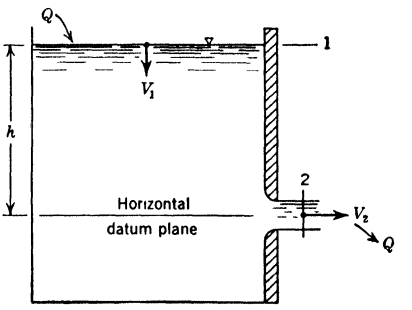


FIG. 34.

$$\frac{p_1}{w} + \frac{V_1^2}{2g} + z_1 = \frac{p_2}{w} + \frac{V_2^2}{2g} + z_2$$

But, since the tank is very large compared to the orifice, V_1 will be very small and when squared usually becomes negligible. The pressure on the reservoir surface, p_1, is atmospheric and may be taken as zero. Atmospheric pressure surrounds the free jet, and thus the pressure in the jet at section 2 will be zero. Obviously, $z_1 = H$ and $z_2 = 0$; therefore, the Bernoulli equation becomes

$$0 + 0 + h = 0 + \frac{V_2^2}{2g} + 0$$

giving

$$V_2 = \sqrt{2gh}$$

as demonstrated by Torricelli.

[1] For a description of the cavitation phenomenon see Appendix V.

Another useful special application of the Bernoulli principle is to the streamtube which approaches and remains adjacent to a solid body placed in a flowing fluid (Fig. 35). Let this streamtube have an infinitesimal cross section and be represented by the streamline AB. Because of the interference of the body, the fluid particles moving on the streamline AB will decelerate as they approach the body and will

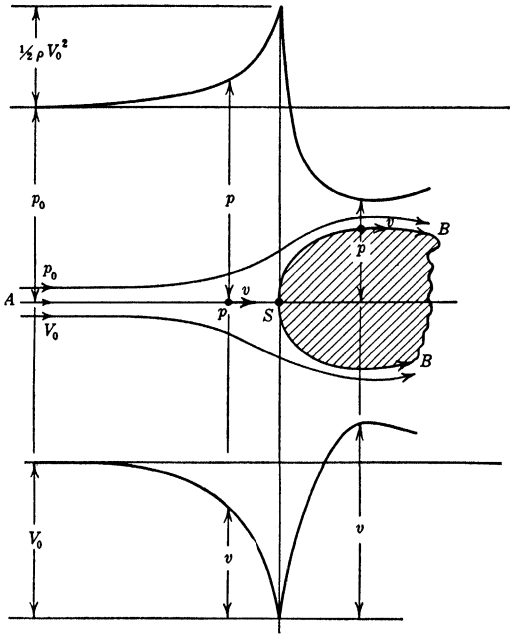


FIG. 35.

temporarily come to rest at the point S, called the stagnation point; they then will move around the contour of the body with a variation in velocity approximately as shown on the figure. From Bernoulli's equation 11 the pressure variation with these velocity changes will be about as shown, and the pressure at the stagnation point, the "stagnation pressure," p_s, may be calculated from

$$p_s + \tfrac{1}{2}\rho V_s^2 = p_o + \tfrac{1}{2}\rho V_o^2$$

p_o and V_o being respectively the pressure and velocity in the undisturbed fluid ahead of the solid body. In this equation $V_s = 0$; therefore

$$p_s = p_o + \tfrac{1}{2}\rho V_o^2 \qquad (13)$$

allowing the pressure developed on the front of objects in a flowing fluid to be readily calculated.

Illustrative Problem

A submarine moves through salt water at a depth of 50 ft and at a speed of 15 mph. Calculate the pressure on the nose of the submarine.

$$p_s = p_o + \tfrac{1}{2}\rho V_o^2$$

$$p_s = 50 \times 64.0 + \frac{1}{2}\frac{64.0}{32.2}\left(\frac{15 \times 5280}{3600}\right)^2$$

$$p_s = 3200 + 480 = 3680 \text{ lb/ft}^2 = 25.6 \text{ lb/in.}^2$$

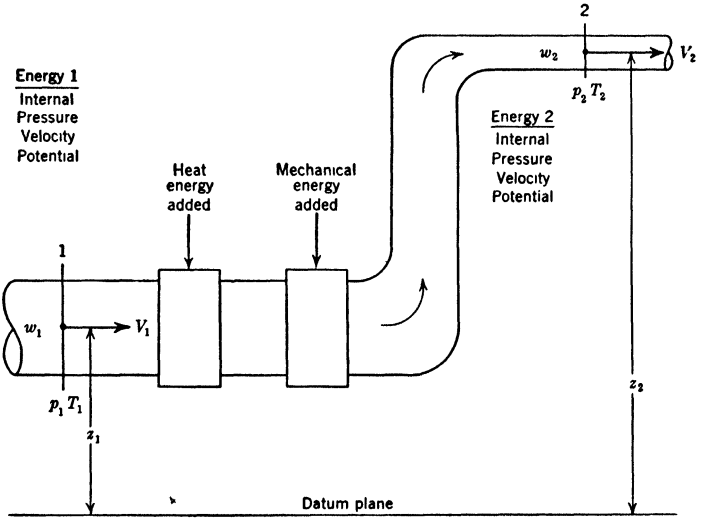


FIG. 36.

20. Energy Relationships. The principles of dynamics and of conservation of mass having been applied to fluid flow in a streamtube, application of the principle of energy conservation is in order.

Figure 36 illustrates, in a qualitative manner, the various types of energy involved in fluid flow and allows the following general energy equation to be written

$$\left\{\begin{matrix}\text{Energy in}\\ \text{fluid at}\\ \text{section 1}\end{matrix}\right\} + \left\{\begin{matrix}\text{Energy added to}\\ \text{fluid between sec-}\\ \text{tions 1 and 2}\end{matrix}\right\} = \left\{\begin{matrix}\text{Energy in}\\ \text{fluid at}\\ \text{section 2}\end{matrix}\right\}$$

The energy which a flowing fluid possesses is composed of four types: internal energy, due to molecular agitation and manifested by tem-

perature; and the energies due to the pressure, velocity, and height of the fluid above datum. Heat energy may be added to or subtracted from a flowing fluid through the walls of the tube, or mechanical energy may be added to or subtracted from the fluid by a pump or turbine. Thus the above equation may be written

$$\left\{\begin{array}{l}\text{Internal energy}\\ +\text{Pressure energy}\\ +\text{Velocity energy}\\ +\text{Potential energy}\end{array}\right\}_1 + \left\{\begin{array}{l}\text{Heat energy}\\ \text{and/or}\\ \text{Mechanical}\\ \text{energy added}\end{array}\right\}_{1\text{-}2} = \left\{\begin{array}{l}\text{Internal energy}\\ +\text{Pressure energy}\\ +\text{Velocity energy}\\ +\text{Potential energy}\end{array}\right\}_2$$

all the energies of which must now be obtained in terms of the variables involved in the flow process. It is most advantageous to write this equation, not in terms of the total energies supplied to or existing in the flowing fluid, but rather in terms of the energies existing in or supplied to a single typical pound of the fluid. Thus, the energies of the equation will have the dimensions of foot-pounds per pound (ft-lb/lb) of the fluid flowing.

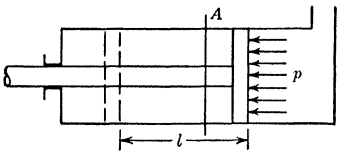


FIG. 37.

Let the internal energy contained in a pound of fluid be I ft-lb. The kinetic energy of a pound of fluid moving with velocity V may be calculated from $MV^2/2$, in which $M = 1/g$, indicating the kinetic energy to be $V^2/2g$ ft-lb/lb. The potential energy of a weight, W, at a height, z, above a plane is given by Wz; therefore, the potential energy of 1 lb of fluid, z ft above the datum, will be z ft-lb.

The pressure energy contained in a pound of fluid may be calculated from the work that may be done by this pressure. If a quantity of fluid at a pressure p is admitted to the cylinder of Fig. 37, the force exerted on the piston is pA; the work done as the piston moves a distance l is pAl; and the weight of fluid which does this work is wAl. Therefore, the pressure energy of, or work done by, a pound of fluid is

$$\frac{pAl}{wAl} = \frac{p}{w} \text{ ft-lb}$$

If the heat energy, in British thermal units, added to a pound of fluid is designated by E_H, its equivalent in foot-pounds will be $778\,E_H$, since 778 ft-lb are equivalent to 1 Btu. Finally, the mechanical energy added to a pound of fluid being designated by E_M ft-lb/lb, the general energy equation becomes

$$I_1 + \frac{p_1}{w_1} + \frac{V_1^2}{2g} + z_1 + 778E_H + E_M = I_2 + \frac{p_2}{w_2} + \frac{V_2^2}{2g} + z_2 \cdot \quad (14)$$

Since this general energy equation is the basis for the solution of the majority of engineering problems on fluid flow, its application to certain important special cases must be examined.

If the temperature of the fluid is nearly equal to that of the surroundings, the heat added to or given off by the fluid is usually negligible. With negligible changes in temperature and density there is negligible change in internal energy. If the fluid passes through no pump or motor, E_M will vanish from the equation. For these special conditions, then, $I_1 = I_2$, $E_H = 0$, $E_M = 0$, $w_1 = w_2 = w$, the general energy equation reduces to the familiar Bernoulli equation,

$$\frac{p_1}{w} + \frac{V_1^2}{2g} + z_1 = \frac{p_2}{w} + \frac{V_2^2}{2g} + z_2$$

Thus, this form of the Bernoulli equation is seen to be an equation of energy as well as an equation of linear distances, a fact which is further confirmed by the equivalence of the dimensions of the unit energy, foot-pounds per pound, and of length, feet.

When a gas or vapor is the fluid flowing, the general energy equation is written

$$778H_1 + \frac{V_1^2}{2g} + z_1 + 778E_H + E_M = 778H_2 + \frac{V_2^2}{2g} + z_2$$

in which

$$778H_1 = I_1 + \frac{p_1}{w_1}$$

$$778H_2 = I_2 + \frac{p_2}{w_2}$$

the term H being called the "total heat content" or the "enthalpy" of the gas or vapor. In problems of gas or vapor flow the difference $z_1 - z_2$ is usually negligible compared to the other terms of the general energy equation. Frequently the flow process is an adiabatic one, occurring so rapidly that no heat energy, E_H, is lost or gained. With no pump or motor involved in the problem, the equation for the adiabatic flow of gases and vapors becomes

$$\frac{V_2^2}{2g} - \frac{V_1^2}{2g} = 778(H_1 - H_2) \tag{15}$$

a familiar flow equation of thermodynamics. In vapor-flow problems H_1 and H_2 are obtained in Btu/lb from tables or diagrams, and since

the equation applies to an adiabatic process conditions 1 and 2 must have the same entropy.

For a perfect gas, thermodynamics shows that

$$778(H_1 - H_2) = \frac{p_1^{\frac{1}{k}}}{w_1} \frac{k}{k-1} \left[p_1^{\frac{k-1}{k}} - p_2^{\frac{k-1}{k}} \right]$$

thus for the adiabatic flow of a perfect gas equation 15 becomes

$$\frac{V_2^2}{2g} - \frac{V_1^2}{2g} = \frac{p_1^{\frac{1}{k}}}{w_1} \frac{k}{k-1} \left[p_1^{\frac{k-1}{k}} - p_2^{\frac{k-1}{k}} \right] \tag{16}$$

This equation may also be obtained directly from Euler's equation

$$\frac{dp}{w} + vdv + dZ = 0 \tag{10}$$

by the assumption of an adiabatic process in Fig. 32. Neglecting the third term of the equation and integrating

$$\int_{p_2}^{p_1} \frac{dp}{w} + \int_{V_2}^{V_1} \frac{vdv}{g} = 0$$

gives

$$\frac{V_2^2}{2g} - \frac{V_1^2}{2g} = \int_{p_2}^{p_1} \frac{dp}{w}$$

and the right-hand side of the equation may be evaluated by the insertion of the adiabatic relation of p and w

$$\frac{p}{w^k} = \frac{p_1}{w_1{}^k}$$

The result is

$$\frac{V_2^2}{2g} - \frac{V_1^2}{2g} = \frac{p_1^{\frac{1}{k}}}{w_1} \frac{k}{k-1} \left[p_1^{\frac{k-1}{k}} - p_2^{\frac{k-1}{k}} \right] \tag{16}$$

as before.

The calculation of the power P of a machine which supplies a unit energy E_M to a flowing fluid is an important engineering problem and may be accomplished readily as follows: The number of pounds of fluid flowing per second will be given by G or Qw, and the energy in foot-pounds given to every pound of the flowing fluid is E_M. Obviously then

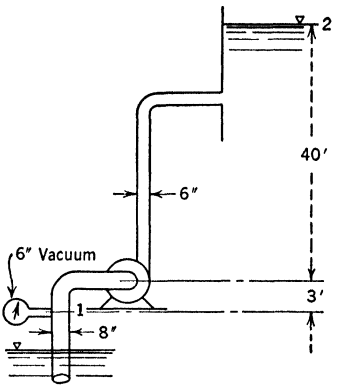
$$P = GE_M = QwE_M \tag{17}$$

therefore

$$\text{Horsepower of machine} = \frac{P}{550} = \frac{GE_M}{550} = \frac{QwE_M}{550} \tag{18}$$

ILLUSTRATIVE PROBLEM

How many horsepower must theoretically be supplied to this pump to maintain a flow of 2.0 cfs under the given pressure conditions? Consider flow from point 1 to point 2, taking datum plane through point 1.



$$p_1 = -\frac{6}{29.92} \times 14.7 \times 144 = -425 \text{ lb/ft}^2$$

$$V_1 = \frac{2.0}{\frac{\pi}{4} \times \left(\frac{8}{12}\right)^2} = 5.72 \text{ ft/sec}$$

$$z_1 = 0, \quad z_2 = 43 \text{ ft}, \quad p_2 = 0, \quad V_2 = 0$$

$$E_1 = \frac{p_1}{w} + \frac{V_1^2}{2g} + z_1 = -\frac{425}{62.4} + \frac{(5.72)^2}{2g} + 0 = -6.3 \text{ ft}$$

$$E_2 = \frac{p_2}{w} + \frac{V_2^2}{2g} + z_2 = 0 + 0 + 43 = 43.0 \text{ ft}$$

$$E_P = E_2 - E_1 = 43 - (-6.3) = 49.3 \text{ ft (ft-lb/lb)}$$

$$\text{Pump horsepower} = \frac{QwE_P}{550} = \frac{2.0 \times 62.4 \times 49.3}{550} = 11.2 \text{ hp}$$

21. Flow of an Incompressible Fluid. A constriction in a stream-tube or pipe line is frequently used as a device for metering fluid flow. Simultaneous application of the continuity and Bernoulli principles to such a constriction will allow direct calculation of the rate of flow when certain variables are measured. To develop these relationships for an incompressible fluid, consider the general type of constriction illustrated in Fig. 38 and write the continuity and Bernoulli equations between sections 1 and 2. For an incompressible fluid, temperature

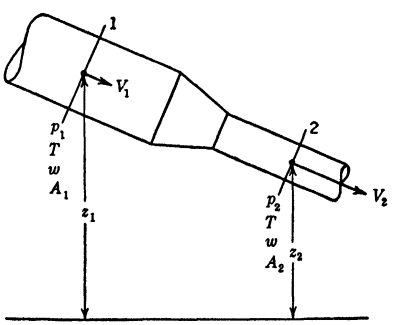


FIG. 38.

and density will not vary appreciably as the pressure changes from p_1 to p_2. Thus the simultaneous equations become

$$\begin{cases} Q = A_1 V_1 = A_2 V_2 \\ \dfrac{p_1}{w} + \dfrac{V_1^2}{2g} + z_1 = \dfrac{p_2}{w} + \dfrac{V_2^2}{2g} + z_2 \end{cases}$$

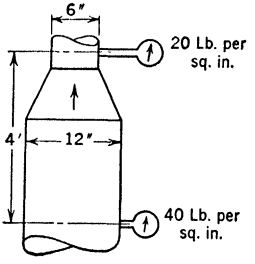
which may be solved for Q by substituting

$$V_1 = \frac{Q}{A_1} \quad \text{and} \quad V_2 = \frac{Q}{A_2}$$

in the second equation, resulting in

$$Q = \frac{A_2}{\sqrt{1 - \left(\dfrac{A_2}{A_1}\right)^2}} \sqrt{2g\left(\frac{p_1}{w} + z_1 - \frac{p_2}{w} - z_2\right)} \tag{19}$$

Thus is becomes evident that the quantity of flow through a constriction in a streamtube (1) is dependent upon the difference of the sums of pressure and potential heads at points 1 and 2 and (2) varies with the square root of this difference.



ILLUSTRATIVE PROBLEM

Calculate rate of flow of water through this pipe line when the gages read as shown.

$$Q = \frac{\dfrac{\pi}{4} \times \left(\dfrac{6}{12}\right)^2}{\sqrt{1 - \left(\dfrac{6}{12}\right)^4}} \sqrt{2g\left[\frac{40 \times 144}{62.4} + 0 - \frac{20 \times 144}{62.4} - 4\right]}$$

$$Q = 10.6 \text{ cfs}$$

22. Flow of a Compressible Fluid. When a compressible fluid, such as a vapor or gas, flows through a constriction (Fig. 39) in a streamtube, large changes in density and temperature may occur as flow takes place. When the constriction is used as a metering device, it is usually short and

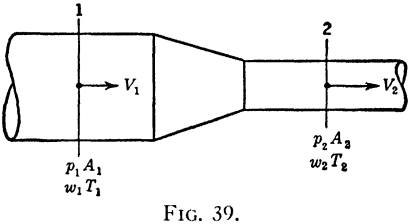


FIG. 39.

thus the expansion from pressure p_1 to pressure p_2 occurs rapidly enough to prevent loss or gain of heat by the fluid, and, therefore, the adiabatic flow equations 15 and 16 may be applied. The simultaneous equations (in which the pressures are absolute) become for a perfect gas

$$\begin{cases} G = A_1 V_1 w_1 = A_2 V_2 w_2 \\ \dfrac{V_2^2}{2g} - \dfrac{V_1^2}{2g} = \dfrac{p_1^{\frac{1}{k}}}{w_1} \dfrac{k}{k-1} \left[p_1^{\frac{k-1}{k}} - p_2^{\frac{k-1}{k}} \right] \end{cases}$$

and when $V_1 = G/A_1 w_1$ and $V_2 = G/A_2 w_2$, from the first equation, are substituted in the second there results

$$G = \frac{A_2 w_2}{\sqrt{1 - \left(\dfrac{w_2}{w_1}\right)^2 \left(\dfrac{A_2}{A_1}\right)^2}} \sqrt{\frac{2gk}{k-1} \frac{p_1^{\frac{1}{k}}}{w_1} \left[p_1^{\frac{k-1}{k}} - p_2^{\frac{k-1}{k}} \right]}$$

This equation may be improved for practical use, and for further analysis by the elimination of w_2 by substituting

$$\frac{w_2}{w_1} = \left(\frac{p_2}{p_1}\right)^{\frac{1}{k}} \quad \text{and} \quad w_2 = w_1 \left(\frac{p_2}{p_1}\right)^{\frac{1}{k}}$$

derived from the adiabatic equation, giving

$$G = \frac{A_2}{\sqrt{1 - \left(\dfrac{p_2}{p_1}\right)^{\frac{2}{k}} \left(\dfrac{A_2}{A_1}\right)^2}} \sqrt{\frac{2gk}{k-1} p_1 w_1 \left[\left(\frac{p_2}{p_1}\right)^{\frac{2}{k}} - \left(\frac{p_2}{p_1}\right)^{\frac{k+1}{k}} \right]} \quad (20)$$

an equation first derived by St. Venant (1839). The equation indicates that rate of flow of a compressible fluid is dependent upon pressure ratios and not upon pressure differences, as was the case for the incompressible fluid. It shows also that the rate of flow cannot be calculated from pressure measurements only, but that the temperature of the fluid at section 1 must be measured to obtain w_1. In most engineering applications of this equation A_2 is small compared to A_1 and thus the term

$$\sqrt{1 - \left(\frac{p_2}{p_1}\right)^{\frac{2}{k}} \left(\frac{A_2}{A_1}\right)^2}$$

may be taken to be unity and the simplified equation becomes

$$G = A_2 \sqrt{\frac{2gk}{k-1} p_1 w_1 \left[\left(\frac{p_2}{p_1}\right)^{\frac{2}{k}} - \left(\frac{p_2}{p_1}\right)^{\frac{k+1}{k}} \right]} \qquad (21)$$

Further investigation of this equation leads to an interesting and significant paradox: If $p_2 = 0$, it seems reasonable to expect flow to occur from section 1 to section 2, yet if $p_2 = 0$ is placed in the equation the weight flow, G, becomes zero also! This inconsistency means that some new factor has entered the problem; this new factor must now be examined.

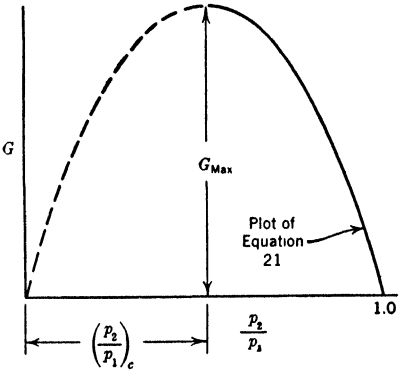


FIG. 40.

If equation 21 is plotted the curve of Fig. 40 results, indicating G be zero where the pressure ratio p_2/p_1 is either zero or unity, and having a maximum value, $G_{max.}$, at a certain "critical pressure ratio," $(p_2/p_1)_c$. The properties of this maximum point on the curve may be obtained by differentiating equation 21 in respect to p_2/p_1 and equating the result to zero. However, differentiation of the whole equation is unnecessary, since the only variables involved are

$$\left[\left(\frac{p_2}{p_1}\right)^{\frac{2}{k}} - \left(\frac{p_2}{p_1}\right)^{\frac{k+1}{k}} \right]$$

and the properties of the maximum point may be obtained from

$$\frac{d}{d\left(\frac{p_2}{p_1}\right)} \left[\left(\frac{p_2}{p_1}\right)^{\frac{2}{k}} - \left(\frac{p_2}{p_1}\right)^{\frac{k+1}{k}} \right] = 0$$

which, when differentiated and solved for p_2/p_1, now $(p_2/p_1)_c$, gives

$$\left(\frac{p_2}{p_1}\right)_c = \left(\frac{2}{k+1}\right)^{\frac{k}{k-1}}$$

showing that the critical pressure ratio is dependent only upon the adiabatic constant, k.

An equation for $G_{max.}$ may now be obtained by substituting this expression in equation 21 and multiplying by $w_2/\sqrt{w_2 w_2}$, giving

$$G_{max.} = w_2 A_2 \sqrt{\frac{2gk}{k-1}\frac{p_1}{w_2}\frac{w_1}{w_2}\left[\left(\frac{2}{k+1}\right)^{\frac{2}{k-1}} - \left(\frac{2}{k+1}\right)^{\frac{k+1}{k-1}}\right]}$$

but from the adiabatic relation between pressure, p, and specific weight, w, at critical pressure conditions

$$p_1 = p_2\left(\frac{2}{k+1}\right)^{-\frac{k}{k-1}}$$

$$\frac{w_1}{w_2} = \left(\frac{2}{k+1}\right)^{-\frac{1}{k-1}}$$

which may be substituted in the above equation, reducing it to

$$G_{max.} = A_2 w_2 \sqrt{\frac{gkp_2}{w_2}} = A_2 w_2 \sqrt{\frac{kp_2}{\rho_2}} \tag{22}$$

From the equation of continuity

$$G_{max.} = A_2 w_2 V_{2max.}$$

and by comparison of these two equations

$$V_{2\,max.} = \sqrt{\frac{kp_2}{\rho_2}}$$

or, in other words, when maximum flow takes place the velocity of flow at the constricted section equals the *acoustic velocity* (Art. 4), the velocity with which a pressure disturbance, such as sound, will travel in the fluid.

The significance of the fluid attaining the acoustic velocity at the constricted section and an explanation of the paradox mentioned above can best be obtained from a study of the flow under various pressure conditions through a constriction formed by a smooth nozzle (Fig. 41) installed in a pipe line. With $p_2 = p_1(A), p_2/p_1 = 1.0$, $p_2 = p_2'$, and no flow will occur. With p_2 less than $p_1(B)$, but with $1.0 > p_2/p_1 > (p_2/p_1)_c$, $p_2 = p_2'$, and flow will take place according to equation 21. As the maximum flow condition is reached, (C) $p_2/p_1 = (p_2/p_1)_c$ and $p_2 = p_2'$ and the velocity of flow from the nozzle equals the acoustic velocity as derived above. If now the pressure p_2,

surrounding the jet of fluid at the nozzle exit, is further lowered, (*D*) no further reduction in p_2', the pressure in the jet, occurs. A discontinuity of pressure then exists between the surrounding fluid and the interior of the jet—a discontinuity which is established and maintained by the acoustic velocity; the outside pressure tends to enter the jet with the velocity of sound, but since the fluid itself is moving with this velocity, the surrounding pressure cannot penetrate the jet. The

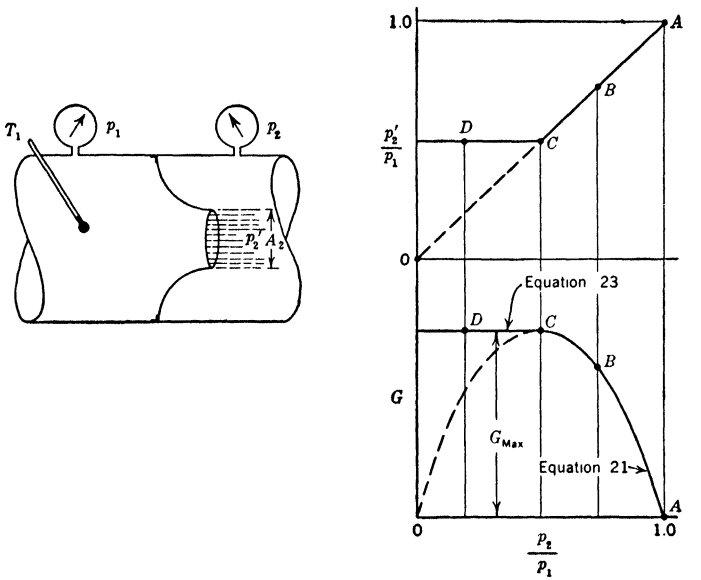


FIG. 41.

pressure in the jet is, therefore, fixed by conditions upstream from the constriction and remains equal to the critical pressure regardless of the magnitude of the surrounding pressure, p_2. With the pressure p_2' remaining constant no change in the flow will occur and thus the *maximum flow will exist for all pressure ratios below the critical.* These facts are shown graphically on Fig. 41, and may be summarized as follows. With

$$\frac{p_2}{p_1} < \left(\frac{p_2}{p_1}\right)_c, \; p_2 < p_c, \; p_2' = p_c, \; \frac{p_2'}{p_1} = \left(\frac{p_2}{p_1}\right)_c$$

In engineering practice it is customary to simplify calculations by designing constrictions so that flow will occur with pressure ratios below the critical. Equation 22 is not convenient for the calculation

of $G_{max.}$ since the temperature at section 2 is not in general measured. This equation may be transformed into

$$G_{max.} = A_2 \sqrt{gkp_1w_1\left(\frac{2}{k+1}\right)^{\frac{k+1}{k-1}}} \tag{23}$$

by the substitution of

$$p_2 = p_1\left(\frac{2}{k+1}\right)^{\frac{k}{k-1}} \quad \text{and} \quad w_2 = w_1\left(\frac{2}{k+1}\right)^{\frac{1}{k-1}}$$

Since $w_1 = p_1/RT_1$, equation 23 becomes

$$G_{max.} = A_2 \sqrt{\frac{gkp_1^2}{RT_1}\left(\frac{2}{k+1}\right)^{\frac{k+1}{k-1}}}$$

a simple equation for calculating flow under maximum conditions after pressure and temperature, p_1 and T_1, are measured. The equation may be further simplified, by collecting the constants, to

$$G_{max.} = \sqrt{\frac{gk}{R}\left(\frac{2}{k+1}\right)^{\frac{k+1}{k-1}}}\frac{A_2p_1}{\sqrt{T_1}} \tag{24}$$

or

$$G_{max.} = Z\frac{A_2p_1}{\sqrt{T_1}}$$

in which

$$Z = \sqrt{\frac{gk}{R}\left(\frac{2}{k+1}\right)^{\frac{k+1}{k-1}}}$$

and is obviously a characteristic constant of the gas, dependent only upon its physical constants, R and k, and upon acceleration due to gravity, g.

When a *vapor* flows through a constriction in a streamtube its behavior is similar to that of a perfect gas, the expansion being adiabatic if rapid and each vapor having a critical pressure ratio below which the conditions of maximum flow will be maintained. Unlike that of perfect gases the critical pressure ratio of a vapor will depend upon its thermodynamic conditions, steam, for example, having a critical pressure ratio of 0.58 when saturated and 0.55 when highly superheated.

The flow of a vapor under adiabatic conditions has been characterized by equation 15 and by the equation of continuity, thus

$$\begin{cases} \dfrac{V_2^2}{2g} - \dfrac{V_1^2}{2g} = 778(H_1 - H_2') \\ G = A_1 V_1 w_1 = A_2 V_2 w_2' \end{cases}$$

which may be solved simultaneously for G, giving

$$G = \frac{223.8 A_2 w_2'}{\sqrt{1 - \left(\dfrac{w_2'}{w_1}\right)^2 \left(\dfrac{A_2}{A_1}\right)^2}} \sqrt{H_1 - H_2'}$$

which simplifies to

$$G = 223.8 A_2 w_2' \sqrt{H_1 - H_2'} \tag{25}$$

if A_2/A_1 is small, which it usually is in engineering practice.

In applying equation 25 to the flow of a vapor through a nozzle installed in a pipe line (Fig. 42) a temperature-entropy or total heat-entropy diagram is used to find the values of H_1 and H_2'. With the

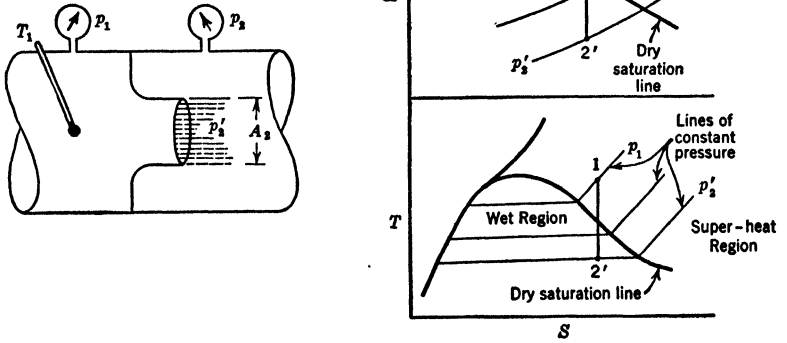


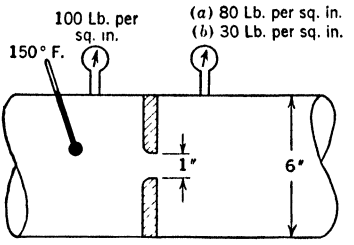
FIG. 42.

thermodynamic properties (pressure, temperature, quality) of the vapor known for section 1 of the streamtube, point 1 may be located on either diagram. Since the process is adiabatic a line of constant entropy (vertical) must be followed to a pressure, p_2', on the diagram, corresponding to section 2 of the streamtube. If the pressure

ratio is above the critical, $p_2' = p_2$; but if below the critical, $p_2' = (p_2/p_1)_c p_1$. With point 2′ established on either diagram the enthalpy, H_2', and the specific volume, v_2', may be obtained, allowing calculation of G, the weight flow.

Illustrative Problem

Calculate the rate of flow of carbon dioxide through this 1-in.-diameter orifice installed in a 6-in. pipe line when the downstream pressure gage reads (*a*) 80 lb/in.^{2}, (*b*) 30 lb/in.^{2} Barometric pressure is 15.0 lb/in.^{2}



$$\left(\frac{p_2}{p_1}\right)_c = \left(\frac{2}{1.30+1}\right)^{\frac{1.30}{1.30-1}} = 0.546$$

(*a*) $$\frac{p_2}{p_1} = \frac{80+15}{100+15} = 0.825$$

$$w_1 = \frac{115 \times 144}{34.9 \times (460+150)} = 0.783 \text{ lb/ft}^3$$

$$G = A_2\sqrt{\frac{2gk}{k-1}p_1 w_1\left[\left(\frac{p_2}{p_1}\right)^{\frac{2}{k}} - \left(\frac{p_2}{p_1}\right)^{\frac{k+1}{k}}\right]}$$

$$G = \frac{\pi}{4} \times \left(\frac{1}{12}\right)^2 \sqrt{\frac{64.4 \times 1.30}{1.30-1}(115 \times 144)0.783\ [(0.825)^{1.54} - (0.825)^{1.77}}$$

$$= 1.89 \text{ lb/sec}$$

(*b*) $$\frac{p_2}{p_1} = \frac{30+15}{100+15} = 0.391$$

$$G_{\max.} = \sqrt{\frac{gk}{R}\left(\frac{2}{k+1}\right)^{\frac{k+1}{k-1}}} \frac{A_2 p_1}{\sqrt{T_1}}$$

$$G_{\max.} = \sqrt{\frac{32.2 \times 1.3}{34.9}\left(\frac{2}{1.3+1}\right)^{7.67}} \frac{\frac{\pi}{4} \cdot \left(\frac{1}{12}\right)^2 115 \times 144}{\sqrt{460+150}} = 2.36 \text{ lb/sec}$$

23. Impulse-Momentum Relationships. The impulse-momentum law provides another useful tool for the solution of fluid flow problems. Its application to complex fluid flow processes sometimes allows circumvention of the complexities and gives a simple answer to problems which cannot be solved by the use of foregoing principles or more advanced energy considerations.

The impulse-momentum law applied to a particle (Fig. 43) is usually stated.

$$F\Delta t = \Delta(MV)$$

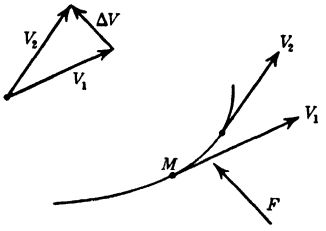


FIG. 43.

in which the product $F\Delta t$ is called the "impulse," the right-hand side of the equation being recognized as the change of momentum. For a particle whose mass, M, remains constant, the above equation may be written

$$F\Delta t = M\Delta V$$

and the impulse-momentum law may be stated: An external force, F, acting on a moving particle of mass M, for a time Δt, will change its velocity by an amount ΔV. Examination of the equation discloses the fact that Δt and M are scalar quantities, and F and ΔV are vector quan-

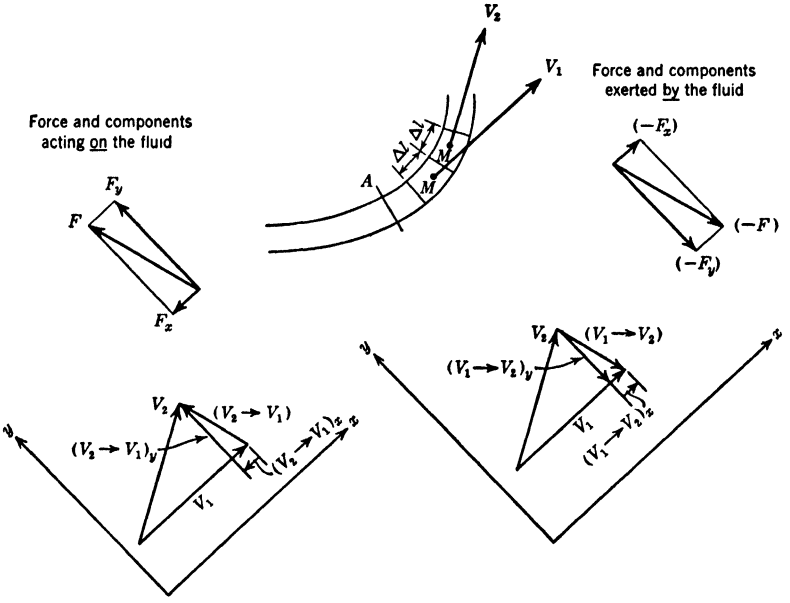


FIG. 44.

tities. Since these vector quantities are related by a simple algebraic equation their directions must be the same. Thus if the direction of ΔV can be obtained the direction of the force becomes established also.

Applying the above principles to the stream of moving fluid of

Fig. 44, the force, F, necessary to change the velocity of the mass M from V_1 to V_2 is given by

$$F\Delta t = M\Delta V$$

in which

$$\Delta V = (V_2 \rightarrow V_1)$$

the $\rightarrow$ indicating a vectorial subtraction carried out as indicated in the vector diagram. The distance Δl is covered by the mass M in time Δt, giving

$$\Delta l = V_1 \Delta t$$

and

$$M = \rho A \Delta l = \rho A V_1 \Delta t = \rho Q \Delta t$$

substitution of these values in the fundamental equation above results in

$$F = Q\rho(V_2 \rightarrow V_1) = \frac{Qw}{g}(V_2 \rightarrow V_1) \tag{26}$$

an equation which may be used for the calculation of force components F_x and F_y as well as the total force, F. Since the direction of F is the same as that of $(V_2 \rightarrow V_1)$

$$\frac{F}{(V_2 \rightarrow V_1)} = \frac{F_x}{(V_2 \rightarrow V_1)_x} = \frac{F_y}{(V_2 \rightarrow V_1)_y}$$

from the similar force and velocity triangles, and, therefore,

$$F_x = \frac{Qw}{g}(V_2 \rightarrow V_1)_x \tag{27}$$

and

$$F_y = \frac{Qw}{g}(V_2 \rightarrow V_1)_y \tag{28}$$

from which the component of force in a given direction necessary to accomplish a component of momentum change in this direction may be calculated.

In the above equations 26, 27, and 28, the forces involved are external forces exerted *on* the fluid in order to accomplish a certain change of velocity. In certain engineering problems, however, the forces exerted *by* the fluid on its surroundings (equal and opposite to

the above forces) are of more immediate practical value. Designating these forces by $(-F)$, $(-F_x)$, and $(-F_y)$, the above equations become

$$(-F) = \frac{Qw}{g}(V_1 \rightarrow V_2)$$

$$(-F_x) = \frac{Qw}{g}(V_1 \rightarrow V_2)_x$$

$$(-F_y) = \frac{Qw}{g}(V_1 \rightarrow V_2)_y$$

The great advantage of the impulse-momentum law is evident from the fundamental equations: the forces are seen to be dependent only upon initial and final velocity conditions and are entirely independent of the flow complexities occurring between these conditions.

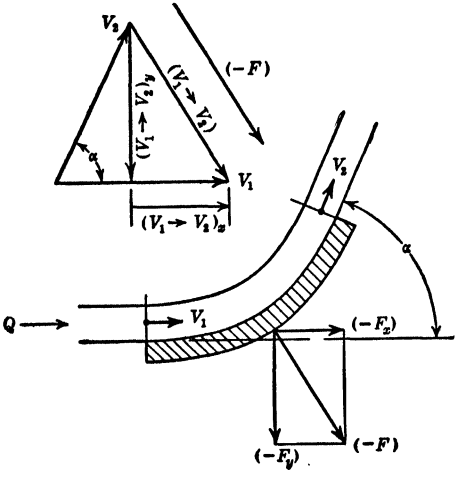


FIG. 45.

The physical meaning of the impulse-momentum law can best be illustrated by its application to a number of specific engineering problems.

The forces on a **fixed blade,** or deflector, as a fluid stream passes over it may be readily calculated. From Fig. 45,

$$(V_1 \rightarrow V_2)_x = V_1 - V_2 \cos \alpha$$

$$(V_1 \rightarrow V_2)_y = V_2 \sin \alpha$$

Therefore

$$(-F_x) = \frac{Qw}{g}(V_1 - V_2 \cos \alpha)$$

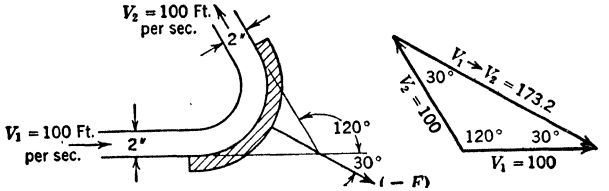
$$(-F_y) = \frac{Qw}{g}(V_2 \sin \alpha)$$

$$(-F) = \frac{Qw}{g}\sqrt{(V_1 - V_2 \cos \alpha)^2 + (V_2 \sin \alpha)^2}$$

Illustrative Problem

A jet of water having 2-in. diameter strikes a fixed blade and is deflected 120° from its original direction. Calculate magnitude and direction of the total force on the blade if velocity of jet is 100 ft/sec.

$$(-F) = \frac{Qw}{g}(V_1 \rightarrow V_2) = \frac{100\,\frac{\pi}{4} \times \left(\frac{2}{12}\right)^2 \times 62.4}{32.2} \times 173.2 = 733 \text{ lb}$$



The computation of the force exerted by a fluid stream on a moving blade forms the basis for elementary calculations on impulse turbines. Let the **single moving blade** of Fig. 46 have a velocity, v, in the same direction as the fluid stream. Since the work done on the blade will be derived from the component of force $(-F_x)$ in the direction of motion, this component only will be calculated. The velocity of fluid *relative to the blade*, u_1, at its entrance will be given by

$$u_1 = V_1 - v$$

and if the blade is assumed frictionless the velocity relative to the blade at exit, u_2, will be the same

$$u_2 = V_1 - v$$

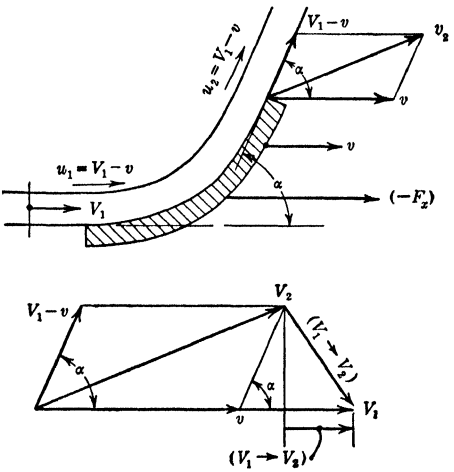


FIG. 46.

The absolute velocity of the fluid stream as it leaves the blade, V_2, will be a composition of its velocity along the blade and the velocity of the blade itself and may be calculated as indicated on the vector diagrams; therefore

$$(V_1 \rightarrow V_2)_x = V_1 - (v + (V_1 - v)\cos\alpha)$$

or

$$(V_1 \rightarrow V_2)_x = (V_1 - v)(1 - \cos \alpha)$$

For a single blade, however, the quantity of flow being deflected per unit of time is not equal to the quantity of flow in the jet since the blade is moving away from the jet. The deflected rate of flow, Q', will be given by

$$Q' = \left(\frac{V_1 - v}{V_1}\right) Q$$

allowing the force component, $(-F_x)$, exerted on the single blade to be calculated as

$$(-F_x) = \frac{Q'w}{g} (V_1 - v)(1 - \cos \alpha)$$

In a closely spaced series of moving blades of the above type such as occurs in an **impulse water turbine** (Fig. 47) all the fluid flowing is

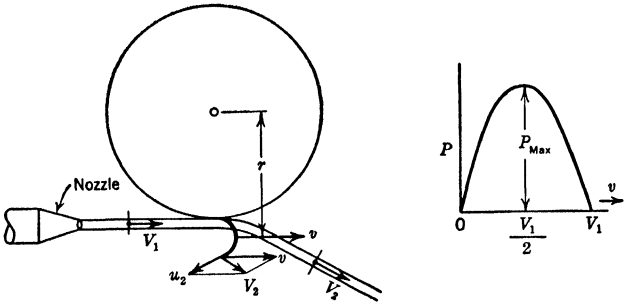


FIG. 47.

deflected by the blades and $Q = Q'$. Thus the force exerted on the blades in the direction of motion may be calculated from

$$(-F_x) = \frac{Qw}{g} (V_1 - v)(1 - \cos \alpha)$$

and since the power transferred from jet to blade is given by

$$P = (-F_x)v$$

$$P = \frac{Qw}{g} (V_1 - v)(1 - \cos \alpha)v$$

allowing the theoretical power developed by the turbine to be calculated. For a given quantity of flow and size of jet, the theoretical

power developed will depend only upon the peripheral speed of the wheel, v, and will be zero when v is zero and when v is equal to the jet velocity V_1. Confirmation of these facts is given by the plot of the above equation in Fig. 47, which also exhibits a point of maximum power at which the turbine should be operated for best efficiency.

The properties of the maximum point on this curve may be obtained by the usual differentiation

$$\frac{d}{dv}\left[\frac{Qw}{g}(V_1 - v)(1 - \cos\alpha)v\right] = 0$$

resulting in $v = V_1/2$ for maximum theoretical power from which the maximum power, $P_{\text{max.}}$, may be calculated by substitution in the general expression, giving

$$P_{\text{max.}} = \frac{Qw}{g}\left(V_1 - \frac{V_1}{2}\right)\left(1 - \cos\alpha\right)\frac{V_1}{2}$$

$$= \frac{Qw}{g}\frac{V_1^2}{4}(1 - \cos\alpha)$$

which becomes

$$P_{\text{max.}} = Qw\frac{V_1^2}{2g}$$

if $\alpha = 180°$. The power available in the jet according to equation 17 is

$$P_{\text{jet}} = Qw\frac{V_1^2}{2g}$$

the same expression as given above. Therefore, all the jet power may be theoretically transferred to the turbine (1) if the speed of operation is correct and (2) if the blades are designed with an angle $\alpha = 180°$.

The force on a **reducer, enlargement, or bend** in a pipe line may be determined from the Bernoulli equation by tedious calculations and graphical integrations, but this force may be obtained directly and easily by use of the impulse-momentum law.

The pipe reducer shown in Fig. 48 represents a typical problem of this type. As flow takes place certain forces act *on* the fluid within the reducer and continually change the momentum of the fluid contained therein. The forces acting on the fluid within the reducer are due to pressure exerted at the ends by the adjacent fluid and at the

sides by the boundary walls. The forces at the ends F_1 and F_2 are given by

$$F_1 = p_1 A_1$$

$$F_2 = p_2 A_2$$

On the side walls a pressure variation about as shown will exist according to the Bernoulli principle. This results in a force indicated sche-

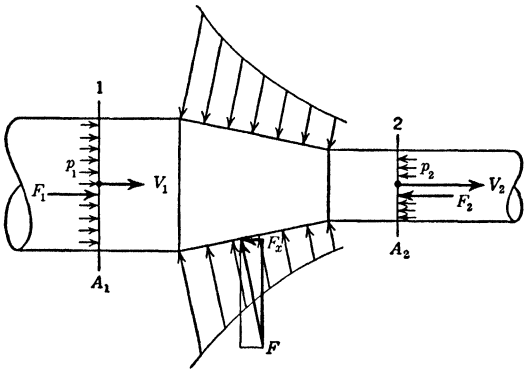


FIG. 48.

matically by F, whose horizontal component is F_x. Applying the impulse-momentum law.

$$F_1 - F_2 - F_x = \frac{Qw}{g}(V_2 \rightarrow V_1)$$

allowing F_x to be calculated.[2] The force exerted by the fluid on the reducer will, of course, be equal to F_x but opposite in direction.

The force on a **reducing pipe bend** may be calculated (Fig. 49) by applying the same principles. With notation similar to that above,

$$F_1 - F_x = \frac{Qw}{g}(V_2 \rightarrow V_1)_x$$

$$F_y - F_2 \sin \alpha = \frac{Qw}{g}(V_2 \rightarrow V_1)_y$$

[2] Note that a net force exerted in a given direction accomplishes a change of momentum in this direction. In this case, the direction of the net force ($F_1 - F_2 - F_x$) is obviously to the right and vectorial considerations indicate the vectorial difference of velocities ($V_2 \rightarrow V_1$) to be to the right also.

from which F_x and F_y may be calculated, the total force, F, exerted by the bend on the fluid being given by

$$F = \sqrt{F_x^2 + F_y^2}$$

and the force exerted by the fluid on the bend is, as before, equal to F but opposite in direction.

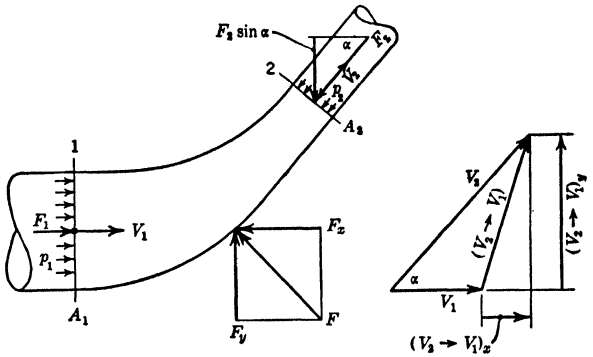
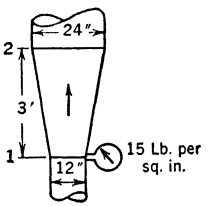


FIG. 49.

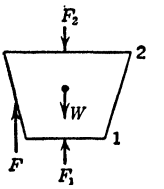
ILLUSTRATIVE PROBLEM

When 10 cfs of water flow upward through this conical enlargement, the pressure gage reads 15 lb/in.^{2} Calculate magnitude and direction of the total force exerted by liquid on enlargement.

$V_1 = 12.72$ ft per sec, $V_2 = 3.18$ ft per sec, $p_2 = 14.72$ lb/in.^{2}



Isolate liquid between sections 1 and 2. The velocity of the liquid is being decreased by a net force acting on the liquid opposed to motion. The net force is $(F_2 + W - F - F_1)$ in which F is the force exerted on the liquid by the enlargement. The decrease of momentum per unit time is $(Qw/g)(V_2 \rightarrow V_1)$.



Equating these,

$$F_2 + W - F - F_1 = \frac{Qw}{g}(V_2 \rightarrow V_1)$$

$$F_2 = 14.72 \times \frac{\pi}{4} \times (24)^2 = 6660 \text{ lb},$$

$$W = \frac{1}{3}\left(\frac{\pi}{4}\left(\frac{24}{12}\right)^2 6 - \frac{\pi}{4}\left(\frac{12}{12}\right)^2 3\right) 62.4 = 343 \text{ lb}.$$

$$F_1 = 15.0 \times \frac{\pi}{4} \times (12)^2 = 1700 \text{ lb}$$

$$6600 + 343 - F - 1700 = \frac{10 \times 62.4}{32.2} (3.18 \rightarrow 12.72) = 185$$

$$F = 5118 \text{ lb}$$

Thus the force exerted *by liquid on enlargement* has a magnitude of 5118 lb and acts vertically downward.

When fluid discharges from an **orifice** in a large container, the jet of fluid will cause a *reactive force* on the container which may be calculated easily by the impulse-momentum law. From Fig. 50 it is obvious that the force exerted on the container will be due to the reduction in pressure on the side of the container which contains the orifice, but this pressure reduction cannot in general be calculated without assumptions or experimental data. Isolating a mass of fluid $ABCD$ from which the jet issues, the horizontal force, F_1, exerted on AD by the

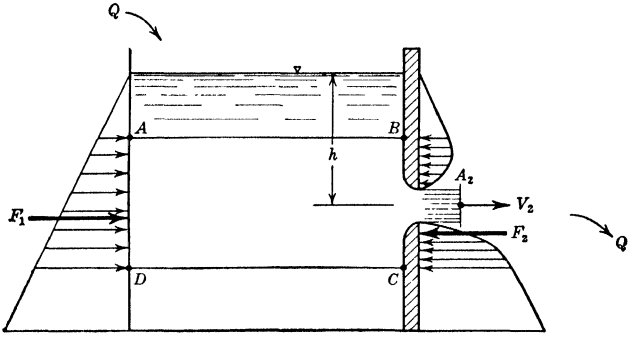


FIG. 50.

vertical wall, may be calculated assuming the fluid to be at rest and using the laws of fluid statics. On the wall BC the pressure distribution will not be static because a pressure reduction will occur, according to the Bernoulli principle, as flow takes place toward the orifice. The force F_2 exerted on BC by the wall will occur from a pressure distribution about as shown and obviously will be less than F_1. Now, applying the impulse-momentum law, F, the net force exerted *by* the container on the fluid, is given by

$$F = F_1 - F_2 = \frac{Qw}{g} (V_2 - V_1)$$

in which V_1, the velocity within the tank, is negligible. Thus

$$F = F_1 - F_2 = \frac{Qw}{g} (V_2)$$

allowing the net force, F, to be calculated and the reactive force exerted by the fluid on the container will be equal to F in magnitude but opposite in direction.

A different expression for F may be obtained by applying Torricelli's theorem and the continuity principle,

$$V_2 = \sqrt{2gh} \quad \text{and} \quad Q = A_2\sqrt{2gh}$$

and substituting these values in the above equation for F,

$$F = \frac{A_2\sqrt{2gh}\,w}{g}\sqrt{2gh} = 2whA_2$$

or, in other words, the reactive force exerted on the container by the moving fluid is just twice the force exerted on an area the size of the orifice submerged at a depth, h, below the liquid surface.

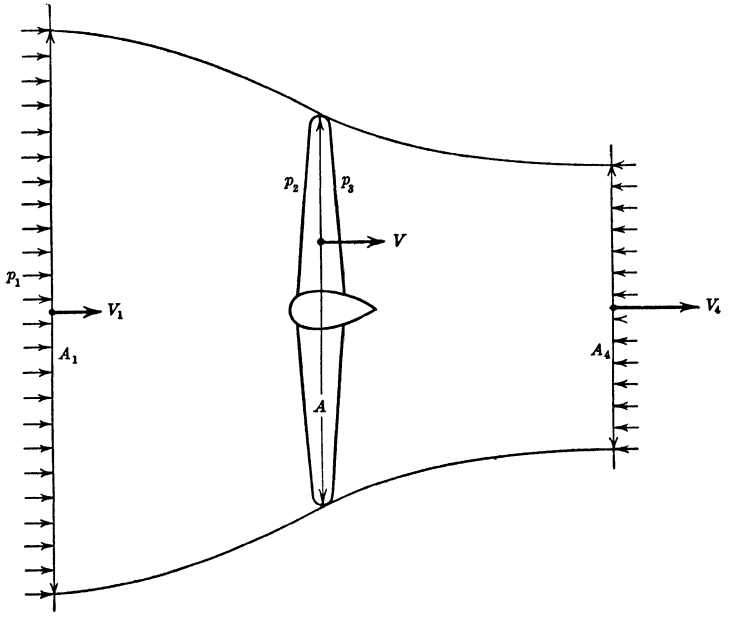


FIG. 51.

Another application of the impulse-momentum law may be made to **ship or airplane propellers** which obtain their thrusts by changing the momentum of a mass of fluid. A screw propeller with its slipstream is shown in Fig. 51 and may be considered to be (1) moving to

the left with a velocity V_1 through still fluid, or (2) stationary in a flow of fluid from left to right with velocity V_1; the relative motion in both cases is the same. For such a propeller operating in an unconfined fluid, the pressures p_1 and p_4, at some distance ahead of and behind the propeller, are obviously the same.

The thrust, F, of the propeller on the fluid results in a change in the velocity of the fluid from V_1 to V_4 and therefore

$$F = \frac{Qw}{g}(V_4 \rightarrow V_1)$$

The useful power output P_o and thrust developed by a propeller moving at a velocity V_1 is $P_o = FV_1$. To obtain this output it is necessary to supply energy enough to create an increase of velocity from V_1 to V_4. From equation 17 the power input, P_i, to create this velocity difference is given by

$$P_i = Qw\left(\frac{V_4^2 - V_1^2}{2g}\right)$$

which may be written

$$P_i = \frac{Qw}{g}(V_4 - V_1)\left(\frac{V_4 + V_1}{2}\right)$$

Thus

$$P_i = F\left(\frac{V_4 + V_1}{2}\right)$$

and the propeller efficiency, η, may be calculated from

$$\eta = \frac{P_o}{P_i} = \frac{FV_1}{F\left(\frac{V_4 + V_1}{2}\right)} = \frac{V_1}{\frac{V_4 + V_1}{2}}$$

which may be placed in better form by adding $\left(\frac{V_1}{2} - \frac{V_1}{2}\right)$ to the denominator; then

$$\eta = \frac{V_1}{\frac{V_4}{2} + \frac{V_1}{2} + \frac{V_1}{2} - \frac{V_1}{2}} = \frac{V_1}{V_1 + \left(\frac{V_4 - V_1}{2}\right)}$$

indicating that the efficiency of a propeller operating in an ideal fluid cannot be 100 per cent [3] since there must always be a sizable velocity

[3] Ship and airplane propellers may have efficiencies of about 80 per cent.

difference $(V_4 - V_1)$, making the denominator of the above expression always greater than the numerator.

Further information on the screw propeller may be obtained by means of the Bernoulli principle. Bernoulli's equation written between sections 1 and 2 is

$$p_1 + \tfrac{1}{2}\rho V_1^2 = p_2 + \tfrac{1}{2}\rho V^2$$

and between sections 3 and 4

$$p_4 + \tfrac{1}{2}\rho V_4^2 = p_3 + \tfrac{1}{2}\rho V^2$$

in which V is the velocity through the plane of the propeller. Since $p_1 = p_4$, subtraction of the first equation from the second results in

$$p_3 - p_2 = \tfrac{1}{2}\rho(V_4^2 - V_1^2)$$

but another equation for the thrust F can be obtained from the pressure difference $(p_3 - p_2)$ acting on the area A, which is

$$F = (p_3 - p_2)A$$

and substituting the equivalent of $(p_3 - p_2)$ from the above equation

$$F = A\tfrac{1}{2}\rho(V_4^2 - V_1^2)$$

This expression may be equated to the impulse-momentum expression for thrust, giving

$$\frac{Qw}{g}(V_4 - V_1) = A\tfrac{1}{2}\rho(V_4^2 - V_1^2)$$

Since $Q = AV$ and $\rho = w/g$, this equation reduces to

$$V = \frac{V_4 + V_1}{2}$$

showing that the velocity through the plane of a propeller operating in an ideal fluid is the numerical average of the velocities at some distance ahead of and behind the propeller.

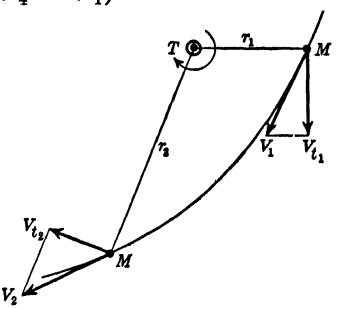


FIG. 52.

The impulse-momentum law, when applied to the *rotation* of a particle about an axis, is stated as

$$T\Delta t = \Delta(MV_t r)$$

in which (Fig. 52) T is the torque which must act on the particle for

time Δt in order to accomplish the change in angular momentum $\Delta(MV_t r)$, M being the mass of the particle, V_t, its tangential component of velocity, and r the distance between the particle and axis of rotation. Since the mass of the particle is constant, the equation may be written

$$T = \frac{M}{\Delta t}\Delta(V_t r)$$

which, for application in fluid problems (as in equation 26), becomes

$$T = \frac{Qw}{g}\Delta(V_t r)$$

or

$$T = \frac{Qw}{g}(V_{t_2} r_2 - V_{t_1} r_1) \tag{29}$$

an equation which forms the basis of reaction turbine and centrifugal pump design.

To illustrate the use of this equation consider its application to a **simplified hydraulic reaction turbine**, sections through which are shown in Fig. 53. Water flows inward through the fixed guide vanes 0–1, acquiring a "whirl," and thus possesses a tangential component of velocity, V_{t_1} as it leaves them. It then passes through the blades 1–2 of the rotating element or "runner," and discharges downward as shown.

As the water leaves the guide vanes at point 1, it will have an absolute velocity V_1, having tangential and radial components, V_{t_1} and V_{r_1}, given by

$$V_{t_1} = V_1 \cos \alpha_1$$

$$V_{r_1} = V_1 \sin \alpha_1$$

The radial component, V_{r_1}, is dependent on the rate of flow through the turbine, Q, and may be calculated by applying the continuity principle, giving

$$Q = V_{r_1} 2\pi r_1 l$$

For best operating conditions the water in leaving the guide vanes must pass smoothly into the moving runner at point 1. To accomplish this the tangential velocity of the runner, ωr_1, at this point must be such that the component of relative velocity, u, is tangential to

the blade as is indicated on the vector diagram. From this vector diagram the following equation for V_{t_1} may be written:

$$V_{t_1} = \omega r_1 + V_{r_1} \cot \beta_1$$

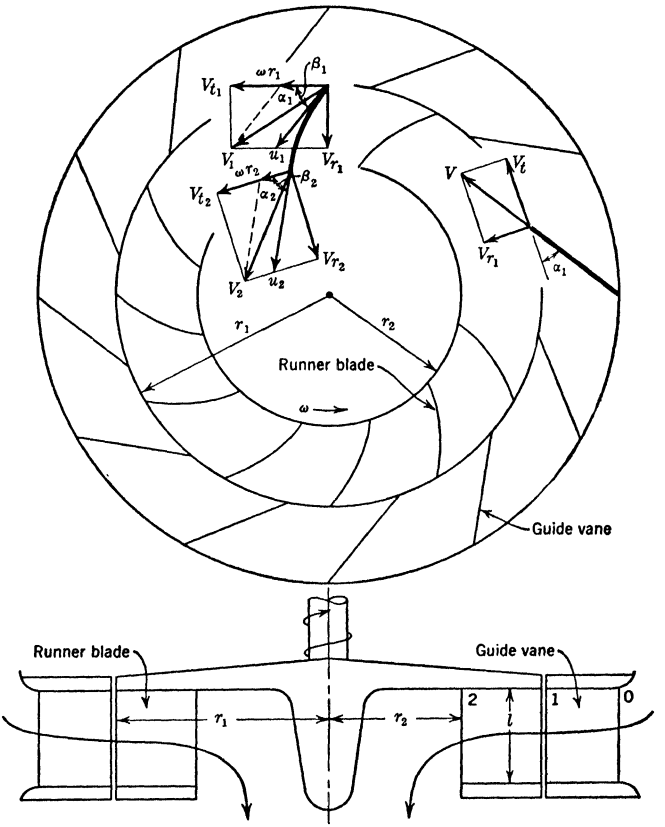


FIG. 53.

At the exit of the runner, the relative velocity, u_2, will be tangential to the blade. The peripheral velocity of the blade, ωr_2, is fixed by the speed of rotation and by the radius at exit, and the component of velocity in a radial direction is determined by the continuity equation

$$Q = V_{r_2} 2\pi r_2 l$$

The vector diagram at the runner exit then becomes as shown and

$$V_{t_2} = \omega r_2 + V_{r_2} \cot \beta_2$$

The torque equation 29 allows calculation of the torque exerted *by* the runner on the fluid. The *torque* exerted by the fluid on the runner will be equal and opposite to this and given by

$$T = \frac{Qw}{g}(V_{t_1}r_1 - V_{t_2}r_2) \tag{30}$$

To obtain a more detailed expression for the theoretical torque exerted on a hydraulic turbine runner when operating under ideal conditions the quantities derived above may be substituted in equation 30; the horse power developed may be calculated from

$$hp = \frac{T\omega}{550}$$

24. Flow Curvatures, Types of Vortices, Circulation. Many foregoing examples have demonstrated the fact that pressure distributions across fluid flows may be calculated from the laws of fluid statics when fluid particles move in straight parallel paths. Since curvilinear fluid motion occurs so frequently in practice it is important to understand the properties of pressure distribution in this type of flow.

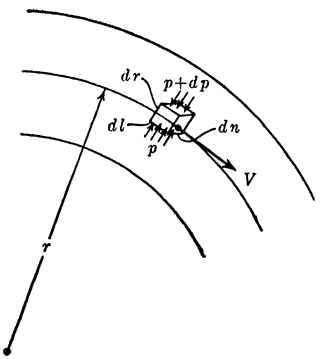


FIG. 54.

In the streamline picture of Fig. 54, a differentially small fluid mass moves along a curved streamline of radius r with a velocity V. If a pressure p exists on the inner face, that on the outer face will be $p + dp$, assuming an increase in pressure with increase in radius. Since the mass of fluid is in equilibrium in a radial direction, the centrifugal force must be balanced by the centripetal force due to pressure. These forces are

$$\text{Centrifugal force} = dM\frac{V^2}{r} = \rho dr dl dn\frac{V^2}{r}$$

$$\text{Centripetal force} = (p + dp)dldn - pdldn = dpdldn$$

which, when equated, give

$$dpdldn = \rho dr dl dn\frac{V^2}{r}$$

or

$$dp = \rho dr \frac{V^2}{r} \tag{31}$$

indicating that pressure will increase with radius in curved flow, or, more generally, pressure at the outside of a curvilinear flow will be greater than that toward the center of curvature.

These facts will explain some of the details of flow through a sharp-edged orifice, a problem which will be treated more exhaustively in a later chapter. Owing to inertia, particles of fluid issuing from the vertical sharp-edged orifice of Fig. 55 will not move horizontally, but rather in smooth curves as shown, the curves resulting in the contraction of the jet to a diameter less than that of the orifice. At the point where the streamlines become parallel at the contracted section of the jet, the pressure in the jet is zero and the velocity is given from Torricelli's theorem (Art. 19) by

$$V_2 = \sqrt{2gh}$$

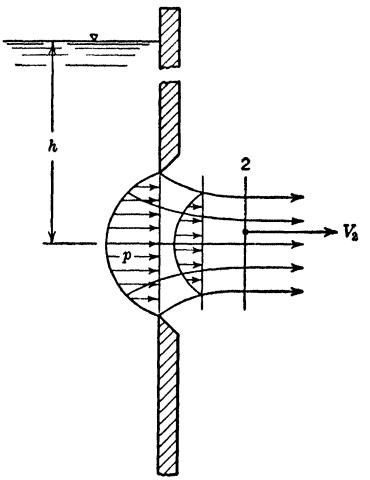


FIG. 55.

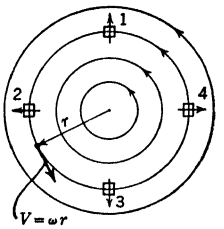
Upstream from point 2, centers of curvature of the jet streamlines are outside of the jet. This means that in moving away from the center of curvature the jet is penetrated, and from equation 31 it may be concluded that the pressure within the curved region of the jet is greater than that outside. This pressure variation is indicated in the figure.

To appreciate more fully the significance of equation 31, let it be applied to two specific types of rotational motion, one of which has been discussed previously (Art. 15).

Certain facts and equations have been brought out concerning the fluid motion obtained by rotating a container of fluid about a vertical axis (Art. 15). After equilibrium sets in, the motion of the fluid at any point in the container is like that of a solid body, possessing a circumferential velocity, V, at a radius, r, given by

$$V = \omega r$$

in which ω is the angular velocity of rotation. If this relation between velocity and radius is substituted in equation 31 the result is



$$dp = \rho dr \frac{\omega^2 r^2}{r}$$

or

$$\frac{dp}{w} = \frac{\omega^2 r dr}{g}$$

the same equation as developed in Art. 15. The streamline picture in this type of rotational motion is shown in Fig. 56, and a particle moving on a streamline is indicated. Inspection of the motion of this particle shows that it will occupy successive positions 1-2-3-4, and as the container makes one revolution the *particle rotates once on its own axis.* Hence it may be concluded that in this type of fluid motion all the fluid particles rotate about their own axes. Such fluid motion is designated as "rotational," and the specific motion indicated in Fig. 56 is sometimes called a "rotational vortex" or "forced vortex."

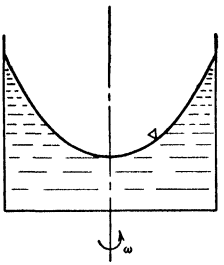


FIG. 56.

Introducing now a new term, Γ (gamma), the "circulation," which will prove useful later, Γ is defined by the equation,

$$\Gamma = \oint v ds$$

in which $\oint$ should be read, "the line integral around a closed curve of —." The meaning of circulation may be obtained from the closed curve drawn in the flow picture of Fig. 57. A differential amount of circulation, $d\Gamma$, is defined as the component, v, of velocity along ds, multiplied by ds, thus

$$d\Gamma = v ds$$

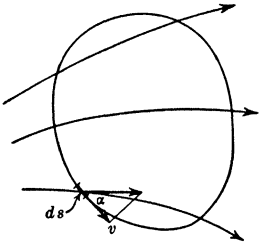


FIG. 57.

and the circulation along the entire closed curve is given by the integration of this expression along the curve. Therefore,

$$\Gamma = \oint v ds$$

Now the circulation around the forced vortex of Fig. 56 may be calculated by taking for simplicity a circle of radius r as the closed curve. The velocity along such a curve is $V = \omega r$, the length of curve is $2\pi r$, and since V does not vary along the curve no integration is necessary. Circulation, Γ, therefore, becomes

$$\Gamma = (\omega r)2\pi r = 2\pi\omega r^2$$

and the circulation is seen to vary with the size and location of the closed curve, another characteristic of "rotational" fluid motion.

Another type of fluid motion is obtained when the sum of the Bernoulli terms for every streamline is the same. Such motion may exist when all the streamlines originate in the same field of energy, such as in the reservoir and pipe bend of Fig. 58. The characteristics of the curved flow in this bend may be obtained from the fact that

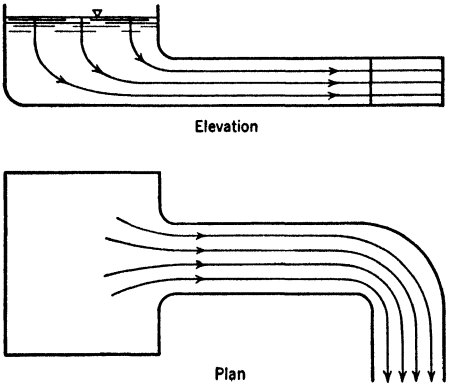


FIG. 58.

$$p + \tfrac{1}{2}\rho V^2 = \text{Constant}$$

at any point on a horizontal plane in the flow. Therefore, by differentiation

$$dp + \rho V dV = 0$$

giving a relation between p and V which may be placed in equation 31. The result is

$$-\rho V dV = \rho dr \frac{V^2}{r}$$

or

$$\frac{dV}{V} - \frac{dr}{r} = 0$$

Integrating,

$$ln V + ln\, r = C = ln C_1$$

and eliminating logarithms

$$Vr = C_1$$

showing that in this case of curved fluid motion the velocities will be least at great distances from the centers of curvature and greatest near these centers.

If flow of this type occurs about a vertical axis a so-called free vortex is formed, such as develops when a container is drained through an opening in the bottom. The streamline picture and hyperbolic velocity variation with radius for such a vortex are shown in the plan view of Fig. 59. The profile of the liquid surface in the vortex may be obtained by neglecting any radial velocity and applying the Bernoulli equation. Over the surface the pressure is zero, and, therefore, this equation becomes

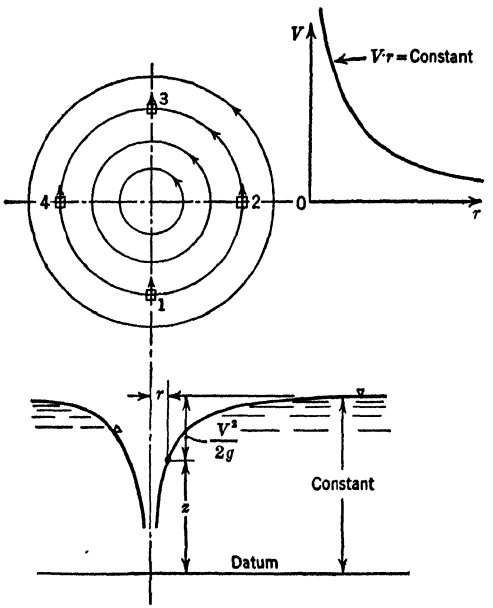


FIG. 59.

$$\frac{V^2}{2g} + z = \text{Constant}$$

the constant being the distance between datum plane and liquid surface at a great distance from the axis of rotation. Thus the surface profile within the vortex may be readily calculated.

To investigate the rotational properties of particles in this fluid flow, let a typical fluid particle be designated as before (Fig. 59). As flow occurs it will be noticed that the particle exhibits no rotation about its own axis as it occupies the successive positions 1-2-3-4. Since none of the particles rotate about their own axes the motion is described as "irrotational" and the free vortex motion described above is termed an "irrotational vortex."

The circulation, Γ, about a free vortex may now be obtained and some useful conclusions drawn from the result. For simplicity select a circular closed curve of radius r, whose center is the center of the vortex. The velocity along such a curve is constant and given by

$$Vr = C_1$$

or

$$V = \frac{C_1}{r}$$

Therefore, the circulation Γ becomes

$$\Gamma = 2\pi r \frac{C_1}{r} = 2\pi C_1$$

showing that the circulation Γ is independent of the size of curve selected for the calculation of the circulation and that the circulation around the center of a free vortex is constant. By a more rigorous and generalized treatment it may be shown that this constant circulation is independent of the *shape* of the closed curve, provided that the vortex center is included within its boundaries.

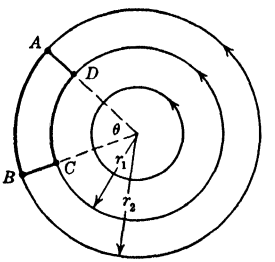


FIG. 60.

In order to obtain more general conclusions concerning the properties of circulation in irrotational motion, the circulation around a closed curve that excludes the center of the vortex may be calculated. A simple curve, $ABCD$, of this type is shown in Fig. 60;

$$\Gamma_{ABCD} = \Gamma_{AB} + \Gamma_{BC} + \Gamma_{CD} + \Gamma_{DA}$$

and may be evaluated from the above principles with the following results

$$\Gamma_{ABCD} = \frac{\theta}{2\pi} 2\pi r_2 \frac{C_1}{r_2} + 0 - \frac{\theta}{2\pi} 2\pi r \frac{C_1}{r_1} + 0 = 0$$

It may be concluded that there is no circulation in irrotational motion around a closed curve which excludes the vortex center. Such a vortex center is called in mathematics a "singular point," and is defined as a point where velocity becomes infinite—a physical impossibility.

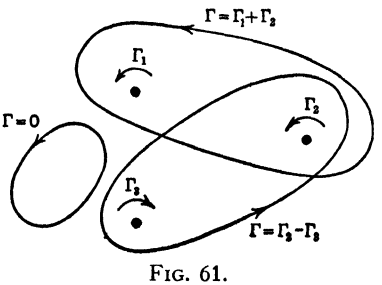


FIG. 61.

The circulation about a vortex center is a constant of the vortex and a measure of its strength. A vortex may, therefore, be designated by $\Gamma \circlearrowleft$ to indicate its strength and direction of rotation. Some other

useful conclusions which may be obtained from further investigation of vortex properties are summarized graphically in Fig. 61.

A combination of the "forced" and "free" vortices, called the "compound" vortex, frequently occurs on the surface of a liquid when the surface is disturbed by a blunt object, such as an oar or paddle, moving through it. The familiar shape of the compound vortex is shown in Fig. 62. In the regions at a distance from the axis of rotation the surface profile of the free vortex appears, but in the center, where the free vortex would require a great drop in the liquid surface, a core of liquid is rotated by the motion of the free vortex. On this core of liquid forms the characteristic paraboloidal surface curve of the forced vortex.

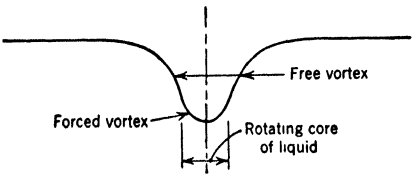


FIG. 62.

BIBLIOGRAPHY

PROPELLERS AND HYDRAULIC TURBINES

W. SPANNHAKE, *Centrifugal Pumps, Turbines and Propellers*, Technology Press, 1934.

PROPELLERS

F. E. WEICK, *Aircraft Propeller Design*, McGraw-Hill Book Co., 1930.

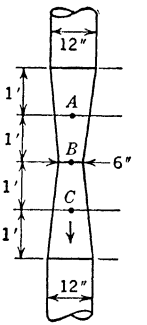
HYDRAULIC TURBINES

R. L. DAUGHERTY, *Hydraulic Turbines*, Third Edition, McGraw-Hill Book Co., 1920.

G. E. RUSSELL, *Textbook on Hydraulics*, fourth edition, Henry Holt & Co., 1934.

A. H. GIBSON, *Hydraulics and Its Applications*, fourth edition, D. Van Nostrand, 1930.

PROBLEMS



135. The flow in this pipe line is reduced linearly from 10 ft^3/sec to zero in 30 sec by a valve at the end of the line. Calculate the local, convective, and total accelerations at points A, B, and C, after 10 sec of valve closure.

136. The velocity of water in a 4-in. pipe line is 7 ft/sec. Calculate the rate of flow in cubic feet per second, gallons per minute, pounds per second, and slugs per second.

137. One hundred pounds of water per minute flow through a 6-in. pipe line. Calculate the velocity.

138. One hundred gallons per minute of glycerine flow in a 3-in. pipe line. Calculate the velocity.

139. Air flows in a 6-in. pipe at a pressure of 20 lb/in.^{2} and a temperature of 100° F. If barometric pressure is 14.7 lb/in^2. and velocity of flow is 12 ft/sec, calculate the weight flow in pounds per second.

140. Water flows in a pipe line composed of 3-in. and 6-in. pipe. Calculate the velocity in the 3-in. pipe when that in the 6-in. pipe is 8 ft/sec. What is its ratio to the velocity in the 6-in. pipe?

141. A smooth nozzle with tip diameter 2 in. terminates a 6-in. water line. Calculate the velocity of efflux from the nozzle when the velocity in the line is 10 ft/sec.

142. Air discharges from a 12-in. duct through a 4-in. nozzle into the atmosphere. The pressure in the duct is 10 lb/in.^{2}, and that in the nozzle stream is atmospheric. The temperature in the duct is 100° F, and that in the nozzle stream 23° F. The barometric pressure is 14.7 lb/in.^{2}, and the velocity in the duct is 73.5 ft/sec. Calculate the velocity of the nozzle stream.

143. Air flows with a velocity of 15 ft/sec in a 3-in. pipe line at a point where the pressure is 30 lb/in.^{2} and temperature 60° F. At a point downstream the pressure is 20 lb/in.^{2} and temperature 80° F. Calculate the velocity at this point. Barometric pressure is 14.7 lb/in.^{2}

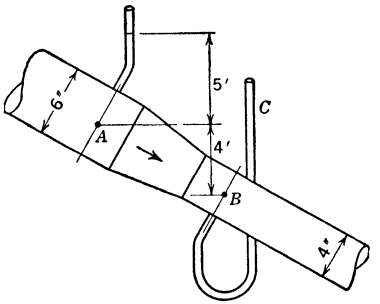
144. At a point in a two-dimensional fluid flow, two streamlines are parallel and 3 in. apart. At another point these streamlines are parallel but only 1 in. apart. If the velocity at the first point is 10 ft/sec, calculate the velocity at the second.

145. Water flows in a pipe line. At a point in the line where the diameter is 7 in., the velocity is 12 ft/sec and the pressure is 50 lb/in.^{2} At a point 40 ft away, the diameter reduces to 3 in. Calculate the pressure here when the pipe is (*a*) horizontal, (*b*) vertical with flow downward.

146. A horizontal 6-in. pipe in which 1000 gpm of carbon tetrachloride is flowing contains a pressure of 30 lb/in.^{2} If this pipe reduces to 4-in. diameter, calculate the pressure in the 4-in. pipe.

147. In a pipe 1 ft in diameter, 10 cfs of water are pumped up a hill. On the hilltop (elevation 160) the line reduces to 8-in. diameter. If the pump maintains a pressure of 100 lb/in.^{2} at elevation 70, calculate the pressure in the pipe on the hilltop.

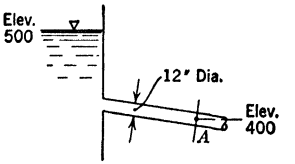
148. In a 3-in. horizontal pipe line containing a pressure of 8 lb/in.^{2} 100 gpm of water flow. If the pipe line reduces to 1-in. diameter, calculate the pressure in the 1-in. section.



PROBLEM 149.

149. If benzene flows through this pipe line and its velocity at *A* is 8 ft/sec, where is the benzene level in the open tube *C*?

150. Water flows through a 1-in. constriction in a horizontal 3-in. pipe line. If the water temperature is 150° F (w = 61.2 lb/ft^3) and the pressure in the line is maintained at 40 lb/in.^{2}, what is the maximum rate of flow which may occur? Barometric pressure is 14.7 lb/in.^{2}



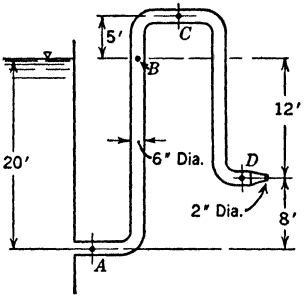
PROBLEM 151.

151. If 8 cfs of water flow through this pipe line, calculate the pressure at point *A*.

152. When the head of water on a 2-in. diameter smooth orifice is 10 ft, calculate the rate of flow therefrom.

153. Five gallons of water flow out of a vertical 1-in. pipe per minute. Calculate the diameter of the stream 2 ft below the end of the pipe.

154. A 3-in. horizontal pipe is connected to a water tank 15 ft below the surface. The pipe terminates in a 1-in. diameter smooth nozzle. Calculate the pressure in the line.



155. Calculate the rate of flow through this pipe line and the pressures at A, B, C, and D.

156. A smooth nozzle 2 in. in diameter is connected to a water tank. Connected to the tank at the same elevation is an open U-tube manometer containing mercury and registering a deflection of 25 in. The lower mercury surface is 20 in. below the tank connection. What flow will be obtained from the nozzle?

157. A 3-in. horizontal pipe is connected to a tank of water 5 ft below the water surface. The pipe is gradually enlarged to 3.5-in. diameter and discharges freely into the atmosphere. Calculate rate of flow and pressure in the 3-in. pipe.

158. A siphon consisting of a 1-in. hose is used to drain water from a tank. The outlet end of the hose is 8 ft below the water surface, and the bend in the hose 3 ft above the water surface. Calculate the rate of flow and pressure in the bend.

159. A 1-in. nozzle on a horizontal 3-in. pipe discharges a stream of water with a velocity of 60 ft/sec. Calculate the pressure in the pipe and the velocity of the nozzle stream at a point 20 ft below the nozzle. (Neglect air friction.)

160. A smooth 2-in. nozzle terminates a 6-in. pipe and discharges water vertically upward. If a pressure gage in the pipe 4 ft below the nozzle tip reads 50 lb/in.^{2}, calculate the velocity at the nozzle tip and rate of flow. What is the velocity of the stream at a point 30 ft above the nozzle tip?

161. Water flows through a 3-in. constriction in a horizontal 6-in. pipe. If the pressure in the 6-in. section is 40 lb/in.^{2} and that in the constriction 20 lb/in.^{2}, calculate the velocity in the constriction and the rate of flow.

162. Water discharges from a tank of water through a 2-in. nozzle into a tank of gasoline (sp. gr. 0.72). The nozzle is 10 ft below the water surface and 11 ft below the surface of the gasoline. Calculate the rate of flow.

163. Water discharges through a 1-in. nozzle under a 20-ft head, into a tank of air in which a vacuum of 10 in. of mercury is maintained. Calculate the rate of flow.

164. A closed tank contains water with air above it. The air is maintained at a pressure of 15 lb/in.^{2}, and 10 ft below the water surface an orifice discharges into the atmosphere. At what velocity will water emerge from the orifice?

165. A pump draws water from a reservoir through a 12-in. pipe. When 12 cfs are being pumped, what is the pressure in the pipe at a point 8 ft above the reservoir surface: (*a*) in pounds per square inch; (*b*) in feet of water?

166. The pressure in the testing section of a wind tunnel is -1.07 in. of water when the velocity is 60 mph. Calculate the pressure on the nose of an object when placed in the testing section of this tunnel. Assume w for air $= 0.0763$ lb/ft^3.

167. The pressure in a 4-in. pipe line carrying 1000 gpm of perfect fluid weighing 70 lb/ft^3 is 20 lb/in.^{2} Calculate the pressure on the upstream end of a small object placed in this pipe line.

168. An airship flies through still air at 50 mph. What is the pressure on the nose of the ship if the air temperature is 40° F and pressure 13.0 lb/in.^{2}?

169. A submarine moves at 10 knots/hr through salt water ($S = 1.025$) at a depth of 50 ft. Calculate the pressure on the bow of the submarine. (1 knot = 6080 ft.)

170. Benzene discharges from an orifice in a tank under a 10-ft head. What pressure will exist on the nose of a small object placed in the jet close to the orifice, in pounds per square inch, in feet of benzene?

171. A circular cylinder 6 in. in diameter is placed in a wind tunnel where the velocity is 80 mph, the air density 0.0763 lb/ft^3. The cylinder is placed with its axis normal to the flow. Calculate the pressure on the front of the cylinder and the pressure at a point on the cylinder's surface 90° from the front where the velocity is 160 mph.

172. The pressure on the front of an object in a stream of water is 8 in. of water above the static pressure in the stream. Calculate the velocity of the stream.

173. A horizontal 6-in. water line contains a flow of 5 cfs and a pressure of 25 lb/in.^{2} Taking a datum 5 ft below the pipe's centerline, calculate the energy available in the flow.

174. A 2-in. nozzle discharges 1 cfs of water vertically upward. Calculate the energy in the jet (*a*) at the tip of the nozzle; (*b*) 20 ft above the nozzle tip, taking a datum plane at the nozzle tip; (*c*) the energy of flow in the pipe (4-in.) 3 ft below the nozzle tip, taking datum plane at the nozzle tip.

175. In a perfectly-insulated section of horizontal 12-in. pipe, 8 cfs of water flow at a pressure of 40 lb/in.^{2} and temperature of 50° F. The pipe bends vertically upward, is reduced to 6-in. diameter, and becomes horizontal again 10 ft above the 12-in section. A heating coil in the vertical section delivers 1000 Btu/sec to the flow. Calculate temperature and pressure in the 6-in. horizontal section assuming that no heat is lost through the pipe walls.

176. Six pounds per second of superheated steam flow upward in a 12-in. pipe line. At elevation 100 the pressure and temperature are 150 lb/in.^{2} and 396° F, and at elevation 200, 138 lb/in.^{2} and 390° F. The barometer reads 15.0 lb/in.^{2} Calculate the heat lost through the pipe walls between the above two points, using the following data from the steam tables:

$$w_{100} = 0.345 \text{ lb/ft}^3$$
$$w_{200} = 0.322 \text{ lb/ft}^3$$
$$H_{100} = 1213.6 \text{ Btu/lb}$$
$$H_{200} = 1212.0 \text{ Btu/lb}$$

177. A tank containing superheated steam at 10 lb/in.^{2} and 314.5° F discharges adiabatically through a small orifice into the atmosphere. Calculate the velocity of the steam jet if steam tables indicate that H in the tank is 1196.1 Btu/lb and in the jet 1155.4 Btu/lb. The barometer reads 15 lb/in.^{2}

178. A tank containing air at 10 lb/in.^{2} and 314.5° F. discharges adiabatically through a small orifice into the atmosphere. Calculate the velocity and temperature of the air jet. The barometer reads 15.0 lb/in.^{2}

179. A pump takes 1000 gpm of benzene from an open tank through an 8-in. pipe. It discharges this flow through a 6-in. pipe, and at a point on this pipe 10 ft above the liquid surface (in the tank) a pressure gage reads 35 lb/in.^{2} What horsepower is being supplied by the pump?

180. A pump having 4-in. suction pipe and 3-in. discharge pipe pumps 500 gpm of water. At a point on the suction pipe a vacuum gage reads 6 in. of mercury; on the discharge pipe 12 ft above this point, a pressure gage reads 48 lb/in.^{2} Calculate the horsepower suplied by the pump.

181. What horsepower pump is theoretically required to raise 200 gpm of water from a reservoir of surface elevation 100 to one of surface elevation 250?

182. Through a 4-in. pipe, 1.0 cfs of water enters a small hydraulic motor and discharges through a 6-in. pipe. The inlet pipe is lower than the discharge pipe, and at a point on the former a pressure gage reads 60 lb/in.^{2}; 14 ft above this on the discharge pipe a pressure gage reads 30 lb/in.^{2} What horsepower is developed by the motor?

183. If 12 cfs of water are pumped over a hill through an 18-in. pipe line, and the hilltop is 200 ft above the surface of the reservoir from which the water is being taken, calculate the pump horsepower required to maintain a pressure of 25 lb/in.^{2} on the hilltop.

184. A hydraulic turbine in a power plant takes 100 cfs of water from a reservoir of surface elevation 235 and discharges it into a river of surface elevation 70. What theoretical horsepower is available in this flow?

185. A pump takes water from a tank and discharges it into the atmosphere through a horizontal 2-in. nozzle. The nozzle is 15 ft above the water surface and is connected to the pump's 4-in. discharge pipe. What horsepower pump is required to maintain a pressure of 40 lb/in.^{2} just behind the nozzle?

186. Water flows through a 4-in. constriction in a horizontal 6-in. pipe. The pressure in the pipe is 40 lb/in.^{2} and in the constriction 25 lb/in.^{2} Calculate the flow.

187. Water flows upward through a 6-in. constriction in a vertical 12-in. pipe. In the constriction there is a vacuum of 8 in. of mercury, and at a point on the pipe 5 ft below the constriction a pressure gage reads 30 lb/in.^{2} Calculate the flow.

188. Carbon tetrachloride flows downward through a 2-in. constriction in a 3-in. vertical pipe line. If a differential manometer containing mercury is connected to the constriction and to a point in the pipe 4 ft above the constriction and this manometer reads 14 in., calculate the rate of flow. (CCl_4 fills manometer tubes to mercury surfaces.)

189. A $1\frac{1}{2}$-in. smooth nozzle is connected to the end of a 6-in. water line. The pressure in the pipe behind the nozzle is 40 lb/in.^{2} Calculate the rate of flow.

190. A smooth 2-in. nozzle terminates a 4-in. pipe line and discharges water vertically upward. If a pressure gage on the pipe 6 ft below the nozzle tip reads 50 lb/in.^{2}, calculate the discharge.

191. Air flows through a 3-in. constriction in a 6-in. pipe. Pressure gages connected to pipe and constriction read respectively 50 lb/in.^{2} and 35 lb/in.^{2} The temperature in the pipe is 200° F, and the barometric pressure 14.7 lb/in.^{2} Calculate the (weight) rate of flow.

192. Solve the preceding problem when the pressure gage reading at the constriction is maintained at (*a*) 15 lb/in.^{2}, (*b*) 5 lb/in.^{2}

193. Carbon dioxide discharges from a 6-in. pipe through a 2-in. nozzle into the atmosphere. If the gage pressure in the pipe is 10 lb/in.^{2}, the temperature 100° F, and the barometric pressure 30.5 in. mercury, calculate the weight of CO_2 discharged per second. Calculate the pressure and temperature within the jet.

194. Solve the preceding problem when the pressure gage reads 20 lb/in.^{2}

195. Superheated steam at 5 lb/in.^{2} and 328° F. (H = 1203.5 Btu/lb) dis-

charges from a 6-in. pipe through a 2-in. nozzle into the atmosphere. Calculate the rate of flow. The barometer reads 15.0 lb/in.^{2} In the steam jet H = 1179.7 Btu/lb, w = 0.0347 lb/ft^3.

196. If in the preceding problem discharge takes place into a tank where the pressure is 8 lb/in.^{2} abs, calculate the rate of flow and pressure in the steam jet. Critical pressure ratio is 0.55 (in jet, H = 1155.8 Btu/lb, w = 0.0274 lb/ft^3).

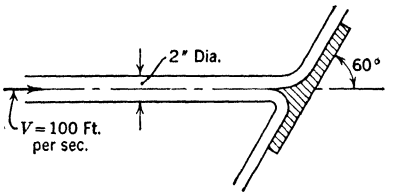
197. A 250-gpm horizontal jet of water 1-in. in diameter strikes a stationary blade which deflects it 60° from its original direction. Calculate the vertical and horizontal components of force exerted by the liquid on the blade. Find the magnitude and direction of the total force on the blade.

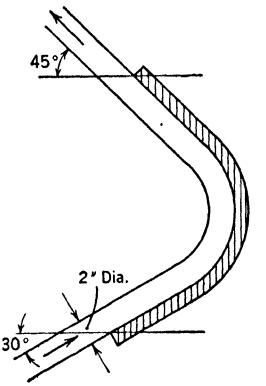
198. Solve the preceding problem with a deflection of 150°.

199. A 2-in. jet of water moving at 120 ft/sec has its direction reversed by a smooth stationary deflector. Calculate the magnitude and direction of the force on the deflector.

200. The jet of the preceding problem strikes a stationary flat plate whose surface is normal to the jet. Calculate the magnitude and direction of the force on the plate.

201. This 2-in. diameter jet moving at 100 ft/sec is

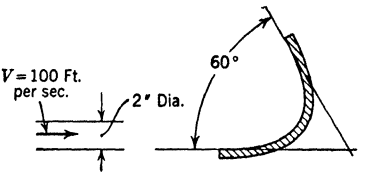




divided in half by a "splitter" on the stationary flat plate. Calculate the magnitude and direction of the force on the plate.

202. Calculate the magnitude and direction of the vertical and horizontal components and the total force exerted on this stationary blade by a 2-in. jet of water moving at 50 ft/sec.

203. Calculate the magnitude and direction of the force required to move this single blade horizontally against the direction of the jet at a velocity of 50 ft/sec. What horsepower is required to accomplish this motion?



204. What force is exerted on a single flat plate moving at 20 ft/sec by a jet of 1-in. diameter having a velocity of 50 ft/sec, if they both move in the same direction and the surface of the plate is normal to the jet?

205. A 6-in. pipe line equipped with a 2-in. nozzle supplies water to an impulse turbine 6 ft in diameter having blade angles of 165°. Plot a curve of theoretical horsepower *vs.* rpm when the pressure behind the nozzle is 100 lb/in.^{2} What is the force on the blades when the maximum horsepower is being developed?

206. A horizontal 6-in. pipe in which 2.2 cfs of water are flowing contracts to 3-in. diameter. If the pressure in the 6-in. pipe is 40 lb/in.^{2}, calculate the magnitude and direction of the horizontal force exerted on the contraction.

207. A horizontal 2-in. pipe in which 400 gpm of water are flowing enlarges to a 4-in. diameter. If the pressure in the smaller pipe is 20 lb/in.^{2}, calculate magnitude and direction of the horizontal force on the enlargement.

208. A conical enlargement in a vertical pipe line is 5 ft long and enlarges the pipe from 12-in. to 24-in. in diameter. Calculate the magnitude and direction of the vertical force on this enlargement when 10 cfs of water flow upward through the line and the pressure at the smaller end of the enlargement is 30 lb/in.^{2}

209. A 2-in. nozzle terminates a 6-in. horizontal water line. The pressure behind the nozzle is 60 lb/in.^{2} Calculate the magnitude and direction of the force on the nozzle.

210. A 90° bend occurs in a 12-in. horizontal pipe in which the pressure is 40 lb/in.^{2} Calculate the magnitude and direction of the force on the bend when 10 cfs of water flow therein.

211. A 6-in. horizontal pipe line bends through 90° and while bending changes its diameter to 3 in. The pressure in the 6-in. pipe is 30 lb/in.^{2}, and the direction of flow is from larger to smaller. Calculate the magnitude and direction of the total force on the bend when 2.0 cfs of water flow therein.

212. Solve the preceding problem if the bend is 120°.

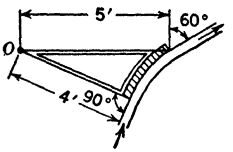
213. A 2-in. smooth nozzle discharges horizontally from a tank under a 30-ft head of water. Calculate the force exerted on the tank.

214. A 3-in. vertical pipe line discharges 50 gpm of water into a tank of water whose free surface is 10 ft below the end of the pipe. What force is exerted on the tank?

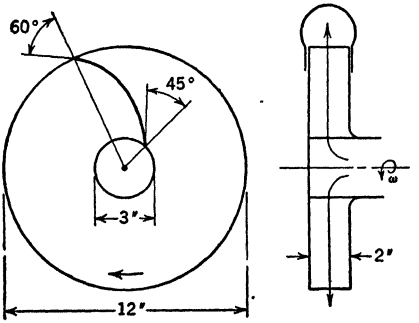
215. An airplane flies at 120 mph through still air (w = 0.0763 lb/ft^3). The propeller is 6 ft in diameter, and its slipstream has a velocity of 200 mph relative to the fuselage. Calculate (*a*) the propeller efficiency, (*b*) the velocity through the plane of the propeller, (*c*) the horsepower input, (*d*) the horsepower output, (*e*) the thrust of the propeller, (*f*) the pressure difference across the propeller plane.

216. A ship moves up a river at 20 mph (relative to shore). The river current has a velocity of 5 mph. The velocity of water a short distance behind the propellers is 40 mph relative to the ship. If the velocity of 100 cfs of water is changed by the propeller, calculate the thrust.

217. This stationary blade is pivoted at point *O*. Calculate the torque exerted thereon when a 2-in. water jet moving at 100 ft/sec passes over it as shown.



218. A radial reaction turbine has



r_1 = 3 ft, r_2 = 2 ft, and its flow cross section is 1 ft high. The guide vanes are set so that α_1 = 30°. When 100 cfs of water flow through this turbine the angle α_2 is found to be 60°. Calculate the torque exerted on the turbine runner. If the angle β_2 is 150°, calculate the speed of rotation of the turbine runner and the angle β_1

necessary for smooth flow into the runner. Calculate the horsepower developed by the turbine at the above speed.

219. A centrifugal pump impeller having dimensions and angles as shown rotates at 500 rpm. Assuming a radial direction of velocity at the blade entrance, calculate the rate of flow, the pressure difference between inlet and outlet of blades, and the torque and horsepower required to meet these conditions.

220. An open cylindrical tank 5 ft in diameter and 10 ft high containing water to a depth of 6 ft is rotated about its vertical axis at 75 rpm. Calculate the Bernoulli constants taking the datum at the bottom of the tank for the two streamlines lying in a horizontal plane 1 ft above the bottom of the tank and having radii of 1 ft and 2 ft. Calculate also the circulation along these streamlines.

221. In a free vortex the velocity 0.5 ft from the center of rotation is 10 ft/sec. Calculate the Bernoulli constants for the two streamlines lying in a horizontal plane 5 ft below the water surface and having radii of 1 ft and 2 ft. Calculate also the circulation along these streamlines.

CHAPTER IV

THE FLOW OF A REAL FLUID

The flow of a real fluid is vastly more complex than that of an ideal one owing to phenomena caused by the existence of viscosity. Viscosity introduces a resistance to motion by causing shear or friction forces to exist between fluid particles. For flow to take place work must be done to overcome these resistance forces, and in the process energy is lost in heat. The study of real fluid flow is essentially one of the relation of viscosity and other variables to these resistance forces and lost energies.

25. Laminar and Turbulent Flow. The effects of viscosity cause the flow of a real fluid to occur under two very different conditions, or regimes: that of "laminar" flow and that of "turbulent" flow. The characteristics of these regimes were first demonstrated by Reynolds,[1] with an apparatus similar to that of Fig. 63. Water flows from a glass

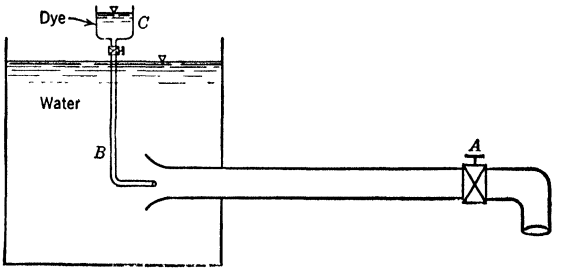


FIG. 63.

tank through a bell-mouthed glass pipe, the flow being controlled by the valve A. A thin tube, B, leading from a reservoir of dye, C, has its opening within the entrance of the glass pipe. Reynolds discovered that, for low velocities of flow in the glass pipe, a thin filament of dye issuing from the tube did not diffuse, but was maintained intact

[1] O. Reynolds, " An experimental investigation of the circumstances which determine whether the motion of water shall be direct or sinuous and of the law of resistance in parallel channels," *Philosophical Transactions of the Royal Society*, Vol. 174, Part III, p. 935, 1883.

throughout the pipe, forming a thin straight line parallel to the axis of the pipe. As the valve was opened, however, and greater velocities obtained, the dye filament wavered and broke, diffusing through the flowing water in the pipe. Reynolds found that the velocity at which the filament of dye diffused was dependent upon the degree of quietness of the water in the tank, higher velocities being obtainable with increased quiescence. He also discovered that if the dye filament had once diffused it became necessary to decrease the velocity in order to restore it, but the restoration always occurred at approximately the same velocity in the pipe.

Since intermingling of fluid particles during flow would cause diffusion of the dye filament, Reynolds deduced from his experiments that at low velocities this intermingling was entirely absent and that the fluid particles moved in parallel layers, or laminae, sliding over particles in adjacent laminae, but not mixing with them; this is the regime of "laminar flow." Since at higher velocities the dye filament diffused through the pipe, it was obvious that some intermingling of fluid particles was occurring, or, in other words, the flow was "turbulent." Laminar flow broke down into turbulent flow at some critical velocity above that at which turbulent flow was restored to the laminar condition; the former velocity is called the upper critical velocity, and the latter, the lower critical velocity.

Reynolds was able to generalize his conclusions from these and other experiments by the introduction of a dimensionless term, N_R, called the Reynolds number, and defined by

$$N_R = \frac{Vd\rho}{\mu}$$

in which V is the average velocity in the pipe, d the diameter of the pipe, and ρ and μ the density and viscosity of the fluid flowing therein. Reynolds found that certain critical values of the Reynolds number, $(N_R)_c$, defined the upper and lower critical velocities for all fluids flowing in all sizes of pipes, thus deducing the fact that a single number defines the limits of laminar and turbulent pipe flow for all fluids.

The upper limit of laminar flow was found by Reynolds to correspond to a Reynolds number of 12,000 to 14,000, but unfortunately this upper critical Reynolds number is indefinite, being dependent upon several incidental conditions such as: (1) initial quietness of the fluid,[2]

[2] Ekman, working in 1910 with Reynolds' original apparatus, was able to obtain laminar flow up to a Reynolds number of 50,000 by quieting the water for days before running his tests.

(2) shape of pipe entrance, and (3) roughness of pipe. However, these high values of the upper critical Reynolds number are of only academic interest and the engineer may take the upper limit of laminar flow to be defined by $(N_R)_c = 2700$ to 4000.

The lower limit of turbulent flow, defined by the lower critical Reynolds number, is of greater engineering importance; it defines a condition below which all turbulence entering the flow from any source will eventually be damped out by viscosity. This lower critical Reynolds number thus sets a limit below which laminar flow will always occur; many experiments have indicated the lower critical Reynolds number to have a value of 2100.

Between Reynolds numbers of 2100 and 4000 a region of uncertainty exists and the engineer must make conservative selection in this region of the variables which are dependent upon the Reynolds number.

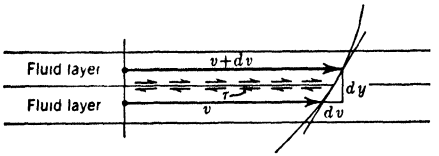


FIG. 64.

In laminar flow, agitation of fluid particles is of a molecular nature only, and these particles are restrained to motion in parallel paths by the action of viscosity. The shearing stress between adjacent moving layers is determined in laminar flow by the viscosity and is completely defined by the differential equation (Art. 5)

$$\tau = \mu \frac{dv}{dy}$$

the stress being the product of viscosity and velocity gradient (Fig. 64).

In turbulent flow, fluid particles are not retained in layers by viscous action, but move in heterogeneous fashion through the flow, sliding past some fluid particles, and colliding with others in an entirely haphazard manner, causing a complete mixing of the fluid as flow takes place. These fluid particles, moving in all directions through the flow, cause at any point a rapid and irregular pulsation in velocity along the general direction of motion and across this direction as well. If the components in the direction of motion of the instantaneous velocities at a point could be measured, a variation of high frequency and small magnitude would be obtained and the time average of all these velocity components would be the velocity which is taken to exist at the point. Across the general direction of motion, rapid variation would be found to exist also, and the time average of these variations would obviously be zero.

Since turbulence is an entirely chaotic motion of individual fluid particles through short distances in every direction as flow takes place, the motion of individual fluid particles is impossible to trace and characterize mathematically, but mathematical relationships may be obtained by considering the average motion of aggregations of fluid particles.

The shear stress between two fluid layers in highly turbulent flow is not due to viscosity, but rather to the momentum exchanges occurring as fluid particles move from one of these layers to the other as the result of the turbulent mixing process. Taking the velocities of fluid particles due to turbulence as v_y and v_x, respectively normal to and along the direction of general motion, it is evident that if homogeneous turbulence is assumed

$$v_x = v_y$$

Using this assumption, Reynolds [3] showed that the shear stress between moving fluid layers in turbulent flow is given by

$$\tau = \rho \overline{v_x v_y}$$

in which $\overline{v_x v_y}$ is the time average of the product of v_x and v_y. Prandtl [4] succeeded in relating the above velocities of turbulence to the general flow characteristics by proposing that fluid particles are transported by turbulence a certain average distance, l, from regions of one velocity to

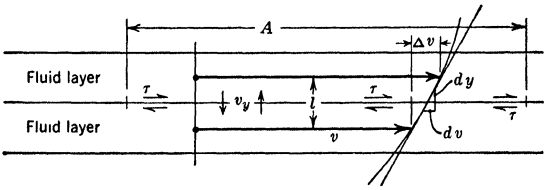


FIG. 65.

regions of another and in so doing suffer changes in their general velocities of motion. Prandtl termed the distance l the "mixing length" and suggested that the change in velocity, Δv, incurred by a fluid particle moving through the distance l was proportional to v_x and to v_y. From Fig. 65,

$$\Delta v = l \frac{dv}{dy}$$

[3] O. Reynolds, "On the dynamical theory of incompressible viscous fluids and the determination of the criterion," *Philosophical Transactions of the Royal Society*, A1, Vol. 186, p. 123, 1895.

[4] L. Prandtl, "Ueber die ausgebildete Turbulenz," *Proceedings Second International Congress Applied Mechanics, Zurich*, 1926, p. 62.

and, from the foregoing statement and substitution of this equation in the Reynolds expression for shear stress, there results

$$\tau \propto \rho l^2 \left(\frac{dv}{dy}\right)^2$$

thus indicating the variables which determine the shear stress in turbulent flow.

ILLUSTRATIVE PROBLEM

Water flows in a 6-in. pipe line at a velocity of 12 ft/sec and at a temperature of 50° F. Is the flow laminar or turbulent?

$$\mu = 0.0000273 \text{ lb sec/ft}^2$$

$$N_R = \frac{Vd\rho}{\mu} = \frac{10 \times \frac{6}{12} \times \frac{62.4}{32.2}}{0.0000273} = 355{,}000$$

Since 355,000 > 2100, flow is turbulent.

26. Fluid Flow Past Solid Boundaries. A knowledge of flow phenomena near a solid boundary is of great value in engineering problems because in actuality flow is never encountered which is not affected by the solid boundaries over which it passes. The classic aeronautical problem is the flow of fluid over the surfaces of an object such as a wing or fuselage, and in other branches of engineering the problem of flow between solid boundaries, such as in pipes and channels, is of paramount importance.

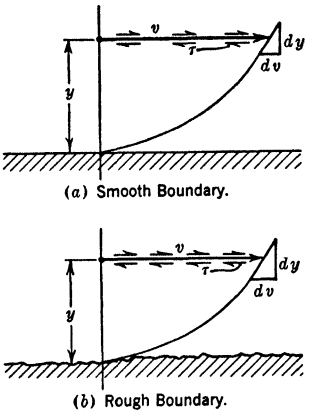


FIG. 66.

One experimentally determined fact concerning fluid flow over smooth solid boundaries is that no motion of fluid particles, relative to the boundary, exists adjacent to the boundary. This means that a diagram of velocity distribution must always indicate a velocity of zero at the boundary. The physical explanation of this phenomenon is that a very thin layer of fluid, possibly having a thickness of but a few molecules, adheres to the solid boundary and motion takes place relative to this layer.

Laminar flow occurring over smooth or rough boundaries possesses the same properties (Fig. 66), the velocity being zero at the bound-

ary, and the shear stress between moving layers at any distance, y, being given by

$$\tau = \mu \left(\frac{dv}{dy}\right)_y$$

Thus, in laminar flow, surface roughness has no effect on the flow properties.

In turbulent flow, however, the roughness of the boundary surface will affect the physical properties of fluid motion. When turbulent flow occurs over smooth solid boundaries it is always separated from the boundary by a film of laminar flow (Fig. 67). This laminar film has been observed experimentally, and its existence may be justified theoretically by the following simple reasoning: The presence of a boundary in a turbulent flow will curtail the freedom of the turbulent mixing process by reducing the available mixing length, and, in a region very close to the boundary, the available mixing length is reduced to zero, resulting in a film of laminar flow over the boundary.

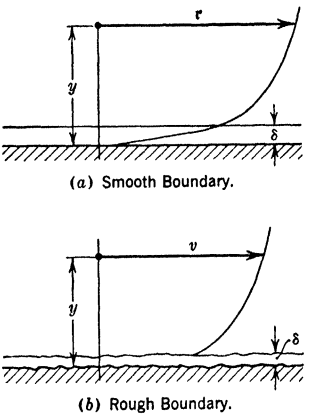


FIG. 67.

In the laminar film the shear stress, τ, is given by

$$\tau = \mu \frac{dv}{dy}$$

and at a distance from the boundary where turbulence is completely developed

$$\tau \propto \rho l^2 \left(\frac{dv}{dy}\right)^2$$

Between the latter region and the laminar film lies a transition region in which shear stress results from a complex combination of turbulent and viscous action, turbulent mixing being restricted by the viscous effects due to the proximity of the wall. The fact that there is a transition from fully developed turbulence to no turbulence at the boundary surface shows that the laminar film, although given an arbitrary thickness, δ, in Fig. 67, possesses no real line of demarcation between the laminar and turbulent regions.

The roughness of boundary surfaces will affect the physical properties of turbulent flow, and the effect of this roughness is dependent upon the thickness of the laminar film. A boundary surface is said to be "smooth" if its projections or protuberances are so completely submerged in the laminar film (Fig. 67*a*) that they have no effect on the turbulent mixing process. However, when the height of the roughness projections is equal to or greater than the thickness of the laminar film (shown schematically in Fig. 67*b*), the projections serve to augment the turbulence and, if roughness is excessive, even to prevent the existence of such a film. Since the thickness of the laminar film, which is a variable quantity, is a criterion of effective roughness, it is possible for the same boundary surface to behave as a smooth one or a rough one, depending upon the thickness of the laminar film which covers it.

Since surface roughness serves to increase the turbulence in a flowing fluid and thus decrease the effect of viscous action some prediction may be made as to the effect of roughness on energy losses. In turbulent flow over rough surfaces energy is consumed by the work done in the continual generation of turbulence by the roughness protuberances. The energy involved in this turbulence is composed of the kinetic energy of fluid masses, which is known to be proportional to the squares of their velocities. Since these velocities are in turn proportional to the velocities of general motion it may be concluded that energy losses caused by rough surfaces vary with the squares of velocities.

As turbulent flow takes place over smooth surfaces, work is done at the expense of available fluid energy against the shear stress due to viscous action in the laminar film. No predictions will be made as to the relation of energy losses and velocities in this case where a combination of turbulent and viscous action exists, but many experiments have indicated that for turbulent flow over smooth surfaces energy losses will vary with the 1.75 to 1.85 power of velocities.

In laminar flow over boundary surfaces, energy losses will subsequently be shown theoretically and experimentally to be directly proportional to velocities.

The velocity profiles of Fig. 67 indicate a small velocity gradient in the turbulent region at a comparatively small distance from the boundary. In other words, flow with a uniform velocity, undisturbed by the presence of the boundary, is taking place in close proximity to it, and this flow, although turbulent, possesses the velocity and pressure characteristics of an ideal fluid flow. The suggestions—

(1) that the viscous action of a real fluid on a solid surface is confined to a thin region close to the boundary, and (2) that outside of this region fluid can be treated as an ideal one—were made by Prandtl[5] and served to revolutionize the treatment of the subject. The suggestions justified the use of the ideal fluid in determining the velocities, pressures, and shapes of the streamlines about an object in a real fluid flow.

27. Fluid Flow between Parallel Plates. To develop some of the fundamental mechanical relationships of fluid flow in passages, consider an incompressible fluid flowing in a section between two vertical parallel plates of infinite extent.

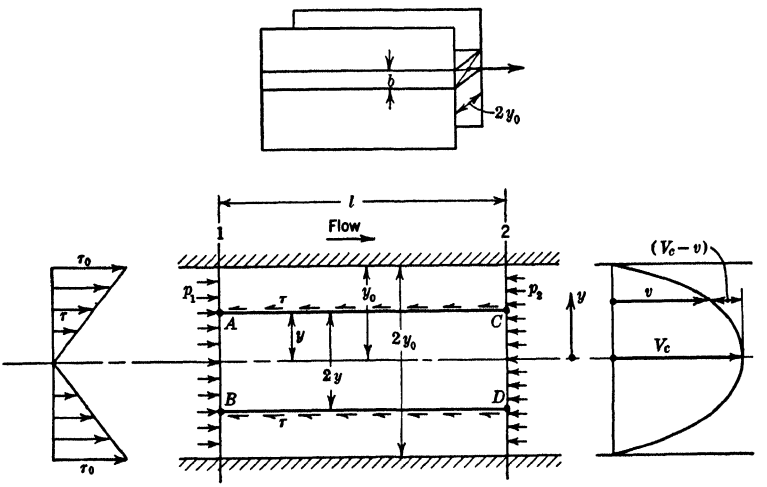


FIG. 68.

Figure 68 represents two such vertical plates with spacing, $2y_o$, between which flow through a section of height b is to be analyzed. From the continuity principle the average velocities of flow, V_1 and V_2, through any two sections, 1 and 2, are the same, and thus any mass of fluid, $ABCD$, of width $2y$, which is isolated in the flow, moves with constant velocity. Constant-velocity motion requires that the net force acting on this fluid mass be zero. Since the force F_τ, due to the shear stress τ, opposes motion, the pressure force F_P, which balances this force, must act in the direction of motion, requiring that $p_1 > p_2$, and showing that a pressure drop occurs in the direction of flow. If sections 1 and 2 are separated by a distance l, and the pressures over

[5] *Proceedings Third International Mathematics Congress*, Heidelberg, 1904.

these sections are uniform, the shear force, F_τ, and pressure force, F_P, may be calculated directly as

$$F_\tau = 2bl\tau$$

and

$$F_P = 2by(p_1 - p_2)$$

which may be equated

$$2bl\tau = 2by(p_1 - p_2)$$

giving the fundamental result

$$\tau = \left(\frac{p_1 - p_2}{l}\right) y$$

and proving that τ varies linearly with y, being zero midway between the two plates and possessing a maximum value, τ_o, at the walls of the passage.

The lost power, P_L, consumed by the total flow through the section of height b in overcoming the shear force F_{τ_o} on its boundary surface may be readily calculated from

$$P_L = F_{\tau_o} V$$

in which

$$F_{\tau_o} = \tau_o 2bl = (p_1 - p_2)2y_o b$$

giving

$$P_L = (p_1 - p_2)2y_o bV$$

but lost power may also be calculated from

$$P_L = QwE_L$$

in which E_L is the lost energy per pound of fluid flowing. Equating these two expressions for lost power in which

$$Q = b2y_o V$$

$$(p_1 - p_2)2y_o bV = 2y_o bwE_L$$

whence

$$E_L = \frac{p_1 - p_2}{w}$$

or the energy consumed per pound of fluid between two sections is simply the loss in pressure head between the two sections. The same

result may be obtained directly from the following energy balance by the Bernoulli equation

$$\frac{p_1}{w} + \frac{V_1^2}{2g} = \frac{p_2}{w} + \frac{V_2^2}{2g} + E_L$$

and since $V_1 = V_2$

$$E_L = \frac{p_1 - p_2}{w}$$

The foregoing developments are perfectly general, applying to both laminar and turbulent flow. Now for mathematical simplicity assume that laminar flow exists between the two parallel plates to illustrate the application of the shear stress equations. In laminar flow the shear stress, τ, is given by [6]

$$\tau = -\mu \frac{dv}{dy}$$

and between parallel plates by

$$\tau = \left(\frac{p_1 - p_2}{l}\right) y$$

For laminar flow between parallel plates both these equations must be satisfied; therefore

$$-\mu \frac{dv}{dy} = \left(\frac{p_1 - p_2}{l}\right) y$$

the variables of which may be separated as follows:

$$-dv = \left(\frac{p_1 - p_2}{\mu l}\right) y dy$$

The left-hand side of this equation may be integrated between the center velocity, V_c, and the variable velocity, v, at a distance, y, from the center; the right-hand side may be integrated between the corresponding limits, zero and y. Integrating

$$-\int_{V_c}^{v} dv = \frac{p_1 - p_2}{\mu l} \int_0^y y dy$$

$$V_c - v = \left(\frac{p_1 - p_2}{2\mu l}\right) y^2 \tag{32}$$

[6] The minus sign appears since y in the above problem is taken in a direction opposite to that assumed in previous problems; here v decreases with increasing y.

showing that for laminar flow between parallel plates the velocity distribution is a parabolic curve having a maximum value midway between the plates, as illustrated in Fig. 68.

28. Flow About Immersed Objects.[7] As real fluid flows in turbulent condition over the surface of a solid object placed in the flow, the effects of viscosity will create velocity conditions at the surface similar to those described above. However, the laminar film which forms over the surface of the object in general is not of constant thickness since it must begin from no thickness at the front of the object where the fluid first contacts it, and increase along the surface of the object in the direction of motion; this type of laminar film is termed a "laminar boundary layer." Under certain conditions this layer may change into a "turbulent boundary layer" which possesses a thin laminar film beneath it and adjacent to the object. These phenomena are illustrated in Fig. 69 for a simple type of object, a smooth flat plate, the thicknesses of the various layers and films being greatly exaggerated. Although the boundary layer occupies an extremely small and usually invisible part of the flow picture it is, nevertheless, of great importance since it is the essential reason for the existence of a frictional "drag" force exerted by the fluid on the object.

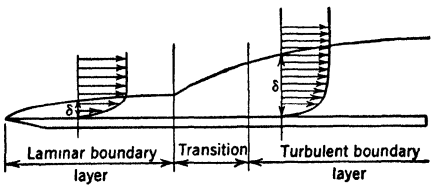


FIG. 69.

The boundary layer in adhering to, or separating from, the object on which it forms brings about different flow phenomena and different effects upon the drag force. On a streamlined object (Fig. 70*a* and *b*) the boundary layer will adhere to the surface of the object and the flow picture appears to be identical with that of an ideal fluid. On a blunt object, however, the boundary layer will cause the flow to separate from the object, resulting in a flow picture (Fig. 70*d*) vastly different from that of an ideal fluid (Fig. 70*c*). The phenomenon of separation thus becomes an important factor in determining the characteristics of fluid flow about objects; its mechanism and properties must now be investigated.

To discover the fundamental properties of separation, compare ideal fluid flow and real fluid flow about a blunt object such as a circular cylinder (Fig. 71). Let the cylinder be placed in an ideal flow possessing a pressure p_o and velocity V_o. A symmetrical streamline picture

[7] See Chapter IX for a more complete treatment of this subject.

and pressure distribution will result, and, of course, no energy will be lost as flow takes place about the object. For a real fluid having the

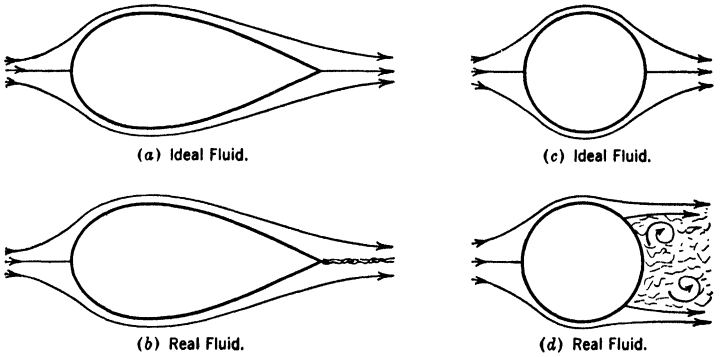


FIG. 70.

same velocity and pressure, energy will be consumed in overcoming resistance caused by the shear stresses in the boundary layer as flow

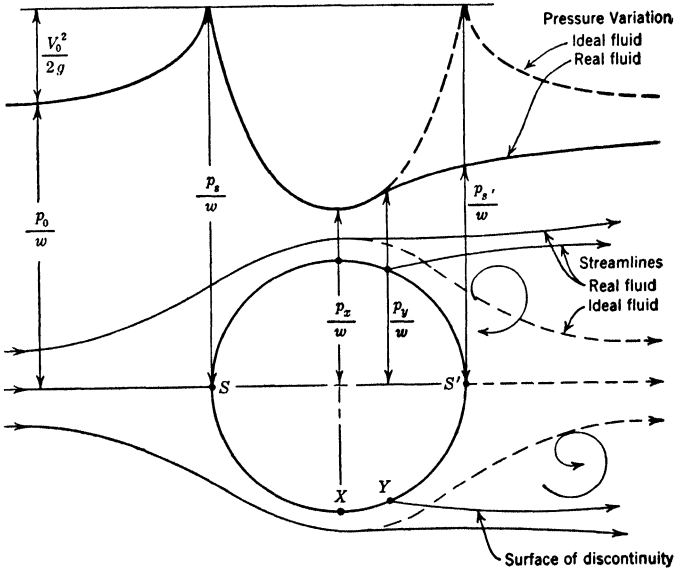


FIG. 71.

passes over the surface of the object. The result is that real fluid particles possess less energy when they arrive at point X than ideal

fluid particles, although these particles started with the same energy content. The fluid particles, in moving from point X to S' along the surface of the object, are moving into a region of high pressure and must possess enough energy to accomplish this motion against the pressure gradient. The ideal fluid particles can do this because of their satisfactory energy content, but the real fluid particles are unable to do the same since some of their energy has been dissipated. The result is that these particles are unable to move beyond a point Y on the rear surface of the cylinder; here they come to rest, accumulate, and are given a rotary motion by the surrounding flow. An eddy of increasing size is then developed at point Y, and the momentum of this eddy becomes so great that the eddy cannot be retained by the cylinder but must break away from it, allowing another one to form and the process to repeat itself.

The result of separation and eddy formation is the formation behind solid objects of a turbulent wake, the turbulence of which is of an "eddying" nature in contrast to the "normal" turbulence discussed in Art. 25. In the creation of the eddies of the turbulent wake, fluid energy has been stored in the eddies and, therefore, made unavailable. As these eddies die out owing to the influence of viscosity, their energy is converted into heat and lost from the fluid flow. The turbulent wake thus becomes another fluid mechanism in which energy may be lost.

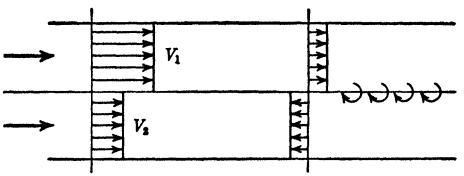


FIG. 72.

The turbulent wake behind a blunt object is separated from the "live" flow by a "surface of discontinuity" on each side of which pressures may be the same, but velocities differ greatly. Such a surface of discontinuity is indicated schematically on Fig. 71. Actually this surface does not possess the symmetry, uniformity, and stability implied by the sketch, but wavers in a transverse direction as the eddies form; besides this property the discontinuity surface itself has an inherent tendency to break up into eddies. To illustrate this tendency, consider a simple type of a discontinuity surface which may be created between adjacent fluid streams moving with different velocities (Fig. 72). If an observer moves in the direction of the streams with a velocity equal to the numerical average of those of the streams, he sees the relative velocity profile shown at the right from which the tendency for eddy creation is immediately evident.

To return now to the problem of drag forces on objects in a fluid flow, the effects of boundary layers, separation, and wakes may be observed. Fundamentally, drag is caused by the components of the normal and tangential forces transmitted from the fluid to the surface elements of the solid object. These normal forces are those of pressure, which in general may be calculated by applying the Bernoulli principle to the streamtube adjacent to the object. The tangential forces are those of shear at the surface of the object arising from viscous effects in the boundary layer. From Fig. 73, the total drag force, D, may be expressed mathematically as

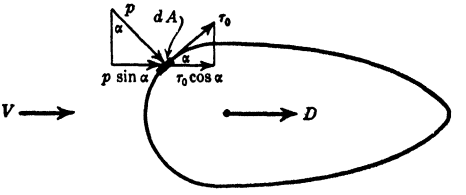


FIG. 73.

$$D = \int^{S} p dA \sin \alpha + \int^{S} \tau_0 dA \cos \alpha \tag{33}$$

in which $\int^{S}$ designates "integral over the surface of the object." The drag resulting from the pressure variation over the surface of the object is called the "form" or "profile" drag, D_p, since its magnitude will be found to depend primarily on the "form" or "profile" of the object. The drag force, D_f, incurred by the shear stresses over the surface of the object due to frictional effects is termed the "frictional" or "skin friction drag." Hence the relations:

$$\text{Profile drag, } D_p = \int^{S} p dA \sin \alpha \tag{34}$$

$$\text{Frictional drag, } D_f = \int^{S} \tau_0 dA \cos \alpha \tag{35}$$

and from equation (33)

$$D = D_p + D_f \tag{36}$$

The approximate relative magnitudes of these drag forces occurring on various objects when placed in a turbulent flow and the effect of the turbulent wake upon them may be obtained from a study of objects having different shapes but the same cross section, placed in the same fluid flow. Three such objects are: the thin circular disk, sphere, and streamlined form of Fig. 74.

For the disk, the streamline picture indicates a stagnation point at the center of the upstream side and a greatly reduced pressure at

the edges. This reduced pressure, being adjacent to the turbulent wake, is transmitted into it, causing the downstream side of the disk to be exposed to reduced pressure which will contribute to the profile drag force. Designating the pressure reduction below that in the

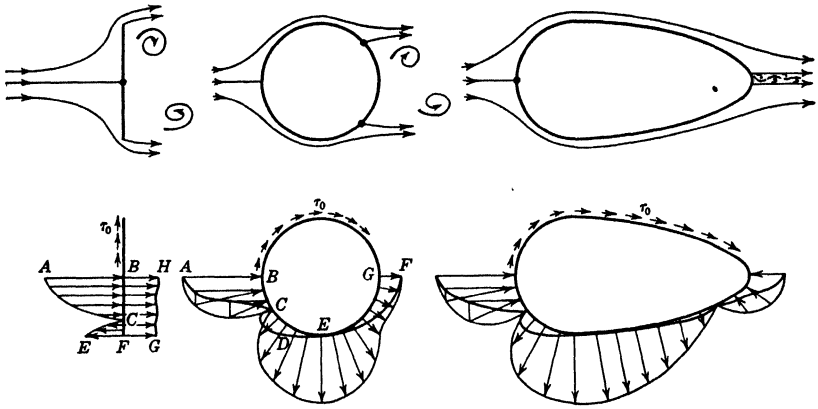


FIG. 74.

undisturbed flow by vectors directed away from the surface of the disk (and that in excess of the pressure in the undisturbed flow by vectors toward the surface), a pressure diagram results whose net area is the profile drag. Thus the profile drag is given by

$$D_p = 2(ABC + BFGH - FCE)$$

and the frictional drag, D_f, will then be zero since none of the shear stresses on the surface of the disk have components in the direction of motion.

For the sphere, the turbulent wake is smaller than that of the disk and, from examination of the streamline picture, will possess a somewhat higher pressure. To obtain the profile drag graphically the diagram of the pressure components is necessary. Here

$$D_p = 2(ABC + EFG - CDE)$$

which is seen to be much smaller than that of the disk, a fact which is confirmed by many experiments indicating the profile drag of the sphere to be roughly one-third that of the disk. The frictional drag of the sphere is a finite quantity since the shear stresses at its surface have components in the direction of motion; however, shear-stress variations are extremely difficult to calculate and their small magni-

tudes will result in a frictional drag which is negligible compared to the profile drag of the sphere.

For the streamlined form the turbulent wake is extremely small and the pressure surrounding it and within it is comparatively large since the gentle contour of the body has allowed deceleration of the flow and consequent regain of pressure, without incurring separation. The pressure diagrams lead directly to the conclusion that the profile drag of the streamlined form is very small, and experimental results indicate it to be about 1/40 that of the disk. The frictional drag for objects of this shape is much greater than that for the sphere since streamlining has brought more surface area into contact with the flow. For well-streamlined objects frictional drag assumes a magnitude comparable to that of profile drag.

The foregoing examples illustrate the fact that the viscosity property of a fluid is the root of the drag problem. Viscosity has been seen to cause drag either by frictional effects on the surface of an object or through profile drag by causing separation and the creation of a low-pressure region behind the object. By streamlining an object the size of its low-pressure turbulent wake is decreased and a reduction in profile drag is accomplished, but in general an increase in frictional drag is incurred.

For an ideal fluid in which there is no viscosity and thus no cause for frictional effects or formation of a turbulent wake, regardless of the shape of the object about which flow is occurring, it is evident that the drag of the object is zero. Two centuries ago, D'Alembert's discovery that all objects in an ideal fluid exhibit no drag was a fundamental and disturbing paradox; today this fact is a logical consequence of the fundamental reasoning presented above.

29. Stability—Secondary Flows. The flow phenomena about a symmetrical body, such as the sphere, suggests the existence of a general law of fluid motion which will prove to be widely applicable. On the front half of the sphere the flow picture has been seen to be practically identical with that of the ideal fluid, but on the rear half, where a turbulent wake forms, the flow picture bears no resemblance to that of the ideal fluid. On the front half of the sphere the flow is being accelerated and pressure head (or energy) is being converted into velocity head. For ideal flow to occur behind the sphere, deceleration equivalent to the above acceleration must occur and velocity head must be reconverted into pressure head. Owing to boundary layer phenomena this deceleration of the fluid flow is not accomplished without the formation of a turbulent wake, the eddies of which serve

to consume fluid energy. This single example illustrates the following general law of fluid motion: Acceleration of a moving fluid, identified by convergent streamlines and a decrease in pressure in the direction of motion, is an efficient and stable fluid process, accompanied by no eddy formation and small energy losses; on the other hand, deceleration of fluid flow is an inefficient process, accompanied by instability, eddy formation, and large energy losses.

These principles may be seen to apply to flow through passages such as the convergent-divergent tube or the nozzle of Fig. 75, where smooth, stable flow exists in the convergent passages but separation and eddying turbulence occur as the flow is decelerated.

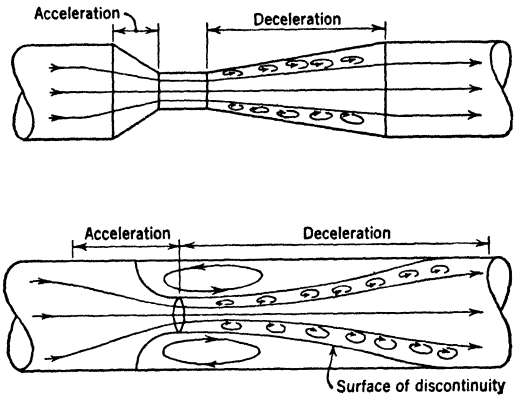


FIG. 75.

Another engineering application of these principles occurs in a comparison of the efficiencies of hydraulic turbines and centrifugal pumps. In the turbine the flow passages are convergent, causing continual acceleration of the fluid through the machine. In the pump, which creates pressure head by dynamic means, the passages are divergent. Hydraulic turbine efficiencies have been obtained up to 94 per cent but maximum centrifugal pump efficiencies range around 87 per cent, and the difference between these efficiencies may be attributed to the inherent efficiency and inefficiency of the acceleration and deceleration processes.

Another consequence of the boundary layer is the creation of a flow within a flow, a "secondary flow" superimposed upon the main, or "primary," flow. A classical and useful example of the creation of an eddy motion and dissipation of energy by a secondary flow occurs when fluid flows through a smooth bend in a circular pipe (Fig. 76).

For an ideal fluid flowing under these conditions it has been shown (Art. 24) that a pressure gradient develops across the bend due to the centrifugal forces of fluid particles as they move through the bend. Stability occurs in the ideal fluid when this pressure gradient brings about a balance between the centrifugal and centripetal forces on the fluid particles. In a real fluid this stability is disrupted by the velocity being reduced to zero at the walls owing to the existence of the laminar film. The reduction of velocity at the outer part (A) of the bend reduces the centrifugal force of the particles moving near the wall, causing the pressure at the wall to be below that which would be maintained in an ideal fluid. However, the velocities of fluid particles

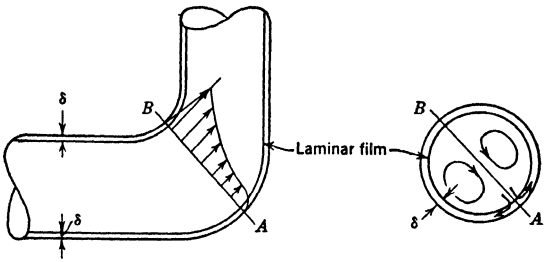


FIG. 76.

toward the center of the bend are about the same as those of the ideal fluid, and the pressure gradient developed by their centrifugal forces is about the same. The "weakening" of the pressure gradient at the outer wall will cause a flow to be set up from the center of the pipe toward the wall which will develop into the twin eddy motion shown, and this secondary motion added to the main flow will cause a double spiral motion, the energy of which will be dissipated in heat as the motion is destroyed by viscosity. The energy of the secondary motion has been derived from the available fluid energy, and as viscosity causes this energy to be dissipated, fluid energy is lost in much the same way as it is lost by eddies in a turbulent wake.

BIBLIOGRAPHY

B. A. BAKHMETEFF, *The Mechanics of Turbulent Flow*, Princeton University Press, 1936.

H. ROUSE, " Modern Conceptions of the Mechanics of Fluid Turbulence," *Trans. A.S.C.E.*, Vol. 102, 1937.

Fluid Mechanics for Hydraulic Engineers, McGraw-Hill Book Co., 1938.

L. PRANDTL and O. G. TIETJENS, *Applied Hydro and Aeromechanics*, McGraw-Hill Book Co., 1934.

L. PRANDTL, *The Physics of Solids and Fluids*, Part II, Blackie & Son, 1936.
C. V. DRYSDALE, *The Mechanical Properties of Fluids*, Blackie & Son, 1925.
R. A. DODGE and M. J. THOMPSON, *Fluid Mechanics*, McGraw-Hill Book Co., 1937.
M. P. O'BRIEN and G. H. HICKOX, *Applied Fluid Mechanics*, McGraw-Hill Book Co., 1937.

PROBLEMS

222. If 30 gpm of water flow in a 3-in. pipe line at 70° F, is the flow laminar or turbulent?

223. Glycerine flows in a 1-in. pipe at a velocity of 1 ft/sec and temperature of 80° F. Is the flow laminar or turbulent?

224. Superheated steam at 400° F and absolute pressure 100 lb/in.^{2} (w = 0.202 lb/ft^3) flows in a 1-in. pipe at a velocity of 5 ft/sec. Is the flow laminar or turbulent?

225. Linseed oil flows at 80° F in a $\frac{1}{2}$-in. pipe at 2 ft/sec. Is the flow laminar or turbulent?

226. Carbon dioxide flows in a 2-in. pipe at a velocity of 5 ft/sec, temperature of 150° F, and pressure 40 lb/in.^{2} The barometer reads 15.0 lb/in.^{2} Is the flow laminar or turbulent?

227. What is the maximum flow of water which may occur in a 6-in. pipe at 80°F at laminar condition?

228. What is the maximum flow of air that may occur at laminar condition in a 4-in. pipe at 30 lb/in.^{2} abs and 100° F.?

229. What is the largest diameter pipe line that may be used to carry 100 gpm of linseed oil at 80° F if the flow is to be laminar?

230. A fluid flows in a 3-in. pipe line which discharges into a 6-in. line. Calculate the Reynolds number in the 6-in. pipe if that in the 3-in. pipe is 20,000.

231. The loss of energy in a certain pipe line flow is 3 ft-lb/lb of fluid flowing. What loss of energy will occur when the flow is doubled, assuming (*a*) laminar flow, (*b*) turbulent flow and smooth pipe, (*c*) turbulent flow and rough pipe?

232. Water flows horizontally between vertical parallel plates spaced 2 ft apart. If the pressure drop in the direction of flow is 4 lb/in.^{2} per 100 ft, calculate the shear stress in the flow at the surfaces of the plates, 3 in., 6 in., and 9 in. from them, and at the midpoint between them.

233. A liquid flows in laminar condition between two parallel plates 2 ft apart. If the velocity at the midpoint between the plates is 4 ft/sec, calculate the velocities at the plates and at distances of 3 in., 6 in., and 9 in. from them. If the viscosity of this liquid is 0.1 lb sec/ft^2 and its density 1.8 slugs/ft^3, calculate the loss of pressure and loss of head in a distance of 100 ft along the flow. What is the rate of flow through a section having b = 3 ft? (See Fig. 68.)

CHAPTER V

SIMILARITY AND DIMENSIONAL ANALYSIS

30. Similarity and Models. Near the latter part of the last century, models began to be used to study flow phenomena which could not be solved by mathematical methods or by means of available experimental results. At the present time the use of models is increasing: the aeronautical engineer obtains data and checks his designs by model tests in wind tunnels; the ship designer tests ship models in towing basins; the mechanical engineer tests models of turbines and pumps and predicts the performance of the full-scale machines from these tests; the civil engineer works with models of hydraulic structures and rivers to obtain more reliable solutions to his design problems. The justification for the use of models is an economic one—a model, being small, costs little compared to the "prototype" from which it is built, and its results may lead to savings of many times its cost; a model also adds a certainty to design which can never be obtained from calculations alone.

Similarity of flow phenomena not only occurs between a prototype and its model but also may exist between various natural phenomena if certain laws of similarity are satisfied. Similarity thus becomes a means of correlating the apparently divergent results obtained from similar fluid phenomena and as such becomes a valuable tool of modern fluid mechanics; the application of the laws of similarity will be found to lead to more comprehensive solutions and thus to a better understanding of fluid phenomena in general.

There are many types of similarity, all of which must be obtained if complete similarity is to exist between fluid phenomena. The first and simplest of these is the familiar geometrical similarity which states that the flow pictures of model and prototype have the same shape, and, therefore, that the ratios between corresponding *lengths* in model and prototype are the same. In the model and prototype of Fig. 77, for example,

$$\frac{d}{d_m} = \frac{l}{l_m}$$

Corollaries of geometric similarity are that areas vary with the squares of lengths, thus

$$\frac{A}{A_m} = \left(\frac{d}{d_m}\right)^2 = \left(\frac{l}{l_m}\right)^2$$

and that volumes vary with the cubes of lengths.

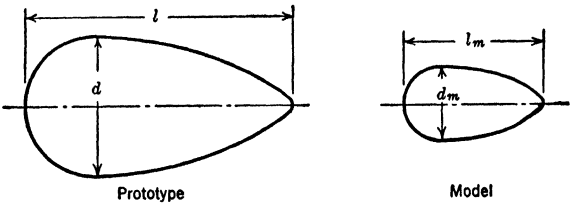


FIG. 77.

If the two similar objects of Fig. 77 are placed in the similar fluid flows of Fig. 78, another type of similarity, kinematic similarity, exists if motion of the fluid about the objects is the same. Such similarity of motion is characterized by ratios of corresponding velocities and accelerations being the same throughout the flow picture; for example,

$$\frac{V_1}{V_{1_m}} = \frac{V_2}{V_{2_m}} \quad \text{and} \quad \frac{a_3}{a_{3_m}} = \frac{a_4}{a_{4_m}}$$

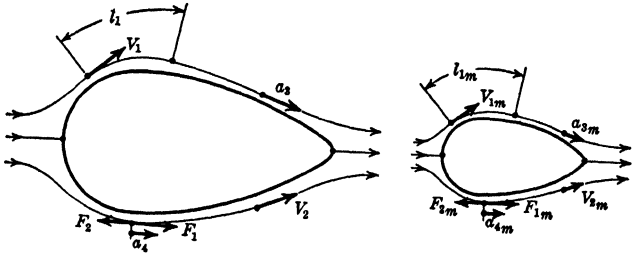


FIG. 78.

In order to maintain geometric and kinematic similarity between flow pictures there must be forces acting on corresponding fluid masses which are related by ratios similar to those above, and this similarity, governed by the existence of such force ratios, is called "dynamic similarity." Without defining the nature of the forces, dynamic similarity may be indicated schematically (Fig. 78) by

$$\frac{F_1}{F_{1_m}} = \frac{F_2}{F_{2_m}}$$

or

$$\left(\frac{F_2}{F_1}\right)_{\text{model}} = \left(\frac{F_2}{F_1}\right)_{\text{prototype}}$$

But these force ratios must be maintained for *all* the corresponding fluid masses throughout the flow pictures, and thus it is evident that they can be governed only by relations between dynamic and kinematic properties of the flow and the physical properties of the fluids involved.

The forces which may act on fluid masses in a fluid flow are those of pressure, F_P; inertia, F_I; gravity, F_G; viscosity, F_V; elasticity, F_E; and surface tension, F_T. Since these forces are taken to be those on *any* fluid mass, they may be generalized by the following fundamental relationships:

$$F_P = pA = pl^2$$

$$F_I = Ma = \rho l^3 \frac{V^2}{l} = \rho V^2 l^2$$

$$F_G = Mg = \rho l^3 g$$

$$F_V = \mu \frac{dv}{dy} A = \mu \frac{V}{l} l^2 = \mu V l$$

$$F_E = EA = El^2$$

$$F_T = Tl$$

To obtain dynamic similarity between two flow pictures when all these forces act, all independent force ratios which can be written must be the same in model and prototype; thus dynamic similarity between two flow pictures when all possible forces are acting is expressed by the following five simultaneous equations:

$$\left\{\begin{array}{l}
\left(\frac{F_P}{F_I}\right)_p = \left(\frac{F_P}{F_I}\right)_m = \left(\frac{p}{\rho V^2}\right)_p = \left(\frac{p}{\rho V^2}\right)_m \\
\left(\frac{F_I}{F_V}\right)_p = \left(\frac{F_I}{F_V}\right)_m = \left(\frac{Vl\rho}{\mu}\right)_p = \left(\frac{Vl\rho}{\mu}\right)_m = \left(\begin{array}{c}\text{Reynolds}\\ \text{number}\end{array}\right)_p = \left(\begin{array}{c}\text{Reynolds}\\ \text{number}\end{array}\right)_m \\
\left(\frac{F_I}{F_G}\right)_p = \left(\frac{F_I}{F_G}\right)_m = \left(\frac{V^2}{lg}\right)_p = \left(\frac{V^2}{lg}\right)_m = \left(\begin{array}{c}\text{Froude}\\ \text{number}\end{array}\right)_p = \left(\begin{array}{c}\text{Froude}\\ \text{number}\end{array}\right)_m \\
\left(\frac{F_I}{F_E}\right)_p = \left(\frac{F_I}{F_E}\right)_m = \left(\frac{\rho V^2}{E}\right)_p = \left(\frac{\rho V^2}{E}\right)_m = \left(\begin{array}{c}\text{Cauchy}\\ \text{number}\end{array}\right)_p = \left(\begin{array}{c}\text{Cauchy}\\ \text{number}\end{array}\right)_m \\
\left(\frac{F_I}{F_T}\right)_p = \left(\frac{F_I}{F_T}\right)_m = \left(\frac{\rho l V^2}{T}\right)_p = \left(\frac{\rho l V^2}{T}\right)_m = \left(\begin{array}{c}\text{Weber}\\ \text{number}\end{array}\right)_p = \left(\begin{array}{c}\text{Weber}\\ \text{number}\end{array}\right)_m
\end{array}\right.$$

in which the quantities, p, V, and l may be any pressure, velocity, and length, provided that the quantities used are the *corresponding* ones in model and prototype; the force ratios are named for the experimenters who first derived and used them.

Fortunately, in most engineering problems the above five equations are not necessary since some of the forces stated above (1) may not act, (2) may be of negligible magnitude, or (3) may be related by certain known laws and, therefore, are not independent. In each new problem of similarity a good understanding of fluid phenomena is necessary to determine how the problem may be satisfactorily simplified by the elimination of irrelevant or negligible forces. The reasoning involved in such an analysis is best illustrated by citing certain simple and recurring engineering examples.

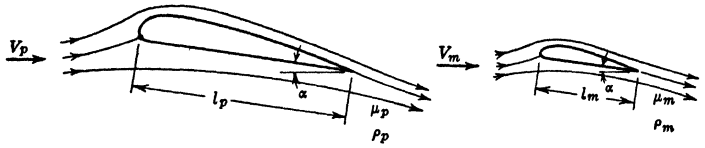


FIG. 79.

In the classical aeronautical problem where a model of a wing is to be built and tested (Fig. 79), the model must first have the same shape as its prototype and be placed in the flow at the same "angle of attack," α. After these requirements are met, dynamic, kinematic, and geometric similarity of the flow pictures will be obtained if all the relevant force ratios are made equal in model and prototype.

Certain forces, however, may be eliminated immediately: Surface tension forces are negligible; if the fluids are taken to be incompressible, the elasticity forces drop out; the gravity forces, although acting on all fluid particles, do not affect the flow picture and, therefore, may be omitted. Thus, in this problem there exist only the forces of pressure, inertia, and viscosity which must be related by some physical equation. Since all corresponding forces in model and prototype have the same ratio only one ratio is necessary to characterize complete dynamic similarity. This ratio is

$$\left(\frac{F_I}{F_V}\right)_p = \left(\frac{F_I}{F_V}\right)_m = \left(\frac{Vl\rho}{\mu}\right)_p = \left(\frac{Vl\rho}{\mu}\right)_m = (N_R)_p = (N_R)_m$$

and from this equation it is evident that complete dynamic similarity fixes no theoretical restrictions as to the fluid which may be used in

the testing of a model; any fluid may be used provided that the Reynolds number of the model can be made equal to the Reynolds number of the prototype.

The above reasoning may be applied without change to the turbulent flow of fluids in circular pipes (Fig. 80). Here geometric similarity requires that the roughness pattern of the pipe surfaces be similar, and complete dynamic similarity is obtained when

$$\frac{V_1 d_1 \rho_1}{\mu_1} = \frac{V_2 d_2 \rho_2}{\mu_2} = (N_R)_1 = (N_R)_2$$

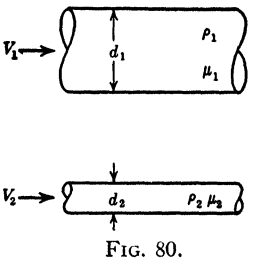


FIG. 80.

Here, again, it is immaterial which fluids are involved; complete dynamic similarity is obtained when the Reynolds numbers of the two flows are the same.[1]

It has been shown (Art. 25) that the laminar flow regime is defined by low values of the Reynolds number and that low Reynolds numbers indicate that inertia forces are small compared to those of viscosity. For laminar flow, pressure forces are relatively large, but, owing to large resistance, fluid motion is slow and inertia forces may be neglected. Complete dynamic similarity is defined in laminar flow by

$$\left(\frac{F_P}{F_V}\right)_p = \left(\frac{F_P}{F_V}\right)_m = \left(\frac{pl}{\mu V}\right)_p = \left(\frac{pl}{\mu V}\right)_m$$

an equation whose shape is confirmed by equation 32, one of the laws of laminar motion between parallel plates.

The laws of ship-model testing were first developed and used by William Froude in England about 1870. In this specialized field of engineering the problems of similarity are different from those presented above, but the fluid phenomena and reasoning involved will find many other useful engineering applications. In this problem the fluids suffer inappreciable compression during flow, and the elasticity forces may be neglected. If the models for testing are not extremely small the forces of surface tension are entirely negligible, leaving the forces of pressure, inertia, viscosity, and gravity to be considered.

As a ship moves through the free surface of a liquid it encounters resistance due to skin friction and to pressure variation, like a sub-

[1] The significance of this simple statement should be fully appreciated. Complete dynamic similarity implies similarity of the complex turbulent flow processes in the two pipes.

merged object (Art. 28). For a surface vessel the pressures over the hull are determined by the Bernoulli equation applied to the stream-tubes adjacent to the hull. This pressure variation, however, is manifested by a rise or depression of the liquid surface since the pressure at a point below the surface is related to its depth by the static law

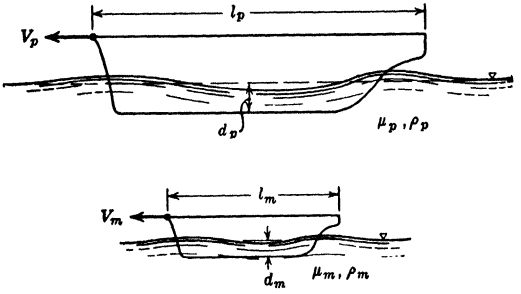


FIG. 81.

$p = wh$. The shape of the water surface adjacent to a surface vessel becomes that of Fig. 81, and, from the static law, the forces of pressure (p) become equivalent to those of gravity (wh). Therefore, pressure forces are eliminated from the problem and complete dynamic similarity is defined by the simultaneous equations

$$\begin{cases} \left(\frac{F_I}{F_G}\right)_p = \left(\frac{F_I}{F_G}\right)_m = \left(\frac{V^2}{lg}\right)_p = \left(\frac{V^2}{lg}\right)_m = (N_F)_p = (N_F)_m \\ \left(\frac{F_I}{F_V}\right)_p = \left(\frac{F_I}{F_V}\right)_m = \left(\frac{Vl\rho}{\mu}\right)_p = \left(\frac{Vl\rho}{\mu}\right)_m = (N_R)_p = (N_R)_m \end{cases}$$

Solution of these equations results in

$$\frac{\nu_p}{\nu_m} = \left(\frac{l_p}{l_m}\right)^{\frac{2}{3}}$$

indicating that a relation between the kinematic viscosities of the fluids involved is determined when the model scale is selected. This means (1) that a fluid for the towing basin must be found whose kinematic viscosity is a certain proportion of that of water, or (2) that if water is used in the towing basin the model scale must be unity, resulting in a full-scale model! This fact proves an unsurmountable obstacle to complete dynamic similarity for ship models and necessitates a

compromise between the Reynolds and Froude laws. This compromise is effected by obtaining "incomplete dynamic similarity" by making the Froude numbers in model and prototype the same and correcting the test results by experimental data dependent upon the Reynolds law. This method of treatment is justified since the flow conditions resulting from viscosity are small compared to those resulting from the wave pattern which is an inertia-gravity phenomenon.

Illustrative Problems

Water flows at 86° F in a 3-in. pipe line at a velocity of 5 ft/sec. With what velocity must linseed oil flow in a 1-in. pipe line at the same temperature for the two flows to be dynamically similar?

The Reynolds numbers for the two flows are the same.

$$\frac{5 \times \frac{3}{12} \times \frac{62.4}{32.2}}{0.00001667} = \frac{V \times \frac{1}{12} \times \frac{62.4}{32.2} \times .93}{0.000692}; \quad V = 37.2 \text{ ft/sec}$$

A surface vessel of 500-ft length is to be tested by a model 10 ft long. If the vessel travels at 25 mph, at what speed must the model move in order to have approximate similarity between model and prototype?

For incomplete similarity the Froude numbers are the same in model and prototype.

$$\frac{\left(25 \times \frac{5280}{3600}\right)^2}{500 \times 32.2} = \frac{V^2}{10 \times 32.2}; \quad V = 518 \text{ ft/sec}$$

31. Dimensional Analysis. Another useful tool of modern fluid mechanics and a necessary adjunct to the principle of similarity is that field of mathematics known as "dimensional analysis," the mathematics of the dimensions of quantities.

The methods of dimensional analysis are built up on the principle of dimensional homogeneity which states that an equation expressing a physical relationship between quantities must be dimensionally homogeneous; i.e., the dimensions of each side of the equation must be the same. This principle has already been utilized in Chapter I in obtaining the dimensions of mass density and kinematic viscosity, and it has been recommended as a valuable means of checking engineering calculations. Now, further investigation of the principle will reveal that it affords a means of constructing physical equations from a knowledge of the variables involved and their dimensions.

Before examining the methods of dimensional analysis, recall that there are two different systems by which the dimensions of physical quantities may be expressed. These systems are the force-length-time system and the mass-length-time system. The former system, generally preferred by engineers, becomes the familiar "foot-pound-second" system when expressed in English dimensions; the latter system in English dimensions becomes the "foot-slug-second" system. The latter system is generally preferred in dimensional analysis, and, since the student is familiar with the former system, the use of the latter will serve to develop versatility in the use of dimensions.

A summary of the fundamental quantities of fluid mechanics and their dimensions in the various systems is given in Table VI, the conventional system of capital letters being followed to indicate the dimensions of quantities. The basic relation between the force-length-time and mass-length-time systems of dimensions is given by the Newtonian law, force or weight = (Mass) × (Acceleration) and, therefore, dimensionally,

$$F = M\frac{L}{T^2}$$

from which the dimensions of any quantity may be converted from one system to the other.

To illustrate the mathematical steps in a simple dimensional problem, consider the familiar equation of fluid statics

$$p = wh$$

but assume that the dimensions of w and h are known and those of p unknown. The dimensions of p can be only some combination of M, L, and T, and this combination may be discovered by writing the equation dimensionally as

Unknown dimensions of p = (Dimensions of w) × (Dimensions of h)

or

$$M^aL^bT^c = \left(\frac{M}{L^2T^2}\right) \times (L)$$

in which a, b, and c are unknowns. The principle of dimensional homogeneity being applied, the exponents of *each* of the quantities is the same on each side of the equation, giving

$$a = 1, \quad b = -2 + 1 = -1, \quad c = -2$$

TABLE VI

DIMENSIONS OF FUNDAMENTAL QUANTITIES USED IN FLUID MECHANICS

Quantity	Symbol	English Engineering Dimensions	Force-Length-Time Dimensions	Mass-Length-Time Dimensions
Acceleration	a	ft/sec^2	L/T^2	L/T^2
Acceleration due to gravity	g	ft/sec^2	L/T^2	L/T^2
Area	A	ft^2	L^2	L^2
Density	ρ	lb sec^2/ft^4	FT^2/L^4	M/L^3
Force	F	lb	F	ML/T^2
Kinematic viscosity	ν	ft^2/sec	L^2/T^2	L^2/T
Length	l	ft	L	L
Mass	M	lb sec^2/ft	FT^2/L	M
Power	P	ft lb/sec	FL/T	ML^2/T^3
Pressure	p	lb/ft^2	F/L^2	M/LT^2
Rate of flow	Q	ft^3/sec	L^3/T	L^3/T
Specific weight	w	lb/ft^3	F/L^3	M/L^2T^2
Time	t	sec	T	T
Velocity	V	ft/sec	L/T	L/T
Viscosity	μ	lb sec/ft^2	FT/L^2	M/LT
Weight	W	lb	F	ML/T^2
Weight rate of flow	G	lb/sec	F/T	ML/T^3

whence

$$\text{Dimensions of } p = ML^{-1}T^{-2} = \frac{M}{LT^2}$$

It is obvious, of course, that this result might have been obtained more directly by cancellation of L on the right-hand side of the equation, for this has been, and will continue to be, the usual method of obtaining the unknown dimensions of a quantity. It is of utmost importance, however, to note the mathematical steps which lie unrevealed in this hasty cancellation, if the basis of dimensional analysis is to be understood.

The above methods may now be used in quite another and more important way. To illustrate by another familiar example, suppose that it is known that the power P, which can be derived from a hydraulic motor, is dependent upon the rate of flow through the motor Q, the specific weight of the fluid flowing w, and the unit energy E which is given up by every pound of fluid as it passes through the

machine. Suppose that the relation between these four variables is unknown but it is known that these are the *only* variables involved in the problem.[2] With this meager knowledge the following mathematical statement may be made:

$$P = f(Q, w, E)$$

From the principle of dimensional homogeneity it is obvious that the quantities involved cannot be added or subtracted since their dimensions are different. This principle limits the equation to a combination of products and quotients of powers and roots of the quantities involved, which may be expressed in the general form

$$P = CQ^a w^b E^c$$

in which C is a dimensionless constant which may exist in the equation but cannot, of course, be obtained by dimensional methods. Writing the equation dimensionally

$$\frac{ML^2}{T^3} = \left(\frac{L^3}{T}\right)^a \left(\frac{M}{L^2T^2}\right)^b (L)^c$$

equations are obtained in the exponents of the dimensions as follows:

$$M : 1 = b$$

$$L : 2 = 3a - 2b - c$$

$$T : -3 = -a - 2b$$

whence

$$a = 1, \quad b = 1, \quad c = 1$$

and resubstitution of these values in the above equation gives

$$P = CQwE$$

The shape of the equation (confirmed by equation 17) has, therefore, been derived *without physical analysis* solely from consideration of the dimensions of the quantities which were known to enter the problem. The magnitude of C may be obtained either (1) from a physical analysis of the problem, or (2) from experimental measurements of P, Q, w, and E.

From the above problem it appears that in dimensional analysis only three equations can be written since there are only three funda-

[2] Note that experience and analytical ability in determining the relevant variables are necessary before the methods of dimensional analysis can be successfully applied.

mental dimensions: M, L, and T. This fact limits the completeness with which a problem with more than three unknowns may be solved, but does not limit the utility of dimensional analysis in obtaining the shape of the equation. This point may be illustrated by considering a more complex problem of fluid mechanics, that of the calculation of the drag of a surface vessel, and in this problem it may also be observed how the similarity principle may be utilized in interpreting the results. Considering the surface vessel of Fig. 81, having a certain shape and draft d, the force [3] D, necessary to tow or propel the ship will depend upon the size of the ship (characterized by its length, l) the viscosity μ, and density ρ of the fluid in which the ship moves, the velocity of motion V, and the acceleration due to gravity g, since it has been shown in Art. 30 that the wave pattern is a gravity phenomenon. Thus, with no further knowledge than the variables involved in the problem, an equation may be written

$$D = f(l, \rho, \mu, V, g)$$

which for dimensional reasons must have the shape

$$D = Cl^a \rho^b \mu^c V^d g^e$$

and the equation of the dimensions of the terms is

$$\frac{ML}{T^2} = (L)^a \left(\frac{M}{L^3}\right)^b \left(\frac{M}{LT}\right)^c \left(\frac{L}{T}\right)^d \left(\frac{L}{T^2}\right)^e$$

resulting in the three equations of the exponents of M, L, and T

$$M : 1 = b + c$$

$$L : 1 = a - 3b - c + d + e$$

$$T : -2 = -c - d - 2e$$

whence

$$b = 1 - c, \quad d = 2 - c - 2e, \quad a = 2 + e - c$$

and substituting these values in the second equation

$$D = Cl^{2+e-c} \rho^{1-c} \mu^c V^{2-c-2e} g^e$$

and by collecting terms

$$D = C\left(\frac{V^2}{lg}\right)^{-e} \left(\frac{Vl\rho}{\mu}\right)^{-c} \rho l^2 V^2$$

[3] The force, D, is the equal and opposite of the total drag of the ship.

But

$$N_F = \frac{V^2}{lg} \quad \text{and} \quad N_R = \frac{Vl\rho}{\mu}$$

allowing the equation to be written in the more general form

$$D = f(N_F, N_R)\rho l^2 V^2$$

The drag of objects moving through a fluid is usually expressed by

$$D = C_D l^2 \frac{\rho V^2}{2}$$

in which C_D is a dimensionless "drag coefficient," the magnitude and properties of which are usually determined by experiment. Comparison of the last two equations reveals that

$$C_D = 2f(N_F, N_R) = f'(N_F, N_R)$$

showing without experiment, but *from dimensional analysis alone*, that the drag coefficient depends upon the Froude and Reynolds numbers.

The principles of dynamic similarity have demonstrated that the flow picture about a surface vessel is completely similar to the flow picture about its model if

$$(N_F)_{\text{prototype}} = (N_F)_{\text{model}}$$

and

$$(N_R)_{\text{prototype}} = (N_R)_{\text{model}}$$

but since

$$C_D = f'(N_F, N_R)$$

it is evident that one of the results of obtaining complete dynamic similarity between a model and prototye is the equality of the drag coefficients in the model and prototype. Thus the fundamental reason for obtaining dynamic similarity between a model and its prototype is to cause their dimensionless coefficients to be the same, allowing them to be measured in the model and used for the prototype.

BIBLIOGRAPHY

SIMILARITY

A. H. Gibson, "The Principle of Dynamic Similarity with Special Reference to Model Experiments," *Engineering*, Vol. 117, 1924, pp. 325, 357, 391, 422.

A. C. CHICK, "The Principle of Similitude," *Hydraulic Laboratory Practice*, p. 796, A.S.M.E. 1929.

K. C. REYNOLDS, "Notes on the Laws of Hydraulic Similitude as Applied to Experiments with Models," *Hydraulic Laboratory Practice*, p. 759, A.S.M.E., 1929.
O. G. TIETJENS, "Use of Models in Aerodynamics and Hydrodynamics," *Trans. A.S.M.E.*, Vol. 54, 1932, p. 225.

DIMENSIONAL ANALYSIS

J. R. FREEMAN, "Introduction," p. 775, *Hydraulic Laboratory Practice*, A.S.M.E., 1929.
A. C. CHICK, "Dimensional Analysis," p. 782, *Hydraulic Laboratory Practice*, A.S.M.E., 1929.
E. BUCKINGHAM, "Model Experiments and the Forms of Empirical Equations," *Trans. A.S.M.E.*, Vol. 37, 1915, p. 263.
P. W. BRIDGMAN, *Dimensional Analysis*, Yale University Press, 1922.

PROBLEMS

234. An airplane wing of chord length 10 ft moves through still air at 60° F and 14.7 lb/in.^{2} at a speed of 200 mph. A 1 : 20 scale model of this wing is placed in a wind tunnel, and dynamic similarity between model and prototype is desired. (*a*) What velocity is necessary in a tunnel where the air has the same pressure and temperature as that in flight? (*b*) What velocity is necessary in a variable-density wind tunnel where pressure is 200 lb/in.^{2} abs and temperature 60° F? (*c*) At what speed must the model move through water (60° F) for dynamic similarity?

235. An airship 600 ft long is to be tested by a 1 : 100 scale model. If the ship moves at 80 mph and the wind-tunnel velocity is 60 mph, calculate model and flight Reynolds numbers, assuming that both tunnel and flight air is the same (14.7 lb/in.^{2}, 60° F).

236. A submerged submarine moves at 10 mph. At what theoretical speed must a 1 : 20 model be towed for dynamic similarity between model and prototype, assuming sea water and towing-tank water the same?

237. It is desired to obtain dynamic similarity between 2 cfs of water at 50° F flowing in a 6-in. pipe and linseed oil flowing at a velocity of 30 ft/sec at 90° F. What size of pipe is necessary for the linseed oil?

238. The flow of air in a 2-in. pipe at 10 lb/in.^{2} and 60° F is to be similar to the water flow of the preceding problem. If barometer is standard, what air velocity is required?

239. Water flows at 60° F in a 3-in. pipe at 5 ft/sec. What velocity must water of the same temperature have in a 6-in. pipe for the two pipe flows to be dynamically similar?

240. Water (60° F) flows in a 2-in. pipe at 3 ft/sec. What velocity must glycerine at 80° F have in a 6-in. pipe for the two flows to be dynamically similar?

241. When castor oil flows at 60° F in a 2-in. horizontal pipe line at 10 ft/sec, a pressure drop of 320 lb/in.^{2} occurs in 200 ft of pipe. Calculate the pressure drop in the same length of 1-in. pipe when linseed oil at 100° F flows therein at a velocity of 1 ft/sec.

242. A ship 200 ft long is to be tested by a 1 : 50 scale model. If the ship is to travel at 30 mph, at what speed must the model be towed to obtain incomplete dynamic similarity with its prototype?

243. A ship model 3 ft in length is tested in a towing basin at a speed of 3 ft/sec. To what ship velocity does this speed correspond if the ship has a length of (*a*) 200 ft, (*b*) 400 ft?

244. The discharge of a perfect fluid through an orifice under a static head is an inertia-gravity phenomenon and one to which the Froude law may be applied. Using such an orifice and a geometrically similar model of the same, derive ratios between the following quantities in model and prototype (in terms of the head): velocity, rate of flow, horsepower of jet.

245. By dimensional analysis prove that: Kinetic energy = constant $\times MV^2$.

246. By dimensional analysis prove that: Centrifugal force = constant $\times MV^2/r$.

247. By dimensional analysis prove that: G = constant $\times AwV$.

248. Prove by dimensional analysis that a body of mass M and radius of gyration r, rotating at angular velocity ω, possesses kinetic energy given by

$$\text{Kinetic energy} = \text{constant} \times Mr^2\omega^2$$

249. Prove by dimensional analysis that: $w = p/RT$.

250. By dimensional analysis, prove that the force F necessary to accomplish a change ΔV in the velocity of a mass M in time t is given by

$$F = \text{constant} \times \frac{M\Delta V}{t}$$

251. By dimensional analysis, prove that: Pressure drop = constant $\times \mu V/l$ in laminar flow. (See equation 32 and Art. 30.)

CHAPTER VI

FLUID FLOW IN PIPES

The problems of fluid flow in pipe lines — the prediction of rate of flow through pipes of given characteristics, the calculation of energy losses therein, etc. — have wide application in engineering practice; they afford an opportunity of applying many of the foregoing principles to fluid flows of a comparatively simple and controlled nature.

32. Energy Relationships. The flow of a real fluid differs from that of a perfect fluid in that energy in the real fluid is continually converted into heat through the processes of turbulence and friction, brought about by the existence of viscosity. Therefore the energy equations of Art. 20 must be modified for application to the real fluid by the introduction of a lost energy term. This being designated as E_L (foot-pounds per pound), or as the "lost head," h_L (feet), it is obvious from previous reasoning that

$$E_L = h_L$$

Introducing the lost energy to the various energy equations, the general energy equation 14

$$I_1 + \frac{p_1}{w_1} + \frac{V_1^2}{2g} + z_1 + 778\,E_H + E_M = I_2 + \frac{p_2}{w_2} + \frac{V_2^2}{2g} + z_2 \quad (14)$$

remains unchanged. This results from the fact that the heat energy generated by the turbulence and frictional processes is merely an exchange of energy between the terms of the equation and hence does not appear therein as a separate term. If we assume that no machine exists between the sections 1 and 2 of the streamtube $E_M = 0$, and write the above equation in differential form

$$778dE_H = dI + d\left(\frac{p}{w}\right) + d\left(\frac{V_2}{2g}\right) + dz$$

substituting for w its equivalent $1/v$, the equation becomes

$$778dE_H = dI + d\,(pv) + d\left(\frac{V^2}{2g}\right) + dz$$

or

$$778dE_H = dI + pdv + vdp + d\left(\frac{V^2}{2g}\right) + dz$$

Considering now the thermodynamic aspects of the problem, the total amount of heat added to every pound of flowing fluid will be the sum of that added from external sources and that generated by frictional processes; thus the total heat added to the fluid becomes

$$778dE_H + dh_L$$

which goes into changing internal energy and doing work upon the flowing fluid. Thus

$$778dE_H + dh_L = dI + pdv$$

Solving this equation simultaneously with the above general energy equation yields

$$vdp + d\left(\frac{V^2}{2g}\right) + dz + dh_L = 0$$

which is the differential form of the Bernoulli equation for the flow of all fluids.

For compressible fluids, the equation becomes, upon substitution of $1/w$ for v and integration,

$$\int_{p_2}^{p_1} \frac{dp}{w} + \frac{V_1^2}{2g} + z_1 = \frac{V_2^2}{2g} + z_2 + h_L \tag{37}$$

in which the evaluation of the integral term is dependent upon the variation of density with pressure.

For fluids which may be treated as incompressible there is no variation of density with pressure, and the integration may be carried out, giving

$$\frac{p_1}{w} + \frac{V_1^2}{2g} + z_1 = \frac{p_2}{w} + \frac{V_2^2}{2g} + z_2 + h_L \tag{38}$$

the familiar Bernoulli equation, modified to include the lost energy term, h_L.

33. General Mechanics of Fluid Flow in Pipe Lines. The meaning of lost head and energy in pipe flow can best be obtained from a study of the mechanics of fluid motion in circular pipes, similar to that of Art. 27. Figure 82 represents a section of a long, straight, uniform,

sloping circular pipe in which laminar or turbulent flow of an incompressible fluid is fully established.[1] Flow being assumed from section 1 to section 2, the Bernoulli equation (38) modified for lost head may be described graphically as indicated, and it is observed: (1) that the "pressure (hydraulic) grade line" must always slope downward in the direction of flow, and (2) that the vertical drop in this grade line between any two points must represent the lost head in the pipe between these two points.

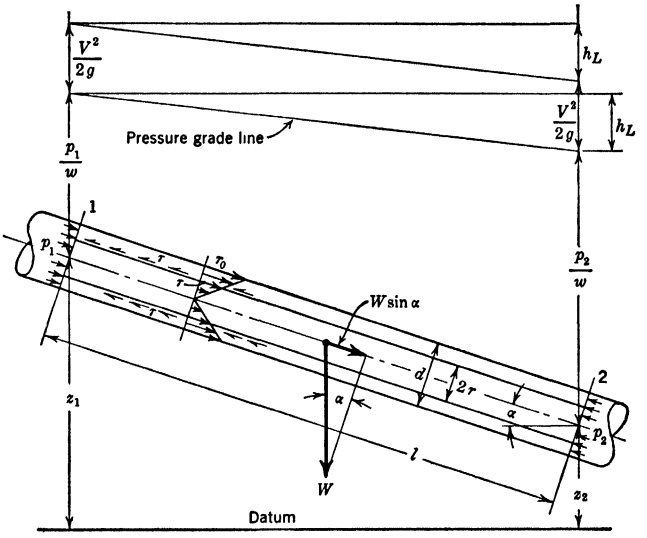


FIG. 82.

Since the pipe is of uniform size, the continuity principle requires motion in the pipe to take place at constant velocity, and constant-velocity motion in turn requires that the net force acting on any moving fluid mass be zero. The forces acting along the axis of the pipe on the fluid mass of length l and radius r are those of pressure on the ends, shear on the sides, and the component of weight in the direction of motion. The equation involving these forces may be seen from the figure to be

$$p_1 \pi r^2 - p_2 \pi r^2 + W \sin \alpha - \tau 2\pi r l = 0$$

or

$$(p_1 - p_2)\pi r^2 + \pi r^2 w l \sin \alpha - \tau 2\pi r l = 0$$

[1] That is, the section considered is a good distance from the pipe entrance or other source of eddying turbulence.

in which $\sin \alpha = \frac{z_1 - z_2}{l}$. Substituting this value and canceling πr,

$$\pi r(p_1 - p_2 + w(z_1 - z_2)) - \tau 2l = 0$$

and dividing by w

$$\pi r\left(\frac{p_1}{w} - \frac{p_2}{w} + z_1 - z_2\right) = \frac{2l\tau}{w}$$

But from the figure

$$h_L = \left(\frac{p_1}{w} - \frac{p_2}{w} + z_1 - z_2\right)$$

giving

$$\tau = \left(\frac{wh_L}{2l}\right) r \tag{39}$$

which shows that here, as between parallel plates (Art. 27), the distribution of shear stress in both flow regimes is linear, shear stress being maximum at the pipe wall and zero at the pipe center. At the wall the shear stress is designated by τ_o, and from the above general equation

$$\tau_o = \frac{wh_L}{2l}\frac{d}{2} = \frac{wdh_L}{4l}$$

The lost power P_L accompanying the lost head h_L may be calculated directly from

$$P_L = Qwh_L$$

but more fruitfully from the work done by the moving fluid against the shear stress, τ_o. Here

$$P_L = (\tau_o \pi dl)V$$

but

$$\tau_o = \frac{wdh_L}{4l}$$

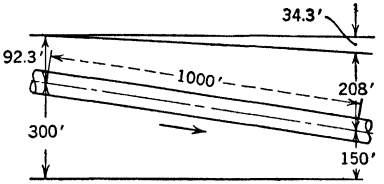
which when substituted above results in

$$P_L = \frac{wdh_L\, \pi dl V}{4l} = \left(\frac{\pi d^2}{4} V\right) wh_L = Qwh_L$$

as before.

ILLUSTRATIVE PROBLEM

Water flows through a section of a 12-in. pipe line 1000 ft long, running from elevation 300 to elevation 150. A pressure gage at elevation 300 reads 40 lb/in.^{2}, and one at elevation 150 reads 90 lb/in.^{2} Calculate loss of head, direction of flow, and shear stress at the wall of the pipe.



$$\left(\frac{p}{w}\right)_{300} = \frac{40 \times 144}{62.4} = 92.3 \text{ ft}$$

$$\left(\frac{p}{w}\right)_{150} = \frac{90 \times 144}{62.4} = 208.0 \text{ ft}$$

$$h_L = 300 + 92.3 - 150 - 208.0 = 34.3 \text{ ft}$$

Direction of flow: downward

$$\tau_o = \frac{wdh_L}{4l} = \frac{62.4 \times 1 \times 34.3}{4 \times 1000} = 0.535 \text{ lb/ft}^2$$

34. Laminar Flow. For laminar flow the relation between shear stress and velocity gradient,

$$\tau = \mu \frac{dv}{dy}$$

allows a simple theoretical derivation of the relationships between the other variables involved, the results of which are confirmed by experiment.

The general equation for the shear stress, τ, has been shown to be

$$\tau = \frac{wh_L}{2l} r$$

but in laminar flow τ is also given by [2]

$$\tau = -\mu \frac{dv}{dr}$$

[2] See footnote 6, page 115.

Equating these two expressions for τ,

$$-\mu \frac{dv}{dr} = \frac{wh_L}{2l} r$$

the variables of which may be separated

$$dv = -\frac{wh_L}{2\mu l} rdr$$

and the relation between velocity and radius obtained by integrating the equation between the center of the pipe, where $r = 0$ and $v = V_c$, and the variable radius, where $r = r$ and $v = v$. Integrating

$$\int_v^{V_c} dv = -\frac{wh_L}{2\mu l} \int_r^0 rdr = V_c - v = \frac{wh_L}{4\mu l} r^2 \tag{40}$$

showing that for laminar flow in circular pipes the velocity profile is a parabolic curve (Fig. 83) having a maximum velocity at the center of the pipe and reducing to zero at the walls.

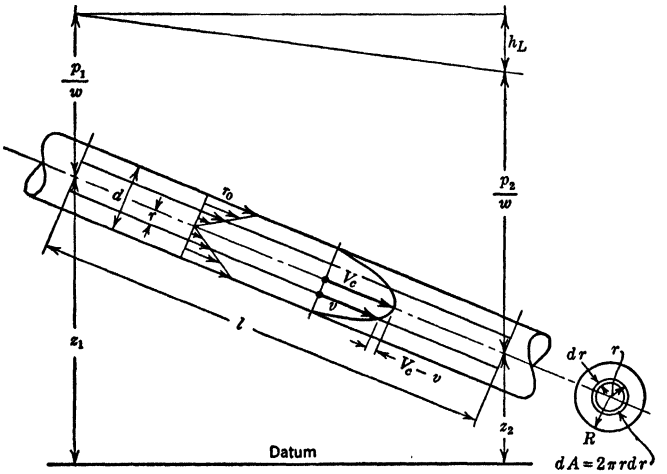


FIG. 83.

From the fact that, when $v = 0, r = R$, the fundamental equation of laminar flow may be obtained from equation 40

$$V_c = \frac{wh_L R^2}{4\mu l} = \frac{wh_L d^2}{16\mu l} \tag{41}$$

The relation between the average velocity and center velocity may

be derived by equating two expressions for the rate of flow, Q. Obviously,

$$Q = V\pi R^2$$

in which V is the average velocity. But

$$Q = \int^{A} vdA = \int_0^{R} v2\pi r dr$$

in which the variable velocity, v, may be shown from equation 40 to be given by

$$v = V_c\left(1 - \frac{r^2}{R^2}\right)$$

Substituting this value for v and integrating,

$$Q = \int_0^{R} V_c\left(1 - \frac{r^2}{R^2}\right)2\pi r dr = \frac{V_c}{2}\pi R^2$$

and equating the two expressions for Q

$$V = \frac{V_c}{2} \tag{42}$$

proving that the average velocity is always one-half of the center velocity for laminar flow in circular pipes.

Equation 41 may now be obtained in terms of the average velocity, V, by substituting $V_c = 2V$, giving

$$V = \frac{wh_L d^2}{32\mu l} \tag{43}$$

a more practical version of the basic laminar flow equation. Transposition of equation 43 allows calculation of lost head occurring in laminar flow from

$$h_L = \frac{32\mu l V}{wd^2} \tag{44}$$

and indicates that the head lost in laminar flow varies directly with the velocity of flow. By multiplying the right-hand side of equation 44 by $2V/2V$ and substituting ρg for w, equation 44 may be transformed for use in subsequent developments to

$$h_L = \frac{32\mu l V}{\rho g d^2}\cdot\frac{2V}{2V} = \left(\frac{64}{\frac{Vd\rho}{\mu}}\right)\frac{l}{d}\frac{V^2}{2g} = \frac{64}{N_R}\frac{l}{d}\frac{V^2}{2g} \tag{45}$$

Another statement of the equation for laminar flow may be derived in terms of the rate of flow, Q, by substituting for V in equation 43 the relation

$$V = \frac{Q}{\frac{\pi d^2}{4}}$$

which gives

$$Q = \frac{\pi d^4 w h_L}{128 \mu l} \tag{46}$$

This equation shows that in laminar flow the rate of flow, Q, which will occur in a circular pipe varies directly with the lost head and with the fourth power of the diameter but inversely with the length of pipe and viscosity of the fluid flowing. These facts of laminar flow were established experimentally, independently, and almost simultaneously by Hagen (1839) and Poiseuille (1840), and thus the law of laminar flow expressed by the above equations is termed the "Hagen-Poiseuille law."

The experimental verification, by Hagen, Poiseuille, and later investigators, of the above theoretical derivations serves to confirm the assumptions (1) that there is no velocity adjacent to a solid boundary and (2) that in laminar flow the shear stress is given by

$$\tau = \mu \frac{dv}{dy}$$

which were taken for granted in the above derivations.

Illustrative Problem

One hundred gallons of oil ($S = 0.90$ and $\mu = 0.0012$ lb sec/ft^2) flow per minute through a 3-in. pipe line. Calculate the center velocity, the lost head in 1000 ft. of this pipe, and the shear stress and velocity at a point 1 in. from the center line.

$$V = \frac{100}{60 \times 7.48} \frac{1}{\frac{\pi}{4}\left(\frac{3}{12}\right)^2} = 4.53 \text{ ft/sec}$$

$$N_R = \frac{Vd\rho}{\mu} = \frac{4.53 \times \frac{3}{12} \times (0.90 \times 1.935)}{0.0012} = 1645$$

Therefore laminar flow exists and $V_c = 2 \times 4.53 = 9.06$ ft/sec

$$h_L = \frac{64}{N_R}\frac{l}{d}\frac{V^2}{2g} = \frac{64}{1645} \times \frac{1000}{\frac{3}{12}} \times \frac{(4.53)^2}{2g} = 49.6 \text{ ft of oil}$$

$$v = V_c\left(1 - \frac{r^2}{R^2}\right) = 9.06\left[1 - \left(\frac{1}{1.5}\right)^2\right] = 5.03 \text{ ft/sec}$$

$$\tau = \frac{wh_L}{2l}r = \frac{62.4 \times 0.90 \times 49.6}{2 \times 1000}\frac{1}{12} = 0.116 \text{ lb/ft}^2$$

35. Dimensional Analysis of the Pipe-Friction Problem. Although Prandtl and von Karman have met with some success in a theoretical treatment of turbulent flow in pipes, the advanced mathematics involved places their analysis of the subject beyond the scope of an elementary textbook.

However, a good understanding of turbulent pipe flow may be attained from a study of experimental results, interpreted by the methods of dimensional analysis and similarity. A general investiga-

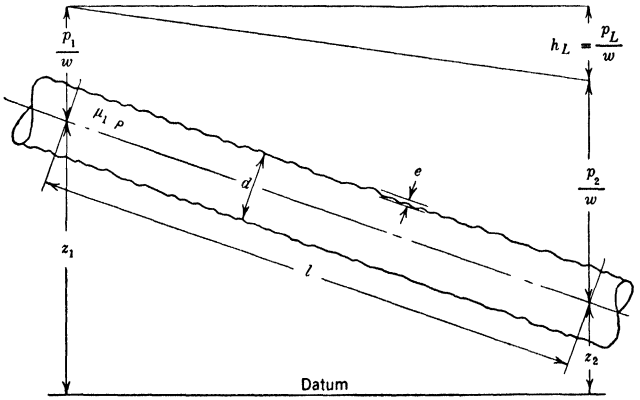


FIG. 84.

tion of pipe flow by these methods will, of course, lead to results which are equally applicable to laminar and turbulent flow and, therefore, will allow the inclusion not only of experimental results of tests in turbulent flow, but also of the relationships of laminar flow which were derived in Art. 34.

For a dimensional analysis of the lost head due to pipe friction, consider a rough pipe (Fig. 84), of diameter d, in which a fluid of viscosity μ and density ρ is flowing with an average velocity V. In a

length of this pipe, l, a lost head, h_L, is caused by pipe friction, and the loss of pressure p_L equivalent to this head loss is given by

$$p_L = wh_L$$

Assume that the roughness of the pipe has a definite pattern and that the average height of the roughness protuberances is e. Making a selection of the variables upon which the lost pressure, p_L, depends,

$$p_L = f(l, V, d, \mu, \rho, e)$$

and by the methods of dimensional analysis,

$$p_L = Cl^a V^b d^c \mu^x \rho^y e^z$$

Before writing the equations involving the dimensions of these quantities it may be predicted that

$$a = 1$$

or, in other words, the loss of head may be expected to vary directly with the length of pipe. The dimensional equation thus becomes

$$\frac{M}{LT^2} = (L)^1 \left(\frac{L}{T}\right)^b (L)^c \left(\frac{M}{LT}\right)^x \left(\frac{M}{L^3}\right)^y (L)^z$$

from which the equations of exponents are

$$M: \quad 1 = x + y$$

$$L: \quad -1 = 1 + b + c - x - 3y + z$$

$$T: \quad -2 = -b - x$$

Solving in terms of x and z

$$b = 2 - x$$

$$c = -1 - x - z$$

$$y = 1 - x$$

which, when substituted above, give

$$p_L = ClV^{2-x} d^{-1-x-z} \mu^x \rho^{1-x} e^z$$

or by arrangement of terms and insertion of 2/2

$$p_L = 2C\rho \frac{l}{d} \frac{V^2}{2} \left(\frac{\mu}{Vd\rho}\right)^x \left(\frac{e}{d}\right)^z$$

but since

$$p_L = wh_L$$

$$h_L = 2C\left(\frac{\mu}{Vd\rho}\right)^x\left(\frac{e}{d}\right)^z\frac{\rho}{w}\frac{l}{d}\frac{V^2}{2}$$

But $w/\rho = g$, $Vd\rho/\mu = N_R$, and since x and z are unknown the equation may be written in the general form

$$h_L = F\left(N_R, \frac{e}{d}\right)\frac{l}{d}\frac{V^2}{2g} \tag{47}$$

The equation used by Darcy (1857), Weisbach, and others for the calculation of lost head due to pipe friction was obtained experimentally from numerous tests on the flow of water in pipes. This so-called "Darcy equation" is the basis of pipe-friction calculations today and is

$$h_L = f\frac{l}{d}\frac{V^2}{2g} \tag{48}$$

in which f is called the "friction factor." The early hydraulic experimenters discovered that the friction factor was apparently dependent upon the pipe diameter d, the average velocity of flow V, and the roughness of the pipe, but with the use of dimensional analysis these facts and more may be safely predicted today without the aid of experiment, as may be seen from a comparison of the last two equations, which gives

$$f = F\left(\frac{Vd\rho}{\mu}, \frac{e}{d}\right) \tag{49}$$

Dimensional analysis has thus allowed isolation of all the variables upon which the friction factor depends and has shown that these variables exist in two dimensionless combinations, $Vd\rho/\mu$, the Reynolds number; and e/d, the "relative roughness"[3] of the pipe. Dimensional analysis has indicated furthermore a single general solution of the pipe-friction problem which is applicable to all fluids.

The physical significance of equation 49 may be stated briefly: The friction factors of pipes will be the same if their Reynolds numbers, roughness patterns, and relative roughnesses are the same. This statement being interpreted by the principle of similarity, it becomes

[3] "Relative" roughness since e/d expresses the size of the roughness protuberances relative to the diameter of the pipe.

evident that its basic meaning is: The friction factors of pipes are the same if their flow pictures are in every detail geometrically and dynamically similar.

Dimensional analysis cannot, of course, give the exact mathematical relationship between f, N_R, and e/d but indicates only that *there is a relationship* between these variables which may be found by a theoretical or experimental analysis. The former has been used in the case of laminar flow, resulting in equation 45

$$h_L = \frac{64}{N_R} \frac{l}{d} \frac{V^2}{2g}$$

which shows that

$$f = \frac{64}{N_R} \tag{50}$$

and that in laminar flow the friction factor f is independent of the surface roughness, bearing out the fact (Art. 26) that surface roughness can have no effect upon laminar flow.

For turbulent flow the following review of experimental results is necessary to obtain the relationship of f, N_R, and e/d.

36. Results of Pipe-Friction Experiments. The results of recent tests by Nikuradse [4] demonstrate perfectly the relationship of f, N_R, and e/d for both laminar and turbulent flow. In these tests geometrical

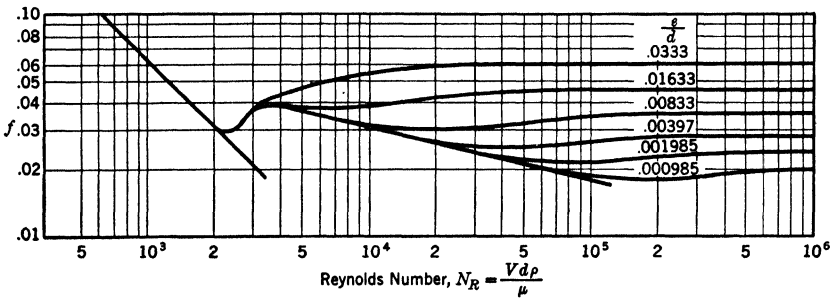


FIG. 85. Relation of friction factor, Reynolds number, and relative roughness for similar pipes.

similarity of the roughness patterns was obtained artificially by fixing a coating of uniform sand grains to the pipe wall. The results of the tests, plotted logarithmically on Fig. 85, illustrate the following important fundamentals.

[4] J. Nikuradse, "Stromungsgesetze in rauhen Rohren," *V. D. I. Forschungsheft*, 361, 1933.

1. The physical difference of the laminar and turbulent flow regimes is indicated by the change in the relationship of f to N_R at the critical Reynolds number of 2100.

2. The laminar regime is characterized by a single curve, given by the equation $f = 64/N_R$ for all surface roughness and thus shows that lost head in laminar flow is independent of surface roughness.

3. In turbulent flow a curve of f *vs.* N_R exists for every relative roughness, e/d, and from the shape of the curves it may be concluded that for rough pipes the roughness is more important than the Reynolds number in determining the magnitude of the friction factor.

4. At high Reynolds numbers, the friction factors of rough pipes become constant dependent wholly upon the roughness of the pipe and thus independent of the Reynolds number. Thus, for highly turbulent flow over rough surfaces the Darcy equation becomes

$$h_L = (\text{Constant}) \frac{l}{d} \frac{V^2}{2g}$$

showing that

$$h_L \propto V^2 \tag{51}$$

for turbulent flow over rough surfaces.

5. In turbulent flow a single curve expresses the relationship of f and N_R for all pipes which are hydraulically smooth, showing that surface roughness, when submerged in the laminar film, can have no effect on the friction factor and thus that lost head in smooth pipes is caused by viscosity effects alone. Using, for simplicity, the equation developed by Blasius,[5] expressing the relation between f and N_R for turbulent flow in smooth pipes,

$$f = \frac{0.3164}{(N_R)^{\frac{1}{4}}} \tag{52}$$

and substituting this in the Darcy equation

$$h_L = \frac{0.3164}{\left(\frac{Vd\rho}{\mu}\right)^{\frac{1}{4}}} \frac{l}{d} \frac{V^2}{2g}$$

it is evident that

$$h_L \propto V^{1.75} \tag{53}$$

[5] H. Blasius, *Forschungsarbeiten auf dem Gebiete des Ingenieurwesens*, 131, 1913.

indicating approximately how head loss varies with velocity for turbulent flow over smooth surfaces.

6. The series of curves for the rough pipes diverge from the smooth pipe curve as the Reynolds number increases. In other words, pipes which are smooth at low values of N_R become rough at high values of N_R. This may be explained by the thickness of the laminar film decreasing (Art. 38) as the Reynolds number increases, thus exposing smaller roughness protuberances to the turbulent region and causing the pipe to exhibit the properties of a rough pipe.

Unfortunately the excellent results of Nikuradse cannot be applied directly to engineering problems since the roughness patterns of commercial pipe are entirely different and much more variable than the artificial roughnesses used by Nikuradse. At present, because of this lack of uniformity, the surface roughnesses encountered in engineering practice cannot be classified practically by anything more than a descriptive statement. This fact gives an inevitable uncertainty to the selection of the friction factor in engineering problems, an uncertainty which may be overcome only by practical experience.

A practical summary of the friction factors for pipes of commercial roughness has been developed by Pigott.[6] A portion of this summary and the Blasius and Nikuradse curves for smooth pipes are presented in Fig. 86 and may be used in the solution of problems.

The accuracy of pipe-friction calculations is necessarily lessened by the unpredictable change in the roughness and friction factor due to the accumulation of dirt and rust on the pipe walls. This accumulation not only increases surface roughness but also reduces the effective pipe diameter as well, and may lead to an extremely large increase in the friction factor after the pipe has been given a long period of service.

Illustrative Problem

If 90 gpm of water at 68° F flow through a smooth 3-in. pipe line, calculate the loss of head in 3000 ft of the pipe.

$$V = \frac{90}{60 \times 7.48} \times \frac{1}{\frac{\pi}{4} \times \left(\frac{3}{12}\right)^2} = 4.08 \text{ ft/sec}$$

$$N_R = \frac{4.08 \times \frac{3}{12} \times 1.935}{0.000021} = 93{,}800$$

[6] R. J. S. Pigott, "The flow of fluids in closed conduits," *Mechanical Engineering*, Vol. 55, No. 8, p. 497, August, 1933.

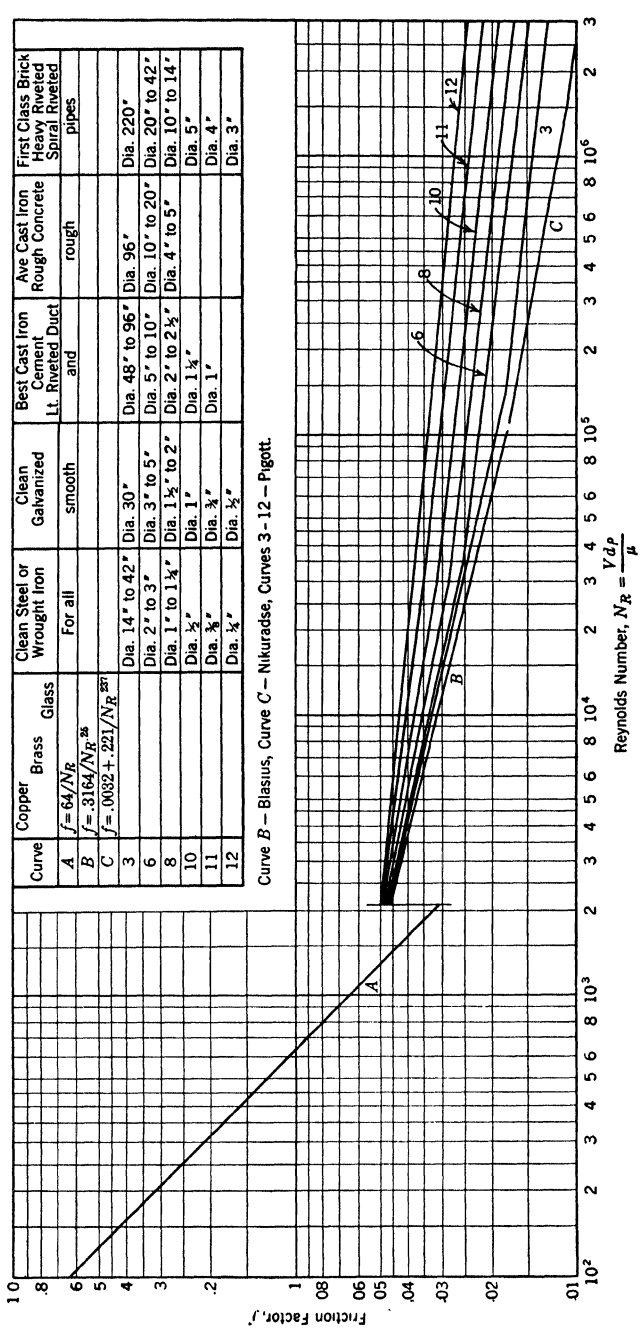


FIG. 86. Relation of friction factor, Reynolds number, and roughness for commercial pipes.

From the Plot of Fig. 86,

$$f = 0.0181$$

$$h_L = f \frac{l}{d} \frac{V^2}{2g} = 0.0181 \frac{3000}{\frac{3}{12}} \frac{(4.08)^2}{2g} = 56.1 \text{ ft}$$

37. Velocity Distribution in Circular Pipes — The Pipe Coefficient. For laminar flow in circular pipes it has been shown theoretically (Art. 34) and may be proved experimentally that the variation of velocity along a diameter follows a parabolic curve, and one of the characteristics of a parabolic velocity distribution in a circular pipe has been seen to be the fixed relationship

$$V_c = 2V$$

between the center velocity and average velocity. This equation may be written

$$\frac{V}{V_c} = \frac{1}{2}$$

in which V/V_c, the ratio of average to center velocity, is frequently called the " pipe coefficient " or " pipe factor."

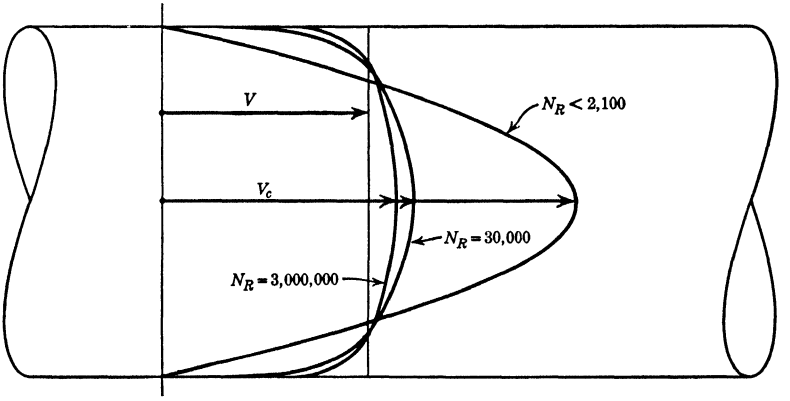


FIG. 87. Velocity distributions in circular pipes.[7]

In turbulent flow the curve of velocity distribution is not determined by viscous shear between moving layers, but depends upon the strength and extent of the turbulent mixing process. Turbulent mix-

[7] H. Rouse, "Modern Conceptions of the Mechanics of Fluid Turbulence," *Trans. A.S.C.E.*, Vol. 102, 1937, p. 463.

ing of fluid particles tends to cause them to move at the same velocity and thus the velocity distribution curve becomes increasingly flattened as the Reynolds number increases, as shown by the curves of Fig. 87, which are drawn for the same average velocity, V. A glance at these curves indicates that the pipe coefficient, V/V_c, increases with the Reynolds number and suggests a practical method of describing velocity distribution properties by the single curve (1) of Fig. 88. A supplementary curve (2) of pipe coefficient *vs.* $V_c d\rho/\mu$ is useful in obtain-

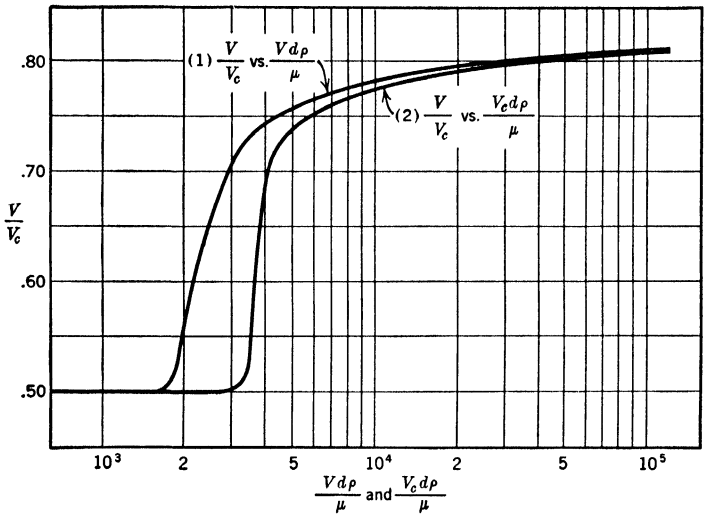


FIG. 88. Relation of pipe coefficient and Reynolds number.[8]

ing direct solutions of problems in which the center velocity is known and the pipe coefficient is to be found.

A relationship between pipe coefficient and friction factor may be obtained from the equation

$$V_c - V = 4.07\sqrt{\frac{\tau_o}{\rho}}$$

which was proposed by Prandtl[9] from the results of Nikuradse's experi-

[8] Data from T. E. Stanton and J. R. Pannell, "Similarity of Motion in Relation to the Surface Friction of Fluids," *Philosophical Transactions of the Royal Society*, A 214, 1914, p. 199.

[9] L. Prandtl, "Neuere Ergebnisse der Turbulenzforschung," *V. d. I. Zeit.*, Vol. 77, No. 5, Feb. 4, 1933.

ments. A more useful expression for τ_o may be calculated from the general equation

$$\tau_o = \frac{wdh_L}{4l}$$

since it is now known that h_L is given by

$$h_L = f\frac{l}{d}\frac{V^2}{2g}$$

Substituting this in the expression for τ_o

$$\tau_o = \frac{wd}{4l} f \frac{l}{d}\frac{V^2}{2g} = \frac{f}{8}\rho V^2 \tag{54}$$

or

$$\sqrt{\frac{\tau_o}{\rho}} = V\sqrt{\frac{f}{8}}$$

in which $\sqrt{\tau_o/\rho}$ is termed the " friction velocity." When this expression for $\sqrt{\tau_o/\rho}$ is substituted in Prandtl's equation above

$$\frac{V_c - V}{V} = \frac{V_c}{V} - 1 = 4.07\sqrt{\frac{f}{8}}$$

giving

$$\frac{V}{V_c} = \frac{1}{4.07\sqrt{\frac{f}{8}} + 1} \tag{55}$$

thus relating pipe coefficient and friction factor.

In deriving the Bernoulli equation from the principle of energy conservation for the perfect fluid (Art. 20), it was seen that the kinetic energy per pound of fluid flowing was given by $V^2/2g$. For the perfect fluid all fluid particles will pass a point in a circular pipe with the same velocity, causing the distribution of velocity to be uniform, as shown in Fig. 89. For the real fluid, however, the existence of a velocity distribution curve having a maximum velocity at the center of the pipe and no velocity at the wall will cause the term $V^2/2g$ to be an erroneous expression for the kinetic energy of the flow.

To demonstrate this fact, consider laminar flow in a circular pipe

(Fig. 89), where the velocity distribution curve is given by the simple equation

$$v = V_c\left(1 - \frac{r^2}{R^2}\right)$$

The power due to the kinetic energy of fluid passing with velocity v through the differential area dA is given by

$$P = dQw\frac{v^2}{2g} = v2\pi rdrw\frac{v^2}{2g}$$

which must be integrated to obtain the total kinetic energy of the flow.

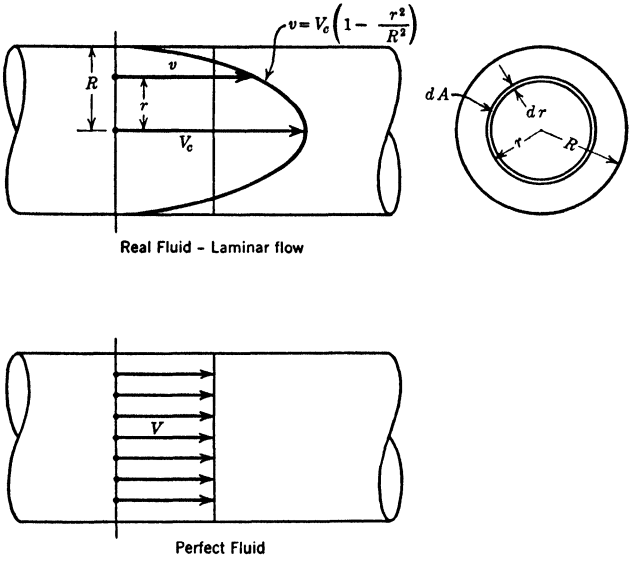


FIG. 89.

Substituting the above expression for v and integrating,

$$\int_0^P dP = \frac{\pi w V_c^3}{g}\int_0^R \left(1 - \frac{r^2}{R^2}\right)^3 rdr$$

results in

$$P = \frac{\pi R^2 V_c^3 w}{8g}$$

But

$$V_c = 2V$$

giving

$$P = (\pi R^2 V)w\frac{V^2}{g} = Qw\frac{V^2}{g}$$

Thus for laminar flow the kinetic energy term is not $V^2/2g$ but V^2/g, and, because of the existence of velocity variation across the pipe in real fluid flow, a correction term, α, must be introduced to the Bernoulli equation, giving

$$\frac{p_1}{w} + \alpha_1 \frac{V_1^2}{2g} + z_1 = \frac{p_2}{w} + \alpha_2 \frac{V_2^2}{2g} + z_2 + h_L$$

in which $\alpha = 2$ for laminar flow. In turbulent flow the flattening of the velocity distribution curve is an approach to the straight-line velocity distribution of the perfect fluid, and hence in turbulent flow the correction term α has a value close to unity, a magnitude of 1.05 being a satisfactory average value for ordinary turbulent flows.

The effect of the term α in many engineering calculations is entirely negligible since the magnitude of the $V^2/2g$ terms are frequently very small compared to the other terms of the Bernoulli equation and a slight change in the velocity-head terms will have no effect upon the final results. The use of the term α is, of course, not justified unless the other Bernoulli terms are known precisely and unless flow cross sections are chosen where known velocity distributions will exist.

38. Approximate Thickness of the Laminar Film. The approximate thickness of the laminar film may be established by the following simple analysis and approximations. Assume for simplicity that the film has a precise thickness, δ (Fig. 90), and that within the film the flow is wholly laminar. Let the velocity at the outer boundary of the film be designated by V_w. At the wall the shear stress is given by

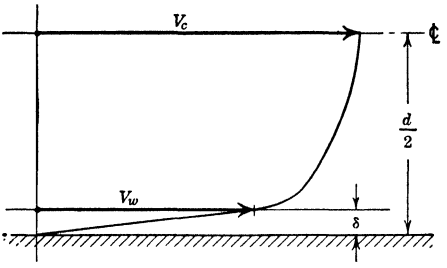


FIG. 90.

$$\tau_o = \mu \frac{dv}{dy}$$

But since δ is very small the velocity distribution within the film may be assumed linear. Thus

$$\frac{dv}{dy} = \frac{V_w}{\delta}$$

and

$$\tau_o = \mu \frac{V_w}{\delta}$$

But τ_o is also given (Art. 37) by

$$\tau_o = \frac{f}{8}\rho V^2$$

Equating the two expressions for τ_o and solving for δ

$$\delta = \frac{8\mu V_w}{f\rho V^2}$$

which, by insertion of d/d, may be written

$$\delta = \frac{8}{f}\frac{V_w}{V}\frac{\mu}{Vd\rho}d$$

and therefore

$$\frac{\delta}{d} = \frac{8}{f}\frac{V_w}{V}\frac{\mu}{Vd\rho} \tag{56}$$

The ratio V_w/V may be found from the relationship of von Karman [10]

$$\frac{V_w}{\sqrt{\frac{\tau_o}{\rho}}} = 11.6$$

for smooth pipes. But (Art. 37)

$$\sqrt{\frac{\tau_o}{\rho}} = V\sqrt{\frac{f}{8}}$$

Thus

$$\frac{V_w}{V} = 11.6\sqrt{\frac{f}{8}} = 4.1\sqrt{f}$$

which may be substituted in equation 56, giving

$$\frac{\delta}{d} = \frac{32.8}{N_R\sqrt{f}} \tag{57}$$

allowing the approximate thickness of the laminar film to be calculated and showing that the thickness of the film relative to the pipe diameter is dependent upon both friction factor and Reynolds number and decreases in thickness with increasing Reynolds number.

[10] Th. von Karman, "Turbulence and Skin Friction," *J. Aero. Sciences*, Vol. I, No. 1, p. 1, January, 1934.

39. Pipe Friction for Compressible Fluids. The calculation of pressure loss due to pipe friction when gases and vapors flow in insulated pipe lines is, in general, a rather complex process and therefore will not be treated exhaustively here. The complications will be evident upon examination of the flow of a gas in a perfectly insulated pipe. Although through the insulation no heat is added to or abstracted from the fluid flowing between sections 1 and 2, the expansion from pressure p_1 to pressure p_2 is not a reversible adiabatic process since heat is generated by fluid friction and is added to the flowing fluid. The expansion thus becomes a polytropic process, the nature of which depends upon the lost pressure, which is unknown. The solution of such a problem can be obtained only by a tedious trial-and-error procedure, applied to short lengths of the pipe.

However, a direct solution for the pipe-friction loss may be obtained for a perfect gas flowing *isothermally* in a pipe line. Isothermal fluid flow can occur only when the transfer of heat through the pipe walls and the addition of heat to the fluid from the pipe friction process are adjusted in such a manner that the temperature of the fluid remains constant. Such an adjustment of heat transfers is approximated naturally in uninsulated pipes where velocities are small and where temperatures inside and outside of the pipe are about the same; frequently the flow of gases in long pipe lines may be treated isothermally.

Gas flow in a uniform pipe line is characterized by the fact that the velocity does not remain constant but continually increases in the direction of flow, the drop in pressure along the line, caused by pipe friction, bringing about a continuous reduction in density in the direction of flow. From the continuity equation

$$G = AwV$$

it is evident that a decrease in specific weight must cause an increase in velocity since the weight flow G and the area A are both constant. The continual change of pressure, velocity, and specific weight as flow takes place necessitates writing the Bernoulli equation in differential form and subsequently integrating to obtain practical results. Neglecting the difference in the h terms, equation 37 may be written in differential form as

$$\frac{dp}{w} + \frac{VdV}{g} + dh_L = 0$$

and applied to the differentially small element of fluid shown in Fig. 91. Substituting the Darcy equation for the lost head term, this equation becomes

$$\frac{dp}{w} + \frac{VdV}{g} + f\frac{dl}{d}\frac{V^2}{2g}$$

Dividing by $V^2/2g$

$$\frac{2gdp}{wV^2} + 2\frac{dV}{V} + \frac{f}{d}dl = 0$$

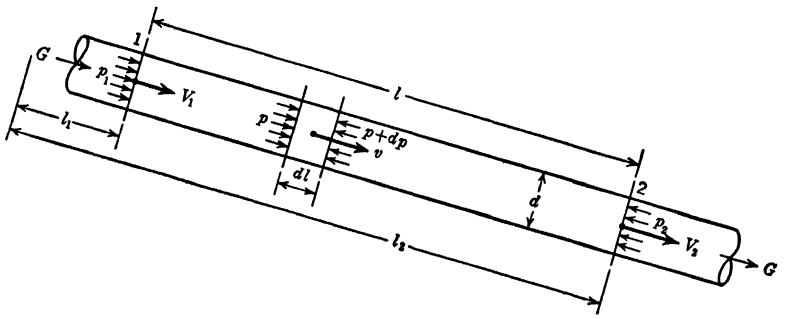


FIG. 91.

But from the continuity principle $V = G/Aw$, which, when substituted in the first term, gives

$$\frac{2gA^2w}{G^2}dp + 2\frac{dV}{V} + \frac{f}{d}dl = 0$$

The specific weight, w, is given by the equation of state of the gas $w = p/RT$, in which, for an isothermal process, T is constant. Substituting this expression for w in the first term, the equation becomes

$$\frac{2gA^2}{G^2RT}\int_{p_1}^{p_2} pdp + 2\int_{V_1}^{V_2}\frac{dV}{V} + \frac{f}{d}\int_{l_1}^{l_2} dl = 0$$

which may be integrated between the indicated limits, giving

$$p_1^2 - p_2^2 = \frac{G^2RT}{gA^2}\left[2ln\frac{V_2}{V_1} + f\frac{l}{d}\right] \tag{58}$$

and allowing the pressure p_2 to be calculated when the other variables are known. Theoretically the solution of the equation must be accomplished by trial since V_2 cannot be calculated until p_2 is known, but

usually the term $2ln(V_2/V_1)$ is so small in comparison to fl/d that it may be neglected, reducing the equation to

$$p_1^2 - p_2^2 = \frac{G^2RT}{gA^2} f \frac{l}{d} \tag{59}$$

thus making possible a direct solution.

The Reynolds number is, of course, necessary to obtain the friction factor, f. Although the velocity and density of the fluid change continually throughout the pipe, the Reynolds number of the flow remains constant and may be calculated as follows:

$$N_R = \frac{Vd\rho}{\mu} = \frac{Vdw}{\mu g}$$

but $V = G/wA$ which, when substituted above, gives

$$N_R = \frac{Gd}{\mu g A}$$

in which all the terms are constant for isothermal flow in a uniform pipe.

Compressible fluids may be frequently treated as incompressible in pipe-friction calculations if the pressure and density changes are not large; the lost head or pressure may be calculated from the Darcy equation

$$h_L = f \frac{l}{d} \frac{V^2}{2g}$$

which, under the above conditions, may be written

$$\frac{p_1 - p_2}{w_1} = f \frac{l}{d} \frac{V_1^2}{2g} \tag{60}$$

The limits of application of equation 60 may be seen by comparing equation 60 with equation 59. To accomplish this, substitute in equation 59 the following relations:

$$p_1^2 - p_2^2 = (p_1 - p_2)(p_1 + p_2)$$

$$\frac{G^2}{A^2} = V_1^2 w_1^2$$

which give

$$(p_1 - p_2)(p_1 + p_2) = w_1^2 RTf \frac{l}{d} \frac{V_1^2}{2g}$$

Rearranging and inserting 2/2 on the right-hand side of the equation,

$$\frac{p_1 - p_2}{w_1} = \left(\frac{2}{p_1 + p_2}\right) w_1 RTf \frac{l}{d} \frac{V_1^2}{2g}$$

Substituting p_1/RT for w_1, this equation becomes

$$\frac{p_1 - p_2}{w_1} = \left(\frac{2p_1}{p_1 + p_2}\right) f \frac{l}{d} \frac{V_1^2}{2g}$$

or

$$\frac{p_1 - p_2}{w_1} = \left(\frac{2}{1 + \frac{p_2}{p_1}}\right) f \frac{l}{d} \frac{V_1^2}{2g} \tag{61}$$

Comparison of equations 60 and 61 shows that equation 60 can be multiplied by a correction factor dependent upon the pressure ratio, p_2/p_1, to obtain the result given by equation 59. For a pressure ratio $p_2/p_1 = 0.96$, the magnitude of the correction factor is 1.02, indicating that an error of 2 per cent is incurred if density change is neglected and pressure drop calculated from equation 60. An allowable error of 2 per cent being assumed, it is apparent that equation 59 must be used when $p_2/p_1 < 0.96$ but that equation 60 will give satisfactory results when $p_2/p_1 > 0.96$.

Illustrative Problem

If 40 lb/min of air flow isothermally through a horizontal, smooth 3-in. pipe line at a temperature of 100° F, and the pressure at a point in this line is 50 lb/in.^{2}, abs, calculate the pressure in the line 2000 ft downstream from this point.

$$N_R = \frac{Gd}{\mu g A} = \frac{\frac{40}{60} \times \frac{3}{12}}{0.000000402 \times 32.2 \times \frac{\pi}{4}\left(\frac{3}{12}\right)^2} = 262{,}000$$

From the plot of Fig. 86,

$$f = 0.0145$$

$$p_1^2 - p_2^2 = \frac{G^2 RT}{gA^2} f \frac{l}{d}$$

$$(50 \times 144)^2 - p_2^2 = \frac{(\frac{40}{60})^2 \times 53.3 \times (100 + 460)}{32.2\left[\frac{\pi}{4}\left(\frac{3}{12}\right)^2\right]^2} 0.0145 \frac{2000}{\frac{3}{12}}$$

$$51{,}900{,}000 - p_2^2 = 19{,}860{,}000$$

$$p_2 = 5660 \text{ lb/ft}^2 = 39.3 \text{ lb/in.}^2 \text{ ab}$$

40. Pipe Friction in Non-Circular Pipes. Although the majority of pipes used in engineering practice are of circular cross section, occasions arise when calculations must be carried out on friction loss in rectangular passages and other conduits of non-circular form. The foregoing equations for circular pipes may be adapted to these special problems by the means of a new term, called the "hydraulic radius."

The hydraulic radius is defined as the *area of flow cross section divided by the wetted perimeter.* In a circular pipe of diameter d,

$$\text{Hydraulic radius } R = \frac{\frac{\pi d^2}{4}}{\pi d} = \frac{d}{4}$$

or

$$d = 4R$$

for a pipe of circular cross section.

This value may be substituted in the Darcy equation for lost head and into the expression for the Reynolds number with the following results:

$$h_L = \frac{f}{4}\frac{l}{R}\frac{V^2}{2g} \tag{62}$$

and

$$N_R = \frac{V4R\rho}{\mu} \tag{63}$$

from which the lost head in conduits of any form may be calculated with the aid of the plot of Fig. 86.

The calculation of lost head in non-circular conduits involves the calculation of the hydraulic radius, R, of the flow cross section and using the friction factor obtained on an "equivalent" circular pipe having a diameter d given by

$$d = 4R$$

In view of the complexities of laminar films, turbulence, roughness, shear stress, etc., it seems surprising at first that a circular pipe "equivalent" to a non-circular conduit may be obtained so easily, and it would, therefore, be expected that the method might be subject to certain limitations. The method gives satisfactory results when the problem is one of turbulent flow over rough surfaces, but if used for laminar flow large errors are introduced.

The foregoing facts may be justified theoretically by examining further the structure of the Darcy equation

$$h_L = \frac{f}{4}\frac{l}{R}\frac{V^2}{2g}$$

in which obviously

$$h_L \propto \frac{1}{R}$$

From the definition of the hydraulic radius, its reciprocal is the "wetted perimeter per unit of flow cross section" and is, therefore, an index of the extent of the rough surface in contact with the flowing fluid. The hydraulic radius may be safely used in the above equation when resistance to flow and head loss are primarily dependent upon the extent of the rough boundary surface, as for turbulent flow in which pipe friction phenomena are confined to a thin region adjacent to the boundary surface and thus vary with the size of this surface. In laminar flow, however, friction phenomena result from the viscosity properties of the fluid and are independent of surface roughness. The magnitude of the boundary surface plays a secondary role in these phenomena, and so in laminar flow the use of the hydraulic radius to obtain a circular pipe equivalent to a non-circular one is not possible.

Illustrative Problem

Calculate the loss of head and pressure drop when air at standard conditions (14.7 lb/in.^{2}, 60° F) flows through 200 ft of 18 in. by 12 in. smooth rectangular duct with an average velocity of 10 ft/sec. Sp. wt. of standard air = 0.0763 lb/ft.^{3}

$$p = \frac{18 \times 12}{2 \times 18 + 2 \times 12} = 3.6 \text{ in.} = 0.30 \text{ ft.}$$

$$N_R = \frac{V \times 4R \times \rho}{\mu} = \frac{10 \times 4 \times .30 \times \dfrac{.0763}{32.2}}{0.000000375} = 75{,}900$$

From the plot of Fig. 86,

$$f = 0.019$$

$$h_L = f\frac{l}{4R}\frac{V^2}{2g} = 0.019 \times \frac{2000}{4 \times .30} \times \frac{\overline{10}^2}{2g} = 49.2 \text{ ft of air}$$

$$p_L = wh_L = 0.0763 \times 49.2 = 5.82 \text{ lb/ft}^2 = 0.0405 \text{ lb/in}^2.$$

41. Pipe-Friction Calculations by the Hazen-Williams Method. In order to circumvent the difficulties encountered because surface roughness is a relative quantity, causing friction factors to be different in pipes having the same roughness but having different diameters, Hazen and Williams[11] proposed a formula in which the friction factor was a function of surface roughness only. The formula was originally proposed for the solution of hydraulic problems but should give correct results for the flow of any fluid provided that flow occurs at high Reynolds numbers. Although the formula is empirical and thus does not possess dimensional homogeneity it gives good results and is in general use by American engineers.

The shape of the Hazen-Williams formula compares favorably with that of the "Chezy equation," which may be derived from the Darcy equation as follows. The Darcy equation states

$$h_L = \frac{f}{4}\frac{l}{R}\frac{V^2}{2g}$$

which may be solved for V, giving

$$V = \sqrt{\frac{8g}{f}}\sqrt{R}\sqrt{\frac{h_L}{l}}$$

in which $\sqrt{8g/f} = C$, the "Chezy coefficient," and $h_L/l = S$, the lost head per foot of pipe; substitution of these values results in

$$V = C\sqrt{RS} = CR^{0.5}S^{0.5} \tag{64}$$

as proposed by Chezy (1775).

Hazen and Williams found that experimental results were best satisfied by the formula

$$V = 1.318C_{hw}\ R^{0.63}S^{0.54} \tag{65}$$

Values of the coefficient C_{hw} are given in Table VII; it is obvious that here again experience is necessary in the selection of coefficients if reliable results are to be obtained.

The advantages and disadvantages of the Hazen-Williams method are evident from the formula and foregoing discussion. Among the advantages are: (1) the coefficient depends only upon roughness, (2) the effect of roughness and the other variables upon the velocity of

[11] A. Hazen and G. S. Williams, *Hydraulic Tables*, Third edition, 1920, John Wiley & Sons.

TABLE VII

HAZEN-WILLIAMS COEFFICIENT, C_{hw}

Pipes extremely straight and smooth	140
Pipes very smooth	130
Smooth wood, smooth masonry	120
New riveted steel, vitrified clay	110
Old cast iron, ordinary brick	100
Old riveted steel	95
Old iron in bad condition	60–80

flow and capacity of pipe are given directly by the formula. Its disadvantages are: (1) its lack of dimensional homogeneity, and (2) the impossibility of applying it to the flow of all fluids under all conditions. Although the formula appears cumbersome with its fractional exponents, this disadvantage is overcome in engineering practice by the use of tables and diagrams in its solution.

ILLUSTRATIVE PROBLEM

If 90 gpm of water flow through a smooth 3-in. pipe line, calculate the loss of head in 3000 ft of this pipe.

$$V = \frac{90}{60 \times 7.48} \times \frac{1}{\frac{\pi}{4}\left(\frac{3}{12}\right)^2} = 4.08 \text{ ft/sec.}$$

$$R = \frac{\frac{\pi}{4}\left(\frac{3}{12}\right)^2}{\pi\left(\frac{3}{12}\right)} = 0.0625 \text{ ft.}$$

From Table VII,

$$C_{hw} = 140$$

$$4.08 = 1.318 \times 140 \times (0.0625)^{0.63} S^{0.54}$$

$$S = 0.0218 = \frac{h_L}{l} = \frac{h_L}{3000}, \quad h_L = 65.3 \text{ ft}$$

Compare results with the illustrative problem of Art. 36.

42. Minor Losses in Pipe Lines. Into the category of minor losses in pipe lines fall those losses incurred by change of section, bends, elbows, valves, and fittings of all types. Although in long pipe lines these are distinctly "minor" losses and can often be neglected

without serious error, in shorter pipe lines an accurate knowledge of their effects must be known for correct engineering calculations.

The general aspects of minor losses in pipe lines may be obtained from a study of the flow phenomena about an abrupt obstruction placed in a pipe line (Fig. 92), which creates flow conditions typical of those which consume energy and cause minor losses. Minor losses generally result from changes of velocity, velocity increases causing small losses but decreases of velocity causing large losses because of the creation of eddying turbulence. In Fig. 92, energy is consumed

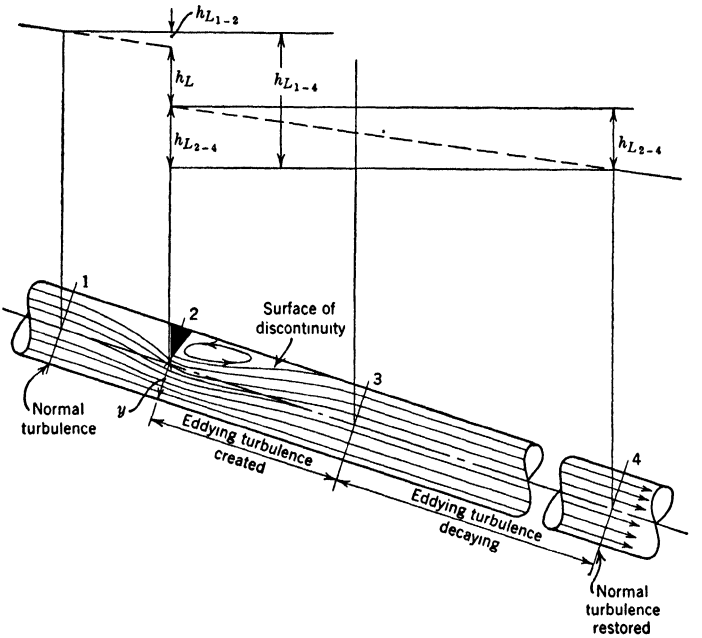


FIG. 92.

in the creation of eddies as the fluid decelerates between sections 2 and 3, and this energy is dissipated in heat as the eddies decay between sections 3 and 4. Minor losses in pipe flow are, therefore, accomplished in the pipe downstream from the source of the eddies, and the pipe friction processes in this length of pipe are hopelessly complicated by the superposition of eddying turbulence upon the normal turbulence pattern. To make minor loss calculations possible it is necessary to assume separate action of the normal turbulence and eddying turbulence although in reality a complex combination and interaction of the two processes exists. Assuming the processes separate allows

calculation of the losses due to normal pipe friction $h_{L_{1-2}}$ and $h_{L_{2-4}}$, and also permits the loss, h_L, due to the obstruction alone, to be assumed concentrated at section 2. This is a great convenience for engineering calculations since the total lost head in a pipe line may be obtained by a simple addition of pipe friction and minor losses without considering the above complications.

In order that they may be inserted readily into the Bernoulli equation, minor losses are expressed by

$$h_L = K_L \frac{V^2}{2g}$$

in which K_L is a coefficient usually determined by experiment. A dimensional analysis of the flow past an obstruction of a given shape (Fig. 92) leads to the conclusion that

$$K_L = f\left(\frac{vd\rho}{\mu}, \frac{e}{d}, \frac{y}{d}\right)$$

or if the shape is changed and the conclusion made more general,

$$K_L = f\left(\frac{vd\rho}{\mu}, \text{roughness, shape}\right)$$

The effect of surface roughness upon minor losses is generally very small since the obstruction is usually short and has little contact with the flowing fluid; however the large irregularities of the obstruction act in similar fashion to the roughness protuberances of a very rough pipe, and Nikuradse's tests (Fig. 85) show that for turbulent flow the friction factors of such pipes are practically independent of the Reynolds number of the flow. From these two statements it may be concluded that for turbulent flow the experimental coefficients, K_L, for most minor losses are dependent primarily upon the shape of the obstruction and are practically independent of roughness and Reynolds number. This conclusion is borne out by experiment and is useful in the interpretation of the following experimental results which were obtained by hydraulic tests; since the hydraulic tests were all made at high Reynolds numbers it may be concluded that these results are adaptable to other fluids at high Reynolds numbers as well.

When a **sudden enlargement** of section (Fig. 93) occurs in a pipe line, a rapid deceleration in flow takes place accompanied by the characteristic eddying turbulence, which may persist in the larger pipe

for a distance of 50 pipe diameters before dying out and allowing restoration of normal turbulence pattern.

In Fig. 92, the distance between the two pressure grade lines at section 2 proved to be the loss of head due to the obstruction. For the

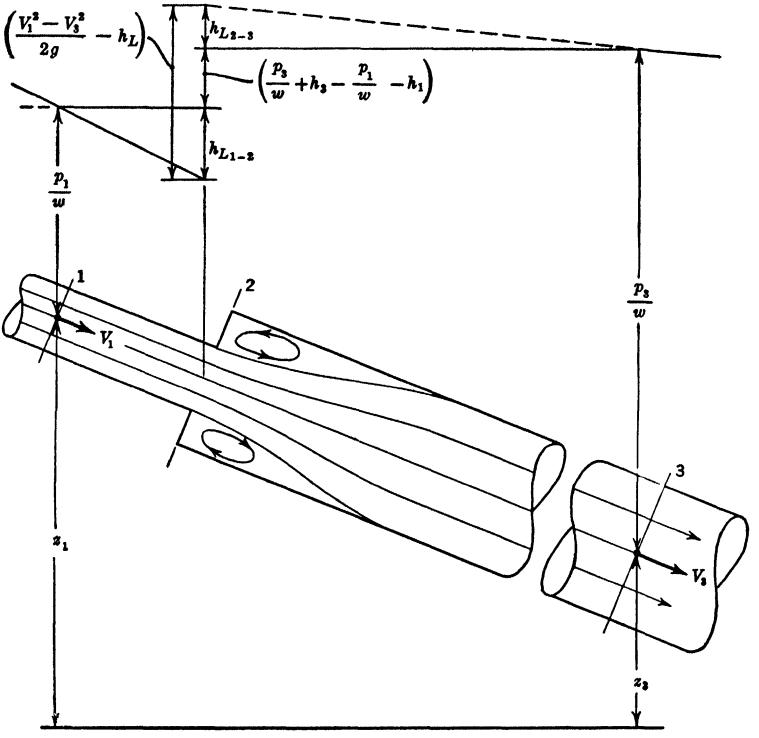


FIG. 93. Sudden Enlargement.

sudden enlargement, however, this does not hold because a change of velocity occurs and brings about a change of pressure according to the Bernoulli principle. The distance between the two grade lines at section 2 may be obtained readily by writing the Bernoulli equation between sections 1 and 3.

$$\frac{p_1}{w} + \frac{V_1^2}{2g} + z_1 = \frac{p_3}{w} + \frac{V_3^2}{2g} + z_3 + h_{L_{1-2}} + h_L + h_{L_{2-3}}$$

whence

$$\frac{p_3}{w} + z_3 - \frac{p_1}{w} - z_1 + h_{L_{1-2}} + h_{L_{2-3}} = \frac{V_1^2}{2g} - \frac{V_3^2}{2g} - h_L \qquad (66)$$

in which the left-hand side of the equation is obviously the vertical distance between the grade lines as shown in Fig. 93.

Application of the impulse-momentum law to the sudden enlargement (Fig. 94) allows theoretical calculation of the lost head h_L, and

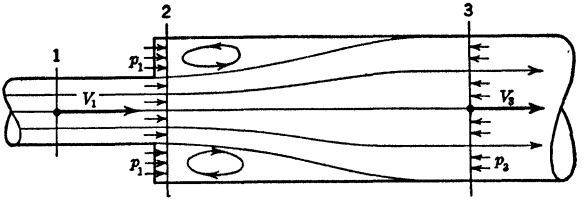


FIG. 94. Sudden Enlargement.

the theoretical analysis gives results which are confirmed closely by experiment. The fluid between sections 2 and 3 experiences a reduction in momentum caused by the difference of pressure $p_3 - p_1$. Neglecting pipe friction

$$p_1 = p_2$$

and the impulse-momentum law gives

$$F = p_3A_3 - p_1A_2 = \frac{Qw}{g}(V_1 - V_3)$$

which may be written (since $A_3 = A_2$)

$$\frac{p_3 - p_1}{w} = \frac{Q}{A_3}\frac{V_1 - V_3}{g} = \frac{V_3(V_1 - V_3)}{g}$$

Neglecting pipe friction, equation 66 becomes

$$\frac{p_3 - p_1}{w} = \frac{V_1^2 - V_3^2}{2g} - h_L$$

giving another expression for $\frac{p_1 - p_3}{w}$. Equating these two expressions

$$\frac{2V_3(V_1 - V_3)}{2g} = \frac{V_1^2 - V_3^2}{2g} - h_L$$

from which

$$h_L = \frac{V_1^2 - V_3^2 - 2V_3V_1 + 2V_3^2}{2g} = \frac{(V_1 - V_3)^2}{2g} \qquad (67)$$

thus allowing calculation of the lost head for any sudden enlargement where the pipe sizes are known. This loss of head due to sudden

enlargement is frequently termed the "Borda-Carnot loss" after the men who made its original development. It may be expressed rigorously as

$$h_L = K_L \frac{(V_1 - V_3)^2}{2g}$$

in which the coefficient K_L has been found experimentally to be close to unity and may be assumed so for most engineering calculations. Empirical formulas are available if greater precision is desired.

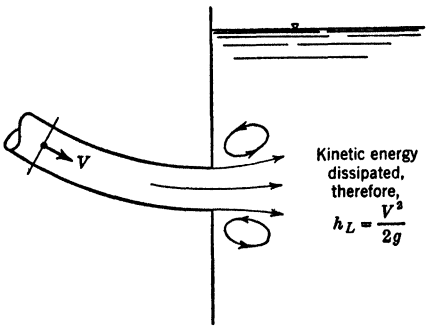


FIG. 95. Pipe Exit.

A special case of a sudden enlargement exists when a pipe discharges into a large tank or reservoir (Fig. 95). Here the velocity downstream from the enlargement may be taken to be zero, and the lost head, called the "exit loss," may be calculated from

$$h_L = \frac{(V_1 - 0)^2}{2g} = \frac{V_1^2}{2g}$$

which simply states that when a pipe discharges into a large volume of fluid the velocity energy of the flow is lost. This agrees with the result that would be expected from a non-mathematical analysis as indicated in Fig. 95.

The loss of head due to **gradual enlargement** is, of course, dependent upon the shape of the enlargement. Tests have been carried out by Gibson on the losses in conical enlargements, or "diffusor tubes," and the results expressed as a proportion of the loss occurring in a sudden enlargement by

$$h_L = K_L \frac{(V_1 - V_2)^2}{2g}$$

in which K_L is primarily dependent upon the cone angle, but is also a function of the area ratio, as shown in Fig. 96. Because of the large surface of the conical enlargement which contacts the fluid, the coefficient K_L embodies the effects of friction as well as those of eddying turbulence. In an enlargement of small central angle, K_L will result

almost wholly from surface friction; but as the angle increases and the enlargement becomes more abrupt, the surfaces are reduced, and here the energy consumed in eddies determines the magnitude of K_L.

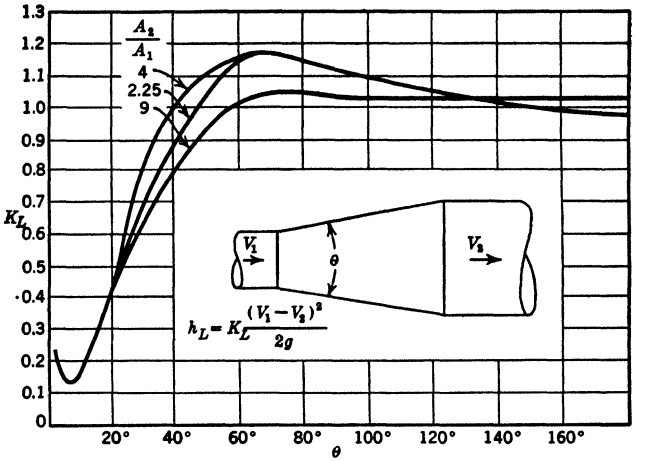


FIG. 96. Loss Coefficients for Conical Enlargements.[12]

From the plot it may be observed that: (1) there is an optimum cone angle of 7° where the combination of the effects of surface friction and eddying turbulence is a minimum; (2) it is better to use a sudden enlargement than one of cone angle around 60°, since K_L is smaller for the former.

ILLUSTRATIVE PROBLEM

A 12-in.-diameter horizontal water line enlarges to a 24-in. line through a 20° conical enlargement. When 10 cfs flow through this line the pressure in the smaller pipe is 20 lb/in.^{2} Calculate the pressure in the larger pipe, neglecting pipe friction.

$$V_{12} = \frac{10}{\frac{\pi}{4}\left(\frac{12}{12}\right)^2} = 12.7 \text{ ft/sec}, \quad V_{24} = 3.18 \text{ ft/sec}$$

From the plot of Fig. 96,

$$K_L = 0.43$$

$$\frac{20 \times 144}{62.4} + \frac{(12.7)^2}{2g} + 0 = \frac{p_{24}}{w} + \frac{(3.18)^2}{2g} + 0 + 0.43\frac{(12.7 - 3.18)^2}{2g}$$

$$\frac{p_{24}}{w} = 47.93 \text{ ft} \quad p = 20.7 \text{ lb/in.}^2$$

[12] A. H. Gibson, *Hydraulics and Its Applications*, Fourth edition, 1930, p. 93, D. Van Nostrand Co.

The physical properties of flow through a **sudden contraction** are shown in Fig. 97. Inertia prevents the fluid from following the solid boundary, and the " live " stream of fluid contracts at section 3 to a

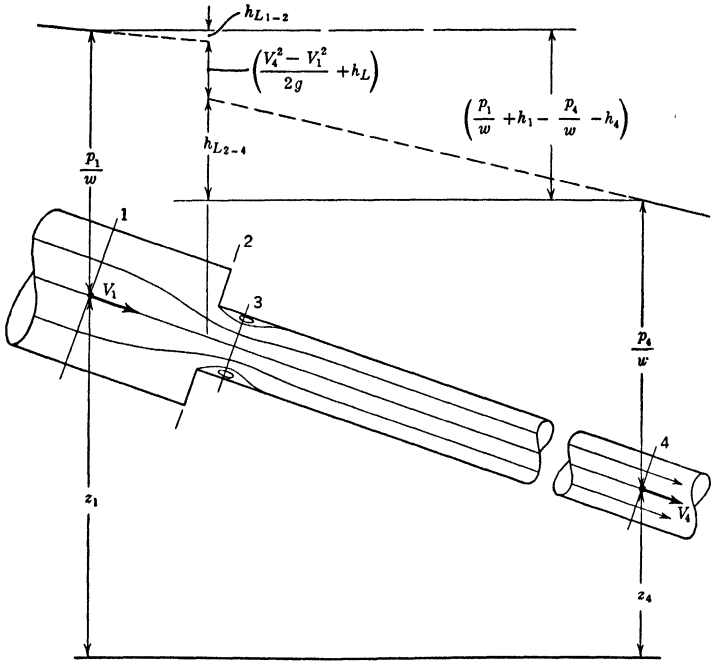


FIG. 97. Sudden Contraction.

diameter less than d_4. From section 3 to section 4 eddying turbulence similar to that of the sudden enlargement accounts for most of the energy which is consumed by the contraction.

Writing Bernoulli's equation between sections 1 and 4

$$\frac{p_1}{w} + \frac{V_1^2}{2g} + z_1 = \frac{p_4}{w} + \frac{V_4^2}{2g} + z_4 + h_{L_{1-2}} + h_L + h_{L_{2-4}}$$

whence

$$\left(\frac{p_1}{w} + z_1 - \frac{p_4}{w} - z_4\right) - h_{L_{1-2}} - h_{L_{2-4}} = \frac{V_4^2}{2g} - \frac{V_1^2}{2g} + h_L$$

which is shown in the figure to be the distance between the two theoretical pressure grade lines.

The loss of head, h_L, in a sudden contraction is expressed by

$$h_L = K_L \frac{V_4^2}{2g}$$

in which V_4 is the velocity in the smaller pipe. The coefficient K_L depends primarily upon the diameter ratio d_4/d_1, which determines the shape of the sudden contraction; the relation of K_L to d_4/d_1 and velocity is shown on Fig. 98.

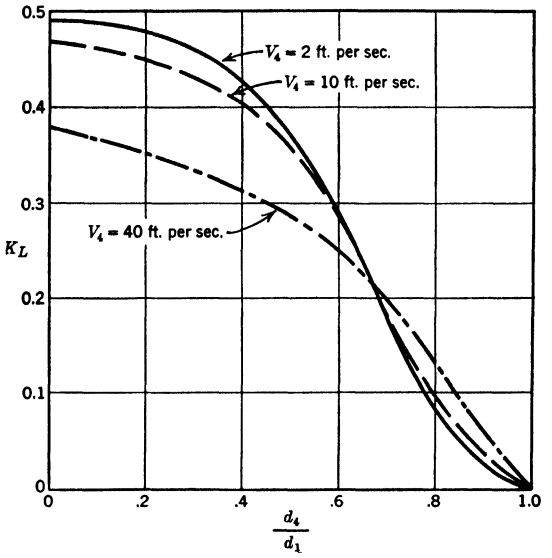


FIG. 98. Loss Coefficients for Sudden Contractions.[13]

A sharp-edged **pipe entrance** from a large body of fluid is given by the condition $d_4/d_1 = 0$ in Fig. 98, and it should be noted that the loss coefficient K_L for such an entrance is close to 0.5 for ordinary velocities. The values of K_L for this and other pipe entrances are shown in Fig. 99, and here again it may be observed that the magnitude of K_L depends primarily upon the amount of deceleration and consequent eddying turbulence caused by the entrance.

Because of smooth acceleration of the fluid in **gradual contractions** the losses are usually so small that they may be neglected in most engineering calculations.

[13] Data from H. W. King and C. O. Wisler, *Hydraulics*, Third edition, 1933, page 182, John Wiley & Sons.

Smooth pipe bends will cause losses of head due to the energy consumed by the twin eddy motion set up by secondary flows (Art. 29). The nature and magnitude of bend losses are shown in Fig. 100; they are comparable to those of Fig. 92. The loss of head in a bend is expressed by

$$h_L = K_L \frac{V^2}{2g}$$

in which V is the average velocity in the pipe. The loss coefficient K_L has been shown experimentally by Hofmann [14] to be a function of shape, roughness, and Reynolds number. Figure 101 gives a partial summary of his results for 90° circular bends, the shape of which may be defined by the simple ratio r/d. The tests were carried out on polished brass bends to obtain the "smooth" curve; the bends were then artificially roughened by applying a mixture of sand and paint, resulting in the "rough" curve. The curves thus give the extremes of roughness variation and illustrate the dependency of K_L upon roughness. Hofmann's tests were made at Reynolds numbers between 60,000 and 225,000, but the curves of Fig. 101 give an approximate summary of his results for Reynolds numbers from 100,000 to 225,000 in which range the values of K_L became practically constant [15] and thus independent of the Reynolds number. Because of the constancy of loss coefficients at high Reynolds numbers, it is probable that

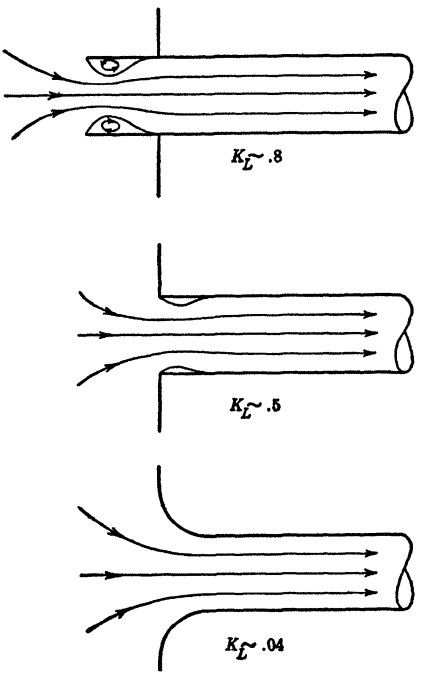


FIG. 99. Pipe Entrances.

[14] *Trans. of the Hydraulic Institute of the Munich Technical University*, Bulletin 3, p. 29, 1935, A.S.M.E.

[15] This constancy of K_L is more true of the rough bends than of the smooth ones. Compare this with the friction factors for smooth and rough pipe, Figs. 85 and 86.

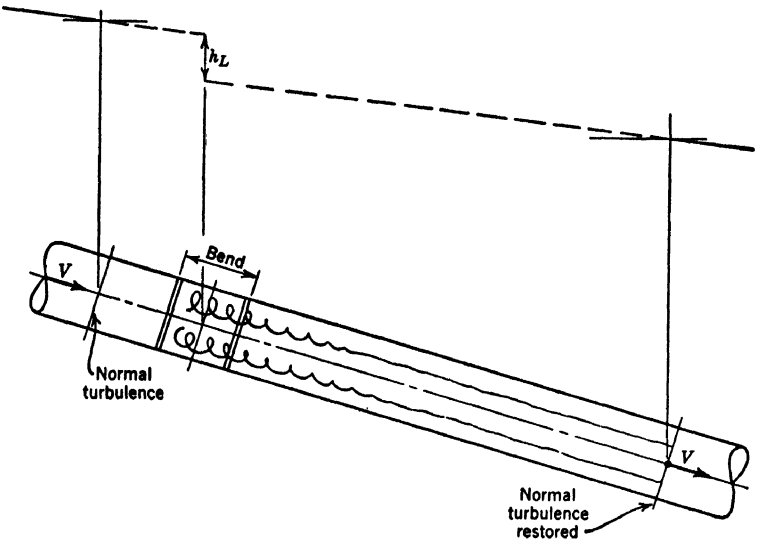


FIG. 100.

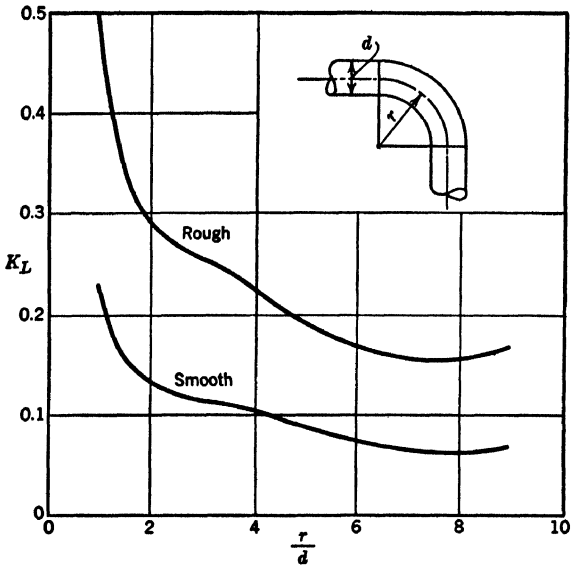


FIG. 101. Loss Coefficients for 90° Circular Bends.

Hofmann's results may be applied beyond the Reynolds numbers attained in his experiments.

The losses of head caused by **commercial pipe fittings** occur because of their rough and irregular shapes which cause excessive turbulence to be created. The shapes of commercial pipe fittings are determined more by structural properties, ease in handling, and production methods than by head-loss considerations, and it is, therefore, not feasible or economically justifiable to build pipe fittings having completely streamlined interiors in order to minimize head loss. The loss of head in commercial pipe fittings is usually expressed by a loss coefficient, K_L, and the velocity head in the pipe, as

$$h_L = K_L \frac{V^2}{2g}$$

in which K_L is a constant (at high Reynolds numbers), the magnitude of which depends upon the shape of the fitting. Values of K_L for various common fittings, compiled by the Crane Co.,[16] are presented in Table VIII.

TABLE VIII

LOSS COEFFICIENT, K_L, FOR COMMERCIAL PIPE FITTINGS

Globe valve, wide open	10.0
Angle valve, wide open	5.0
Gate valve, wide open	.19
$\frac{3}{4}$ open	1.15
$\frac{1}{2}$ open	5.6
$\frac{1}{4}$ open	24.0
Return bend	2.2
Standard tee	1.8
90° elbow	.90
45° elbow	.42

It is generally recognized that when fittings are placed in close proximity the total loss obtained through them is less than their numerical sum obtained by the foregoing methods. Systematic tests have not been made on this subject because a simple numerical sum of the losses gives a result in excess of the actual losses and thus produces an error on the conservative side when predictions of pressures and rates of flow are to be made.

[16] *Engineering Data on Flow of Fluids in Pipes and Heat Transmission*, 1935.

43. The Pressure Grade Line and Its Use. The utility of plotting above the center line of a pipe the pressure head therein has been apparent in many of the foregoing examples. The result is the hydraulic or pressure grade line which may be used to give a graphical significance to the equations of pipe flow.

Some of the properties of the pressure grade line which have been noted in the preceding problems are (1) its characteristic downward slope in the direction of flow due to pipe friction, (2) the increase of this slope with velocity, and (3) the rather abrupt rises and drops in the grade line when minor losses are incurred.

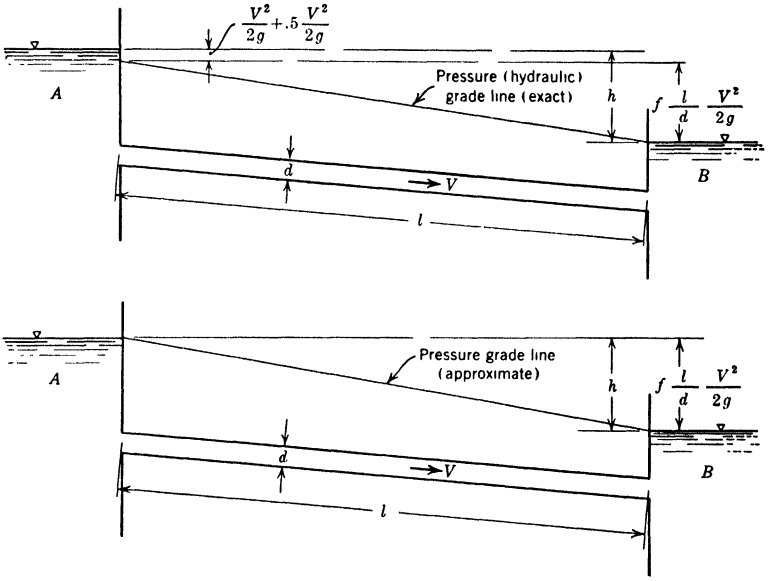


FIG. 102.

Several illustrations of the meaning of the pressure grade line and its relation to the Bernoulli equation are given in the following examples. Frequently, in long pipe lines where velocities are small and minor losses of little significance, an approximate grade line may be sketched which will allow useful engineering conclusions to be drawn directly.

In a long pipe line between two reservoirs (Fig. 102) the exact and approximate hydraulic grade lines are as shown. A drop in the exact grade line occurs as the fluid enters the pipe, caused by (1) the increases of velocity at the expense of pressure and (2) the head lost

at the pipe entrance. Considering minor losses and velocity heads and writing Bernoulli's equation between the two reservoir surfaces

$$0 + 0 + h = 0 + 0 + 0 + 0.5\frac{V^2}{2g} + f\frac{l}{d}\frac{V^2}{2g} + \frac{V^2}{2g}$$

From the exact pressure grade line of Fig. 102

$$h = \frac{V^2}{2g} + 0.5\frac{V^2}{2g} + f\frac{l}{d}\frac{V^2}{2g}$$

the same result as obtained from the Bernoulli equation but of more significance because all the terms may be visualized graphically.

The minor losses and velocity heads being neglected, the Bernoulli equation becomes

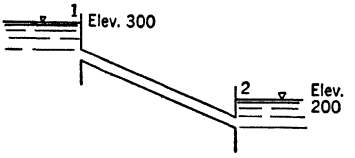
$$0 + 0 + h = 0 + 0 + 0 + f\frac{l}{d}\frac{V^2}{2g}$$

and similarly from the approximate pressure grade line

$$h = f\frac{l}{d}\frac{V^2}{2g}$$

Illustrative Problem

A 6-in. pipe line 2000 ft long connects two reservoirs, one of surface elevation 300, the other of surface elevation 200. Assuming that $f = 0.024$, calculate the rate of flow through the line (*a*) including and (*b*) neglecting minor losses.



(*a*) $$0 + 0 + 300 = 0 + 0 + 200 + 0.5\frac{V^2}{2g} + 0.024\frac{2000}{\frac{6}{12}}\frac{V^2}{2g} + \frac{V^2}{2g}$$

$$V = 8.13 \text{ ft/sec} \qquad Q = 1.595 \text{ cfs}$$

(*b*) $$0 + 0 + 300 = 0 + 0 + 200 + 0.024\frac{2000}{\frac{6}{12}}\frac{V^2}{2g}$$

$$V = 8.20 \text{ ft/sec} \qquad Q = 1.61 \text{ cfs}$$

Consider now a pipe line of more complicated nature (Fig. 103) consisting of three pipes of different sizes, with enlargement, contrac-

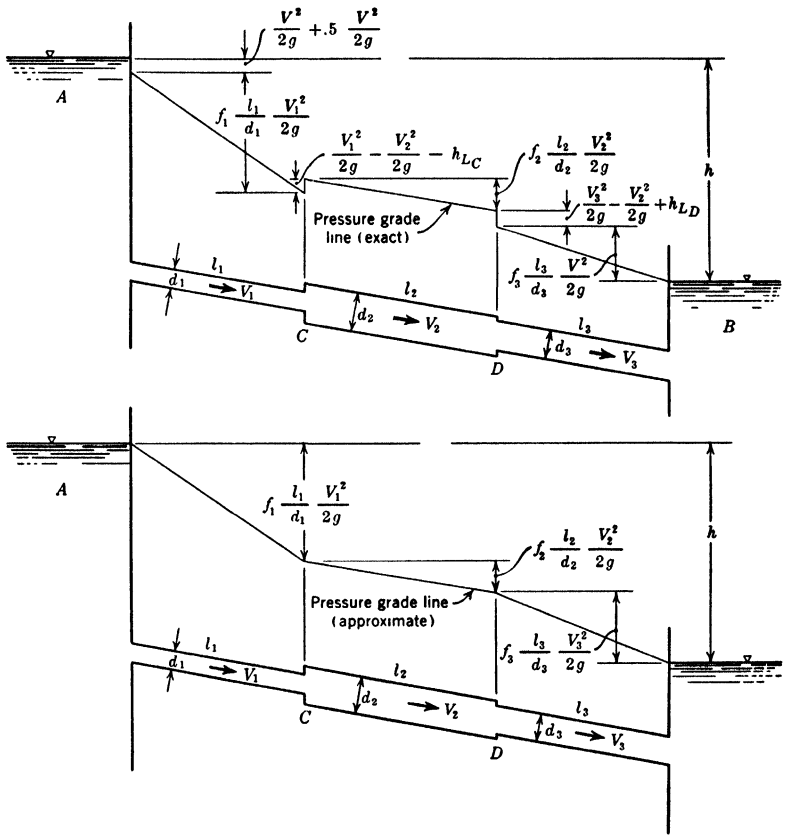


FIG. 103.

tion, entrance, and exit losses. The Bernoulli equation may be written as before

$$0 + 0 + h = 0 + 0 + 0 + 0.5\frac{V_1^2}{2g} + f_1\frac{l_1}{d_1}\frac{V_1^2}{2g} + h_{L_C} + f_2\frac{l_2}{d_2}\frac{V_2^2}{2g} + h_{L_D} + f_3\frac{l_3}{d_3}\frac{V_3^2}{2g} + \frac{V_3^2}{2g}$$

From the exact pressure grade line

$$h = 0.5\frac{V_1^2}{2g} + \frac{V_1^2}{2g} + f_1\frac{l_1}{d_1}\frac{V_1^2}{2g} - \left(\frac{V_1^2}{2g} - \frac{V_2^2}{2g} - h_{L_C}\right) + f_2\frac{l_2}{d_2}\frac{V_2^2}{2g} + \left(\frac{V_3^2}{2g} - \frac{V_2^2}{2g} + h_{L_D}\right) + f_3\frac{l_3}{d_3}\frac{V_3^2}{2g}$$

which is identical with the result obtained from the Bernoulli equation.

Neglecting minor losses and pressure variation incurred by velocity changes, the Bernoulli equation gives

$$0 + 0 + h = 0 + 0 + 0 + f_1 \frac{l_1}{d_1} \frac{V_1^2}{2g} + f_2 \frac{l_2}{d_2} \frac{V_2^2}{2g} + f_3 \frac{l_3}{d_3} \frac{V_3^2}{2g}$$

and from the approximate pressure grade line the same result

$$h = f_1 \frac{l_1}{d_1} \frac{V_1^2}{2g} + f_2 \frac{l_2}{d_2} \frac{V_2^2}{2g} + f_3 \frac{l_3}{d_3} \frac{V_3^2}{2g}$$

is obtained.

The above examples serve to illustrate the properties of the exact and approximate pressure grade lines and the use of these lines in lending a significance to pipe flow problems which cannot be obtained from equations alone.

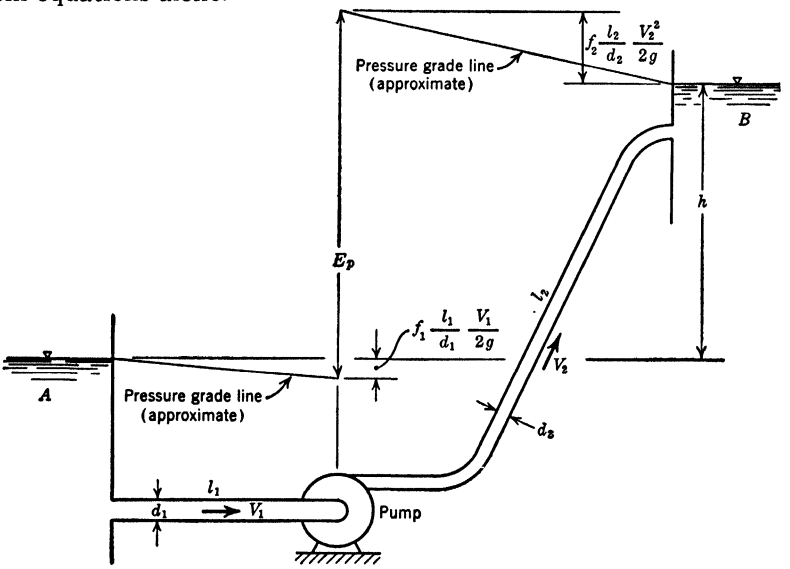


FIG. 104.

When a pump or motor is present in a pipe line the pressure grade line assumes a special shape as a result of the fluid energy which is given to or taken from the fluid by the machine. The approximate grade line for a pipe in which a pump is installed is shown in Fig. 104. Here as the flow takes place from A to B the pump must supply

sufficient energy (1) to raise the fluid through a height h, and (2) to overcome the friction loss in the line. This is seen clearly from the pressure grade line, which gives

$$E_p = h + f_1 \frac{l_1}{d_1} \frac{V_1^2}{2g} + f_2 \frac{l_2}{d_2} \frac{V_2^2}{2g}$$

The same result may, of course, be obtained by writing the Bernoulli equation between the reservoir surfaces; here

$$0 + 0 + 0 + E_p = 0 + 0 + h + f_1 \frac{l_1}{d_1} \frac{V_1^2}{2g} + f_2 \frac{l_2}{d_2} \frac{V_2^2}{2g}$$

At points in a pipe line where the velocity is high or where the elevation of the pipe is well above the datum plane, the pressure grade line may be below the pipe (Fig. 105). According to the method of plotting the grade line, the pressure in a pipe which lies above the grade line must have a negative value and thus be less than the atmospheric pressure. Regions of negative pressure in pipe lines are frequently a source of trouble in pipe-line operation since gases dissolved in the flowing fluid tend to come out of solution and collect

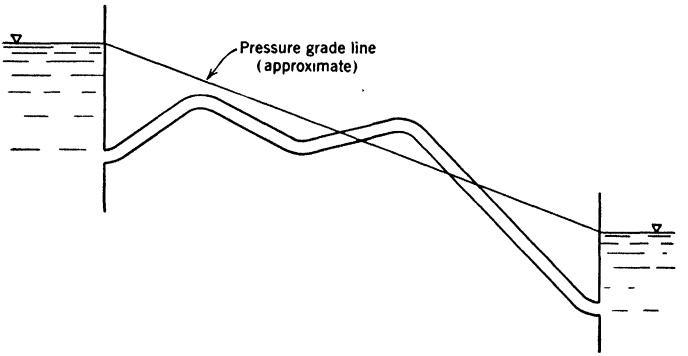


FIG. 105.

in the line, thus reducing the capacity of the line; negative pressures within the line also give an opportunity for air to leak into the line, increase the pressure, and reduce the flow. Regions of negative pressure are avoided as much as possible in the design of pipe lines, but where they exist a source of vacuum is required to draw off collections of gas. Gases which collect at high points in a pipe line when the pipe is below the hydraulic grade line may be vented by opening a cock at the highest point in the pipe and allowing the pressure of the fluid to force the gases out.

If the curves in the elevational view of a pipe line are abrupt, they are frequently loosely termed "siphons," although the only resemblance to siphonic action occurs in a pipe which is convex upward and runs above the hydraulic grade line. Pipe-line curves which are convex upward are called "siphons" whether they are above or below the hydraulic grade line; curves which are convex downwards are termed "inverted siphons," an obvious misnomer. This confused situation may be somewhat clarified by the study of the action of the "true siphon" of Fig. 106 and by comparison of true siphonic action with that occurring in the vertical curves of a pipe line. The distinc-

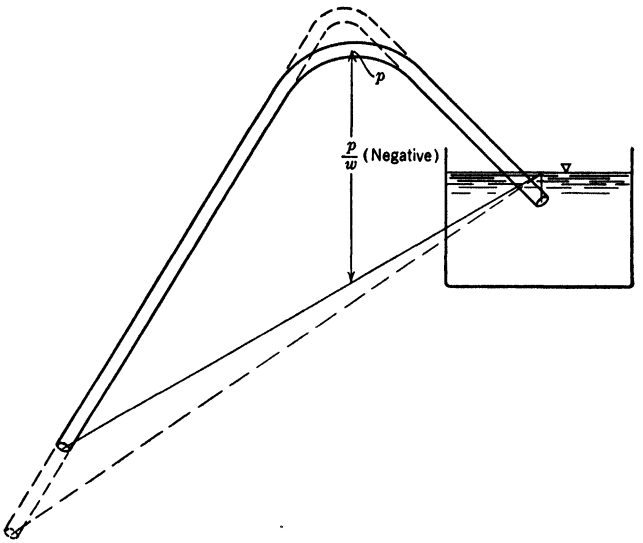


FIG. 106.

tive characteristic of the true siphon is that practically its entire length lies above the hydraulic grade line. The factor which determines its successful operation is the maximum negative pressure, which exists at the crown of the siphon. The magnitude of this negative pressure is, of course, limited by the barometric height and vapor pressure of the liquid,[17] but it should not be concluded that such a negative pressure may be obtained in practice; actually disruption of the flow occurs at negative pressures well below the maximum, due to the liberation of entrained gases. Obviously, then, the factors which change the negative pressure at the crown of the siphon

[17] See Appendix V.

are the factors which are fundamental to its successful operation. From the approximate pressure grade line it may be concluded directly that (1) raising the crown of the siphon and (2) lowering the free end of the pipe both increase this negative pressure and that these, therefore, are the fundamental variables which determine the success or failure of siphon operation. Although these conclusions might have been reached by several applications of the Bernoulli principle the utility of the hydraulic grade line has been shown again in discovering the fundamental factors of a problem quickly and efficiently.

44. Branching Pipes. Some of the more complicated problems of pipe-line design involve the flow of fluids in pipes which intersect.

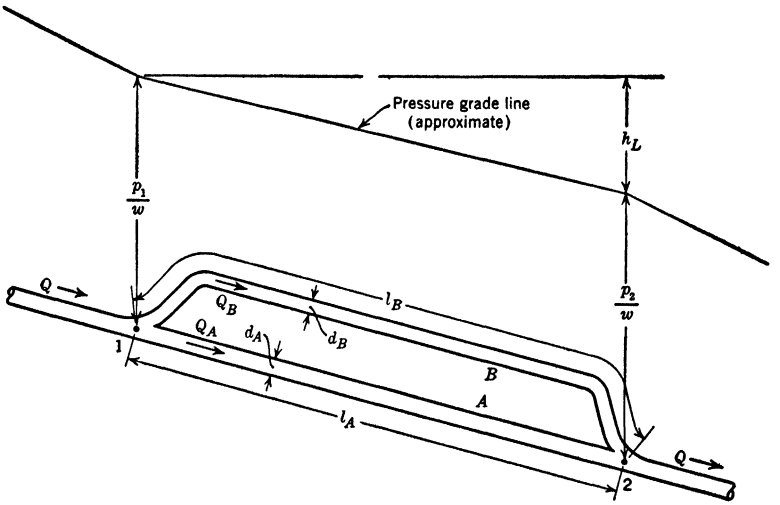


FIG. 107.

The principles involved in problems of this type may be obtained by a study of pipes which (1) divide and rejoin and (2) lead from regions of different pressure and meet at a common point.

In pipe-line practice, "looping" or laying a line, B, parallel to an existing pipe line, A, and connected with it (Fig. 107), is a standard method of increasing the capacity of the line. Here there is an interesting analogy between fluid flow and the characteristics of a parallel electric circuit, if head lost is compared with drop in potential and rate of flow with electric current.

Obviously as flow takes place from point 1 to point 2 through either pipe A or pipe B the same lost head, h_L, is accomplished and from the continuity principle the sum of the flows in pipes A and B must be the

total flow in the single pipe line. Neglecting minor losses, these two facts allow the writing of the equations

$$\begin{cases} f_A \dfrac{l_A}{d_A} \dfrac{V_A^2}{2g} = f_B \dfrac{l_B}{d_B} \dfrac{V_B^2}{2g} \\ Q = Q_A + Q_B \end{cases}$$

which may be placed in terms of Q for simultaneous solution by inserting the relations

$$V_A = \frac{4Q_A}{\pi d_A^2} \quad \text{and} \quad V_B = \frac{4Q_B}{\pi d_B^2}$$

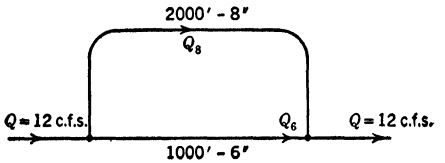
giving

$$\begin{cases} \dfrac{f_A}{2g} \dfrac{l_A}{d_A} \left(\dfrac{4Q_A}{\pi d_A^2}\right)^2 = \dfrac{f_B}{2g} \dfrac{l_B}{d_B} \left(\dfrac{4Q_B}{\pi d_B^2}\right)^2 \\ Q = Q_A + Q_B \end{cases}$$

which would allow calculation of the division of a flow, Q, into two flows, Q_A and Q_B, when the sizes and friction factors of the pipes are known.

Illustrative Problem

A 12-in. water line, in which 12 cfs flow, branches into a 6-in. line 1000 ft long and an 8-in. line 2000 ft long which rejoin and continue as a 12-in. line. Calculate the flow through the two branch lines assuming that $f = 0.022$ for both of these.



$$V_6 = \frac{Q_6}{\frac{\pi}{4} \times \left(\frac{6}{12}\right)^2} = 5.1\, Q_6$$

$$V_8 = \frac{Q_8}{\frac{\pi}{4}\left(\frac{8}{12}\right)^2} = 2.87 Q_8$$

$$(h_L)_6 = (h_L)_8 = 0.022 \times \frac{1000}{\frac{6}{12}} \times \frac{(5.1Q_6)^2}{2g} = 0.022 \times \frac{2000}{\frac{8}{12}} \times \frac{(2.87Q_8)^2}{2g}$$

Solving $\begin{cases} Q_8 = 1.455 Q_6 \end{cases}$

but $\begin{cases} Q = Q_8 + Q_6 = 12 \end{cases}$

$$Q_6 = 4.89 \text{ cfs} \qquad Q_8 = 7.11 \text{ cfs}$$

Another engineering example of branching pipes is that typified by the "three-reservoir problem" of Fig. 108 which may be solved advantageously by application of hydraulic grade line principles.

Here flow may take place. (1) from reservoir A into reservoirs B and C, or (2) from reservoir A to C without inflow or outflow from reservoir B, or (3) from reservoirs A and B into reservoir C. The approximate hydraulic grade lines representing these conditions are indicated on

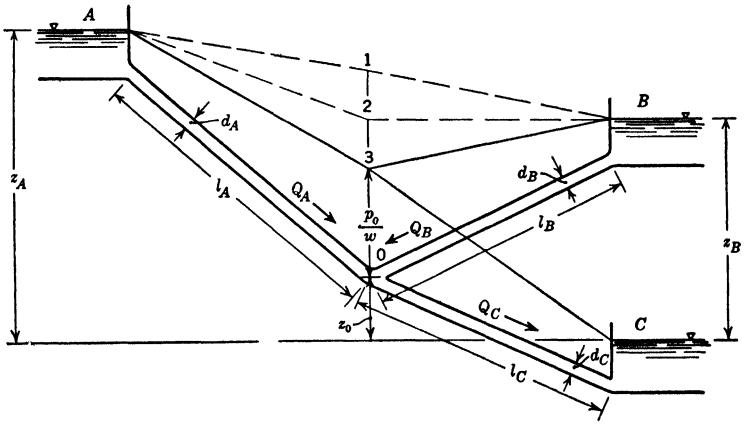


FIG. 108.

the figure, and it is obvious that the slopes of these lines and the above flow conditions are determined by the magnitude of the pressure head at the junction, O. Assuming flow to take place from reservoirs A and B into C, the following equations may be written directly from inspection of the hydraulic grade lines.

$$z_A = z_o + \frac{p_o}{w} + f_A \frac{l_A}{d_A} \frac{1}{2g} \left(\frac{4Q_A}{\pi d_A^2}\right)^2$$

$$z_B = z_o + \frac{p_o}{w} + f_B \frac{l_B}{d_B} \frac{1}{2g} \left(\frac{4Q_B}{\pi d_B^2}\right)^2$$

$$z_o + \frac{p_o}{w} = f_C \frac{l_C}{d_C} \frac{1}{2g} \left(\frac{4Q_C}{\pi d_C^2}\right)^2$$

and from the continuity principle

$$Q_A + Q_B = Q_C$$

These four simultaneous equations may be solved readily by trial (if pipe sizes, friction factors, and elevations are known), by assuming a value of p_o/w and solving the first three equations for Q_A, Q_B, and Q_C. The solution of the problem is completed when these values of Q_A, Q_B.

and Q_C satisfy the fourth equation, thus allowing prediction of the rates of flow for a given or existing pipe system.

The above type of solution is not that encountered in design problems where the desired rates of flow are known, the pipe-line elevations fixed by topography and other considerations, and the problem is to build the most economical pipe system to transmit these flows. In this case the assumption of a value of p_o/w immediately fixes the diameters and, therefore, the initial and operation costs of the pipes. Various assumptions of p_o/w may be made and the resulting total costs plotted agains p_o/w. The value of p_o/w resulting in the minimum total cost will determine all the pipe sizes for the most economical design.

BIBLIOGRAPHY

(See also Bibliography for Chapter IV.)

R. L. DAUGHERTY, *Hydraulics*, Fourth Edition, McGraw-Hill Book Co., 1937.
H. W. KING and C. O. WISLER, *Hydraulics*, Third Edition, John Wiley & Sons, 1933.
G. E. RUSSELL, *Textbook on Hydraulics*, Fourth Edition, Henry Holt & Co., 1934.
H. W. KING, *Handbook of Hydraulics*, Third Edition, McGraw-Hill Book Co., 1939.
A. H. GIBSON, *Hydraulics and Its Applications*, Fourth Edition, D. Van Nostrand, 1930.

PROBLEMS

252. When 10 cfs of water flow through a 6-in. constriction in a 12-in. horizontal pipe line, the pressure at a point in the pipe is 50 lb/in.^{2}, and the head lost between this point and the constriction is 10 ft. Calculate the pressure in the constriction.

253. A 2-in. nozzle terminates a vertical 6-in. pipe line in which water flows downward. At a point on the pipe line a pressure gage reads 40 lb/in.^{2} If this point is 12 ft above the nozzle tip and the head lost between point and tip is 5 ft, calculate the rate of flow.

254. A 12-in. pipe leaves a reservoir of surface elevation 300 at elevation 250 and drops to elevation 150, where it terminates in a 3-in. nozzle. If the head lost through line and nozzle is 30 ft, calculate the rate of flow.

255. An 18-in. pipe line runs from a reservoir of surface elevation 350 and discharges into the atmosphere at elevation 250. If the loss of head in this pipe line is 90 ft, what flow can be expected?

256. A vertical 6-in. pipe leaves a water tank of surface elevation 80. Between the tank and elevation 40 on the line, 8 ft of head is lost when 2 cfs flow through the line. If an open piezometer tube is attached to the pipe at elevation 40, what will be the elevation of the water surface in this tube?

257. What horsepower pump is required to pump 20 cfs of water from a reservoir of surface elevation 100 to one of surface elevation 250, if in the pump and pipe line 40 ft of head are lost?

258. Through a hydraulic turbine flow 100 cfs of water. On the 42-in. inlet pipe at elevation 145, a pressure gage reads 50 lb/in.^{2} On the 60-in. discharge pipe at

elevation 130 a vacuum gage reads 6 in. of mercury. If the total head lost through pipes and turbine between elevations 145 and 130 is 30 ft, what horsepower may be expected from the machine?

259. In a 9-in. pipe line 5 cfs of water are pumped from a reservoir of surface elevation 100 over a hill of elevation 165. What horsepower pump is required to maintain a pressure of 50 lb/in.^{2} on the hilltop if the head lost between reservoir and hilltop is 20 ft?

260. Water flows downward through a 1000-ft section of 12-in. pipe line running from elevation 200 to elevation 100. The pressure at elevation 200 is 40 lb/in.^{2}, and the velocity in the line is 10 ft/sec. The head lost in this section is 5 ft. Calculate: (*a*) the total energy at elevations 200 and 100, taking datum at sea level; (*b*) the pressure at elevation 100; (*c*) the shear stress at the wall of the pipe, 3 in. from the center and on the centerline; (*d*) the lost horsepower in the 1000-ft section for this flow.

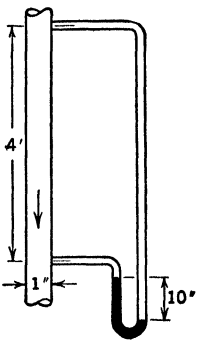
261. When a liquid flows in a horizontal 6-in. pipe, the shear stress at the walls is 1.3 lb/ft.^{2} Calculate the pressure drop in 100 ft of this pipe line.

262. If 2 cfs of glycerine at 50° F flow in a 6-in. pipe, calculate: (*a*) the velocity at the center of the pipe; (*b*) the loss of head in 100 ft of the pipe by equations 44 and 45; (*c*) the velocity 2 in. from the centerline; (*d*) the shear stress at the wall; (*e*) the shear stress 2 in. from the centerline.

263. Oil of viscosity 0.01 lb sec/ft^2 and specific gravity 0.90 flows with an average velocity of 5 ft/sec in a 12-in. pipe line. Calculate the shear stress at the wall and 3 in. from the center line.

264. In a section of 2-in. pipe line 500 ft long running from elevation 130 to elevation 90 flow 30 gpm of linseed oil at 80° F. If flow is downward and pressure at elevation 130 is 30 lb/in.^{2}, calculate the pressure at elevation 90. Check for laminar flow before calculating this pressure.

265. If 0.25 gpm of oil of specific gravity 0.92 flow in laminar condition through this vertical 1-in. pipe line, calculate the viscosity of the oil if the manometer deflection is 10 in.



266. Water flows at 50° F from a reservoir through a 1-in. pipe line 2000 ft long which discharges into the atmosphere at a point 1 ft below the reservoir surface. Calculate the flow, assuming it to be laminar and neglecting the velocity head in the pipe line. Check the assumption of laminar flow.

267. Glycerine flows through a 2-in. horizontal pipe line, leading from a tank and discharging into the atmosphere. If the pipe line leaves the tank 20 ft below the liquid surface and is 100 ft long, calculate the flow when the glycerine has a temperature of (*a*) 50° F, (*b*) 70° F.

268. What horsepower pump is required to pump 50 gpm of linseed oil from a tank of surface elevation 40 to one of elevation 60 through 1500 ft of 3-in. pipe, if the oil is at (*a*) 80° F, (*b*) 100° F?

269. If 180 gpm of water at 70° F flow in a 6-in. pipe line having roughness protuberances of average height 0.030 in. and if similar roughness having height 0.015 in. exists in a 3-in. pipe, what flow of linseed oil (100° F) must take place therein for the friction factors of the two pipes to be the same?

270. In a 12-in. pipe line, 15 cfs of water flow upward. At a point on the line at

elevation 100, a pressure gage reads 130 lb/in.^{2} Calculate the pressure at elevation 150, 2000 ft up the line, assuming the friction factor to be 0.02.

271. Given that 250 gpm of carbon tetrachloride flow downward through 200 ft of 3-in. pipe, from elevation 100 to elevation 40; the pressure at the former point is 30 lb/in.^{2}, and that at the latter 50 lb/in.^{2} Calculate the friction factor.

272. Calculate the loss of head in 1000 ft of 3-in. brass pipe when water at 80° F flows therein at an average velocity of 10 ft/sec.

273. In a 2-in. pipe line, 25 gpm of glycerine flow at 70° F. Calculate the loss of head in 200 ft of this pipe.

274. If 100 lb/min of air flow in a 3-in. horizontal clean steel pipe line at 175 lb/in.^{2} ab and 80° F, calculate the loss of head and pressure drop in 300 ft of this pipe.

275. If 2 cfs of water flow at 50° F in a clean 6-in. cast-iron pipe line, calculate the loss of head per 100 ft of line.

276. If 12 cfs of water flow in a 12-in. spiral riveted pipe at 70° F, calculate the loss of head in 500 ft of this pipe.

277. Castor oil flows in a 1-in. pipe line at 50° F at a velocity of 2 ft/sec. Calculate the loss of head in 100 ft of this pipe.

278. A 3-in. brass pipe line 100 ft long carries 100 gpm of linseed oil. Calculate the head loss when the oil is at (*a*) 80° F, (*b*) 110° F.

279. Solve the preceding problem when the liquid is castor oil.

280. In a laboratory test 490 lb/min of water at 60° F flow through a section of 2-in. brass pipe 30 ft long. A differential manometer connected to the ends of this section shows a reading of 14.2 in. If the fluid in the bottom of the manometer has a specific gravity of 3.20, calculate the friction factor and the Reynolds number.

281. Water flows from a tank through 200 ft of horizontal 2-in. brass pipe and discharges into the atmosphere. If the water surface in the tank is 4 ft above the pipe, calculate the rate of flow, considering losses due to pipe friction only, when the water temperature is (*a*) 50° F, (*b*) 100° F. (Trial and error solution or by Blasius' equation for f.)

282. A 1-in. clean galvanized pipe 400 ft long leaves a water tank at elevation 30 and discharges into the atmosphere at elevation 27. If the water surface in the tank has elevation 35 and the water is at 70° F, calculate the rate of flow considering losses due to pipe friction only. (Trial and error solution.)

283. In a horizontal 8-in. clean steel pipe line, 5.0 lb/sec of superheated steam flow at an absolute pressure of 250 lb/in.^{2} If the steam is superheated 100° F, calculate loss of head and loss of pressure in 500 ft of this pipe.

284. Carbon dioxide flows in a 4-in. horizontal clean steel pipe line at a velocity of 10 ft/sec. At a point in the line a pressure gage reads 100 lb/in.^{2} and the temperature is 100° F. What pressure is lost due to friction in 100 ft of this pipe? Barometric pressure 14.7 lb/in.^{2}

285. What loss of head occurs in 100 ft of a $\frac{1}{2}$-in. galvanized pipe when water flows therein at 60° F and 30 ft/sec?

286. If 2.5 cfs of water flow in an 18-in. clean steel pipe line at 40° F, calculate (*a*) the shear stress at the pipe walls and (*b*) the velocity on the pipe centerline from Fig. 88 and equation 55.

287. Water flows in a 6-in. pipe line at 60° F. If the velocity on the pipe's centerline is 3 ft/sec, what is the rate of flow?

288. Linseed oil flows in an 8-in. pipe line at 80° F. The center velocity is 6 ft/sec. Calculate the rate of flow.

289. Glycerine flows in a 2-in. pipe at 50° F and with a center velocity of 8 ft/sec. Calculate the rate of flow through the line.

290. Carbon dioxide flows in a 3-in. pipe at 50 lb/in.^{2} ab and 50° F. If the center velocity is 2 ft/sec, calculate the weight rate of flow.

291. If 250 gpm of water flow at 40° F in a 6-in. smooth pipe line, calculate the approximate thickness of the laminar film, the center velocity, and the velocity V_w.

292. Prove that, for smooth pipes having Reynolds numbers below 100,000,

$$\frac{\delta}{d} = \frac{58.3}{N_R^{\frac{7}{8}}}$$

provided that δ is small.

293. Air flows isothermally in a 3-in. pipe line at a velocity of 10 ft/sec, an absolute pressure of 40 lb/in.^{2}, and temperature of 50° F. If pressure is lost by friction, calculate the velocity where the pressure is 30 lb/in.^{2} abs.

294. Through a horizontal 6-in. clean cast-iron pipe line 1000 ft long in which the temperature is 60° F, 200 lb/min. of air flow isothermally. If the pressure at the upstream end of this pipe length is 30 lb/in.^{2} abs, calculate the pressure at the downstream end and the velocities at these two points.

295. Carbon dioxide flows isothermally in a 2-in. horizontal clean steel pipe line and at a certain point the velocity is 60 ft/sec, pressure 60 lb/in.^{2} abs, and temperature 80° F. Calculate the pressure and velocity 500 ft down stream from this point.

296. Air at 14.7 lb/in.^{2} abs and 60° F flows in a 12 in. by 3 in. horizontal clean galvanized duct at a velocity of 15 ft/sec. Calculate the loss of head and loss of pressure per foot of duct.

297. Air at 14.7 lb/in.^{2} abs and 60° F flows in a horizontal triangular clean galvanized duct having 8-in. sides, at a velocity of 12 ft/sec. Calculate the head and pressure lost per foot of duct.

298. Ten cubic feet of water flow per second in a smooth 9-in. square duct at 50° F. Calculate the head lost in 100 ft of this duct.

299. A brick conduit of cross-sectional area 10 ft^2 and wetted perimeter 12 ft carries water at 50° F at a velocity of 8 ft/sec. Calculate the head lost in 200 ft of this conduit.

300. A semicircular good brick conduit 5 ft in diameter carries water at 70° F at a velocity of 10 ft/sec. Calculate the loss of head per foot of conduit.

301. A reservoir has surface elevation 200. A 24-in. old cast-iron pipe line 2 miles long leaves the reservoir at elevation 180 and discharges freely at elevation 100. Calculate the flow through the line.

302. A new riveted steel 12-in. pipe line 1 mile long runs from elevation 350 to elevation 325. If the pressure at both of these points is 50 lb/in.^{2}, calculate the rate of flow.

303. A new riveted steel 18-in. pipe line 1000 ft long runs from elevation 150 to elevation 200. If the pressure at the former point is 100 lb/in.^{2} and at the latter 72 lb/in.^{2}, what rate of flow can be expected through the line?

304. A 3-ft square smooth masonry conduit is 3 miles long and connects two reservoirs having a difference in their surface elevations of 60 ft. What flow can be expected through the conduit?

305. If 200 cfs of water are to be carried through a smooth wooden pipe line which leaves a reservoir (surface elevation 290) at elevation 250 and runs 3 miles

to elevation 200, where a pressure of 30 lb/in.^{2} is to be maintained, what size pipe line is required?

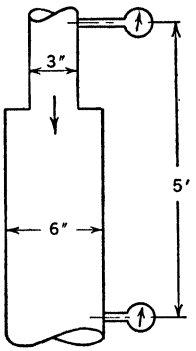
306. If 60 cfs of water are to be pumped from a reservoir of surface elevation 150 to one of surface elevation 200 through 2 miles of 30-in. old cast-iron pipe, what horsepower pump is required?

307. What diameter smooth masonry pipe is necessary to carry 50 cfs between two reservoirs of surface elevations 250 and 100 if the pipe line is to be 2 miles long?

308. An extremely smooth 12-in pipe line leaves a reservoir of surface elevation 500 at elevation 460. A pressure gage is located on this line at elevation 400 and 1000 feet from the reservoir (measured along the line). Calculate the gage reading when 10 cfs flow in the line, using: (*a*) the Hazen-Williams formula, (*b*) Fig. 86. (Temperature 68° F.)

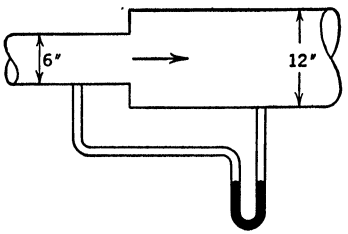
309. Calculate, by the Hazen-Williams method, the head lost in the brick conduit of Problem 299.

310. If 5 cfs of water flow through a 6-in. horizontal pipe which suddenly enlarges to 12-in. diameter, and if the pressure in the smaller pipe is 20 lb/in.^{2}, calculate that in the 12-in. pipe. neglecting pipe friction.



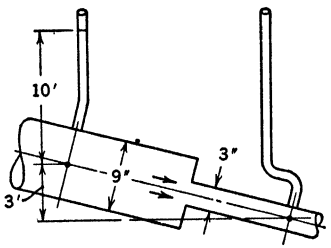
311. Estimate the rate of flow of benzene through this sudden enlargement if the upper gage reads 20 lb/in.^{2} and the lower one 23 lb/in.^{2}

312. Calculate the manometer reading when 8 cfs of water flow through this enlargement.



313. Solve Problem 312 assuming conical enlargements of 70° and 7°.

314. A 4-in. pipe suddenly contracts to a 2-in. pipe in which the velocity is 10 ft/sec. Calculate the loss of head through the contraction if water is flowing.



315. The velocity of water in a 6-in horizontal pipe is 3 ft/sec. Calculate the loss of head through a sudden contraction to 2-in. diameter. If the pressure in the 6-in. pipe is 50 lb/in.^{2}, what is the pressure in the 2-in. pipe, neglecting pipe friction?

316. Calculate the height to which water will rise in the downstream piezometer tube when 1.0 cfs flows through this contraction.

317. Water flows at 10 ft/sec in a 6-in. pipe line which contracts abruptly to a 3-in. pipe. Calculate the velocity and diameter of the live stream at the contracted section (3, Fig. 97).

318. If 2 cfs of water leave a reservoir in a 6-in. pipe line, calculate the lost head

caused by the pipe entrance assuming it to be the "re-entrant," "sharp," and "rounded" entrances of Fig. 99.

319. A 90° smooth bend in a 12-in. pipe line has a radius of 4 ft. Calculate the loss of head when 15 cfs of fluid flow through this bend.

320. A horizontal 2-in. pipe line leaves a water tank 20 ft below the water surface. If this line has a sharp entrance and discharges into the atmosphere, calculate the rate of flow neglecting and considering the entrance loss, if the pipe length is (*a*) 15 ft, (*b*) 150 ft. Assume f to be 0.025.

321. A 15-in. pipe line connects two reservoirs having surface elevations 150 and 90. If the line is 1 mile long and has a sharp entrance, calculate the rate of flow including and neglecting minor losses. Assume that $f = 0.020$.

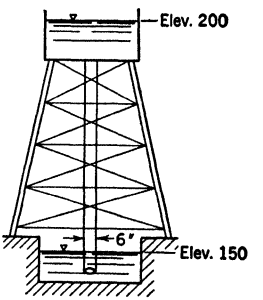
322. A 12-in. horizontal pipe 1000 ft long leaves a reservoir of surface elevation 200 at elevation 180. This line connects to a 6-in. pipe 1000 ft long running to elevation 100, where it enters a reservoir of surface elevation 130. Assuming that $f = 0.02$, and neglecting minor losses, calculate the flow through the line and sketch the approximate hydraulic grade line, showing its elevation at the contraction.

323. At the rate of 50 gpm, linseed oil is to be pumped through 1000 ft of 2-in. brass pipe line between two tanks having difference of surface elvation 10 ft. Neglecting minor losses, what pump horsepower is required if the oil temperature is (*a*) 80° F, (*b*) 120° F?

324. A horizontal 2-in. brass pipe line leaves (sharp entrance) a water tank 10 ft below its free surface. At 50 ft from the tank, it suddenly enlarges to a 4-in. pipe which runs 100 ft horizontally to another tank entering it 2 ft below its surface. Calculate the flow through the line when the water temperature is 68° F, neglecting no losses. (Trial and error solution.)

325. A pipe line running between two reservoirs having surface elevations of 500 and 300 consists of 1000 ft of 10-in, 8-in., and 6-in. pipe in that order downstream, connected by sudden contractions. Assuming that $f = 0.023$ for all pipes, calculate the rate of flow and sketch the hydraulic grade line showing all important elevations (*a*) including and (*b*) neglecting the minor losses. Assume that the line has a sharp entrance.

326. Calculate the rate of flow from this water tank if the 6-in. pipe line has $f = 0.02$ and is 50 ft long.



327. A 12-in. pipe line 1500 ft long leaves a reservoir of surface elevation 500 at elevation 460 and runs to elevation 390, where it discharges into the atmosphere. Calculate the flow and sketch accurately the hydraulic grade line (assuming that $f = 0.022$): (*a*) for the conditions above, and (*b*) when a 3-in. nozzle is attached to the end of the line, assuming the lost head in the nozzle to be 5 ft.

328. A 6-in. horizontal pipe line 1000 ft long leaves a reservoir of surface elevation 300 at elevation 250. The line terminates in a 2-in. nozzle. Calculate the discharge from the nozzle and the horsepower available in the nozzle stream, and sketch the hydraulic grade line. Assume that $f = 0.025$ and neglect entrance and nozzle loss.

329. A pump close to a reservoir of surface elevation 100 pumps water through a 6-in. pipe line 1500 ft long and discharges it at elevation 200 through a 2-in. nozzle. Calculate the pump horsepower necessary to maintain a pressure of 50 lb/in.^{2} behind

the nozzle, and sketch accurately the hydraulic grade line, neglecting loss in the nozzle and taking $f = 0.02$.

330. A 24-in. pipe line 3000 ft long leaves (sharp entrance) a reservoir of surface elevation 500 at elevation 450 and runs to a turbine at elevation 200. Water flows from the turbine through a 36-in. vertical pipe ("draft tube") 20 ft long to tailwater of surface elevation 185. When 30 cfs flow through pipe and turbine, what horsepower is developed? What are the pressures at the entrance and exit of the turbine? Take $f = 0.02$; include exit loss; neglect other minor losses and those within the turbine.

331. The siphon of Fig. 106 consists of a 2-in. hose having $f = 0.025$. The crown of the siphon is 10 ft above and the free end 15 ft below the water level in the tank. If the hose is 60 ft long and the bend is at its third point, calculate the flow and the pressure at the crown.

332. What is the maximum flow which may be obtained theoretically in problem 322 when the 6-in. and 12-in. pipes are interchanged?

333. The horizontal 8-in. suction pipe of a pump is 500 ft long and is connected to a reservoir of surface elevation 300, 10 ft below the water surface. From the pump, the 6-in. discharge pipe runs 2000 ft to a reservoir of surface elevation 420, which it enters 30 ft below the water surface. Taking f to be 0.02 for both pipes, calculate the pump horsepower required to pump 3.0 cfs from the lower reservoir. Sketch accurately the approximate hydraulic grade line. What is the maximum theoretical flow which may be pumped through this system: (*a*) with the 8-in. suction pipe, (*b*) with a 6-in. suction pipe?

334. A 12-in. pipe line 2 miles long runs on an even grade between reservoirs of surface elevations 500 and 400, entering the reservoirs 30 ft below their surfaces. The flow through the line is inadequate, and a pump is installed at elevation 420 to increase the capacity of the line. Assuming f as 0.02, what pump horsepower is required to pump 6.0 cfs downhill through the line? Sketch accurately the approximate hydraulic grade line before and after the pump is installed. What is the maximum theoretical flow which may be obtained through the line?

335. A 24-in. pipe line branches into a 12-in. and an 18-in. pipe, each of which is 1 mile long and rejoin to form a 24-in. pipe. If 30 cfs flow in the main pipe, how will the flow divide? Assume that $f = 0.018$ for both branches.

336. A 24-in. pipe line carrying 30 cfs divides into 6-in., 8-in., and 12-in. branches, all of which are the same length and enter the same reservoir below its surface. Assuming that $f = 0.020$ for all pipes, how will the flow divide?

337. An 18-in. pipe divides into 12-in. and 6-in. branches which rejoin. If the 6-in. branch is 1 mile long, how long must the 12-in. branch be for the flow to divide equally when 10 cfs flow in the 18-in. pipe? Assume that $f = 0.019$ throughout.

338. A 36-in. pipe divides into three 18-in. pipes at elevation 400. The 18-in. pipes run to reservoirs which have surface elevations of 300, 200, and 100, these pipes having respective lengths of 2, 3, and 4 miles. When 42 cfs flow in the 36-in. line, how will the flow divide? Assume that $f = .017$ for all pipes.

339. Reservoirs A, B, and C have surface elevations of 500, 400, and 300, respectively. A 12-in. pipe 1 mile long leaves reservoir A and runs to point 0 at elevation 450. Here the pipe divides and an 8-in. pipe 1 mile long runs from 0 to B and a 6-in. pipe $1\frac{1}{2}$ miles long runs from 0 to C. Assuming that $f = 0.02$, calculate the flows in the lines.

340. A straight 12-in. pipe line 3 miles long is laid between two reservoirs of surface elevations 500 and 350 entering these reservoirs 30 ft beneath their free surfaces. To increase the capicity of the line a 12-in. line 1.5 miles long is laid from the original line's midpoint to the lower reservoir. What increase in flow is gained by installing the new line? Assume that $f = 0.02$ for all pipes.

341. Three pipes join at a common point at elevation 350. One, a 12-in. line 2000 ft long, goes to a reservoir of surface elevation 400; another, a 6-in. line 3000 ft long, goes to a reservoir of surface elevation 500; the third (6-in.) runs 1000 ft to elevation 250, where it discharges into the atmosphere. Assuming that $f = 0.02$, calculate the flow in each line.

CHAPTER VII

FLUID FLOW IN OPEN CHANNELS

Open-channel flow embraces that variety of problems which arise when water flows in natural water courses, regular canals, irrigation ditches, sewer lines, flumes, etc.—a province of paramount importance to the civil engineer. Although open-channel problems practically always involve the flow of water, and although the experimental results used in these problems were obtained by hydraulic tests, modern fluid mechanics indicates the extent to which these results may be applied to the flow of other fluids in open channels.

45. Fundamentals. In the problems of pipe lines, as may be seen from the hydraulic grade line, the pressures in the pipe may vary along the pipe and depend upon energy losses and the conditions imposed upon the ends of the line. Open flow, however, is characterized by

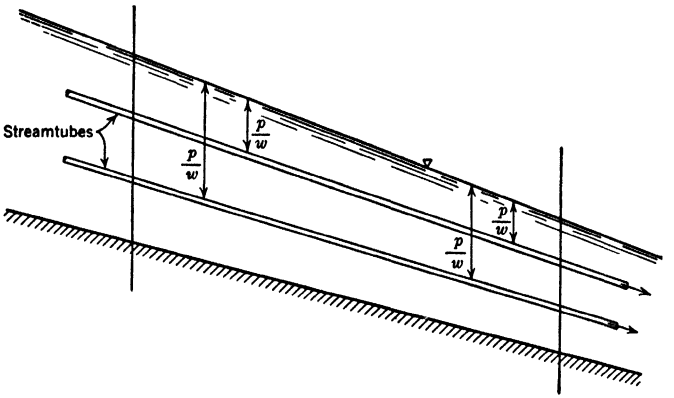


FIG. 109.

the fact that pressure conditions are determined by the constant pressure, usually atmospheric, existing on the entire surface of the flowing liquid. In general, pressure variations within a liquid flowing in an open channel are determined by the principles of fluid statics (Art. 8) unless the flow is sharply divergent, convergent, or curved; the latter conditions are accompanied by vertical accelerations or

decelerations which disrupt the laws of static pressure distribution (Art. 15). Therefore, with the foregoing exceptions, the pressure head equivalent to the pressure at a point in open-channel flow is exactly equal to the depth of submergence of the point (Fig. 109). This leads to the conclusion that the hydraulic grade lines for all the streamtubes which compose open-channel flow lie in the liquid surface.

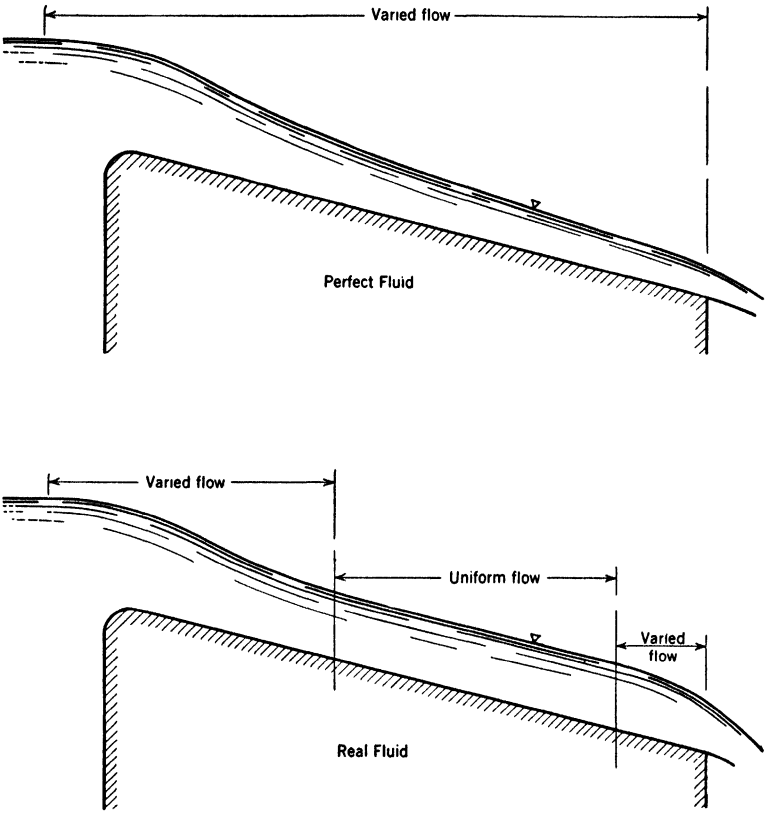


FIG. 110.

Open-channel flow may be laminar or turbulent, steady or unsteady, "uniform" or "varied," "tranquil" or "rapid." The laminar flow of liquids in open channels has few practical engineering applications, and the problem of unsteady flow in open channels is an exceedingly complex one; the following discussion will therefore be confined to steady turbulent flow. The definitions of tranquil and rapid flow will be presented subsequently, but the significance, causes, and limits

of uniform and varied flow must now be examined. The meaning of these terms and the fundamentals of open-channel flow may be seen from a comparison of perfect fluid flow and real fluid flow in similar channels of unchanging shape leading from reservoirs of the same surface elevation (Fig. 110).[1] No resistance will be encountered by the perfect fluid as it flows down the channel, and because of this lack of resistance it will continually accelerate under the influence of gravity. Thus, the velocity of flow in the channel continually increases, and with this velocity increase, a reduction in flow cross section is required by the continuity principle. Reduction in flow cross section is characterized by a decrease in depth of flow; since the depth of flow continually "varies" when the forces acting on fluid particles are unbalanced, this type of fluid motion is termed *varied flow.*

When real fluid flows in the same channel, motion encounters resistance forces due to fluid viscosity and channel roughness. Analysis of the resistance forces originating from these same properties in pipes has shown the forces to depend upon the velocity of flow (equation 54). Thus, in the upper end of the channel where motion is slow, resistance forces are small but the components of gravity forces in the direction of motion are the same as for the ideal fluid. The resulting unbalanced forces in the direction of motion bring about acceleration and varied flow in the upper reaches of the channels. However, with an increase of velocity, the forces of resistance increase until they finally balance those caused by gravity. Upon the occurrence of this force balance, constant-velocity motion is attained, which is characterized by no change of flow cross section and thus no change in the depth of flow —the depth of flow remains constant, hence the term *uniform flow.* Toward the lower end of the channel, pressure forces exceed resistance forces and varied flow again results.

Obviously, an inequality of the above forces is more probable than a balance of these forces, and hence varied flow occurs in practice to a far greater extent than uniform flow. In short channels, for example, uniform-flow conditions may never be attained because of the long reach of channel necessary for the establishment of uniform flow. However, in many problems a rigorous treatment of varied flow is not necessary, and approximate calculations of varied flow may be carried out with the equations of uniform flow. Solution of the uniform-flow problem forms the basis of open-channel-flow calculations.

[1] The channel slopes in most of the illustrations in this chapter have been exaggerated to emphasize their existence. In open-channel practice, slopes are very seldom encountered which are greater than 1 ft in 100 ft, or 0.01.

46. Uniform Flow—The Chezy Equation. The fundamental equation for uniform open-channel flow may be derived readily by equating the equal and opposite forces due to gravity and resistance and applying some of the fundamental notions of fluid mechanics obtained in the analysis of pipe flow. Consider the uniform flow of a liquid between sections 1 and 2 of the open channel of Fig. 111.

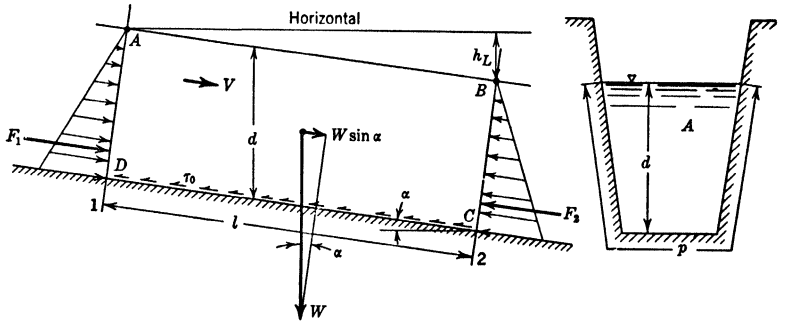


FIG. 111.

The forces acting upon the mass of fluid, $ABCD$, contained between sections 1 and 2 are: (1) the forces of static pressure F_1 and F_2, acting on the ends of the mass; (2) the component of weight in the direction of motion, $W \sin \alpha$; and (3) the force of resistance, F_τ, resulting from the shear stresses, τ_o, on the bottom and sides of the channel. A summation of these forces gives

$$F_1 + W \sin \alpha - F_2 - F_\tau = 0$$

But obviously

$$F_1 = F_2$$

and therefore

$$F_\tau = W \sin \alpha$$

But $W = Awl$, $\sin \alpha = h_L/l$, and $\tan \alpha = S$, in which S is the slope of the channel bed and of the liquid surface as well. For the small slopes encountered in open-channel practice

$$\tan \alpha = \sin \alpha = S$$

Taking τ_o to be the average shear stress on the sides and bottom of the channel the resistance force, F_τ, may be expressed by

$$F_\tau = \tau_o pl$$

Substituting these relationships in the above force equation

$$\tau_o pl = AwlS$$

or

$$\tau_o = w\frac{A}{p}S$$

in which A/p is recognized as the hydraulic radius, R. Therefore

$$\tau_o = wRS \tag{68}$$

In pipe flow, τ_o was shown to be given (equation 54) by

$$\tau_o = f\rho\frac{V^2}{8}$$

in which f, the friction factor, was dependent upon surface roughness and the Reynolds number, but more dependent upon the magnitude of the former for highly turbulent flow. The mechanism of real fluid motion is similar in pipes and open channels, and hence as an approximation it may be concluded that for turbulent flow in open channels

$$\tau_o = KV^2 \tag{69}$$

in which K is a coefficient depending primarily upon the roughness of the channel lining. Substituting this expression in equation 68

$$KV^2 = wRS$$

and thus

$$V = \sqrt{\frac{w}{K}}\sqrt{RS}$$

or, if $C = \sqrt{w/K}$,

$$V = C\sqrt{RS} \tag{70}$$

called the "Chezy equation"[2] after the French hydraulician who established this relationship experimentally in 1775. By applying the continuity principle, the equation may be placed in terms of Q as

$$Q = CA\sqrt{RS} \tag{71}$$

the fundamental equation of uniform flow in open channels.

47. The Chezy Coefficient. Many experiments have been carried out to determine the magnitude of the Chezy coefficient, C, and its dependence upon other variables. A theoretical basis for these experi-

[2] Compare the above derivation of the Chezy equation with that of Art. 41.

mental results may be obtained by the application of some of the fundamental notions of fluid mechanics in the following manner:

From equation 69

$$K = \frac{f\rho}{8}$$

and substituting this expression in the equation for C above,

$$C = \sqrt{\frac{w}{K}} = \sqrt{\frac{8w}{f\rho}} = \sqrt{\frac{8g}{f}}$$

With g a constant, the Chezy coefficient, C, is thus dependent upon the friction factor, f, of the channel. Expressing this in a more general fashion

$$C = F_1(f)$$

But from a study of flow in circular pipes which all have the same shape,

$$f = F_2\left(\frac{Vd}{\nu}, \text{ roughness}\right)$$

In open-channel flow the frictional processes are the same as those in pipes, but the shapes of open channels are quite different and this variation in shape must affect the friction factor. Hence, for open channels

$$f = F_3\left(\frac{VR}{\nu}, \text{ roughness, shape}\right)$$

Designating roughness by n, and recalling (Art. 40) that the hydraulic radius, R, characterizes the shape of the section as regards frictional effects in turbulent flow, this equation may be written

$$f = F_3\left(\frac{VR}{\nu}, n, R\right)$$

or more generally

$$f = F_4(V, \nu, n, R)$$

and, since

$$C = F_1(f),$$

$$C = F_5(V, \nu, n, R)$$

For water flowing in open channels within the usual range of temperature the kinematic viscosity, ν, varies little; taking ν as a constant

$$C = F_6(V, n, R)$$

From the Chezy equation

$$V = F_7(C, R, S)$$

Substituting this relationship in the one above,

$$C = F_8(n, R, S)$$

Theoretical reasoning thus leads to the conclusion that for the turbulent flow of water in open channels the Chezy coefficient is dependent upon the roughness, hydraulic radius, and slope of the channel.

This conclusion is confirmed by the formula for C proposed by Ganguillet and Kutter,[3] two Swiss engineers, in 1869. Their formula was derived from experimental results obtained from hydraulic tests on artificial and natural channels of all descriptions, ranging in size from small laboratory channels up to large rivers. The formula has come to be used widely in this country and abroad, although recently its accuracy has been criticized because of errors in some of the tests on which the formula is based. The formula is

$$C = \frac{41.65 + \dfrac{0.00281}{S} + \dfrac{1.811}{n}}{1 + \left(41.65 + \dfrac{0.00281}{S}\right)\dfrac{n}{\sqrt{R}}}$$

in which S has no dimensions, R is in feet, and n may be obtained from the partial list of values of Table IX. Tables and diagrams are available in the hydraulic literature for the solution of the formula. A graphical method of solution is indicated on Fig. 112.

TABLE IX

VALUES OF THE ROUGHNESS COEFFICIENT, n

Smooth cement, planed timber	0.010
Rough timber, canvas	0.012
Good ashlar masonry or brickwork	0.013
Vitrified clay	0.015
Rubble masonry	0.017
Firm gravel	0.020
Canals and rivers in good condition	0.025
Canals and rivers in bad condition	0.035

[3] *General Formula for the Uniform Flow of Water in Rivers and Other Channels*, translated by R. Hering and J. C. Trautwine, Jr., Second edition, 1893, John Wiley & Sons.

Another expression for the Chezy coefficient may be derived from an analysis by Manning[4] resulting in the formula

$$V = KR^{\frac{2}{3}}S^{\frac{1}{2}}$$

for uniform open channel flow. Comparing the Manning and Chezy formulas,

$$C = KR^{\frac{1}{6}}$$

in which K is dependent upon roughness and is given by $1.486/n$. Thus, Manning's proposal leads to

$$C = \frac{1.486}{n} R^{\frac{1}{6}}$$

which, because of simplicity and satisfactory accuracy, is increasingly preferred over the more cumbersome Kutter formula.

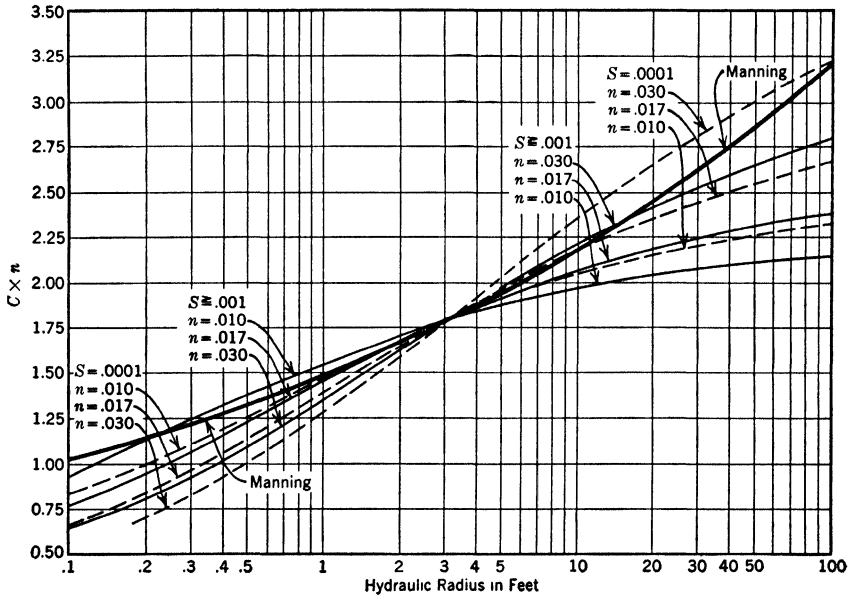


FIG. 112.

The results of the Kutter and Manning formulas may be easily compared and presented for practical use by plotting the product $(C \times n)$ against the hydraulic radius, R (Fig. 112). On such a plot,

[4] *Trans. Inst. Civil Engineers of Ireland*, Vol. 20, 1890, p. 161.

the Manning formula appears as a single line and the Kutter formula as a series of curves whose location depends upon slope and roughness.

Another advantage of the Manning formula is that its simplicity allows it to be inserted into the Chezy equation,

$$Q = \frac{1.486}{n} R^{\frac{1}{6}} A\sqrt{RS}$$

giving

$$Q = \frac{1.486}{n} AR^{\frac{2}{3}} S^{\frac{1}{2}} \tag{72}$$

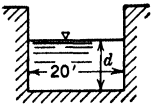
and allowing calculations to be carried out without the necessity for tables or diagrams of C. The equation also shows clearly that an error in the selection of the roughness coefficient, n, causes an error of the same magnitude in the calculated quantity of flow, Q. It is evident from Table IX that experience is essential to the selection of n and the accurate prediction of rates of flow.

ILLUSTRATIVE PROBLEM

A rectangular channel lined with rubble masonry is 20 ft wide and laid on a slope of 0.0001. Calculate the depth of uniform flow in this channel when 400 cfs flow therein

$$n = 0.017, \quad A = 20d, \quad R = \frac{20d}{20 + 2d}$$

Using the Manning equation



$$400 = \frac{1.486}{0.017}(20d)\left(\frac{20d}{20 + 2d}\right)^{\frac{2}{3}}(0.0001)^{\frac{1}{2}}$$

whence

$$\left(\frac{20d}{20 + 2d}\right)^{\frac{2}{3}} d = 22.9$$

Solving by trial, $d = 8.34$ ft

48. Best Hydraulic Cross Section. It is obvious from

$$Q = CA\sqrt{RS}$$

that for a given area of flow cross section, A, and for a given slope, S, the rate of flow, Q, through a channel of given roughness will be maximum when the hydraulic radius, R, is maximum. It becomes important, therefore, for best engineering design to proportion the dimensions

of the channel cross section to give an hydraulic radius which is as large as is practically possible. From the definition of hydraulic radius

$$R = \frac{A}{p}$$

it is obvious that a cross section of maximum hydraulic radius is a cross section of minimum wetted perimeter, p. Minimum wetted perimeter means a minimum of lining material, grading, and general construction work. Hence, a channel cross section having maximum hydraulic radius not only results in the best hydraulic design but tends toward a section of minimum cost as well. It, therefore, becomes of practical interest to investigate certain channel shapes to discover how they may be proportioned in order to have maximum hydraulic radii.

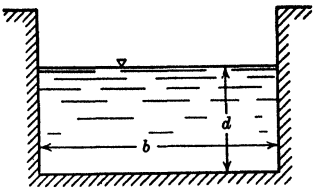


FIG. 113.

For a rectangular cross section of width b and depth d, having a fixed cross-sectional area A, Fig. 113, the dimensions for the conditions of maximum hydraulic radius may be calculated by writing a general expression for the hydraulic radius and obtaining its maximum by differentiating and equating to zero. From Fig. 113,

$$R = \frac{A}{b + 2d}$$

and

$$b = \frac{A}{d}$$

giving

$$R = \frac{A}{\frac{A}{d} + 2d} = \frac{Ad}{A + 2d^2}$$

Differentiating in respect to d and equating to zero

$$\frac{dR}{dd} = \frac{(A + 2d^2)A - Ad(0 + 4d)}{(A + 2d^2)^2} = 0$$

gives

$$A = 2d^2$$

But since A is also given by

$$A = bd$$

comparison of these expressions shows that

$$b = 2d$$

or, in other words, the breadth of a rectangular channel must be twice the depth for a condition of maximum hydraulic radius. The magnitude of the hydraulic radius when maximum may be calculated by substituting the above expressions in the general equation for hydraulic radius as follows:

$$R = \frac{A}{b + 2d} = \frac{2d^2}{2d + 2d} = \frac{d}{2}$$

Thus, when the hydraulic radius is maximum for a rectangular channel it is equal to one-half of the depth of flow.

For the trapezoidal[5] section of Fig. 114, the cross-sectional area is given by

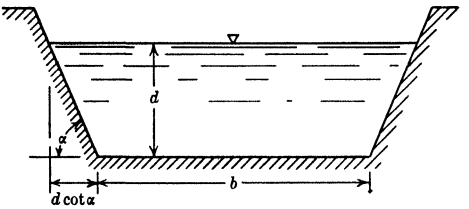


FIG. 114.

$$A = bd + d^2 \cot \alpha$$

from which

$$b = \frac{A}{d} - d \cot \alpha$$

and the wetted perimeter by

$$p = b + 2d \csc \alpha$$

Substituting the above expression for b

$$p = \frac{A}{d} - d \cot \alpha + 2d \csc \alpha$$

Thus the hydraulic radius may be stated

$$R = \frac{A}{p} = \frac{A}{\frac{A}{d} - d \cot \alpha + 2d \csc \alpha}$$

Differentiating in respect to d and equating to zero, the conditions for maximum hydraulic radius are obtained, given by

$$A = d^2(2 \csc \alpha - \cot \alpha)$$

[5] The angle of side slope, α, is generally limited in an earth canal by the angle of repose of the soil. If the canal is lined α may have any value.

Substituting this in the general expression for R,

$$R = \frac{d}{2}$$

as was obtained in the rectangular channel for conditions of maximum hydraulic radius.

ILLUSTRATIVE PROBLEM

What are the best dimensions for a rectangular channel which is to carry 400 cfs if the channel is lined with rubble masonry and is laid on a slope of 0.0001 ?

$$n = 0.017, \quad A = 2d^2, \quad R = \frac{d}{2}$$

$$400 = \frac{1.486}{0.017} \times 2d^2 \times \left(\frac{d}{2}\right)^{\frac{2}{3}} (0.0001)^{\frac{1}{2}}$$

whence

$$d^{\frac{8}{3}} = 364, \quad d = 9.15 \text{ ft}$$

$$b = 2d = 18.30 \text{ ft}$$

or

$$\begin{cases} 400 = \dfrac{1.486}{0.017} (bd) \left(\dfrac{bd}{b + 2d}\right)^{\frac{2}{3}} (0.0001)^{\frac{1}{2}} \\ \dfrac{d}{2} = \dfrac{bd}{b + 2d} \end{cases}$$

and solving these equations simultaneously

$$b = 18.30 \text{ ft} \qquad d = 9.15 \text{ ft}$$

49. Variation of Velocity and Rate of Flow with Depth in Closed Conduits. Frequently in civil engineering practice, particularly in sewer problems, closed conduits that do not flow full are used to convey liquids. Conduits of this type, in which flow does not occur under pressure, satisfy the definition of open channels and must be considered as such. Open-channel flow in closed conduits possesses certain special features because of the convergence of the side walls at the top of the conduit. For sewer design it is essential to have available the relations of velocity and rate of flow to depth for conduits of various shapes; the depth at which the maximum quantity of flow will occur must be known for capacity calculations, and the variation of velocity with depth must also be understood since certain velocities must be maintained in order to transport suspended solid matter.

A simple analysis of these features may be carried out by using the Manning form of the Chezy equation for rate of flow and velocity

$$Q = \frac{1.486}{n} AR^{\frac{2}{3}}S^{\frac{1}{2}}$$

$$V = \frac{1.486}{n} R^{\frac{2}{3}}S^{\frac{1}{2}}$$

For a conduit of a certain roughness, n, laid on a given slope, S, it is obvious that

$$Q \propto AR^{\frac{2}{3}}$$

$$V \propto R^{\frac{2}{3}}$$

and that A and R are both functions of the depth d. Hence Q and V may be plotted against the depth by assuming various values of d, and calculating the corresponding velocities and rates of flow. By dividing these velocities and flow rates by those obtained when the conduit flows full a more generally useful diagram is obtained in which the velocities and rates of flow are both unity when the conduit flows full.

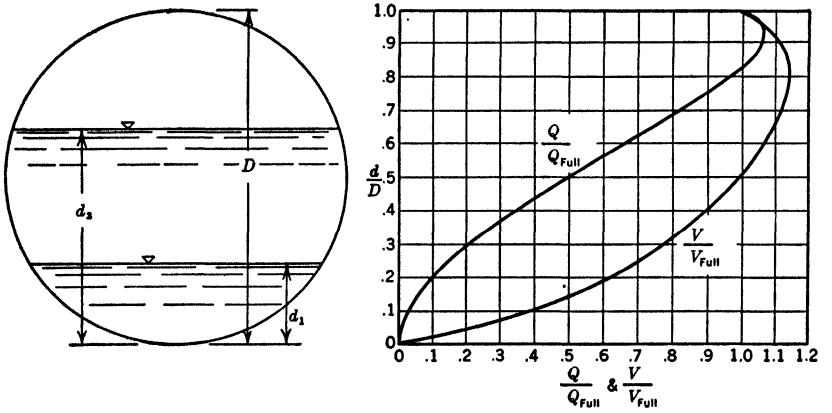


FIG. 115.

A diagram of this type is shown for a circular conduit in Fig. 115; it gives, for any depth, the ratio of rate of flow and velocity at that depth to those when the conduit flows full; with rate of flow and velocity for the full conduit easily obtainable from the Chezy equation, rates of flow and velocities for a partially full conduit are readily found with the aid of the diagram.

The depths at which maximum flow and maximum velocity occur may be obtained directly from the diagram; they are seen to be $0.94D$ and $0.80D$, respectively, for the conduit of circular cross section. These depths may be obtained more accurately by stating $AR^{\frac{2}{3}}$ and $R^{\frac{2}{3}}$ in terms of d, differentiating the expressions in respect to d, equating the results to zero, and solving the resulting equations for d.

50. Specific Energy. Many modern problems in open-channel flow are solved by means of energy calculations. The "specific energy" and its diagram, which were introduced by Bakhmeteff in 1911, have proved fruitful in the explanation of new and old problems of open-channel flow. Today a knowledge of specific energy fundamentals is absolutely necessary in coping with the advanced problems of open

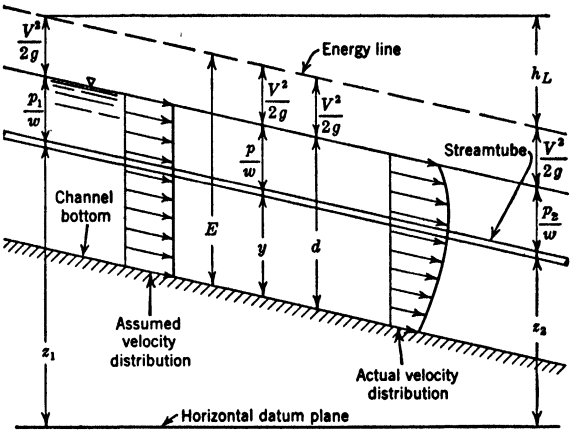


FIG. 116.

flow; these fundamentals and a few of their applications are developed in the succeeding paragraphs.

Consider the uniform flow shown in Fig. 116. Here, for a given slope, roughness, shape, and rate of flow, the depth may be calculated from the Chezy equation. Assuming a uniform velocity distribution, the Bernoulli equation may be written for a typical streamtube as

$$\frac{p_1}{w} + \frac{V_1^2}{2g} + z_1 = \frac{p_2}{w} + \frac{V_2^2}{2g} + z_2 + h_L$$

which indicates that energy is lost as flow occurs. However, if the sloping channel bottom is taken as a datum plane the energy becomes

$$E = y + \frac{p}{w} + \frac{V^2}{2g}$$

which is the same at sections 1 and 2. The term E is called the "specific energy"; from the figure,

$$y + \frac{p}{w} = d$$

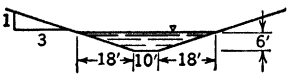
and the definition of specific energy may be simplified to

$$E = d + \frac{V^2}{2g} \qquad . \quad (73)$$

showing that specific energy in open-channel flow is simply the sum of the depth and the velocity head in the channel.

ILLUSTRATIVE PROBLEM

In a trapezoidal channel having a bottom width of 10 ft, 1000 cfs flow at a depth of 6 ft. If the side slopes of the channel are 1 on 3, calculate the specific energy.



$$A = 10 \times 6 + 6 \times 18 = 168 \text{ ft}^2$$

$$V = \frac{1000}{168} = 5.95 \text{ ft/sec}$$

$$E = d + \frac{V^2}{2g} = 6 + \frac{(5.95)^2}{2g} = 6.55 \text{ ft}$$

In uniform open-channel flow Bernoulli energy is lost as flow takes place but specific energy remains constant. In varied flow Bernoulli energy is continually lost, but it will be seen later that specific energy may be lost or gained as varied flow occurs.

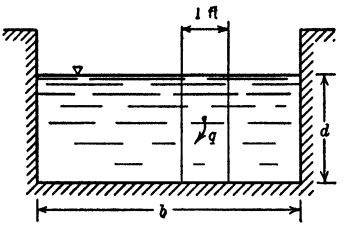


FIG. 117.

It is convenient at this point to deal with flow in a channel of rectangular cross section, whose simple geometrical form will allow the use of simple equations to illustrate the fundamentals. The principles involved may be applied to channels of other shape, but the resulting equations are larger and more difficult to handle.

If a uniform velocity distribution is assumed in the rectangular channel of Fig. 117, the unit rate of flow, q, through a vertical strip of 1-ft width will be given by

$$q = Vd$$

which will eliminate the width of channel, b, from subsequent equations. Obviously q is related to the total rate of flow, Q, by

$$Q = bq$$

From the foregoing equation for q, $V = q/d$, which may be substituted in the equation for specific energy giving

$$E = d + \frac{q^2}{2gd^2} \tag{74}$$

a more useful expression for specific energy, and relating this quantity with depth and rate of flow. A thorough understanding of this equation and its physical meaning may be obtained most easily by: (1) assuming q constant and studying the relation of E and d, and (2) taking E constant and examining the relation of q and d.

In the flow of a certain quantity of liquid in open channels of various slopes, it is evident that steep slopes will tend toward high velocities and small depths, and mild slopes toward low velocities and large depths. The slopes thus determine the depths, but the depths in turn determine the specific energy since q is constant in

$$E = d + \frac{q^2}{2gd^2} \tag{74}$$

Plotting of this equation gives the "specific energy diagram" of Fig. 118 and introduces some new concepts to open-channel flow.

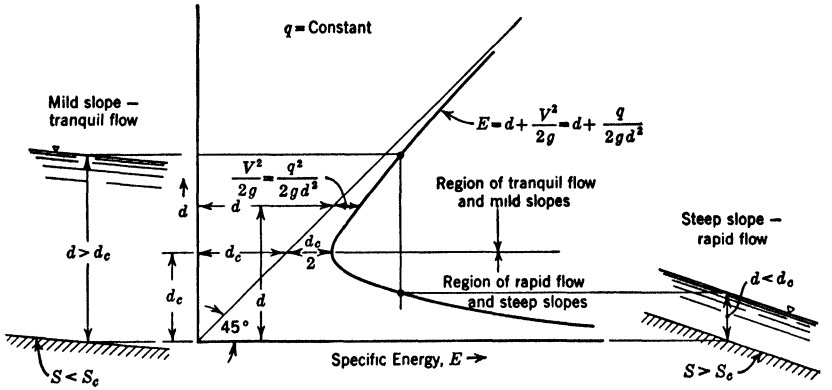


FIG. 118. The Specific Energy Diagram.

The specific-energy curve possesses a point of minimum energy at which the depth is termed the "critical depth." For every specific energy, E, there are two "alternate" depths at which flow may take

place, one greater and one less than the critical depth. If the depth of flow is greater than the critical the flow is said to be "tranquil" and the slopes which bring about such flows are designated as "mild" slopes. The flow is said to be "rapid" if its depth is less than the critical depth; rapid flows are caused by "steep" slopes. Uniform flow at the critical depth will occur when the channel has a "critical slope," S_c.

Certain general characteristics of open-channel flow may be deduced from the specific-energy curve. In the region of flow near the critical depth, the depth may change for practically constant specific energy. Physically this means that, since many depths may occur for approximately the same specific energy content, flow near the critical depth will possess a certain instability (which frequently manifests itself by undulations in the liquid surface). It is also evident from the curve that a loss of specific energy will be accompanied by a reduction in depth in tranquil flow, but in rapid flow an increase of depth is associated with a loss of specific energy.

The relation between depth and rate of flow for constant specific energy may be obtained by solving equation 74 for q, resulting in

$$q = \sqrt{2gd^2E - 2gd^3} \tag{75}$$

From this equation may be plotted the "q-curve"[6] of Fig. 119. The physical meaning of such a curve may be determined by assuming a

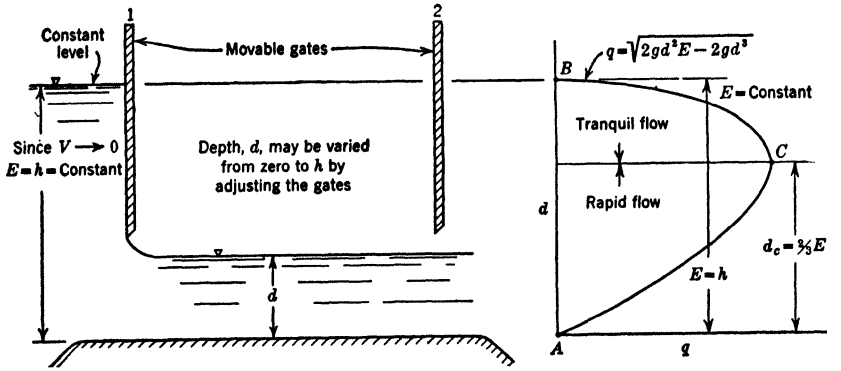


FIG. 119. The q-Curve.

reservoir of a constant surface elevation which discharges into an open channel with movable gates at each end. If the velocity in the

[6] Originally suggested by Koch. For a summary of his work see A. Koch and M. Carstanjen, *Bewegung des Wassers*, 1926.

reservoir is neglected the specific energy here will be constant and equal to the height h throughout manipulation of the gates. If it is assumed that no energy is lost as flow passes the first gate the fluid flowing in the channel will possess the constant specific energy h. By adjusting the gates the depth of liquid in the channel may be varied between zero and h without changing the specific energy, and during this variation the relation between rate of flow and depth is given by the "q-curve" — point A occurs when gate 1 is completely closed, point B when gate 1 is open but gate 2 completely closed, and point C when both gates are removed and unobstructed flow takes place. The last condition brings about a maximum rate of flow which occurs at the critical depth since the point of maximum flow for a given specific energy content is the same as that of minimum energy for a given rate of flow. Hence the regions of rapid and tranquil flow may be indicated on the q-curve as shown.

51. Critical-Depth Relationships. The calculation of critical depth is necessary to the identification of tranquil and rapid flow, and the derivation of the equations of critical flow lends a further significance to the critical depth.

Since critical depth occurs when specific energy is minimum for a given rate of flow the equations of critical flow may be obtained by differentiating equation 74 and equating the result to zero. Performing this operation,

$$\frac{dE}{dd} = \frac{d}{dd}\left(d + \frac{q^2}{2gd^2}\right) = 1 + \frac{q^2}{2g}\left(-\frac{2}{d_c^3}\right) = 0$$

in which d has become d_c after differentiation. From this equation there results

$$q^2 = gd_c^3 \tag{76}$$

which when substituted in the general specific-energy equation gives

$$E_c = d_c + \frac{gd_c^3}{2gd_c^2} = \frac{3}{2}d_c \tag{77}$$

Other important critical-flow equations may be readily derived from equation 76, and these are

$$q = \sqrt{gd_c^3} \tag{78}$$

or

$$d_c = \sqrt[3]{\frac{q^2}{g}} \tag{79}$$

or since

$$q = V_c d_c$$

$$V_c = \sqrt{g d_c} \tag{80}$$

Since these equations may also be obtained by the differentiation of equation 75, the maximum point of the q-curve must correspond to the minimum point of the specific-energy curve, indicating that the former point occurs at the critical depth as stated above.

The foregoing equations demonstrate and suggest certain points concerning critical flow. Equation 79 shows that critical depth depends only upon the rate of flow in the channel. It is a characteristic parameter of the flow which may be determined as soon as q is known. Equation 78 suggests utilizing critical flow as a means of metering open-channel flow. If critical flow may be caused to exist in a channel its depth may be measured and the rate of flow calculated.

Equation 80 is the same as another equation of fluid mechanics

$$V = \sqrt{gd}$$

which gives the velocity of propagation of a small wave on the surface of a body of liquid of depth d. The similarity of these equations offers a rough means of identifying rapid, tranquil, and critical flows in the field. Since critical flow takes place at a velocity exactly equal to the velocity of propagation of a small surface wave, such a wave which is created on the surface of a critical flow cannot progress upstream but will remain stationary because of the equality of velocities. In tranquil and rapid flows, velocities are respectively less than and more than $\sqrt{gd}$; thus in tranquil flow small surface waves will progress upstream, but in rapid flow such waves will be swept downstream.[7]

ILLUSTRATIVE PROBLEM

When 400 cfs flow at a depth of 4 ft in a rectangular channel 20 ft wide, is the flow tranquil or rapid?

$$d_c = \sqrt[3]{\frac{q^2}{g}} = \sqrt[3]{\frac{\left(\frac{400}{20}\right)^2}{32.2}} = 2.32 \text{ ft}$$

Since $4 > 2.32$ ft, flow is tranquil.

52. Occurrence of Critical Depth. The critical depth will occur in open-channel flow when a change in channel slope brings about

[7] The similarity between wave velocity phenomena in open flow and acoustic velocity phenomena in gas flow (Art. 22) should be noted.

a change from tranquil to rapid flow or from rapid to tranquil flow. Two occurrences of critical depth are shown in Fig. 120, where a change from a mild slope to a steep slope causes the flow to pass through the critical depth in its smooth transition from tranquil to rapid flow. An abrupt change from rapid to tranquil flow, the "hydraulic jump,"

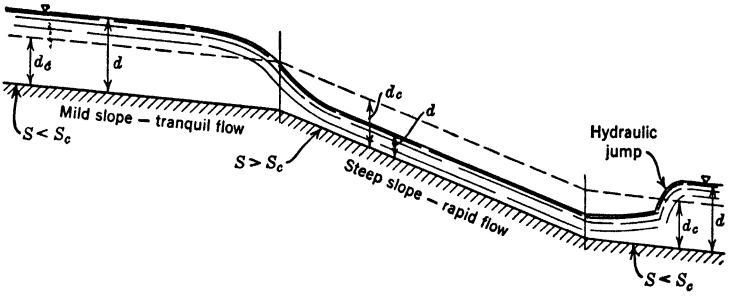


FIG. 120.

occurs when the slope of the channel is changed again to a mild slope; here again the flow passes through the critical depth.

At free outfall from a channel of mild slope (Fig. 121), the critical depth will occur a short distance upstream from the brink. The reason for this is apparent from the specific-energy diagram (Fig. 118). With no obstruction to maintain the depth, the depth may fall from the normal depth of tranquil flow (existing at a great distance up the channel) to the critical depth but may fall no more since further reduction in depth necessitates a gain in specific energy and there is no energy supply from which an energy increase may be drawn. The fact that the brink depth, d_o, is less than the critical is no violation of this principle; here the flow curvatures induce accelerations which upset the simple laws of specific energy. Rouse [8] has found that for very mild slopes the brink depth is a fixed proportion of the critical depth given by

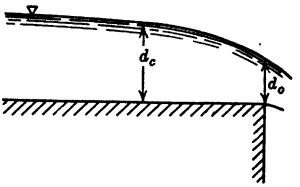


FIG. 121. Free Overfall.

$$\frac{d_o}{d_c} = 0.715 \quad \text{or} \quad d_c = 1.4 d_o$$

[8] H. Rouse, "Discharge Characteristics of the Free Overfall," *Civil Engineering*, Vol. 6, No. 4, p. 257, April, 1936.

He proposes using the brink depth as a means of calculating the rate of flow with the aid of equation 78,

$$q = \sqrt{g d_c^3}$$

Substituting the above relation in this expression

$$q = \sqrt{g(1.4 d_o)^3} = 1.66\sqrt{g}\, d_o^{\frac{3}{2}}$$

or

$$Q = 1.66 b\sqrt{g}\, d_o^{\frac{3}{2}} \tag{81}$$

thus allowing rate of flow to be calculated from measurement of the brink depth.

Flow at critical depth occurs on the crest of a broad-crested weir (Fig. 122), owing to circumstances similar to those of the free outfall. Here, as before,

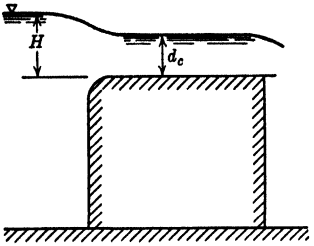


FIG. 122. Broad-Crested Weir.

$$q = \sqrt{g d_3^c}$$

but, friction losses and velocity in the reservoir above the weir being neglected, the specific energy, E_c, of the critical flow, is given by

$$E_c = H$$

But from equation 77

$$d_c = \tfrac{2}{3} E_c$$

and therefore

$$d_c = \tfrac{2}{3} H$$

Substituting above this expression for d_c

$$q = \sqrt{g(\tfrac{2}{3}H)^3}$$

which may be written for comparison with later weir equations

$$Q = 0.578 \times \tfrac{2}{3} b\sqrt{2g}\, H^{\frac{3}{2}} \tag{82}$$

Neglecting friction loss causes this equation to be somewhat in error, and tests on broad-crested weirs indicate the coefficient to be from 0.50 to 0.57 (depending upon the weir shape) instead of the above-derived 0.578.

Critical depth is obtained for purposes of flow measurement by contracting the sides of a channel to form a "venturi flume" or by

raising the channel bottom sufficiently (Fig. 123). The latter problem is essentially one of a submerged broad-crested weir but it presents a means of measuring open-channel flow without the necessity of an inconvenient and costly drop in the channel. Difficulties involved in this method of flow measurement are due to the critical depth location changing as the flow picture changes with varying rates of flow.

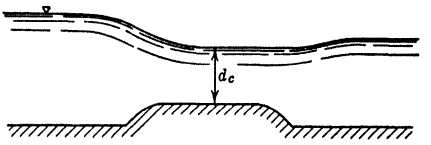


FIG. 123.

As flow passes through the critical depth in its transition from tranquil to rapid flow in the foregoing examples, a "control" is formed. At a "control" in an open channel the depth of flow is determined by the unique relation between depth and rate of flow (equation 79), and depths upstream from this point are "controlled" by the critical depth since occurrences downstream from this point cannot alter the flow above the control. Thus "controls" in an open channel are points where the depths may be calculated directly; depths above and below such controls may be established by the principles of varied flow.

53. Varied Flow. Calculations on varied flow are based on the assumption that the loss of energy in a short reach of channel is the same for varied flow as for a uniform flow having a velocity and hydraulic radius equal to the numerical averages of the velocities and hydraulic radii of the sections at the ends of the reach. This assumption has never been confirmed by experiment, but errors arising from it are likely to be small compared to those incurred in the selection of roughness coefficients. The assumption is undoubtedly more true of varied flow in which the velocity increases than that in which the velocity decreases since in the former energy loss is caused by frictional effects only whereas in the latter the losses due to eddying turbulence are added to those of friction.

Considering the varied flow of Fig. 124, in which the changes of depth and velocity are assumed small,

$$z_1 + d_1 + \frac{V_1^2}{2g} = d_2 + \frac{V_2^2}{2g} + h_L$$

Obviously

$$z_1 = S_o l$$

and

$$h_L = Sl$$

in which S is the slope of the "energy line," which may be assumed to be a straight line over short reaches of channel, l. Substituting these values in the first equation

$$S_o l + d_1 + \frac{V_1^2}{2g} = d_2 + \frac{V_2^2}{2g} + Sl$$

and solving for l

$$l = \frac{\left(d_1 + \frac{V_1^2}{2g}\right) - \left(d_2 + \frac{V_2^2}{2g}\right)}{S - S_o} \tag{83}$$

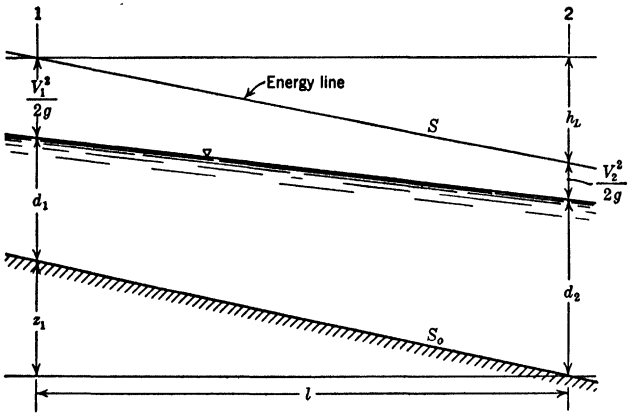


FIG. 124. Varied Flow.

Using now the basic assumption mentioned above, S may be calculated from the Chezy equation for a uniform flow of average velocity and hydraulic radius. Using the Manning coefficient

$$V_{\text{av.}} = \frac{1.486}{n} R_{\text{av.}}^{\frac{2}{3}} S^{\frac{1}{2}}$$

whence

$$S = \left(\frac{n V_{\text{av.}}}{1.486 R_{\text{av.}}^{\frac{2}{3}}}\right)^2$$

in which

$$V_{\text{av.}} = \frac{V_1 + V_2}{2}$$

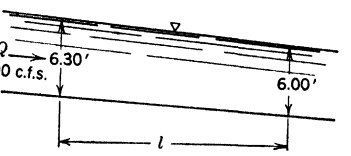
and

$$R_{\text{av.}} = \frac{R_1 + R_2}{2}$$

The general method of making varied-flow calculations is to start at a point in the channel where depth and velocity (say d_2 and V_2) are known, assume a depth, d_1, slightly different from d_2, calculate V_1 and S, and solve equation 83 for the length of reach, l. A fairly accurate profile of the liquid surface in the channel may be obtained by this method if the difference between the known and assumed depths is taken small.

ILLUSTRATIVE PROBLEM

Four hundred cubic feet per second flow in a rectangular channel 20 ft wide, lined with rubble masonry and laid on a slope of 0.0001. The channel ends in a free outfall, and at a point in the channel the depth is 6.00 ft. How far upstream from this point will the depth be 6.30 ft?



$$V_1 = \frac{400}{6.30 \times 20} = 3.18 \text{ ft/sec}$$

$$V_2 = \frac{400}{6.00 \times 20} = 3.33 \text{ ft/sec}$$

$$E_1 = d_1 + \frac{V_1^2}{2g} = 6.30 + \frac{(3.18)^2}{2g} = 6.46 \text{ ft}$$

$$E_2 = d_2 + \frac{V_2^2}{2g} = 6.00 + \frac{(3.33)^2}{2g} = 6.17 \text{ ft}$$

$$V_{av.} = \frac{3.18 + 3.33}{2} = 3.255 \text{ ft/sec}$$

$$R_{av.} = \frac{3.77 + 3.75}{2} = 3.81 \text{ ft}$$

$$S = \left(\frac{0.017 \times 3.255}{1.486 \times (3.81)^{\frac{2}{3}}}\right)^2 = 0.000233$$

$$l = \frac{6.46 - 6.17}{0.000233 - 0.0001} = 2180 \text{ ft}$$

54. The Hydraulic Jump. When a transition of flow occurs from the rapid state to the tranquil state a varied-flow phenomenon results known as the "hydraulic jump" in which the elevation of the liquid surface increases rather abruptly in the direction of flow. Until the last few decades the hydraulic jump was considered by many to be a mysterious and complex phenomenon, but at the present time a com-

plete theoretical solution of the problem involves only a simple application of the laws of fluid statics, impulse-momentum, and specific energy; the results obtained from such a theoretical analysis exhibit close conformity with the results of experimental observations.

An hydraulic jump in a channel of small slope is shown in Fig. 125. It is characterized by an increase of depth,[9] a surface roller, eddying turbulence, and an undulating liquid surface downstream from the jump. Since the jump can occur only as a change from rapid to tranquil flow the depth in changing must pass through the critical depth. In engineering practice the hydraulic jump frequently occurs below a spillway or sluice gate where velocities are high. From Fig. 125 it is obvious that in passing the jump the fluid loses velocity, and the

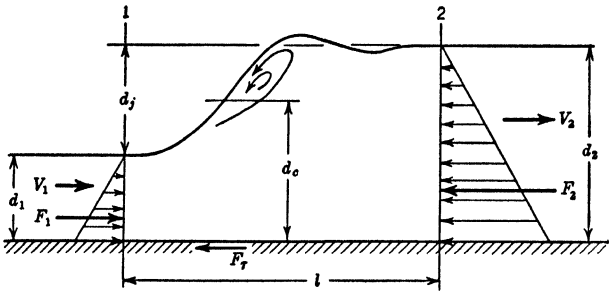


FIG. 125. Hydraulic Jump

jump is often used in this capacity as a dissipator of the kinetic energy of an open flow in order to prevent scour of channel lining.

Between sections 1 and 2 of Fig. 125 there occurs a decrease of velocity from V_1 to V_2 and consequent decrease in the momentum of the flowing liquid which, according to the impulse-momentum law, must be caused by forces continually acting on the liquid mass between these sections. Since the decrease in velocity is in a horizontal direction, the imposed forces are horizontal also and arise (1) from pressure on the ends of the liquid mass and (2) from frictional effects at the sides and bottom of the mass. The pressure forces being designated as F_1 and F_2, and the friction force as F_τ, the impulse-momentum law gives

$$F_2 + F_\tau - F_1 = \frac{Qw}{g}(V_1 - V_2)$$

[9] The jump is not as steep as shown in the figure; the length of jump, l, is usually 4 to 5 times its height, d_j.

in which F_r, resulting from frictional effects over the short distance, l, is safely negligible. The equation, therefore, reduces to

$$F_2 - F_1 = \frac{Qw}{g}(V_1 - V_2)$$

By the principles of fluid statics (Art. 11),

$$F_1 = A_1 w h_{g_1}$$

$$F_2 = A_2 w h_{g_2}$$

Substituting these relationships and $V_1 = Q/A_1$ and $V_2 = Q/A_2$ in the above equation,

$$A_2 h_{g_2} - A_1 h_{g_1} = \frac{Q^2}{g}\left(\frac{1}{A_1} - \frac{1}{A_2}\right) \tag{84}$$

which is the basic general equation for the hydraulic jump in channels of any shape.

Assuming, now, a rectangular channel in order to demonstrate principles and methods with a minimum of mathematical complexity, the above equation reduces through substitution of the following relationships

$$A_1 = bd_1 \qquad A_2 = bd_2$$

$$h_{g_1} = \frac{d_1}{2} \qquad h_{g_2} = \frac{d_2}{2}$$

$$Q = bq$$

to

$$\frac{d_2^2}{2} - \frac{d_1^2}{2} = \frac{q^2}{g}\left(\frac{1}{d_1} - \frac{1}{d_2}\right)$$

which may be written

$$\frac{q^2}{gd_1} + \frac{d_1^2}{2} = \frac{q^2}{gd_2} + \frac{d_2^2}{2} \tag{85}$$

which allows the vertical dimensions of the hydraulic jump to be obtained since if the rate of flow and one depth are known, the other depth may be calculated.

Illustrative Problem

If 400 cfs flow in a rectangular channel 20 ft wide at a depth of 1.00 ft, what depth will exist after an hydraulic jump has occurred from this flow?

$$q = \frac{400}{20} = 20 \frac{\text{ft}^3/\text{sec}}{\text{ft}}$$

$$d_2 = \frac{1}{2}\left[-1 + \sqrt{1 + \frac{8 \times (20)^2}{32.2 \times (1)^3}}\right] = 4.50 \text{ ft}$$

Although special expressions for d_1 and d_2 may be obtained [10] from equation 85, it proves more fruitful to solve the equation by graphical methods. Taking

$$M = \frac{q^2}{gd} + \frac{d^2}{2}$$

it is obvious (1) that, for a given rate of flow, M is a function of d only, and (2) that solution of the equation is given by

$$M_1 = M_2$$

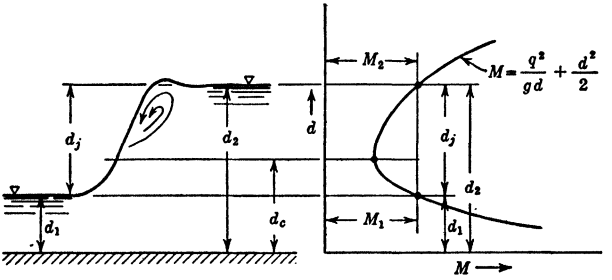


FIG. 126. Hydraulic Jump and M-curve.

The curve obtained (Fig. 126) from plotting M against d possesses a minimum value of M at the critical depth and is similar in shape to the specific-energy diagram. After construction of this curve and with one depth known, the corresponding, or "conjugate," depth may be

[10] Solution of equation 85 gives

$$d_2 = \frac{d_1}{2}\left[-1 + \sqrt{1 + \frac{8\,q^2}{gd_1^3}}\right]$$

or

$$d_1 = \frac{d_2}{2}\left[-1 + \sqrt{1 + \frac{8\,q^2}{gd_2^3}}\right]$$

found by passing a vertical line through the point of known depth. Since a vertical line is a line of constant M, the intersection of this line and the other portion of the curve gives a point where M_1 is equal

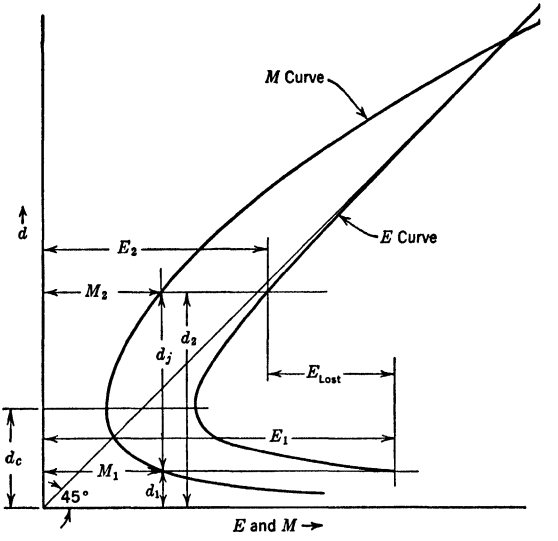


FIG. 127.

to M_2, and allows the conjugate depth and height of jump, dj, to be taken directly from the plot.

By plotting the M-curve and specific-energy curve on the same

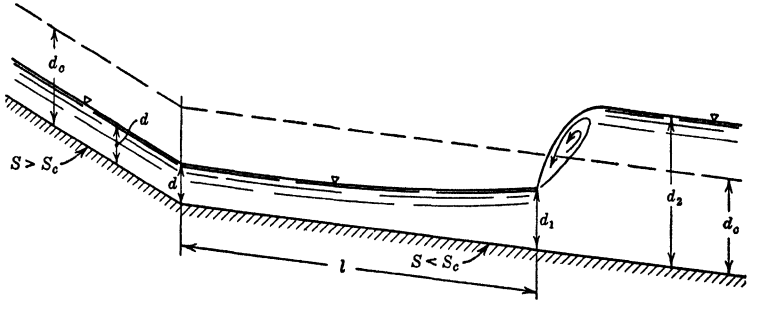


FIG. 128.

diagram, the loss of energy in the jump may be obtained graphically by the methods of Fig. 127, and from the lost energy the horsepower consumed in the jump may be calculated by the usual methods.

A simple problem in locating a hydraulic jump is shown in Fig. 128.

Here a channel of steep slope in which uniform flow is established discharges into a channel of mild slope of sufficient length to contain uniform flow. For a certain rate of flow the depths d and d_2 may be calculated from the Chezy equation. From d_2, d_1 may be obtained from the M-curve or by solution of equation 85. Flow in the reach of channel of length l is of a gradually varied nature, and this length may be obtained by solutions of equation 83; the larger the difference between d_1 and d, the greater the number of solutions necessary for an accurate value of l.

BIBLIOGRAPHY

B. A. BAKHMETEFF, *Hydraulics of Open Channels*, McGraw-Hill Book Co., 1932.

M. P. O'BRIEN and G. H. HICKOX, *Applied Fluid Mechanics*, McGraw-Hill Book Co., 1937.

B. A. BAKHMETEFF and A. E. MATZKE, "The Hydraulic Jump in Terms of Dynamic Similarity," *Trans. A.S.C.E.*, Vol. 101, 1936, p. 630.

H. ROUSE, *Fluid Mechanics for Hydraulic Engineers*, McGraw-Hill Book Co., 1938.

PROBLEMS

342. Water flows uniformly at a depth of 4 ft in a rectangular flume 10 ft wide, laid on a slope of 1 ft per 1000 ft. What is the average shear stress at the sides and bottom of the flume?

343. Calculate the average shear stress over the wetted perimeter of a circular sewer 10 ft in diameter in which the depth of flow is 3 ft and whose slope is 0.0001.

344. What is the average shear stress over the wetted perimeter of a triangular flume 8 ft deep and 10 ft wide at the top, when the depth of water flow is 6 ft? The slope of the flume is 1 in 200.

345. Calculate the friction factor f equivalent to a Chezy coefficient of 120.

346. Calculate the Chezy coefficient which corresponds to a friction factor f of 0.030.

347. For an open channel of hydraulic radius 40 ft, value of n 0.017, and slope 0.0001, check the values of $(C \times n)$ given in Fig. 112.

348. For an open channel of hydraulic radius 0.8 ft, value of n 0.017, and slope 0.001, check the values of $(C \times n)$ given in Fig. 112.

349. What uniform flow will occur in a rectangular planed timber flume 5 ft wide and having a slope of 0.001 when the depth therein is 3 ft. Using: (*a*) Manning C; (*b*) Kutter C.

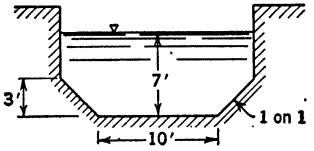
350. Calculate the uniform flow in an earth-lined ($n = 0.020$) trapezoidal canal having bottom width 10 ft, sides sloping 1 on 2, laid on a slope of 0.0001, and having a depth of 6 ft, using: (*a*) Manning C; (*b*) Kutter C.

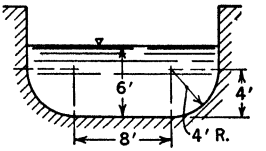
351. What uniform flow exists in a circular brick conduit 5 ft in diameter when the depth of flow is 2 ft, if it is laid on a slope of 0.0005, using: (*a*) Manning C; (*b*) Kutter C.

352. What uniform flow occurs in a river of flow cross section 10,000 ft, wetted perimeter 550 ft, if its slope is 1 in 5000, using: (*a*) Manning C; (*b*) Kutter C? n is 0.025.

353. A rough timber flume in the form of an equilateral triangle (apex down) of 4-ft sides is laid on a slope of 0.01. Calculate the uniform flow which occurs at a depth of 3 ft, using: (*a*) Manning *C*; (*b*) Kutter *C*.

354. What uniform flow will occur in this cross section, if it is laid on a slope of 1 in 2000 and has $n = 0.017$, using (*a*): Manning *C*, (*b*) Kutter *C*?





355. What uniform flow will occur in this open channel if it is laid on a slope of 0.0002 and has a value of n of 0.015, using: (*a*) Manning *C*; (*b*) Kutter *C*?

356. A flume of planed timber has its cross section an isosceles triangle (apex down) of 8-ft base and 6-ft altitude. At what depth will 180 cfs flow uniformly in this flume if it is laid on a slope of 0.01? Use Chezy-Manning equation 72.

357. At what depth will 150 cfs flow uniformly in a rectangular channel 12 ft wide lined with rubble masonry and laid on a slope of 1 in 4000? Chezy-Manning equation 72.

358. At what depth will 400 cfs flow uniformly in an earth-lined ($n = 0.025$) trapezoidal canal of base width 15 ft having side slopes 1 on 3, if the canal is laid on a slope of 1 in 10,000? Chezy-Manning equation 72.

359. Calculate the depth at which 25 cfs will flow uniformly in a smooth cement-lined circular conduit 6 ft in diameter, laid on a slope of 1 in 7000. Chezy-Manning equation 72.

360. An earth-lined ($n = 0.020$) trapezoidal canal of base width 10 ft and side slopes 1 on 3 is to carry 100 cfs uniformly at a maximum velocity of 2 ft/sec. What is the maximum slope that it may have?

361. What slope is necessary to carry 400 cfs uniformly at a depth of 5 ft in a rectangular channel 12 ft wide, having $n = 0.017$?

362. A trapezoidal canal of side slopes 1 on 2 and having $n = 0.017$ is to carry 1300 cfs on a slope of 0.005 at a depth of 5 ft. What base width is required?

363. Rectangular channels of flow cross section 50 ft^2 have dimensions (width $\times$ depth) of (*a*) 25 ft by 2 ft; (*b*) 12.5 ft by 4 ft; (*c*) 10 ft by 5 ft; (*d*) 5 ft by 10 ft. Calculate the hydraulic radii of these sections.

364. What are the best dimensions for a rectangular channel having a flow cross section of 100 ft^2?

365. What are the best dimensions of a trapezoidal channel having a flow cross section of 150 ft^2 and sides sloping at 30°?

366. What are the best dimensions for a rectangular rough timber channel to carry 120 cfs on a slope of 1 in 8000?

367. What are the best dimensions for a trapezoidal canal having side slopes 1 on 3 if it is to carry 1400 cfs on a slope of 0.009? ($n = 0.020$.)

368. What is the minimum slope at which 200 cfs may be carried uniformly in a rectangular channel (having a value of n of 0.014) at a velocity of 3 ft/sec?

369. What is the minimum slope at which 1000 cfs may be carried at a velocity of 2 ft/sec in a trapezoidal canal having $n = 0.025$ and sides sloping 1 on 4?

370. Prove that the best form for a V-shaped open-channel section is one of vertex angle 90°

371. What rate of uniform flow occurs at a depth of 3 in. in a vitrified clay sewer line of 12-in. diameter laid on a slope of 0.003? What is the velocity of this flow?

372. What rate of uniform flow occurs in a 5-ft circular brick conduit laid on a slope of 0.001 when the depth of flow is 3.5 ft? What is the velocity of this flow?

373. At what depth will 800 cfs flow in a circular ashlar masonry conduit 10 ft in diameter, laid on a slope of 0.006? What is the velocity of flow?

374. Solve problem 359 using the plot of Fig. 115. What is the velocity of flow?

375. Plot curves similar to those of Fig. 115 for an isosceles triangle (apex up) whose base is equal to its altitude. Find the maximum points of the curves mathematically.

376. Plot curves similar to those of Fig. 115 for an equilateral triangle (apex up). Find the maximum points of the curves mathematically.

377. Plot curves similar to those of Fig. 115 for a square laid with diagonal vertical. Find the maximum points of the curves mathematically.

378. Calculate the specific energy when 225 cfs flow in a 10-ft rectangular channel at depths of (*a*) 1.5 ft; (*b*) 3 ft; (*c*) 6 ft.

379. Calculate the specific energy when 300 cfs flow at a depth of 4 ft in a trapezoidal channel having base width 8 ft and sides sloping at 45°.

380. What is the specific energy when 60 cfs flow at a depth of 5 ft in a circular channel 6 ft in diameter?

381. Calculate the specific energy when 100 cfs flow at a depth of 3 ft in a triangular (apex down) flume, if the width at the water surface is 4 ft.

382. At what depths may 30 cfs flow in a rectangular channel 6 ft wide if the specific energy is 4 ft?

383. At what depths may 800 cfs flow in a trapezoidal channel of base width 12 ft and sides slopes 1 on 3 if the specific energy is 7 ft?

384. Eight hundred cubic feet per second flow in a rectangular channel of 20 ft width having $n = 0.017$. Plot accurately the specific-energy diagram for depths from 0 to 10 ft, using the same scales for d and E. Determine from the diagram: (*a*) the critical depth; (*b*) the minimum specific energy; (*c*) the specific energy when the depth of flow is 7 ft; (*d*) the depths when the specific energy is 8 ft. What type of flow exists when the depth is (*e*) 2 ft, (*f*) 6 ft, and what are the channel slopes necessary to maintain these depths? What type of slopes are these, and (*g*) what is the critical slope?

385. Flow occurs in a rectangular channel of 20-ft width and has a specific energy of 10 ft. Plot accurately the q-curve. Determine from the curve: (*a*) the critical depth; (*b*) the maximum rate of flow; (*c*) the flow at a depth of 8 ft; (*d*) the depths at which a flow of 1000 cfs may exist and the flow condition at these depths.

386. Five hundred cubic feet per second flow in a rectangular channel 15 ft wide at a depth of 4 ft. Is the flow rapid or tranquil?

387. If 300 cfs flow in a rectangular channel 12 ft wide having $n = 0.015$ and laid on a slope of 0.005, is the flow tranquil or rapid?

388. If 400 cfs flow in a rectangular channel 18 ft wide with a velocity of 5 ft/sec, is the flow tranquil or rapid?

389. Calculate and check the critical depths of problems 384 and 385.

390. What is the maximum flow which may occur in a rectangular channel 8 ft wide for a specific energy of 5 ft?

391. An open rectangular channel 5 ft wide and laid on a mild slope ends in a free outfall. If the brink depth is measured as 0.865 ft, what flow exists in the channel?

392. Calculate the critical depth for 50 cfs flowing in a rectangular channel 8 ft wide. If this channel is laid on a mild slope and ends in a free outfall, what is the depth at the brink?

393. What theoretical flow will occur over a broad-crested weir 30 ft long when the head thereon is 2 ft?

394. The elevation of the crest of a broad-crested weir is 100.00 ft. If the length of this weir is 12 ft and the flow over it 200 cfs, what is the elevation of the water surface upstream from the weir?

395. The critical depth is maintained at a point in a rectangular channel 6 ft wide by building a gentle hump in the bottom of the channel. When the depth over the hump is 2.20 ft, calculate the flow. Sketch the energy line and water surface showing all possible vertical dimensions.

396. If 150 cfs flow in a rectangular channel 10 ft wide, laid on a slope of 0.0004 and having $n = 0.014$, what is the minimum height of hump that may be built across this channel to create critical depth over the hump? Sketch the energy line and water surface, showing all vertical dimensions. Neglect energy losses.

397. A rectangular channel 12 ft wide is narrowed to 6-ft width to cause critical flow in the contracted section. If the depth in this section is 3 ft, calculate the flow and the depth in the 12-ft section, neglecting energy losses in the transition. Sketch energy line and water surface, showing all pertinent vertical dimensions.

398. One hundred and fifty cubic feet per second flow in a rectangular channel 10 ft wide having $n = 0.014$, and laid on a slope of 0.0004. This channel is to be narrowed to cause critical flow in the contracted section. What is the maximum width of contracted section which will accomplish this? Neglect energy losses, and sketch the energy line and water surface, showing vertical dimensions.

399. If 543 cfs flow in a rectangular channel 12 ft wide having $n = 0.017$ laid on a slope of 0.00228 and ending in a free outfall, calculate and plot the water-surface profile from the brink upstream to the region of uniform flow, taking increments of depth of 0.2 ft. How far from the brink does a depth of 5.0 ft occur?

400. The channel of the preceding problem discharges into a channel of the same width and roughness, but having a slope of 0.0293. Calculate and plot the water-surface profile downstream to the region of uniform flow, taking decrements of depth of 0.2 ft. How far from the point of slope change does a depth of 3.0 ft exist?

401. In a rectangular channel 12 ft wide having $n = 0.017$ and laid on a slope of 0.0293, 543 cfs flow uniformly. This channel discharges into one of the same width and roughness laid on a slope of 0.00228. Calculate and plot the water-surface profile downstream until a depth of 3.00 ft is reached, using depth increments of 0.2 ft. How far from the point of slope change does a depth of 2.6 ft exist?

402. Eight hundred cubic feet per second flow in a rectangular channel of 20-ft width. Plot the M curve of hydraulic jumps on the specific-energy diagram of problem 384. From these curves determine: (*a*) the depth after a hydraulic jump has taken place from a depth of 1.5 ft; (*b*) the height of this jump; (*c*) the specific energy before the jump; (*d*) the specific energy after the jump; (*e*) the loss of energy in the jump; (*f*) the total horsepower lost in the jump.

403. A flow of 200 cfs takes place in a rectangular channel 15 ft wide at a depth of 0.5 ft. Calculate the depth after a hydraulic jump has taken place from this flow.

Calculate F_1, F_2, and the change of momentum per second, and check the relationship between these terms.

404. If 543 cfs flow in a rectangular channel 12 ft wide having $n = 0.017$ and laid on a slope of 0.00228, what depth of flow must exist in this channel for a jump to occur resulting in uniform flow? How far downstream from the point of change of slope of problem 401 will such a jump be located?

CHAPTER VIII

FLUID MEASUREMENTS

In engineering and industrial practice one of the fluid problems most frequently encountered by the engineer is the measurement of many of the fluid characteristics discussed in the foregoing chapters. Efficient and accurate measurements are also absolutely essential for correct conclusions in the various fields of fluid research. Whether the necessity for precise measurements is economic or scientific, the engineer of today must be well equipped with a knowledge of the fundamentals and existing methods of measuring various fluid properties and phenomena. It is the purpose of this chapter to indicate only the basic principles of fluid measurements; the reader will find available in the engineering literature [1] the details of installation and operation of the various measuring devices. Although many of the following devices frequently appear in engineering practice as appurtenances in various designs where they are not used for measuring purposes, a study of them as measuring devices will make obvious their applications in other capacities.

55. Measurement of Fluid Properties. Of the fluid properties: density, viscosity, elasticity, surface tension, and vapor pressure, the engineer is usually called upon to measure only the first two. Since measurements of elasticity, surface tension, and vapor pressure are normally made by physicists and chemists, the various experimental techniques for measuring these properties will not be discussed here.

The density of liquids may be determined by the following methods, listed in approximate order of their accuracy: (1) weighing a known volume of liquid; (2) hydrostatic weighing; (3) Westphal balance, (4) hydrometer, and (5) U-tube.

To weigh accurately a known volume of liquid a device called a "pycnometer" is used. This is usually a glass vessel whose weight, volume, and variation of volume with temperature have been accurately determined. If the weight of the empty pycnometer is W_1, and the weight of the pycnometer, when containing a volume V of liquid

[1] See bibliography at end of chapter.

at temperature t is W_2, the specific weight of the liquid, w_t, at this temperature may be calculated directly from

$$w_t = \frac{W_2 - W_1}{V}$$

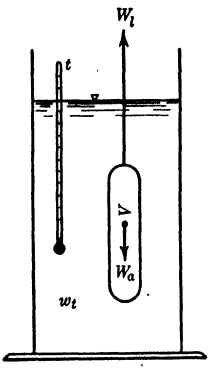


FIG. 129.

Density determination by hydrostatic weighing consists essentially of weighing a plummet of known volume (1) in air and (2) in the liquid whose density is to be determined (Fig. 129). If the weight of the plummet in air is W_a, its volume, V, and its weight when suspended in the liquid, W_l, the equilibrium of vertical forces on the plummet gives

$$W_l + w_t V - W_a = 0$$

and results in

$$w_t = \frac{W_a - W_l}{V}$$

allowing the specific weight, w_t, at the temperature t to be calculated directly.

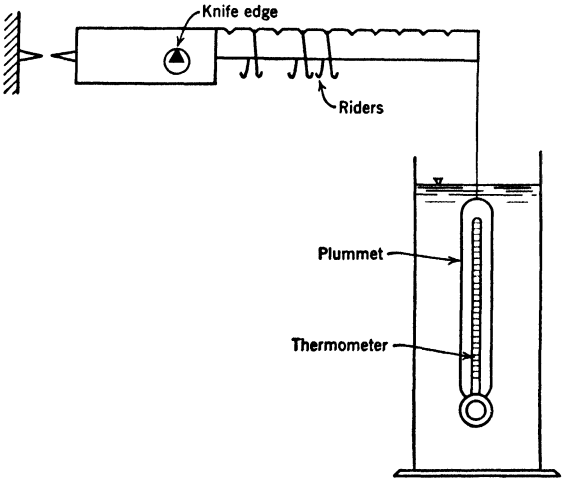


FIG. 130. Westphal Balance.

Like the above method of hydrostatic weighing, the Westphal balance (Fig. 130) utilizes the buoyant force on a plummet as a measure of specific gravity. Balancing the scale beam with special riders placed at special points allows direct and precise reading of specific gravity.

Probably the most common means of obtaining liquid densities is with the hydrometer (Fig. 131), whose operation is governed by the fact that a weighted tube will float with different immersions in liquids of different densities. To create a great variation of immersion for small density variation and, thus, to give a sensitive instrument, changes in the immersion of the hydrometer occur along a slender tube,

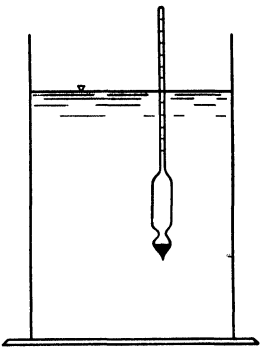


FIG. 131. Hydrometer.

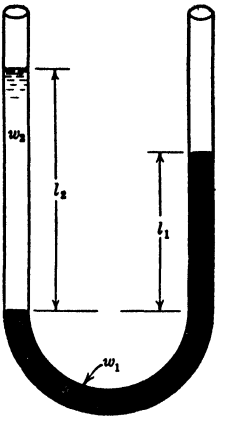


FIG. 132.

which is graduated to read the specific gravity of the liquid at the point where the liquid surface intersects the tube.

The unknown density of a liquid 1 may be obtained approximately from the known density of a liquid 2 (if the liquids are not miscible) by placing them in an open U-tube and measuring the lengths of liquid columns, l_1 and l_2 (Fig. 132). From manometer principles,

$$w_1 l_1 = w_2 l_2$$

and thus

$$w_1 = \frac{l_2}{l_1} w_2$$

This method is not a precise one because the various menisci prevent accurate measurement of the lengths of the liquid columns.

Viscosity measurements are made with devices known as "viscosimeters" or "viscometers," which may be classified as "rotational," "falling-sphere," or "tube" devices according to their construction or operation. The operation of all these viscometers depends upon the existence of laminar flow under certain controlled conditions.

In general, however, these conditions involve too many complexities to allow the constants of the viscometer to be calculated theoretically; and they are, therefore, usually obtained by calibration with a liquid of known viscosity. Because of the variation of viscosity with temperature all viscometers must be immersed in constant-temperature baths and provided with thermometers for taking the temperatures at which the viscosity measurements are made.

Two viscometers of the rotational type are the MacMichael and Stormer viscometers, whose essentials are shown diagrammatically in Fig. 133. Both consist of concentric cylinders, the space between which contains the liquid whose viscosity is to be measured. In the

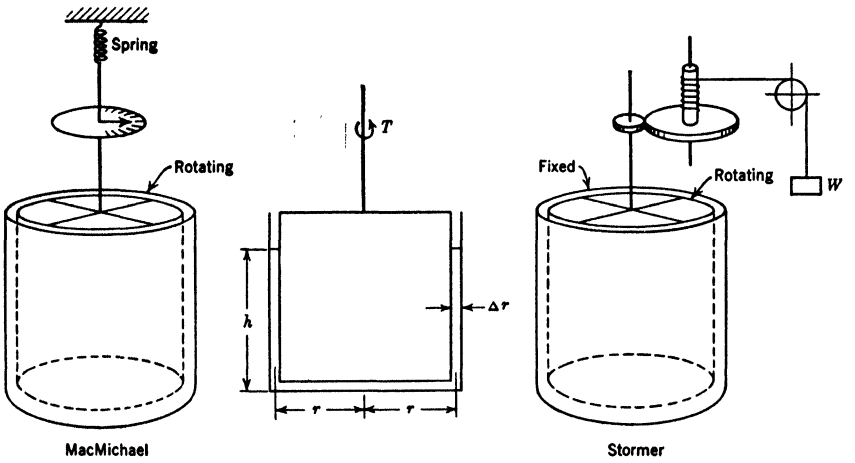


FIG. 133. Rotational Viscometers (Schematic).

MacMichael type, the outer cylinder is rotated at constant speed and the rotational deflection of the inner cylinder (accomplished against a spring) becomes a measure of the liquid viscosity. In the Stormer instrument, the inner cylinder is rotated by a falling-weight mechanism, and the time necessary for a fixed number of revolutions becomes a measure of the liquid viscosity.

The measurement of viscosity by the above variables may be justified by a simplified mechanical analysis, using the dimensions of Fig. 133. Assuming Δr small, and the peripheral velocity of the moving cylinder to be V, the torque, T, is given (neglecting shear stress on the bottom of the cylinder) by

$$T = (\tau 2\pi rh)r = \mu \frac{dv}{dr} 2\pi r^2 h$$

in which

$$dv = V \quad \text{and} \quad dr = \Delta r$$

therefore

$$T = \mu \frac{V}{\Delta r} 2\pi r^2 h$$

But if N = revolutionary speed in revolutions per second, $V = 2\pi rN$, thus

$$T = \mu \frac{2\pi rN}{\Delta r} 2\pi r^2 h$$

or

$$T = K\mu N$$

in which K is a constant whose magnitude depends on the size, proportions, and depth of filling of the viscometer. This equation may be written

$$\mu = \frac{T}{KN}$$

and since the torsional deflection, θ, of the spring is proportional to the torque, the equation becomes for the MacMichael viscometer

$$\mu = K_1 \frac{\theta}{N}$$

showing that liquid viscosity, μ, may be measured by the torsional deflection θ obtained at a speed N. In the Stormer viscometer the torque, T, is maintained constant by the weight mechanism, and thus

$$\mu = \frac{K_2}{KN}$$

If t is the time necessary for a fixed number of revolutions, obviously

$$\mu = K_3 t$$

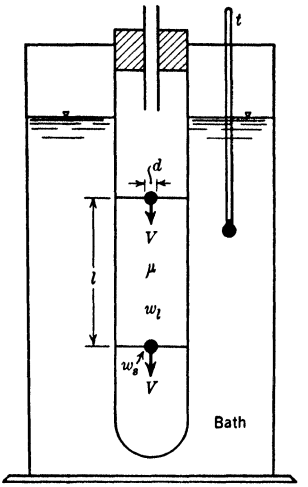
and this time becomes a measure of liquid viscosity.

The falling-sphere type of viscometer is shown in Fig. 134. In this type of viscometer the time t required for a small sphere to fall at constant velocity through a distance l in a liquid becomes a direct measure of the liquid's viscosity. Here again an approximate analysis

justifies the above. From Stokes' law (Art. 77) the drag D of a sphere of diameter d, moving under laminar conditions at a velocity V, through a fluid of infinite extent, is given by

$$D = 3\pi\mu Vd$$

If the proximity of the boundary walls is neglected, this equation may be applied for an approximate analysis of the viscometer. This drag force acts upward on the sphere and acting in the same direction is the buoyant force, F_B, given by



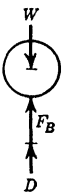


FIG. 134. Falling-Sphere Viscometer.

$$F_B = \frac{\pi}{6} d^3 w_l$$

Acting downward on the sphere is its own weight, W, given by

$$W = \frac{\pi}{6} d^3 w_s$$

For constant-velocity motion the net force on the moving sphere is zero, giving

$$D - W + F_B = 0$$

or

$$3\pi\mu Vd = \frac{\pi}{6} d^3 (w_s - w_l)$$

Solving for μ

$$\mu = \frac{K(w_s - w_l)}{V} = \frac{K(w_s - w_l)t}{l}$$

Thus viscosity in this instrument is measured by time of fall but density of sphere and liquid must be known before viscosity can be calculated.

Two typical tube-type viscometers are the Ostwald and Saybolt instruments of Fig. 135. Similar to the Ostwald is the Bingham type, and similar to the Saybolt are the Redwood and Engler viscometers. All these instruments involve the unsteady laminar flow of a fixed quantity of liquid through a small tube under fixed head conditions. The time for the quantity of liquid to pass through the tube becomes a measure of the *kinematic viscosity* of the liquid.

The Ostwald viscometer is filled to level A, and the meniscus of the liquid in the right-hand tube is then drawn up to a point above B. The time for the meniscus to fall from B to C becomes a measure of the kinematic viscosity. In the Saybolt viscometer the outlet is plugged and the reservoir filled to level A, the plug is then removed and the time required to collect a fixed quantity of liquid in the vessel B is measured. This time then becomes a direct measure of the kinematic viscosity of the liquid.

The relation between time and kinematic viscosity for the tube type of viscometer may be indicated approximately by applying the Hagen-Poiseuille law for laminar flow in a circular tube (Art. 34). The approximation involves the application of a law of *steady established* laminar motion to a condition of unsteady flow in a tube which is too short for established laminar flow to exist and therefore cannot give a complete or perfect relationship between efflux time and kinematic viscosity; it will serve, however, to indicate elementary principles. From equation 46

$$Q = \frac{\pi d^4 w h_L}{128 \mu l}$$

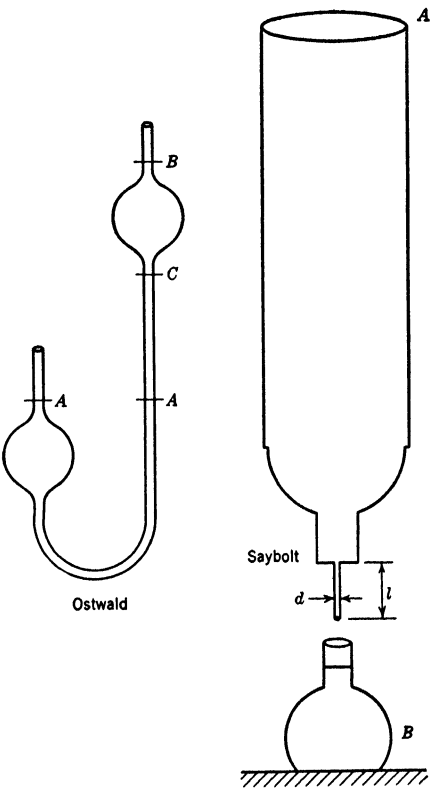


FIG. 135. Tube Viscometers (Schematic)

for steady laminar flow in a circular tube. But $Q = V/t$ (approximately), in which V is the volume of liquid collected in time t. Thus,

$$\frac{V}{t} = \frac{\pi d^4 w h_L}{128 \mu l}$$

and solving for μ

$$\mu = \frac{\pi d^4 w h_L t}{128 V l}$$

The lost head, h_L, however, is nearly constant since it is nearly equal to the imposed head which varies between fixed limits. Since d and l are constants of the instrument the equation reduces to

$$\mu = Kwt$$

or

$$\mu = K\rho gt = K_1\rho t$$

thus

$$\frac{\mu}{\rho} = \nu = K_1 t \qquad \text{(approximately)}$$

The correct empirical equation relating ν and t for the Saybolt Universal viscometer is

$$\nu \text{ in ft}^2/\text{sec} = 0.000002365t - \frac{0.001935}{t} \quad (\text{for } 100 > t > 32)$$

in which t is the time in seconds (called "Saybolt seconds"), and in which the negative term appears as a correction embodying the neglected factors of the above simplified analysis.

Of the tube viscometers the Saybolt, Engler, and Redwood are built of metal to rigid specifications and hence may be used without calibration. Since the dimensions of the glass viscometers such as the Bingham and Ostwald cannot be perfectly controlled, these instruments must be calibrated before viscosity measurements can be made.

56. Measurement of Static Pressure. The accurate measurement of pressure in a fluid at rest may be accomplished with comparative

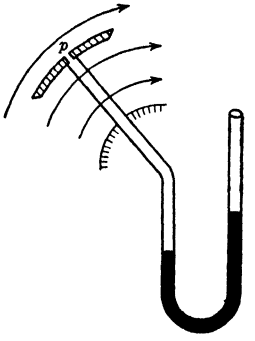


FIG. 136.

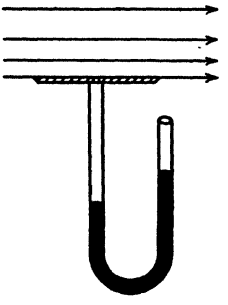


FIG. 137.

ease since it depends only upon the accuracy of the gage or manometer used to record this pressure and is independent of the details of the connection between fluid and recording device. To measure the static

pressure within a moving fluid with perfect accuracy is quite another matter, however, and depends upon painstaking attention to the details of the connection between flowing fluid and measuring device.

To measure the static pressure in the curved flow of Fig. 136, for example, a device must be introduced which *fits the streamline picture perfectly and thus does not disturb the flow at all*, and such a device must contain a small smooth hole, called a "piezometer opening," whose axis is normal to the direction of motion at the point where the static pressure is to be measured; to this opening may be connected a manometer or pressure gage to register the pressure transmitted into the opening. Although meeting these requirements perfectly is a virtual impossibility, the attempt nevertheless illustrates the problem involved in the measurement of static pressure. The above device is a practical one for use in rectilinear flows (Fig. 137), where the difficulties of alignment with the flowing fluid are not so great. In both cases it is apparent that the insertion of a solid device of this type is certain to disturb the fluid flow to some extent, and hence it should be observed that such devices should be made as small as possible.

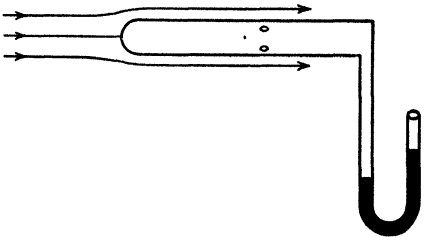
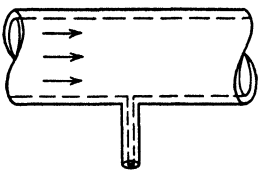


FIG. 138. Static Tube.



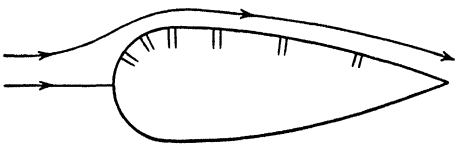


FIG. 139.

A "static tube" (Fig. 138) may be used for measurement of the static pressure in a flowing fluid. Such a tube is merely a smooth cylinder carefully aligned with the flow and having a smooth upstream end. In the side of the cylinder are piezometer holes drilled radially, or a circumferential slot, through which pressure is transmitted to a recording device. Since the introduction of the static tube disturbs the flow and causes the velocity along its surface to be greater than that in the undisturbed flow, the pressure transmitted through the piezometer openings must,

according to the Bernoulli principle, be less than the true static pressure in the undisturbed flow. This error, of course, may be minimized by making the tube as small as possible and is usually safely negligible for most engineering considerations.

The static pressure in the fluid passing over an existing solid surface (such as a pipe wall or the surface of an object in the flow, Fig. 139) may be measured by small smooth piezometer holes drilled normal to the solid surface, since the surface for each of these conditions "fits" the flow perfectly, being a streamline of the flow. Such piezometer openings measure only the local static pressures at their locations on the solid surface and cannot, in general, measure the pressures at a distance from this surface since such pressures are obviously different from those at the surface because of flow curvatures and accelerations. Where no flow curvatures exist, as in a straight pipe, a wall piezometer opening will measure the pressure throughout the cross section of pipe in which the piezometer is located.

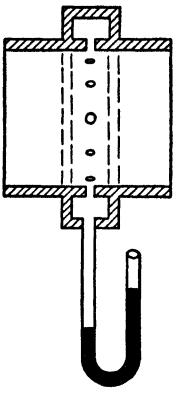


FIG. 140. Piezometer Ring.

Frequently in pipe-line practice a large number of piezometer openings are drilled in the pipe wall at the same cross section and led into a "piezometer ring" (Fig. 140), whence the pressure is transferred to a recording device. The pressure taken from the piezometer ring is considered more reliable than that obtained from a single piezometer opening, since probability dictates that the errors

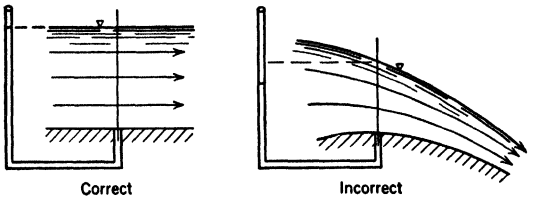


FIG. 141. Measurement of Surface Elevation by Piezometer Columns.

incurred by the inevitable imperfections of single openings will tend to cancel if numerous openings are used and the results averaged; the piezometer ring automatically approximates such an average.

57. Measurement of Surface Elevation. The elevation of the surface of a liquid at rest may be determined by manometer, piezometer column, or pressure-gage readings (Art. 10).

The same methods may be applied to flowing liquids if the above precautions in the construction of piezometer openings are followed and if the piezometer method is used only where the streamlines of the flow are *straight and parallel.* Correct and incorrect measurements of a liquid surface by piezometer openings are illustrated in Fig. 141.

For direct measurements to a liquid surface the hook gage and point gage (Fig. 142) are common. The hook gage is generally used in a stilling well connected to the liquid at the point where its surface elevation is to be measured but may be used directly on the liquid surface if velocities are not large. To set the point of the hook in the

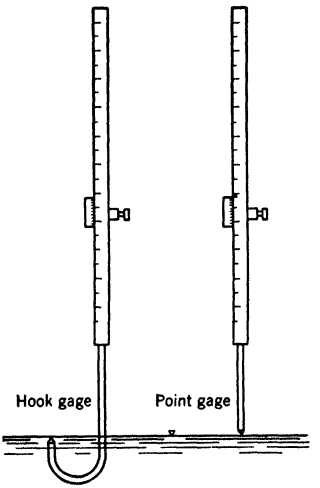


FIG. 142. Gages for Measurement of Surface Elevation.

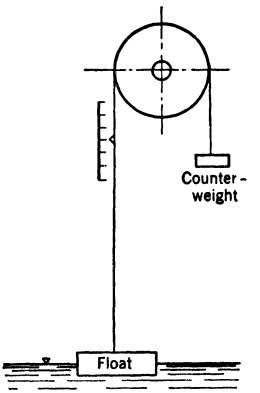


FIG. 143. Float for Measurement of Surface Elevation. (Schematic.)

liquid surface, it is first placed below the surface and then raised until a small pimple appears on the surface—at this condition the point of the hook is above the liquid surface. When the hook is lowered until the pimple just disappears, its point is accurately at the same elevation as the liquid surface. From a graduated scale and vernier on the hook gage shaft, the surface elevation of the liquid may be read precisely.

A point gage is suitable for swiftly flowing liquids in which the presence of a hook below the liquid surface would cause local disturbances. In measuring, the point gage is lowered until it just contacts the liquid surface (noted by slight disturbances of the surface) and then read by scale and vernier located on the gage shaft.

Floats are often used in connection with chronographic water-level recorders for measuring liquid-surface elevations. The arrangement of such floats is indicated schematically in Fig. 143. As the liquid level varies, the motion of the cable is measured on a scale or plotted automatically on a chronographic record sheet.

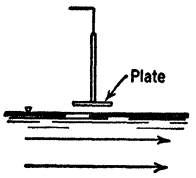


FIG. 144.

An electrical method of liquid surface measurement has recently been somewhat successful. It consists of using a small fixed metal plate, and the liquid surface as a condenser (Fig. 144). Variation of liquid-surface elevation varies the capacitance of the condenser, which may be measured electrically, and after calibration of the device

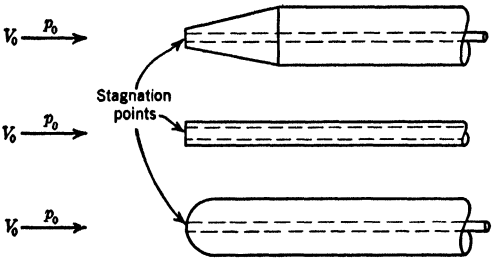


FIG. 145.

electrical measurements become a measure of surface elevation.

Staff gages give comparatively crude but direct measurements of liquid-surface elevation. From casual observation, the reader is familiar with their use as tide gages, in the measurement of reservoir levels and in registering the draft of ships.

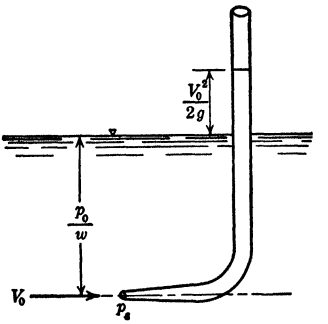


FIG. 146. Pitot Tube.

58. Measurement of Stagnation Pressure. The stagnation,[2] or total, pressure, $p_o + \frac{1}{2}\rho V_o^2$, may be measured accurately by placing in the flow a small solid object having a small piezometer hole at the stagnation point. The piezometer opening may be easily located at the stagnation point if the hole is drilled along the axis of a symmetrical object such as a cylinder, cone, or sphere (Fig. 145). When the axis of the object is aligned with the direction of

[2] See Art. 19.

flow the piezometer opening is automatically located at the stagnation point and the pressure there may be transferred through the piezometer opening to a recording device. Theoretically, the upstream end of solid objects for the above purpose may be of any shape since the shape of the object does not affect the magnitude of the stagnation pressure; in practice, however, the upstream end should be made convergent (conical or hemispherical) in order to fix the location of the stagnation point and to cause its location to be insensitive to small variations in alignment.

A small bent tube, with open end facing upstream, provides an excellent and simple means of measuring stagnation pressure. Tubes of this type are called Pitot tubes after Henri Pitot, who found (1732) that, when they were placed in an open flow at a point where the velocity was V_o (Fig. 146), the liquid in the tube rose above the free surface of the liquid a distance $V_o^2/2g$. Obviously, Pitot's results agree with those obtained by applying the foregoing reasoning on the magnitude of stagnation pressure.

MEASUREMENT OF VELOCITY

59. The Pitot (Pitot-Static) Tube. From the stagnation pressure equation

$$p_s = p_o + \tfrac{1}{2}\rho V_o^2$$

or

$$V_o = \sqrt{\frac{2}{\rho}(p_s - p_o)}$$

it is evident that fluid velocities may be obtained by the measurement of stagnation pressure, p_s, and static pressure, p_o. It has been shown that stagnation pressure may be measured easily and accurately by a Pitot tube and static pressure by various methods, such as tubes, flat plates, and wall piezometers. Any combination of stagnation- and static-pressure-measuring devices is called loosely a " Pitot tube " in most fields of engineering, although Pitot's original device was designed to measure stagnation pressure only. Aeronautical practice takes cognizance of this fact by terming a device which measures both stagnation and static pressures a " Pitot-static tube."

Pitot tubes may be divided into two classes: (1) those in which static and stagnation pressure connections are "separate," and (2) those having "combined" stagnation- and static-pressure-measuring devices.

"Separate" types of Pitot tubes are shown in Fig. 147 as used in obtaining the velocity profile in a pipe or as an air-speed indicator in aeronautical practice. Such tubes are simple in construction, but they cause inconvenience in pipe lines because of the necessity of two

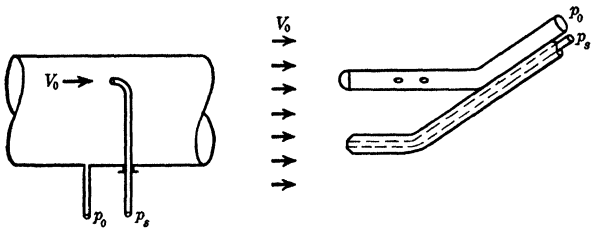


FIG. 147. Pitot Tubes. (Separate.)

pipe connections and the difficulties of obtaining correct static pressure by a single piezometer opening.

Modern practice favors the "combined" type of Pitot tube, two types of which (for general and aircraft use) are illustrated in Fig. 148. Here the static tube jackets the stagnation pressure tube, resulting

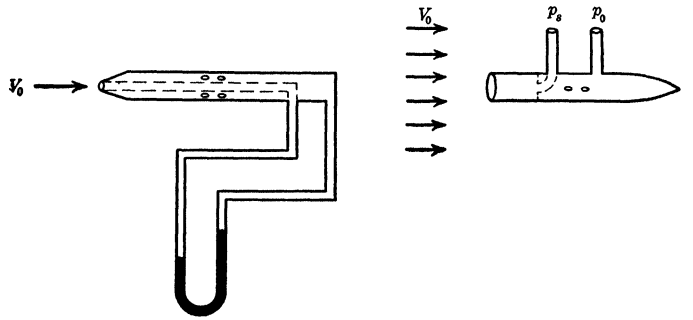


FIG. 148. Pitot Tubes. (Combined.)

in a compact, efficient velocity-measuring device. When connected to a differential manometer which records the pressure difference, $p_s - p_o$, the manometer reading becomes a direct measure of the velocity, as may be seen from the Pitot tube equation

$$V_o = \sqrt{\frac{2}{\rho}(p_s - p_o)}$$

A static tube has been shown to record a pressure slightly less than the true static pressure, owing to the increase in velocity along the

tube (Art. 58). This means that the above equation must be modified by an experimental coefficient, C_I, called the coefficient of the instrument, to

$$V_o = C_I \sqrt{\frac{2}{\rho}(p_s - p'_o)}$$

in which p'_o is the pressure measured by the static tube. Since p'_o is less than p_o it is obvious that C_I will always be less than unity. However, for most engineering problems the value of C_I may be taken as 1.00 for the conventional types of Pitot tubes (Fig. 149), since the

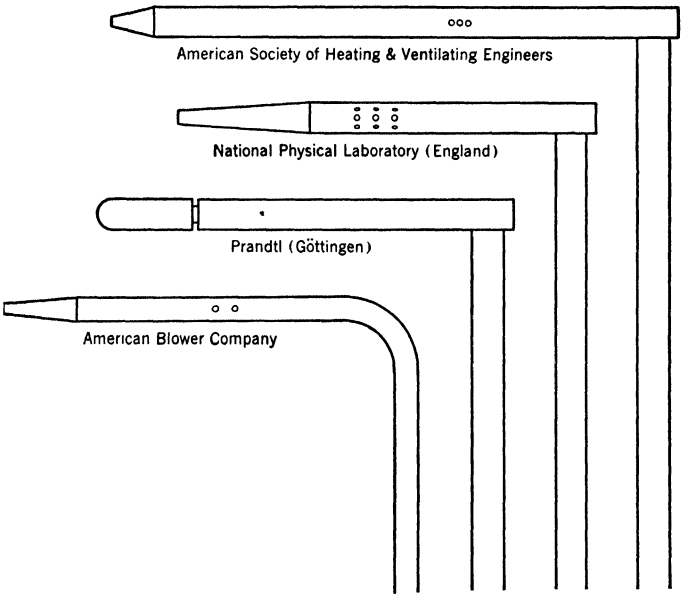


FIG. 149. Pitot Tubes (to Scale).

differences between p_0 and p'_o are very small. Prandtl has designed a Pitot tube in which the difference between p_o and p'_o is completely eliminated by ingenious location of the static-pressure opening. The opening is so located (Fig. 150) that the underpressure caused by the tube is exactly compensated by the overpressure due to the stagnation point on the leading edge of the stem, thus giving the true static pressure at the piezometer opening.

There are many variations on the Pitot-tube idea resulting in devices of various shapes and coefficients. Probably the most popular of these is the Cole Pitometer, a " reversed " type of Pitot tube.

The Pitometer consists of two similar Pitot tubes, one facing upstream, the other downstream (Fig. 151). The tube facing upstream measures the stagnation pressure properly, but the one facing downstream

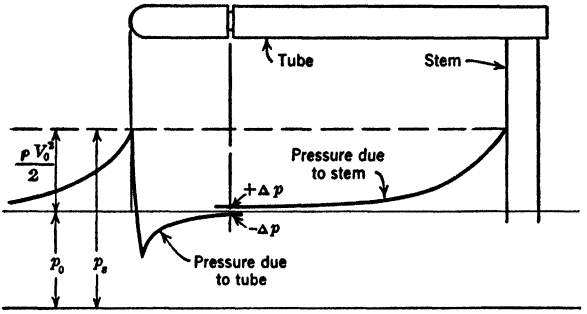


FIG. 150. Prandtl's Pitot Tube.

measures the pressure in the turbulent wake behind itself, which is less (Art. 28) than the true static pressure, p_0. The coefficient of the Pitometer is, therefore, much less than unity; experiments have shown it to have values between 0.84 and 0.87. The advantages of the Pitometer are its ruggedness and a compactness which allows it to be slipped easily through a cock in the wall of a pipe line.

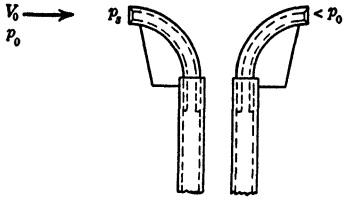


FIG. 151. Cole Pitometer.

A consideration of velocity-measuring devices is their sensitivity to obliquity or angle of yaw (Fig. 152). Since it is always difficult to secure perfect alignment of tube with flow, it is obviously advantageous to have a Pitot tube which gives the smallest possible error when perfect alignment does not exist. The Prandtl-Pitot tube, designed to be

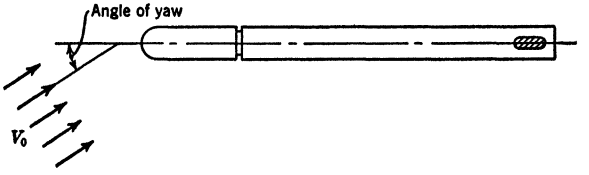


FIG. 152.

insensitive to small angles of yaw, gives a variation of only 1 per cent in its coefficient at an angle of yaw of 19°. For the same percentage variation in coefficient the American Society of Heating and Ventilat-

ing Engineers' Pitot tube may have an angle of yaw of 12°, and that of the National Physical Laboratory only 7°.[3]

Illustrative Problem

A Pitot tube having a coefficient of 0.98 is placed at the center of a pipe line in which benzene is flowing. A manometer attached to the Pitot tube contains mercury and registers a deflection of 3 in. Calculate the velocity at the centerline of the pipe.

$$p_s - p_o' = \tfrac{3}{12} \times 62.4 \times 13.55 - \tfrac{3}{12} \times 62.4 \times 0.89 = 197 \text{ lb/ft}^2$$

$$V = C_I \sqrt{\frac{2}{\rho}(p_s - p_o')} = C_I \sqrt{2g\left(\frac{p_s - p_o'}{w}\right)}$$

$$V = 0.98 \sqrt{64.4\left(\frac{197}{0.89 \times 62.4}\right)} = 14.8 \text{ ft/sec}$$

60. The Venturi Tube. A convergent-divergent tube called a "Venturi tube" has had some success in aeronautical practice as an air-speed-measuring device. A Venturi tube is shown in Fig. 153, and from the familiar Bernoulli principle it is evident that the pressure difference $p_o - p_2$ created by flow through the tube is a measure of the velocity V_o. Neglecting the losses which occur in the short distance between sections 0 and 2 of the streamtube which passes through the Venturi tube, the Bernoulli equation is

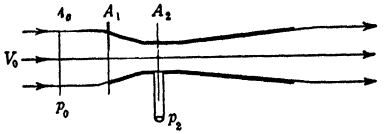


FIG. 153. Venturi Tube.

$$p_o + \tfrac{1}{2}\rho V_o^2 = p_2 + \tfrac{1}{2}\rho V_2^2$$

and assuming an incompressible fluid

$$V_o A_o = V_2 A_2$$

Therefore

$$p_o - p_2 = \tfrac{1}{2}\rho\left(V_o \frac{A_o}{A_2}\right)^2 - \tfrac{1}{2}\rho V_o^2$$

or

$$p_o - p_2 = \tfrac{1}{2}\rho V_o^2\left(\frac{A_o^2}{A_2^2} - 1\right)$$

[3] Data from K. G. Merriam and E. R. Spaulding, *N.A.C.A. Technical Note* 546, 1935.

in which A_o is unknown but dependent upon the area A_1 and the shape of the tube. Introducing an experimental coefficient to express the ratio of A_o to A_1

$$C = \frac{A_o}{A_1} \quad \text{or} \quad A_o = CA_1$$

Introducing this relationship in the above equation and solving for V_o

$$V_o = \frac{1}{\sqrt{\frac{C^2A_1^2}{A_2^2} - 1}} \sqrt{\frac{2}{\rho}(p_o - p_2)}$$

in which C must be found by calibration of the tube in an air stream of known velocity. After calibration the Venturi tube, like the Pitot tube, offers a means of measuring a pressure difference and calculating the

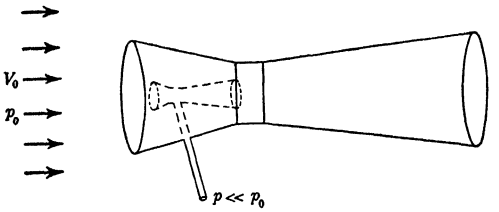


FIG. 154. Double Venturi.

velocity which has created it. Venturi tubes have been generally abandoned as air-speed indicators for aircraft, because of their sensitivity to yaw and their susceptibility to icing difficulties. However, they are still used in engineering practice as a source of low pressure and frequently appear as such in the form of the "double-Venturi" of Fig. 154, one of the flow elements of the standard carburetor.

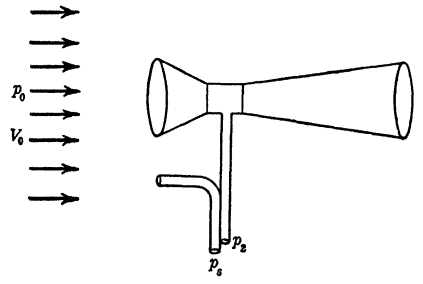


FIG. 155. Pitot-Venturi.

61. The Pitot-Venturi. The Pitot tube and Venturi principles are combined in a velocity-measuring device called the "Pitot-Venturi" (Fig. 155), which for the same velocity gives a pressure difference

($p_s - p_2$) larger than that of Pitot or Venturi alone. Here as in the foregoing examples

$$p_s - p_o = \tfrac{1}{2}\rho V_o^2$$

$$p_o - p_2 = \tfrac{1}{2}\rho V_o^2 \left(\frac{C^2 A_1^2}{A_2^2} - 1\right)$$

Adding these equations gives

$$p_s - p_2 = \tfrac{1}{2}\rho V_o^2 \left(\frac{C^2 A_1^2}{A_2^2}\right)$$

and solving for V_o

$$V_o = \frac{A_2}{CA_1}\sqrt{\frac{2}{\rho}(p_s - p_2)}$$

Here again an experimentally determined value of C is essential to velocity measurements with the Pitot-Venturi.

62. Anemometers and Current Meters. Mechanical devices of similar characteristics are utilized in the measurement of velocity in air and water flow. Those for air are called "anemometers"; those for water, "current meters." These devices consist essentially of a rotating element whose speed of rotation varies with the velocity of flow and for which the relation between these variables must be found by calibration. Anemometers and current meters fall into two main classes, depending upon the design of the rotating elements, which may be of the cup type or vane (propeller) type, as illustrated in Fig. 156.

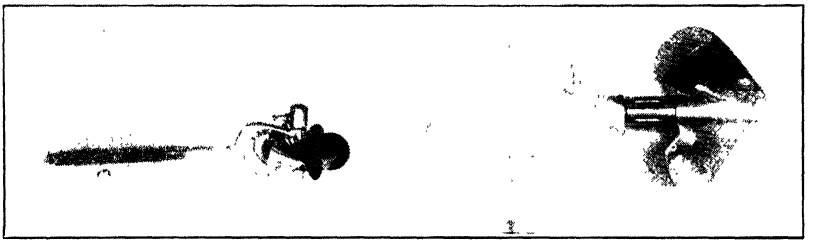
Anemometers and current meters differ slightly in shape, ruggedness, and appurtenances because of the different conditions under which they are used. The cup-type anemometer for the measurement of wind velocity is usually mounted on a rigid shaft; the vane-type anemometer is held in the hand while readings are taken. The current meters are usually suspended in a river or canal by a cable, and hence must have empennages and weights to hold them in fixed positions in the flow.

Another type of anemometer which has been very successful in the field of aeronautical research is the hot-wire anemometer, one type of which is shown diagrammatically in Fig. 157. The device consists of a fine platinum wire exposed to the velocity V_o which is to be measured. The fact that various velocities will have various cooling effects upon the hot wire, which will change its resistance, allows relating by



Cup Type *N. Y. U.* Vane Type *N. Y. U.*

Anemometers



Cup Type *N. Y. U.* Vane Type *A. S. M. E.*

Current Meters

FIG. 156.

calibration the velocity V_o and certain electrical measurements. The hot-wire anemometer of Fig. 157 is of the constant-voltage type,[4] and during its operation the voltage across its terminals is maintained constant. Variation of velocity will change the resistance of the wire and, thus, the ammeter reading; the ammeter reading thus becomes, after calibration, a measure of the velocity. The advantage of the hot-wire anemometer lies in the fact that it may be built in extremely small sizes and so may be employed in obtaining the velocity profiles in boundary layers, etc., where a Pitot tube cannot be used. It must always be calibrated before use, and calibration is generally made against Pitot-tube measurements of velocity.

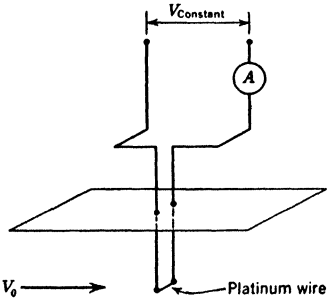


FIG. 157. Hot-Wire Anemometer.

[4] Constant-current and constant-resistance types are also used.

MEASUREMENT OF RATE OF FLOW

63. Total-Quantity Methods. Rate of fluid flow (Q or G) may be obtained by measurement of the total quantity of fluid collected in a measured time. Such collections may be made by weight or volume and are the primary means of measuring fluid flow, but usually such measurements can be employed for only comparatively small flows under laboratory conditions.

Measurement of rate of flow by weighing consists of collecting the flowing liquid in a container placed on a scales and measuring the weight of liquid accumulated in a certain time. There are, of course, many commercial variations of this method and many automatic devices are applied to it, but the principle remains the very simple one indicated above.

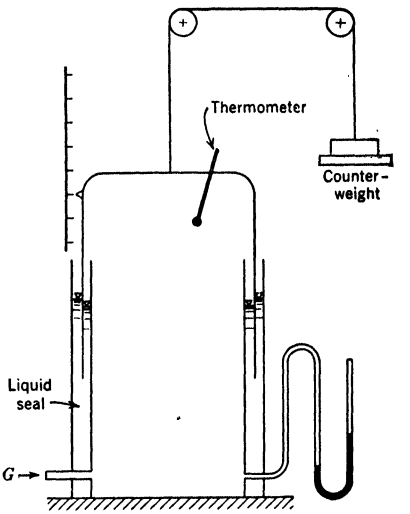


FIG. 158. Gasometer.

Volumetric measurements of rate of flow are carried out by allowing the liquid to collect in a container whose internal dimensions have been accurately determined. By noting the rise in the liquid surface in a measured time, or by noting the number of fillings of the container in a measured time, the rate of flow may be easily calculated. The accuracy of volumetric measurements is not in general so high as that of weighing methods because of the larger number of variables to be measured.

Gases may be measured volumetrically with a "gasometer" (Fig. 158), a device in which constant pressure and temperature are maintained while a volume of gas is collected. With pressure and temperature constant, the rate of rise of the movable top becomes a measure of the rate of flow into the gasometer, and after pressure and temperature are noted the rate of flow may easily be calculated. A correction or automatic compensation must be made for the variable buoyant force acting on the top due to varying immersion.

64. Venturi Meters. A constriction in a streamtube has been seen[5] to cause a pressure variation which is directly related to the rate

[5] Articles 21 and 22.

of flow, and thus is an excellent fluid meter in which rate of flow may be calculated from pressure measurements. Such constrictions used as fluid meters are obtained by Venturi meters, nozzles, and orifices.

A Venturi meter is shown in Fig. 159. It consists of a smooth entrance cone of angle about 20°, a short cylindrical section having diameter $\frac{1}{4}$ to $\frac{1}{2}$ of the pipe diameter, and a diffusor cone having a 5° to 7° total angle in order to minimize energy losses.[6] For satisfactory

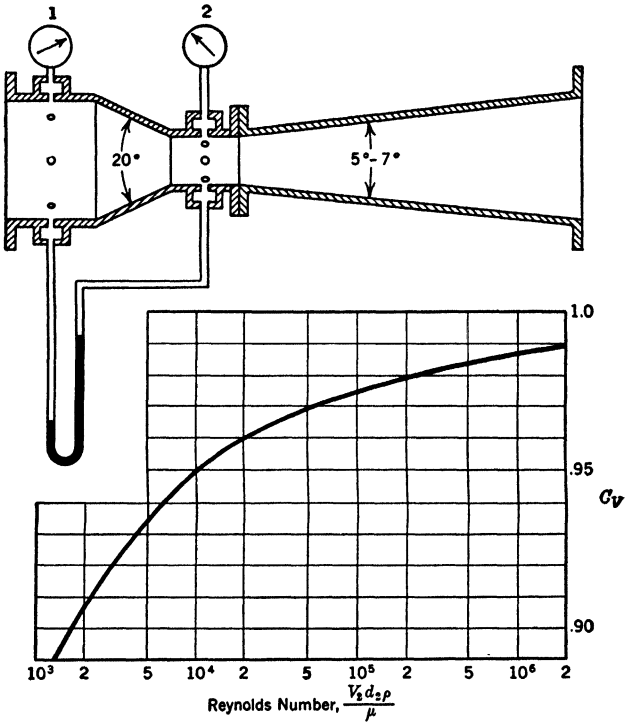


FIG. 159. Venturi Meter.[7]

operation of the meter, the flow should possess "normal" turbulence as it passes section 1. To insure this it should be installed after a section of straight and uniform pipe, free from fittings and other sources of eddying turbulence, and having a length of at least 30 pipe diameters. Straightening vanes may also be placed upstream from the meter for elimination of excessive turbulence of an eddying nature.

[6] See Art. 42.

[7] Data from *Fluid Meters, Their Theory and Application*, Third Edition, A.S.M.E., 1930. More comprehensive data are available in the Fourth Edition of this publication.

The pressures at the base of the meter (section 1) and at the throat or constriction (section 2) are obtained by piezometer rings, and the pressure difference between these points is usually measured by a differential manometer. An accurate measurement of pressure and temperature at section 1 will be seen to be necessary in the metering of gases and vapors, but for liquids the pressure difference between base and throat of the meter will allow calculation of the rate of flow.

Utilizing now the equations for flow of a *perfect* fluid through a constriction in a horizontal streamtube (Arts. 21 and 22):

For incompressible fluids

$$Q = \frac{A_2}{\sqrt{1 - \left(\frac{A_2}{A_1}\right)^2}} \sqrt{2g\left(\frac{p_1 - p_2}{w}\right)}$$

For compressible fluids

$$G = \frac{A_2 w_2}{\sqrt{1 - \left(\frac{A_2}{A_1}\right)^2 \left(\frac{p_2}{p_1}\right)^{\frac{2}{k}}}} \sqrt{\frac{2gk}{k-1} \frac{p_1^{\frac{1}{k}}}{w_1} \left[p_1^{\frac{k-1}{k}} - p_2^{\frac{k-1}{k}}\right]}$$

But since $V_2 = Q/A_2$ and $V_2 = G/A_2 w_2$ the equation for velocity may be written:

For incompressible fluids

$$V_2 = \frac{1}{\sqrt{1 - \left(\frac{A_2}{A_1}\right)^2}} \sqrt{2g\left(\frac{p_1 - p_2}{w}\right)}$$

For compressible fluids

$$V_2 = \frac{1}{\sqrt{1 - \left(\frac{A_2}{A_1}\right)^2 \left(\frac{p_2}{p_1}\right)^{\frac{2}{k}}}} \sqrt{\frac{2gk}{k-1} \frac{p_1^{\frac{1}{k}}}{w_1} \left[p_1^{\frac{k-1}{k}} - p_2^{\frac{k-1}{k}}\right]}$$

These velocities will not be obtained with real fluids because of frictional resistance and energy losses occurring between sections 1 and 2, and the above expressions must be corrected by an experimental coefficient, C_v, the " coefficient of velocity," to bring them into con-

formity with reality. When this coefficient is inserted the original expressions become

$$Q = \frac{C_v A_2}{\sqrt{1 - \left(\frac{A_2}{A_1}\right)^2}} \sqrt{2g\left(\frac{p_1 - p_2}{w}\right)} \tag{86}$$

for the real incompressible fluid, and

$$G = \frac{C_v A_2 w_2}{\sqrt{1 - \left(\frac{A_2}{A_1}\right)^2 \left(\frac{p_2}{p_1}\right)^{\frac{2}{k}}}} \sqrt{\frac{2gk}{k-1} \frac{p_1^{\frac{1}{k}}}{w_1} \left[p_1^{\frac{k-1}{k}} - p_2^{\frac{k-1}{k}} \right]}$$

or

$$G = \frac{C_v A_2 w_2}{\sqrt{1 - \left(\frac{A_2}{A_1}\right)^2 \left(\frac{p_2}{p_1}\right)^{\frac{2}{k}}}} \sqrt{\frac{2gk}{k-1} \frac{p_1}{w_1} \left[1 - \left(\frac{p_2}{p_1}\right)^{\frac{k-1}{k}} \right]} \tag{87}$$

for the real compressible fluid.

The significance of the coefficient of velocity C_v and its relation to head losses may be better understood if the derivation of equation 86 is considered. For a horizontal pipe and constriction the Bernoulli equation is

$$\frac{p_1}{w} + \frac{V_1^2}{2g} = \frac{p_2}{w} + \frac{V_2^2}{2g} + h_L$$

and the equation of continuity

$$Q = A_1 V_1 = A_2 V_2$$

Simultaneous solution of these equations to give equation 86 can result only when

$$h_L = \left(\frac{1}{C_v^2} - 1\right)\left(1 - \left(\frac{A_2}{A_1}\right)^2\right)\frac{V_2^2}{2g} = K\frac{V_2^2}{2g}$$

is inserted in the first equation. In the above equation, K is the minor loss coefficient for the passage between sections 1 and 2, and it is noted that K is related to C_v by

$$K = \left(\frac{1}{C_v^2} - 1\right)\left(1 - \left(\frac{A_2}{A_1}\right)^2\right)$$

Thus, the lower the value of C_v (the greater the difference between real and perfect fluids), the greater will be the magnitude of K and the energy loss. Since the energy loss characterized by K results from frictional effects rather than from eddying turbulence, it may be concluded that the variation of K with the Reynolds number will be similar to that exhibited by the friction factor, f, which decreases as the Reynolds number increases. Therefore, the variation of C_v with the Reynolds number may be expected to follow a trend opposite to those of K and f, and increase with increasing Reynolds number, a fact which is borne out by the experimental results of Fig. 159.

The form of equation 87 makes it too unwieldy for engineering practice and too difficult of rapid solution, but these inconveniences may be overcome by the application of the following graphical methods. Equation 87 for the compressible fluid may be placed in the form of equation 86 if a correction factor, Y,[8] is applied. The equation for compressible fluid flow may therefore be written

$$G = \frac{YC_vA_2w_1}{\sqrt{1 - \left(\frac{A_2}{A_1}\right)^2}} \sqrt{2g\left(\frac{p_1 - p_2}{w_1}\right)} \tag{88}$$

and used conveniently after an expression for Y has been found. This may be done by equating the above equation to

$$G = \frac{C_vA_2w_2}{\sqrt{1 - \left(\frac{A_2}{A_1}\right)^2\left(\frac{p_2}{p_1}\right)^{\frac{2}{k}}}} \sqrt{\frac{2gk}{k-1}\frac{p_1}{w_1}\left[1 - \left(\frac{p_2}{p_1}\right)^{\frac{k-1}{k}}\right]}$$

and solving for Y, with the result that

$$Y = \sqrt{\frac{1 - \left(\frac{A_2}{A_1}\right)^2}{1 - \left(\frac{A_2}{A_1}\right)^2\left(\frac{p_2}{p_1}\right)^{\frac{2}{k}}} \frac{\frac{k}{k-1}\left(\frac{p_2}{p_1}\right)^{\frac{2}{k}}\left[1 - \left(\frac{p_2}{p_1}\right)^{\frac{k-1}{k}}\right]}{1 - \frac{p_2}{p_1}}}$$

Although this calculation seems at first to complicate the problem, closer inspection indicates that Y is dependent on only three variables:

[8] Since the term Y accounts only for the expansion of the gas as it passes from section 1 to section 2 of the constriction, it is called the "expansion factor."

the pressure ratio p_2/p_1, the area ratio A_2/A_1, and the adiabatic constant k. This means that Y may be calculated for various values of these variables once for all, plotted, and thus made readily usable for engineering calculations. A plot of the expansion factor, Y, is given in Fig. 160 for the solution of problems.

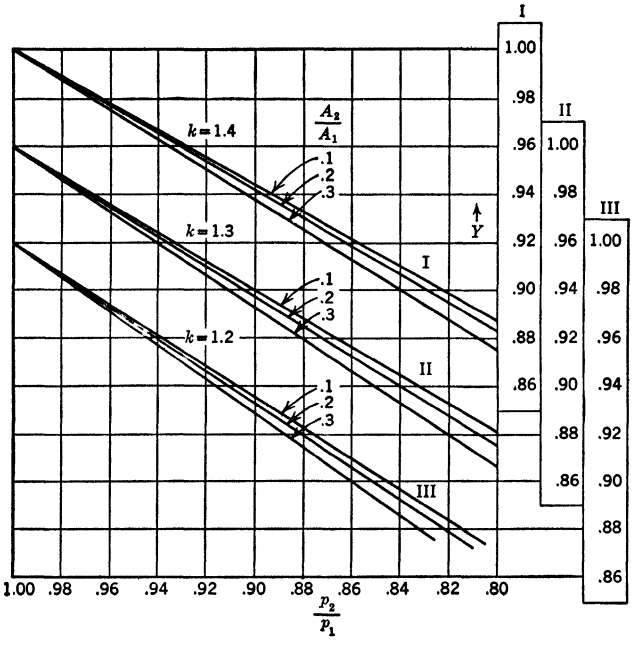


FIG. 160. The Expansion Factor, Y.

From the above facts it is observed that the one equation,

$$G = \frac{YC_vA_2w_1}{\sqrt{1 - \left(\frac{A_2}{A_1}\right)^2}} \sqrt{2g\left(\frac{p_1 - p_2}{w_1}\right)} \tag{89}$$

will allow calculation of fluid flow through a pipe-line constriction such as a Venturi meter, whether the fluid is perfect, real, compressible, or incompressible.

ILLUSTRATED PROBLEM

Air flows through a 6 in. by 3 in. Venturi meter having a coefficient C_v of 0.98. The gage pressure is 20 lb/in.^{2} and the temperature 60° F at the base of the meter,

and the differential manometer registers a deflection of 6 in. of mercury. The barometric pressure is 14.7 lb/in.^{2} Calculate the flow.

$$k = 1.40, \qquad \frac{p_2}{p_1} = \frac{\left(\frac{20 + 14.7}{14.7}\right)29.92 - 6}{\left(\frac{20 + 14.7}{14.7}\right)29.92} = 0.915$$

$$\frac{A_2}{A_1} = \left(\frac{3}{6}\right)^2 = 0.25 \qquad w_1 = \frac{(20 + 14.7)144}{53.3(100 + 460)} = 0.180 \text{ lb/ft}^3$$

From the plot of Fig. 160,

$$Y = 0.95.$$

$$G = \frac{YC_vA_2w_1}{\sqrt{1 - \left(\frac{A_2}{A_1}\right)^2}}\sqrt{2g\left(\frac{p_1 - p_2}{w_1}\right)}$$

$$G = \frac{0.95 \times 0.98 \times \left(\frac{\pi}{4} \times \left(\frac{3}{12}\right)^2\right) \times 0.180}{\sqrt{1 - (0.25)^2}}\sqrt{2g\left(\frac{6 \times \frac{14.7}{29.92} \times 144}{0.180}\right)}$$

$$G = 3.31 \text{ lb/sec}$$

65. Nozzles. Nozzles are used in engineering practice for the creation of jets and streams for all purposes as well as for fluid metering; when placed in or at the end of a pipe line as metering devices they are generally termed "flow nozzles." Since a thorough study of flow nozzles will develop certain general principles which may be applied to other special problems, the flow nozzle only will be treated here.

Flow nozzles are illustrated in Figs. 161 and 162. They are designed to be clamped between the flanges of a pipe, generally possess rather abrupt curvatures of the converging surfaces, terminate in short cylindrical tips, and are essentially Venturi meters with the diffusor cone omitted. Since the diffusor cone exists primarily to minimize the energy losses caused by the meter, it is obvious at once that larger energy losses will result from flow nozzles than occur in Venturi meters and that herein lies a disadvantage of the flow nozzle; this disadvantage is somewhat offset, however, by the lower initial cost of the flow nozzle.

Extensive research on flow nozzles, recently sponsored by the American Society of Mechanical Engineers and the International Standards Association, has resulted in the accumulation of a large amount of reliable data on nozzle installation, specifications, and

experimental coefficients. Only the barest outline of these results can be presented here; the reader is referred to the original papers of these societies for more detailed information.

The A.S.M.E. "long-radius" flow nozzle is shown in Fig. 161. Section 1 is taken one pipe diameter upstream from the nozzle and section 2 at the nozzle tip. It has been found that the pressure at the latter point may be measured successfully by a wall piezometer con-

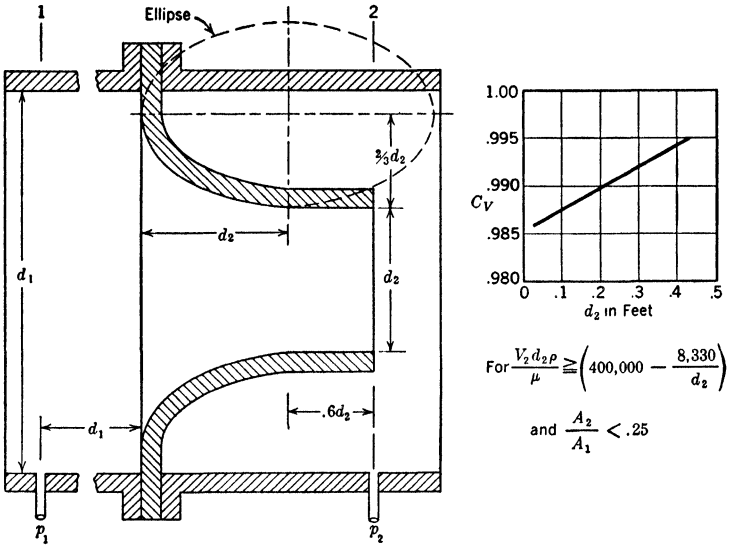


FIG. 161. A.S.M.E. Long-Radius Flow Nozzle.[9]

nection opposite the nozzle tip which leads fortunately to the simplification of the nozzle installation since a wall piezometer is easier to construct than a direct connection to the tip of the nozzle.

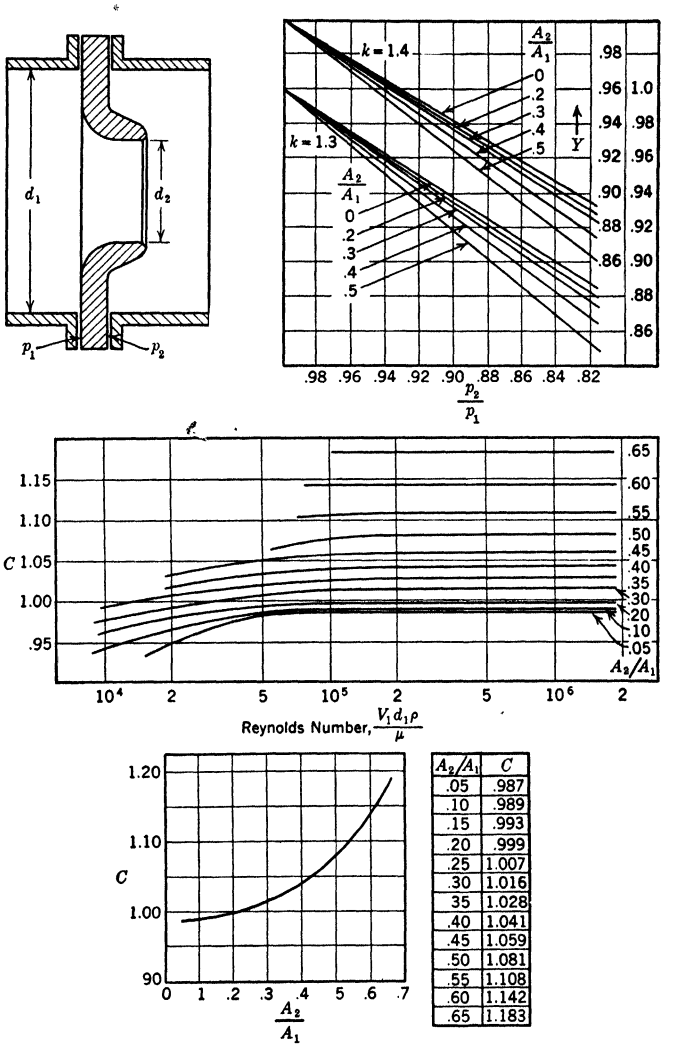
The equation derived for the Venturi meter may be applied directly to the nozzle. This is

$$Q = \frac{YC_v A_2 w_1}{\sqrt{1 - \left(\frac{A_2}{A_1}\right)^2}} \sqrt{2g\left(\frac{p_1 - p_2}{w_1}\right)}$$

for compressible fluids and reduces to

$$Q = \frac{C_v A_2}{\sqrt{1 - \left(\frac{A_2}{A_1}\right)^2}} \sqrt{2g\left(\frac{p_1 - p_2}{w}\right)}$$

[9] *Fluid Meters, Their Theory and Application*, Fourth Edition, A.S.M.E., 1937.



A_2/A_1	C
.05	.987
.10	.989
.15	.993
.20	.999
.25	1.007
.30	1.016
35	1.028
.40	1.041
.45	1.059
.50	1.081
.55	1.108
.60	1.142
.65	1.183

FIG. 162. I.S.A. (German Standard) Flow Nozzle.[10]

for incompressible ones. Values of Y may be obtained from Fig. 160, and values of C_v (over the limited range of tests to date) may be taken from the plot of Fig. 161.

The I.S.A. (German Standard) nozzle shown to scale in Fig. 162

[10] Data from *Regeln für die Durchflussmessung mit genormten Düsen und Blenden*, V.d.I. Verlag, 1935.

differs from the A.S.M.E. nozzle in shape and in the location of the piezometer connections, which are made by holes or slots adjacent to the faces of the nozzle. This method of pressure connection is convenient in that the nozzle, complete with pressure connections, may be built as a unit and installed between the flanges of a pipe line without the necessity of drilling piezometer holes in the pipe.

Although the pressure connections for this nozzle are not made in the conventional way at pipe and constriction, the flow equations

$$G = \frac{YC_vA_2w_1}{\sqrt{1 - \left(\frac{A_2}{A_1}\right)^2}} \sqrt{2g\left(\frac{p_1 - p_2}{w_1}\right)}$$

and

$$Q = \frac{C_vA_2}{\sqrt{1 - \left(\frac{A_2}{A_1}\right)^2}} \sqrt{2g\left(\frac{p_1 - p_2}{w}\right)}$$

may be applied if it is kept in mind that a nozzle is essentially a means of securing a regular pressure variation which, with other factors, is related to the rate of flow. A change in piezometer location, however, alters the values of Y and necessitates the calculation of a special plot for this variable (Fig. 162). Another difference between A.S.M.E. and I.S.A. nozzles is in the definition of the coefficient of the latter as

$$C = \frac{C_v}{\sqrt{1 - \left(\frac{A_2}{A_1}\right)^2}}$$

thus reducing the flow equations to

$$G = YCA_2w_1 \sqrt{2g\left(\frac{p_1 - p_2}{w_1}\right)}$$

and

$$Q = CA_2 \sqrt{2g\left(\frac{p_1 - p_2}{w}\right)}$$

Obviously the coefficient C depends upon the area ratio and, through the coefficient of velocity C_v, upon the Reynolds number as well. The variation of C with these variables is given in the plots of Fig. 162. The constancy of C at high Reynolds numbers and the characteristic decrease of C with decreasing Reynolds numbers should be noted.

Illustrative Problem

An A.S.M.E. long-radius flow nozzle of 3-in. diameter is installed in a 6-in. water line. The attached differential manometer contains mercury and registers a deflection of 6 in. Calculate the rate of flow and the loss of head caused by the nozzle.

From the plot of Fig. 161, $C_v = 0.991$.

$$Q = \frac{C_v A_2}{\sqrt{1 - \left(\frac{A_2}{A_1}\right)^2}} \sqrt{2g\left(\frac{p_1 - p_2}{w}\right)} = \frac{0.991 \times \frac{\pi}{4} \times \left(\frac{3}{12}\right)^2}{\sqrt{1 - (\frac{3}{6})^4}} \sqrt{2g(\tfrac{6}{12}[13.55 - 1])}$$

$$Q = 1.01 \text{ cfs}$$

Loss of head is composed of frictional effects between sections 1 and 2 ($h_{L_{1-2}}$) and loss due to turbulence downstream from the nozzle ($h_{L_{2-3}}$).

$$V_2 = \frac{1.01}{\frac{\pi}{4} \times \left(\frac{3}{12}\right)^2} = 20.55 \text{ ft/sec}$$

$$h_L = \left(\frac{1}{C_v^2} - 1\right)\left(1 - \left(\frac{A_2}{A_1}\right)^2\right)\frac{V_2^2}{2g} = \left(\frac{1}{(0.991)^2} - 1\right)\left(1 - (\tfrac{3}{6})^4\right)\frac{(20.55)^2}{2g} = 0.11 \text{ ft}$$

Calculating $h_{L_{2-3}}$ as a sudden enlargement,

$$h_{L_{2-3}} = \frac{(V_2 - V_3)^2}{2g} = \frac{(20.55 - 5.14)^2}{2g} = 3.70 \text{ ft}$$

$$h_L = h_{L_{1-2}} + h_{L_{2-3}} = 0.11 + 3.70 = 3.81 \text{ ft}$$

66. Orifices. Like nozzles, orifices serve many purposes in engineering practice other than the metering of fluid flow, but the study of the orifice as a metering device will allow the application of principles to other problems, some of which will be treated subsequently.

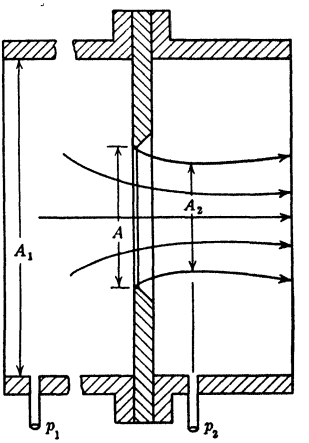


FIG. 163. Sharp-Edged Orifice.

The conventional orifice for use as a metering device in a pipe line consists of a concentric square-edged circular hole in a thin plate which is clamped between the flanges of the pipe line (Figs. 163 and 164). The orifice differs from the nozzle as to flow characteristics in that the constricted section of flow occurs not within the orifice but downstream from it owing to the non-axial direction of fluid

particles as they approach the orifice. This seems to complicate the problem since, in the flow equations between pipe and constriction,

$$G = \frac{YC_vA_2w_1}{\sqrt{1 - \left(\frac{A_2}{A_1}\right)^2}} \sqrt{2g\left(\frac{p_1 - p_2}{w_1}\right)}$$

and

$$Q = \frac{C_vA_2}{\sqrt{1 - \left(\frac{A_2}{A_1}\right)^2}} \sqrt{2g\left(\frac{p_1 - p_2}{w}\right)}$$

A_2 is unknown. At this point another experimental coefficient C_c, the " coefficient of contraction," may be advantageously introduced, C_c being defined by

$$C_c = \frac{A_2}{A}$$

It is simply the ratio between the unknown area A_2 and the known area of the orifice A. When this relationship is introduced in the flow equations, they become

$$G = \frac{YC_vC_cAw_1}{\sqrt{1 - C_c^2\left(\frac{A}{A_1}\right)^2}} \sqrt{2g\left(\frac{p_1 - p_2}{w_1}\right)}$$

and

$$Q = \frac{C_vC_cA}{\sqrt{1 - C_c^2\left(\frac{A}{A_1}\right)^2}} \sqrt{2g\left(\frac{p_1 - p_2}{w}\right)}$$

in which the " orifice coefficient," C, is defined by

$$C = \frac{C_cC_v}{\sqrt{1 - C_c^2\left(\frac{A}{A_1}\right)^2}}$$

This reduces the above equations to

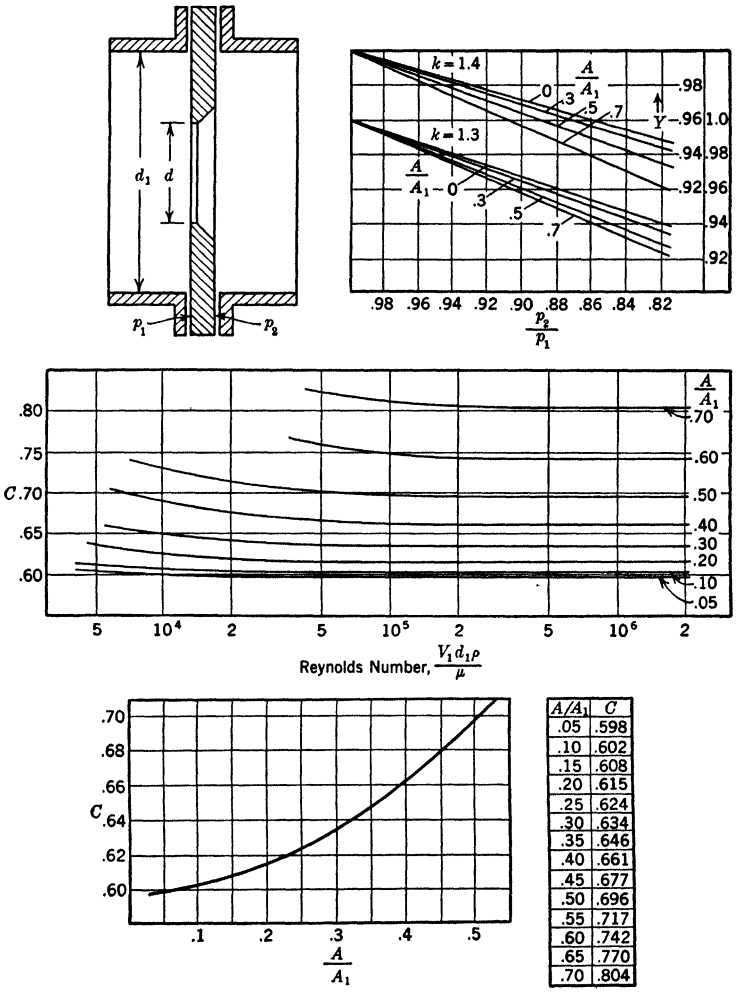
$$G = YCAw_1 \sqrt{2g\left(\frac{p_1 - p_2}{w_1}\right)}$$

and

$$Q = CA \sqrt{2g\left(\frac{p_1 - p_2}{w}\right)}$$

which differ from the equations for the I.S.A. nozzle only in that A_2 has been replaced by A.

The International Standards Association and the American Society



A/A_1	C
.05	.598
.10	.602
.15	.608
.20	.615
.25	.624
.30	.634
.35	.646
.40	.661
.45	.677
.50	.696
.55	.717
.60	.742
.65	.770
.70	.804

FIG. 164. I.S.A. (German Standard) Orifice.[10]

of Mechanical Engineers have undertaken the standardization of orifices, approaching the problem in two different ways. The A.S.M.E. has made available data on orifices for various locations of piezometer

[10] See footnote on p. 257.

connections, but lack of space prevents inclusion of this material here.[11]

The International Standards Association proposes the I.S.A. (German Standard) orifice with only one possible pair of piezometer connections located—as for the I.S.A. nozzle—adjacent to the orifice plate, resulting in the concise presentation of data given in Fig. 164.

The variation of C with the Reynolds number is of some interest since it exhibits a trend opposite to that of the nozzle and Venturi meter. This may be explained from the equation for C

$$C = \frac{C_v C_c}{\sqrt{1 - C_c^2 \left(\frac{A}{A_1}\right)^2}}$$

and must result from an increase of C_c with decreasing Reynolds number. Since the size of the area A_2 would be expected to increase as the flow assumed a more viscous character (lower Reynolds number), the coefficient C (which varies directly with C_c) would be expected to increase also.

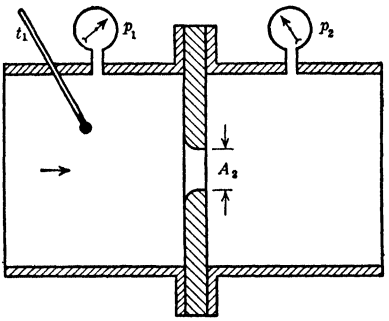


FIG. 165. Rounded Orifice.

Rounded (bell-mouthed) orifices (which are really short nozzles) are frequently used in the metering of gases and vapors. Such an orifice is shown in Fig. 165, and, for gas flow with pressure ratio below the critical, equation 24, Art. 22, modified by a coefficient of velocity, C_v, may be applied directly, giving

$$G = C_v Z \frac{A_2 p_1}{\sqrt{T_1}}$$

in which the value of C_v will be close to unity, 0.995 being a reasonable coefficient to select if calibration of the orifice is not possible.

In using the orifice of Fig. 165 in metering the flow of a vapor the methods of Fig. 42, Art. 22, should be followed and a coefficient C_v introduced in equation 25, giving for vapor flow

$$G = 223.8 C_v A_2 w_2' \sqrt{H_1 - H_2'}$$

[11] See *Fluid Meters—Their Theory and Application*, A.S.M.E., Fourth Edition, 1937.

The value of C_v is probably close to 0.995, but unless other measurements are very precise its inclusion in the equation is usually not justified.

The orifice is frequently encountered in engineering practice operating under a static head where it may not be used as a metering device but rather as a special feature in an hydraulic design.[12]

The general features of an orifice of the above type may be determined from the study of the submerged orifice of Fig. 166, operating

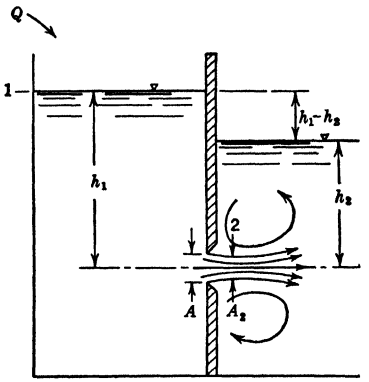


FIG. 166. Submerged Orifice.

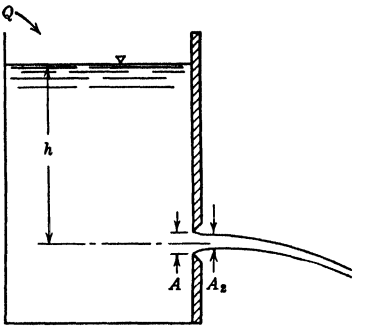


FIG. 167. Orifice Discharging Freely.

under steady-flow conditions. Assuming a perfect fluid and applying the Bernoulli equation between sections 1 and 2

$$0 + 0 + h_1 = h_2 + \frac{V_2^2}{2g} + 0$$

or

$$V_2 = \sqrt{2g(h_1 - h_2)}$$

for the perfect fluid. For the real fluid, frictional effects will prevent the attainment of this velocity and the coefficient of velocity C_v must be introduced, resulting in

$$V_2 = C_v \sqrt{2g(h_1 - h_2)}$$

and the rate of flow through the orifice becomes

$$Q = A_2 V_2 = C_v A_2 \sqrt{2g(h_1 - h_2)}$$

[12] For example, as a sluice gate in a dam, Fig. 169.

As in the pipe-line orifice the area A_2 is unknown but must have a special relation to the orifice area A, depending upon the shape of the orifice, velocity of flow, etc. This relation is expressed by the "coefficient of contraction" C_c, defined (as before) by

$$C_c = \frac{A_2}{A} \quad \text{or} \quad A_2 = C_c A$$

which when substituted above gives

$$Q = C_v C_c A \sqrt{2g(h_1 - h_2)}$$

Orifices and their Coefficients

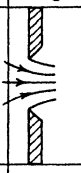
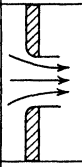
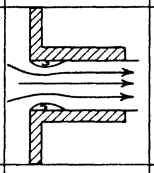
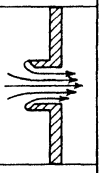
	Sharp edged	Rounded	Short tube	Borda
				
C	.61	98	~ 75	.51
C_c	.62	1.00	1 00	.52
C_v	98	.98	~ 75	98

FIG. 168.

in which the two coefficients are combined into the "coefficient of discharge," C, defined by

$$C = C_c C_v$$

The above equation may now be written

$$Q = CA \sqrt{2g(h_1 - h_2)}$$

allowing prediction of the rate of flow for a given difference in surface elevation, after the coefficient C has been experimentally determined.

When the orifice discharges freely into the atmosphere (Fig. 167), the head h_2 becomes zero and the equation reduces to [13]

$$Q = CA \sqrt{2gh}$$

[13] See Art. 20.

The dependency of the various orifice coefficients upon shape of orifice is illustrated by Fig. 168. The coefficients given are approximate values for large orifices ($d > 1$ in.) operating under comparatively large heads of water ($h > 4$ ft). Above these limits of head and size various experiments have shown that the coefficients become substantially constant. Experimental determinations of orifice coefficients at low heads and for small orifices indicate that the coefficients vary with head and orifice size, but the results of reliable experiments are so divergent that little can be stated as to the best values of orifice coefficients in this range. If orifices are to be small or to be operated under low heads and great accuracy is required they should be calibrated in place.

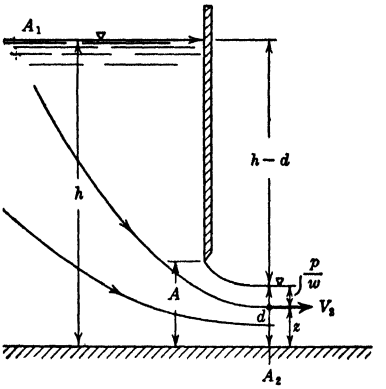


FIG. 169. Sluice Gate.

A special problem of orifice flow is that of the sluice gate of Fig. 169, in which contraction can take place on only one side of the jet. Assuming a perfect fluid and applying Bernoulli's equation to the typical streamtube between the liquid surface and contracted section, taking the base of the structure as datum,

$$0 + 0 + h = \frac{p}{w} + \frac{V_2^2}{2g} + z$$

since the pressure distribution at the contracted section 2, where no flow curvatures exist, is a static one. Obviously,

$$\frac{p}{w} + z = d$$

and therefore

$$h = d + \frac{V_2^2}{2g}$$

which gives

$$V_2 = \sqrt{2g(h - d)}$$

for the perfect fluid. For a real fluid

$$V_2 = C_v \sqrt{2g(h - d)}$$

and

$$Q = A_2 C_v \sqrt{2g(h - d)}$$

or

$$Q = C_c A C_v \sqrt{2g(h - d)}$$

or, introducing the coefficient of discharge, $C = C_v C_c$

$$Q = CA \sqrt{2g(h - d)}$$

for the sluice gate. Since the coefficient C will depend upon the head h and the gate opening A, the relation between these variables must be determined experimentally before the sluice-gate problem can be treated completely.

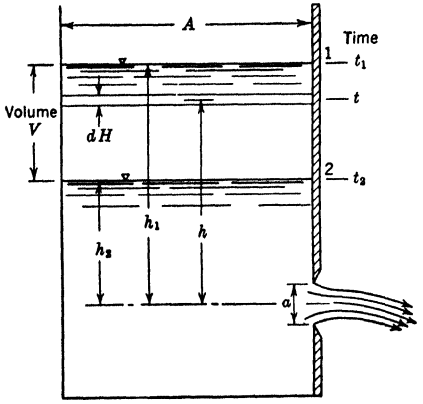


FIG. 170.
Orifice Discharging under Falling Head.

Another problem of orifice flow which frequently arises in engineering practice is that of discharge from an orifice under falling head—a problem of unsteady flow. With no inflow to the container of Fig. 170, the free surface will fall as flow takes place through the orifice. Thus the head on the orifice h, and the rate of flow Q, will vary with time, and the flow becomes an unsteady[14] one. The time necessary for the liquid surface to fall from elevation 1 to elevation 2 may be calculated by writing the equations of flow for a differential time dt. At time t, the head on the orifice is h and the rate of flow is therefore

$$Q = Ca \sqrt{2gh}$$

In time dt the differential volume of fluid, dV, passing from the container is given by the two expressions

$$dV = Qdt$$

and

$$dV = -Adh$$

which may be equated to give

$$Qdt = -Adh$$

[14] See Art. 16.

or by substituting the equation for Q

$$Ca\sqrt{2gh}\,dt = -Adh$$

Solving for dt

$$dt = -\frac{A}{Ca\sqrt{2g}}h^{-\frac{1}{2}}\,dh$$

Integrating between the corresponding limits of t and H

$$\int_{t_1}^{t_2} dt = -\frac{A}{Ca\sqrt{2g}}\int_{h_1}^{h_2} h^{-\frac{1}{2}}\,dh$$

gives the elapsed time, $t_2 - t_1$, as

$$t_2 - t_1 = \frac{2A}{Ca\sqrt{2g}}(h_1^{\frac{1}{2}} - h_2^{\frac{1}{2}})$$

The form of this equation may be simplified by multiplying and dividing by $(h_1^{\frac{1}{2}} + h_2^{\frac{1}{2}})$. This gives

$$t_2 - t_1 = \frac{A(h_1 - h_2)}{\frac{Ca\sqrt{2gh_1} + Ca\sqrt{2gh_2}}{2}}$$

or since V, the total volume discharged in time $t_2 - t_1$, is given by

$$V = A(h_1 - h_2)$$

$$t_2 - t_1 = \frac{V}{\frac{Q_1 + Q_2}{2}}$$

for a container of uniform horizontal cross-sectional area.

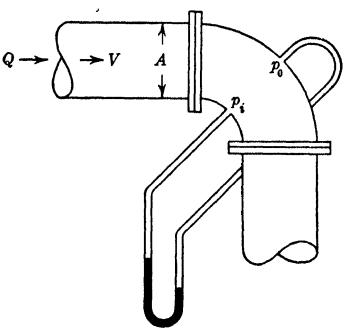


FIG. 171. Flow Bend.

67. Flow Bends. The orifice, nozzle, and Venturi meter as applied in the measurement of pipe line flow have been seen to be fundamentally methods of producing a regular and reproducible pressure difference which is related to rate of flow. For this reason they are sometimes called "pressure-difference meters" or "head meters." Another type of pressure-difference meter is the "flow bend" which utilizes the difference between the pressures at the inside and outside of a pipe bend (Fig. 171) created by centrifugal force as fluid flows through

the bend. Lansford [15] has recently obtained the experimental coefficients of a variety of standard 90° flanged elbows which allows their use as a successful and economical type of fluid meter. He proposes the equation

$$\frac{p_o - p_i}{w} = C_k \frac{V^2}{2g}$$

with coefficient C_k ranging between 1.3 and 3.2, the magnitudes depending upon the size and shape of the flow bend. This equation may be solved for V

$$V = \sqrt{\frac{1}{C_k}} \sqrt{2g\left(\frac{p_o - p_i}{w}\right)}$$

and leads to the flow equation of the familiar form

$$Q = \frac{1}{\sqrt{C_k}} A \sqrt{2g\left(\frac{p_o - p_i}{w}\right)}$$

or, if

$$C = \frac{1}{\sqrt{C_k}},$$

$$Q = CA \sqrt{2g\left(\frac{p_o - p_i}{w}\right)}$$

in which C will have values between 0.56 and 0.88.

68. Pitot-Tube Methods. The rate of flow in pipe lines is frequently measured by means of the Pitot tube and Pitometer. These devices have been seen to be primarily velocity-measuring instruments which may be employed in pipe lines to establish the distribution of velocity; their use in measuring rate of flow is essentially an integration of the product of velocity and area through which the velocity exists.

One method of obtaining rate of flow from velocity measurements is to divide the pipe cross section into a number of equal annular areas (B, C, D, Fig. 172) and to measure the average velocities through these areas by placing the velocity-measuring device at points where these average velocities are assumed to exist. These points are taken to be at the midpoints of the areas, i.e., at points where circles divide these *areas* in half. This is really assuming the velocity to vary linearly over the areas considered which (in turbulent flow) is obviously more

[15] W. M. Lansford, "The Use of an Elbow in a Pipe Line for Determining the Flow in the Pipe," *Bulletin* 289, Eng. Exp. Station, Univ. of Illinois, 1936.

true near the center of the pipe than near the walls; this assumption does not cause serious errors, however, if a large number of annular areas are taken. In general, the velocity distribution is not symmetri-

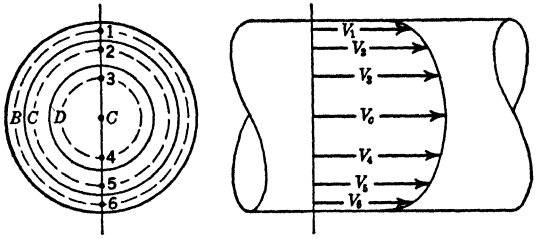


FIG. 172.

cal about the pipe centerline, and the average velocity through an annular area is taken to be the numerical average of the two velocities measured in this area. Thus (Fig. 172)

$$Q_B = \left(\frac{V_1 + V_6}{2}\right)\frac{A}{3}, \quad Q_C = \left(\frac{V_2 + V_5}{2}\right)\frac{A}{3}, \quad Q_D = \left(\frac{V_3 + V_4}{2}\right)\frac{A}{3}$$

but the rate of flow, Q, in the line is given by

$$Q = Q_B + Q_C + Q_D$$

or by substitution of the above values,

$$Q = A\left(\frac{V_1 + V_2 + V_3 + V_4 + V_5 + V_6}{6}\right)$$

This means that the average velocity in the pipe line is given by

$$V = \frac{V_1 + V_2 + V_3 + V_4 + V_5 + V_6}{6}$$

a simple numerical average of the velocities existing at certain special points on the diameter of the pipe line.

Another method of obtaining rate of flow from velocity distribution is by graphical integration. From Fig. 173, it is obvious that

$$Q = \int^{A} v dA$$

or since $dA = 2\pi r\, dr$

$$Q = \pi \int_{o}^{R} v 2r dr$$

but

$$2rdr = d(r^2)$$

thus

$$Q = \pi \int_o^{R^2} v d(r^2)$$

This equation suggests plotting velocity against the square of the radius at which the velocity occurs. The area under the resulting curve (Fig. 173) is equivalent to $\int_o^{R^2} v d(r^2)$ and may be obtained by planimeter or other means. The rate of flow, Q, thus becomes

$$Q = \pi \text{ (Area under } v \textit{ vs. } r^2 \text{ curve)}$$

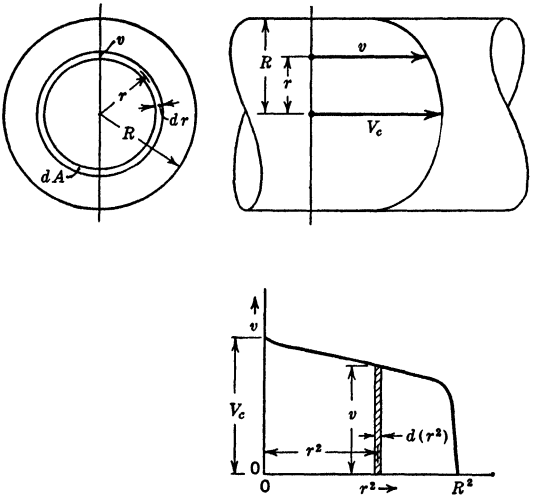


FIG. 173.

The numerical average method is the faster way of obtaining rate of flow in a pipe line by Pitot tube or Pitometer, and although the graphical method is theoretically the more accurate in all probability the two methods will give about the same accuracy in most of their applications in actual practice.

69. Dilution and Thermal Methods. Dilution methods for measuring rate of flow consist essentially of introducing at a steady rate a concentrated foreign substance to the flow, measuring the concentration of the substance after thorough mixing has taken place, and calculating from the dilution of the substance the rate of flow which has brought about this dilution.

A concentrated salt solution has been used in Europe in applying this method to the calculation of flow in small mountain streams and in this country to the calculation of the flow through the turbines of hydroelectric power plants. If the rate of flow of salt solution into the unknown flow is Q_s, and the concentration of salt in this solution C_1 lb/ft^3, the number of pounds per second of salt added to the unknown flow is given by Q_sC_1. If the concentration of salt in the unknown flow after mixing has occurred is C_2, the number of pounds of salt flowing in the stream per second is also given by $(Q + Q_s)C_2$. Therefore,

$$Q_sC_1 = (Q + Q_s)C_2$$

or

$$\frac{Q + Q_s}{Q_s} = \frac{C_1}{C_2}$$

Since Q_s is extremely small compared to Q, it may be eliminated from the numerator of the expression, giving

$$Q = Q_s \frac{C_1}{C_2}$$

Hence by controlling and measuring Q_s and obtaining C_1 and C_2 by titration methods, the unknown rate of flow Q may be found.

Analogous to the above dilution method is the "thermal" method of flow measurement wherein heat is added at a constant rate to a flowing fluid and the rate of flow deduced from the temperature rise caused by this addition of heat. This method, illustrated diagrammatically in Fig. 174, has been applied successfully in measuring the

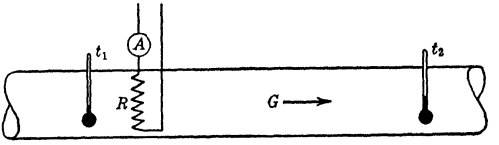


FIG. 174.

flow of gases in pipe lines. It consists essentially of a resistance coil, R, and two thermometers, one upstream from the coil, the other at a point downstream, where turbulent mixing has produced a uniform temperature across the pipe. If I is the current through the coil in amperes, and R the resistance of the coil in ohms, the heat added to the flowing fluid is expressed by I^2R watts. The heat added to the flow in British thermal units per second is, therefore, given by $I^2R/1055$.

If the specific heat of the fluid is c Btu/lb/°F, the heat received by the flow may be expressed as $Gc\ (t_2 - t_1)$. Equating the expressions for heat supplied and heat received

$$\frac{I^2R}{1055} = Gc(t_2 - t_1)$$

and solving for G, the weight flow

$$G = \frac{I^2R}{1055\ c(t_2 - t_1)}$$

Thus by taking measurements of temperature difference and electric current and knowing the specific heat of the gas and the resistance of the coil, the rate of flow may be calculated.

70. Salt-Velocity Method. An ingenious method of flow measurement which has met with success in the measurement of rate of flow to hydroelectric power plants is the salt-velocity method developed by Allen and Taylor.[16] In this method a quantity of concentrated salt solution is introduced suddenly to the flow and the average velocity is

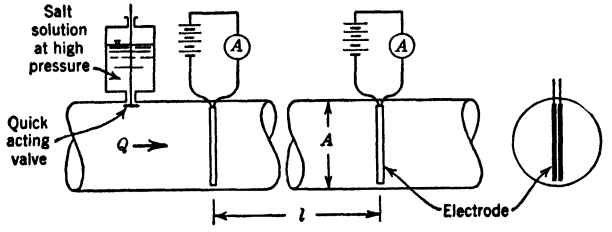


FIG. 175.

obtained by measuring the velocity of the salt solution as it moves with the flow.

The essential feature of the method (illustrated in simplified form in Fig. 175) consists essentially of a device for introducing suddenly the salt solution, and two similar electrodes and circuits. The passage of the salt charge between the plates of an electrode may be recorded by a momentary increase in the ammeter reading due to the greater conductivity of the salt solution. By noting the time t between the deflections of the two ammeter needles, and knowing the distance l

[16] C. M. Allen and E. A. Taylor, "The Salt Velocity Method of Water Measurement," *Trans A.S.M.E.*, Vol. 45, 1923, p. 285.

between electrodes, the average velocity in the pipe may be calculated from

$$V = \frac{l}{t}$$

and the rate of flow by

$$Q = AV$$

The details involved in the salt-velocity method are far more complex than the above statement of principles implies, owing primarily to the use of a chronographic device to record automatically (1) the variation of electrical current with the passage of the salt charge and (2) the time of passage of the charge between electrodes.

71. Weirs. For measuring large and small open flows in field and laboratory, the weir finds wide application. A weir may be defined in a general way as "any regular obstruction in open flow over which

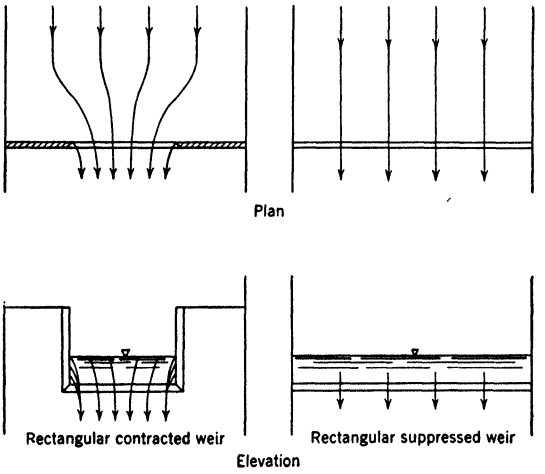


FIG. 176. Sharp-Crested Weirs.

flow takes place." Thus, for example, the spillway of a dam is a special type of weir and may be utilized for flow measurement. However, weirs for measuring purposes are usually of more simple and reproducible form, consisting of smooth, vertical, flat plates with upper edges sharpened. Such weirs, called sharp-crested weirs, appear in a variety of forms, the most popular of which is the rectangular weir which has a straight, horizontal crest. Rectangular weirs appeared originally as notches in a more or less uniform and thin vertical wall and as such developed contraction of the overfalling sheet (nappe) of

liquid (Fig. 176), similar to the contraction of the jet from a sharp-edged orifice; because of these nappe contractions at the ends of the weir, rectangular notches are also called contracted weirs. Obviously when rectangular weirs extend from wall to wall of an open channel these contractions are eliminated or suppressed, and for this reason this type of weir is termed a suppressed weir. Measuring weirs appear in many shapes other than rectangular, the triangular (V-notch) and trapezoidal weir being the more popular of these other types.

The flow of liquid over a weir is at its best an exceedingly complex problem and one difficult of rigorous theoretical solution. An appreciation for the complexities, however, is necessary to an understanding of experimental results and the deficiencies of simplified weir formulas. These complexities may be discovered by considering the flow over the sharp-crested suppressed weir shown in Fig. 177. Although it is obvi-

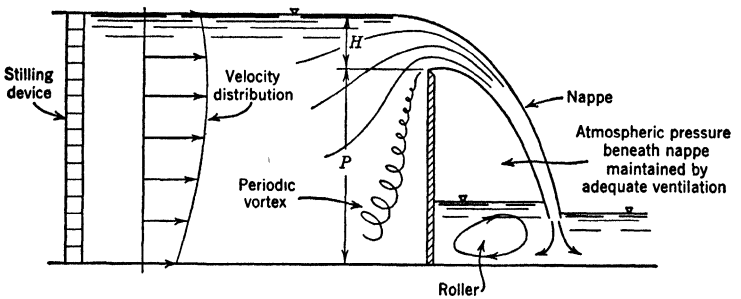


FIG. 177. Weir Flow (Actual).

ous at once that the head H on the weir is the primary factor causing the flow Q to occur, no simple relationship between these two variables can be derived for two fundamental reasons: (1) the geometrical form and (2) the effect of turbulence and frictional processes cannot be calculated. The more important factors which affect the shape of weir flow are the head on the weir H, the weir height P, and the extent of ventilation beneath the nappe. Although the effect of these factors may be found experimentally, there is no simple method of predicting the flow picture from values of H, P, and pressure beneath the nappe. The effects of turbulence and friction not only cannot be predicted but cannot even be isolated for experimental measurement. It may be noted, however, that frictional resistance at the side walls will affect the rate of flow to an increasing extent as the channel becomes narrower and the weir length, b, smaller. Fluid turbulence and frictional processes at the sides and bottom of the approach channel contribute

to the velocity distribution in an unknown way. The effects of velocity distribution on weir flow have been shown by Schoder and Turner [17] to be appreciable, and an effort should be made in all weir installations to provide a good length of approach channel, with stilling devices such as racks and screens for the even distribution of turbulence and the prevention of abnormal velocity distribution. Another influence of frictional processes is the creation of a periodic, helical secondary flow immediately upstream from the weir plate, resulting in a vortex (Fig. 177), which influences the flow in an unknown and unpredictable way. The free liquid surfaces of weir flow also bring surface-tension forces into the problem, and these forces, although small, affect the flow picture appreciably, particularly at low heads and small flows.

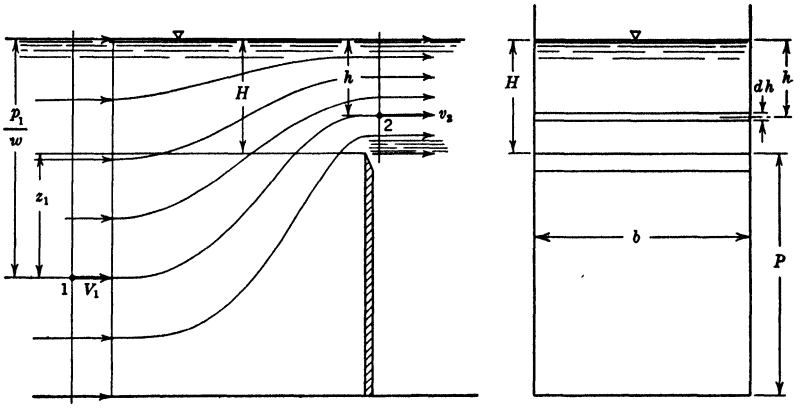


FIG. 178. Weir Flow (Simplified.)

To derive a simple weir equation in the light of the above complexities will obviously require a vast and artificial simplification of the problem. Such simplification will lead to an approximate result which must be corrected by the introduction of experimental coefficients. To derive a simple weir equation, let it be assumed that (1) velocity distribution is uniform, (2) that all fluid particles move horizontally as they pass the weir crest, (3) that the pressure in the nappe is zero, and (4) that the influence of viscosity, turbulence, secondary flows, and surface tension may be neglected. These assumptions produce the flow picture of Fig. 178. Taking section 1 in the approach channel well upstream from the weir and section 2 slightly downstream from

[17] E. W. Schoder and K. B. Turner, "Precise Weir Measurements," *Trans., A.S.C.E.*, Vol. 93, 1929, p. 999.

the weir crest, Bernoulli's equation may be applied to a typical streamline to find the velocity v_2. Taking the streamline 1–2 as a typical one

$$(z + H) + \frac{V_1^2}{2g} - z = 0 + \frac{v_2^2}{2g} + (H - h)$$

which gives

$$v_2 = \sqrt{2g\left(h + \frac{V_1^2}{2g}\right)}$$

and shows that v_2 depends upon h. Because of the dependence of v_2 upon h, v_2 can be considered to be the average velocity through an area of only differential height dh, and the flow, dq, through this area may be written as

$$dq = v_2 b dh = b\sqrt{2g\left(h + \frac{V_1^2}{2g}\right)}\, dh$$

Integration of this equation between the indicated limits

$$\int_o^Q dq = b\sqrt{2g}\int_o^H \left(h + \frac{V_1^2}{2g}\right)^{\frac{1}{2}} dh$$

leads to

$$Q = \tfrac{2}{3} b\sqrt{2g}\left[\left(H + \frac{V_1^2}{2g}\right)^{\frac{3}{2}} - \left(\frac{V_1^2}{2g}\right)^{\frac{3}{2}}\right]$$

giving an approximate relationship between Q and H for rectangular weirs. If V_1 is negligible (as it frequently is), this equation reduces to

$$Q = \tfrac{2}{3} b\sqrt{2g}\, H^{\frac{3}{2}}$$

the basic flow equation for rectangular weirs.

Into the above equation must be inserted an experimental coefficient C which not only embraces the effects of the various phenomena which have been disregarded in the above analysis, but may be made to include the effect of velocity of approach as well. Therefore, real weir flow may be characterized by the equation

$$Q = C\tfrac{2}{3} b\sqrt{2g}\, H^{\frac{3}{2}} \qquad (90)$$

The coefficient C is essentially a factor which transforms the assumed weir flow of Fig. 178 into the real weir flow of Fig. 177, and its magnitude is thus fixed by the most important difference between these flows, which is obviously the shape of the flow picture. Thus the coefficient C is in a sense primarily a coefficient of contraction which expresses the extent of contraction of the true nappe below that

assumed in the theoretical analysis. Since the size of the weir coefficient depends primarily on the shape of the flow picture, the effect of other fluid properties and phenomena may usually be discovered by examining their influence upon the shape of the flow picture.

Although a dimensional analysis of the weir problem must necessarily be incomplete because of the impossibility of including all the pertinent factors it will provide a rational basis for a graphical comparison of the weir coefficients proposed by various experimenters. Neglecting the effect of surface tension, the expressible variables entering the weir problem may be stated as

$$Q = F(b, P, H, \nu, g)$$

which leads by the methods of dimensional analysis to

$$Q = F_1\left(\frac{P}{H}, \frac{\sqrt{2gH}\,H}{\nu}\right)\tfrac{2}{3}b\sqrt{2g}\,H^{\frac{3}{2}}$$

and shows by comparison with equation 90 that

$$C = F_1\left(\frac{P}{H}, \frac{\sqrt{2gH}\,H}{\nu}\right)$$

in which the first ratio is one of linear dimensions and indicates the general shape of the flow picture. The second ratio is recognized as a Reynolds number which for water flow is determined primarily by the size of H since the other terms are substantially constant; therefore

$$C = F_2\left(\frac{P}{H}, H\right)$$

The dependence of the weir coefficient on head and weir height has been noted by many experimenters, who have proposed the following empirical equations for the coefficients of sharp-crested suppressed weirs

Bazin:[18] $$C = \left(0.6075 + \frac{0.01476}{H}\right)\left(1 + 0.55\left[\frac{H}{P+H}\right]^2\right)$$

Frese:[19] $$C = \left(0.615 + \frac{0.00689}{H}\right)\left(1 + 0.55\left[\frac{H}{P+H}\right]^2\right)$$

[18] H. Bazin, *Annales des ponts et chaussées*, 1888–1898. Summarized by G. W. Rafter in "On the Flow of Water Over Dams," *Trans. A.S.C.E.*, Vol. 44, p. 220, 1900.

[19] F. Frese, "Versuche über den Abfluss des Wassers bei vollkommenden Überfällen," *Zeitschrift des V. d. I.*, Dec. 20, 1890, Vol. 34, No. 51, p. 1337.

Swiss Society of Engineers and Architects:[20]

$$C = 0.615\left(1 + \frac{1}{305H + 1.6}\right)\left(1 + 0.5\left[\frac{H}{P + H}\right]^2\right)$$

Rehbock:[21] $$C = \left(0.6035 + 0.0813\frac{H}{P} + \frac{0.000295}{P}\right)\left(1 + \frac{0.00361}{H}\right)^{\frac{3}{2}}$$

These equations are difficult to analyze, but dimensional analysis has suggested plotting C against H for various constant values of P/H, which allows ready comparison of the equations. This has been done in Fig. 179, which may be used to avoid solution of the equations and

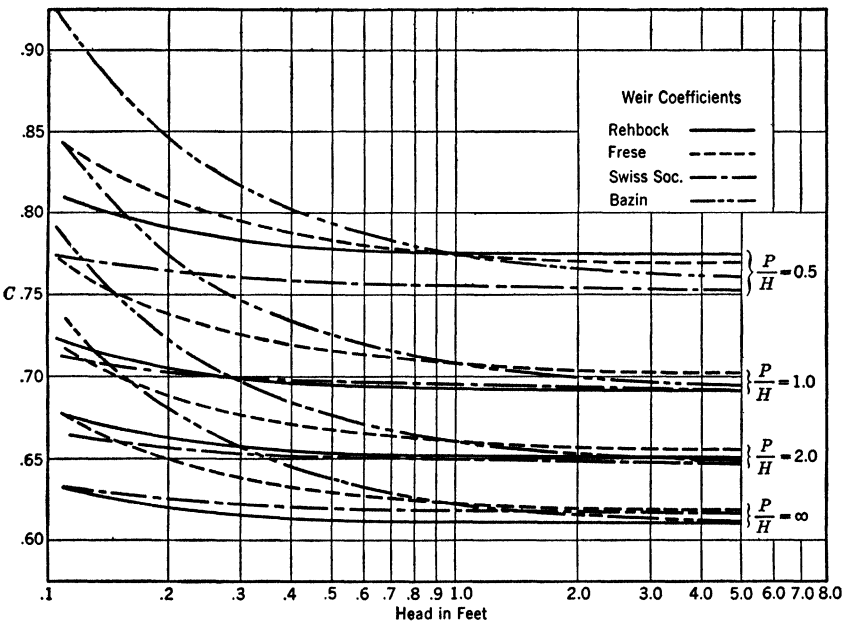


FIG. 179. Coefficients for Sharp-Crested Rectangular Weirs.

to draw some general conclusions on weir coefficients. From this plot it is immediately evident that: (1) the coefficient tends to increase with decreasing head and weir height; (2) in spite of precise experimental measurements very different weir coefficients are found by different experimenters; and (3) the divergence of results is small at

[20] *Code for Measuring Water*, Swiss Ingenieur and Architeckten Verein, 1924.

[21] Th. Rehbock, "Wassermessung mit scharfkantigen Überfallwehren," *Zeitschrift des V. d. I.*, June 15, 1929, Vol. 73, No. 24.

high heads but increases rapidly as low heads are attained. The Rehbock formula is generally considered the most reliable for the selection of the coefficients of a weir which cannot be calibrated in place.

Illustrative Problem

Calculate the rate of flow and velocity of approach when a head of 6 in. exists on a sharp-crested rectangular suppressed weir 4 ft long and 3 ft high.

$$\frac{P}{H} = \frac{3}{0.5} = 6.0$$

From the plot of Fig. 179, C (according to Rehbock) = 0.62, approximately.
From formula, C (according to Rehbock) = 0.623.

$$Q = C\tfrac{2}{3}b\sqrt{2g}\,H^{\frac{3}{2}}$$

$$Q = 0.623 \times \tfrac{2}{3} \times 4\sqrt{2g}\,(\tfrac{6}{12})^{\frac{3}{2}} = 4.73 \text{ cfs}$$

$$V_1 = \frac{4.70}{(3 + \frac{6}{12})4} = 0.338 \text{ ft/sec}$$

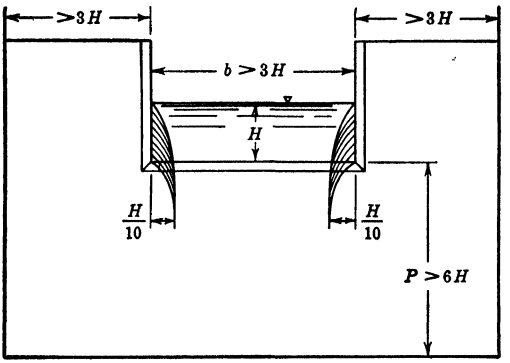


Fig. 180. Rectangular Contracted Weir.

The rectangular contracted weir (Fig. 180) may be treated by the method suggested by Francis,[22] who found experimentally that the end contraction varied directly with the head on the weir and was equal to one-tenth of the head. He reasoned that the end contrac-

[22] J. B. Francis, *Lowell Hydraulic Experiments*, Fourth Edition, 1883, Van Nostrand.

tions reduced the effective weir length from b to $(b - 2H/10)$, and proposed the equation

$$Q = C\frac{2}{3}\left(b - \frac{2H}{10}\right)\sqrt{2g}\,H^{\frac{3}{2}} \tag{91}$$

for rectangular contracted weirs having negligible velocity of approach. Complete contraction of the nappe is dependent upon sufficient distance between ends of weir and channel walls and will exist if the dimensions of Fig. 180 are maintained. If the contracted weir of Fig. 180 cannot be calibrated, the selection of a coefficient of 0.62 seems reasonable in the light of suppressed weir experiments; such a weir must be calibrated in place if great accuracy is desired.

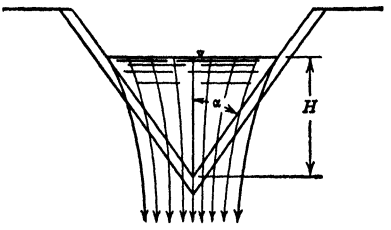


FIG. 181. Triangular Weir.

Triangular or V-notch weirs (Fig. 181) prove advantageous for measuring small rates of flow. A simplified analysis of the triangular weir gives the relationship between head and rate of flow

$$Q = \tfrac{8}{15}\tan\alpha\,\sqrt{2g}\,H^{\frac{5}{2}}$$

if velocity of approach is negligible, as it practically always is for weirs of this type. Introducing the experimental coefficient results in

$$Q = C\,\tfrac{8}{15}\tan\alpha\,\sqrt{2g}\,H^{\frac{5}{2}} \tag{92}$$

Early experiments by Thomson [23] on a weir of notch angle (2α) of 90° indicated C to have an average value of 0.593. Experiments by Barr [24] on the same type of weir made of polished brass led him to propose

$$Q = 2.48H^{2.48}$$

which is equivalent to stating that the coefficient is given by

$$C = \frac{0.580}{H^{0.02}}$$

[23] J. Thomson, "Experiments on Triangular Weirs," *British Assoc. Repts.*, 1861.
[24] J. Barr, "Experiments upon the Flow of Water over Triangular Notches," *Engineering*, April 8, 15, 1910.

Later King,[25] after experiments on the same type of weir constructed of rough steel plate, suggested

$$Q = 2.52H^{2.47}$$

as a flow equation for the 90° triangular weir. King's equation leads to a coefficient given by

$$C = \frac{0.589}{H^{.03}}$$

A comparison of the results of Thomson, Barr, and King, presented graphically in Fig. 182, gives striking confirmation of the effects of details upon weir flow. Roughness or minor obstructions on the weir

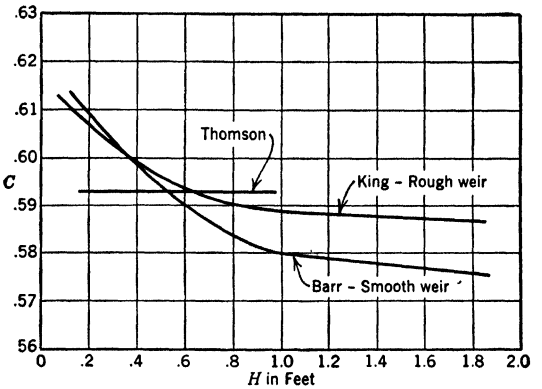


FIG. 182. Coefficients for Triangular Weirs.

plate affect the coefficient of the weir appreciably, by reducing velocities adjacent to the plate, thus reducing the nappe contraction and increasing the coefficient of the weir.

A trapezoidal weir of ingenious design was proposed by Cipoletti[26] in order to compensate automatically for the end contractions of a rectangular notch. Cipoletti expanded the contracted weir formula (91) of Francis to

$$Q = C\tfrac{2}{3}b\sqrt{2g}\,H^{\frac{3}{2}} - C\tfrac{4}{30}\sqrt{2g}\,H^{\frac{5}{2}}$$

[25] H. W. King, *Handbook of Hydraulics*, Second Edition, p. 93, McGraw-Hill Book Co., 1929.

[26] The results of Cipoletti's weir investigations are summarized in *Engineering Record*, Vol. 26, No. 11, p. 168, Aug. 13, 1892.

and considered the negative part as a loss of flow due to the existence of contraction. He proposed compensating for this loss by cutting back the corners of the rectangular contracted weir, in effect adding a half triangular weir at each end. For the proper value of α, the flow which would be lost by contraction is supplied by the triangular weir and thus

$$C\tfrac{4}{30}\sqrt{2g}\,H^{\frac{5}{2}} = C\tfrac{8}{15}\tan\alpha\sqrt{2g}\,H^{\frac{5}{2}}$$

whence

$$\tan\alpha = \tfrac{1}{4}$$

if the two coefficients are assumed equal. Thus to this type of trapezoidal weir (Fig. 183), the rectangular suppressed-weir equation

$$Q = C\tfrac{2}{3}b\sqrt{2g}\,H^{\frac{3}{2}}$$

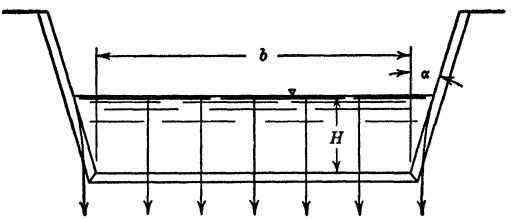


FIG. 183. Trapezoidal Weir.

may be applied in which C, determined by Cipoletti, may be taken as 0.63.

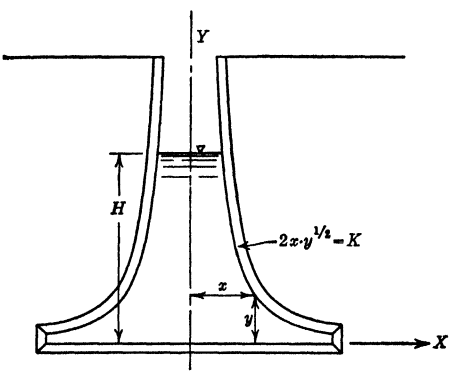


FIG. 184. Proportional Weir.

One of the characteristics of rectangular weirs has been seen to be the variation of Q with $H^{\frac{3}{2}}$, whereas for the triangular weir Q has been seen to vary with $H^{\frac{5}{2}}$. This leads to the conclusion that the geometrical shape of the weir determines the magnitude of the exponent and suggests the possibility of designing a weir in which Q varies linearly with H. Such a weir, termed a "proportional" or "Sutro" weir, finds wide application in water-level control where a simple relationship between head and rate of flow is desired.

Rettger [27] has shown that a proportional weir (Fig. 184) having horizontal crest and sides formed of hyperbolas given by the equation

$$2xy^{\frac{1}{2}} = K$$

results in a theoretical flow equation

$$Q = K\frac{\pi}{2}\sqrt{2g}\,H$$

and a linear relation between Q and H. Introducing the experimental weir coefficient, C, the practical equation for the proportional weir becomes

$$Q = CK\frac{\pi}{2}\sqrt{2g}\,H$$

Broad-crested weirs and spillways occur as overflow devices in hydraulic structures and are seldom used for measuring purposes; they are, however, rectangular weirs of special form to which the

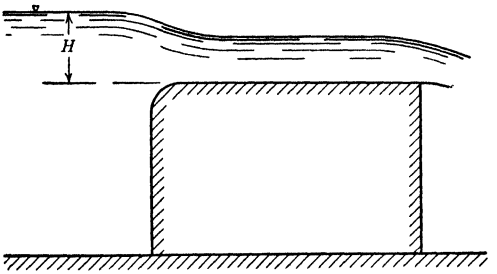


FIG. 185. Broad-Crested Weir.

foregoing rectangular weir equations may be applied. The broad-crested weir (Fig. 185) operates on the critical-depth principle modified for friction and flow curvatures and has been treated briefly in Art. 52. The rectangular-weir equation

$$Q = C\tfrac{2}{3}b\sqrt{2g}\,H^{\frac{3}{2}}$$

may be applied in which C ranges from 0.50 to 0.57, depending primarily upon the shape of the weir.

[27] E. W. Rettger, "A Proportional Flow Weir," *Engineering News*, Vol. 71, No. 26, June 25, 1914.

The "ogee" type of spillway is shown in Fig. 186. Major considerations in the design of such a spillway are structural stability against hydrostatic pressure and other loads and prevention of reduced

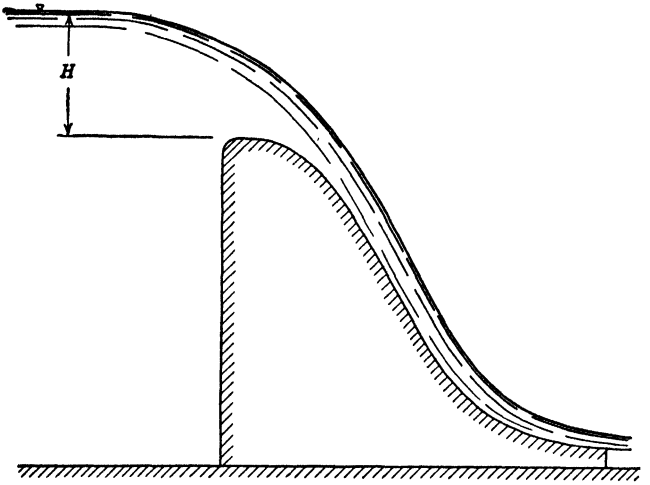


FIG. 186. Ogee Spillway.

pressures on the downstream face due to separation of the sheet of water from this surface. The rectangular-weir equation may be applied to the ogee spillway, the coefficient C ranging from 0.60 to 0.75. The relatively high value of C may be explained by a comparison of a sharp-crested weir (Fig. 187) and an ogee spillway designed exactly to fit the curvature of the lower side of the nappe of this weir. Obviously, with a fixed reservoir surface the flow over the two structures will be approximately the same, but the heads for each structure will be measured from their respective crests and will, therefore, be different, the head on the weir being greater than the head on the spillway. If the coefficient of the weir is C_w, the spillway coefficient, C_s, is seen to be the larger if the rates of flow are equated

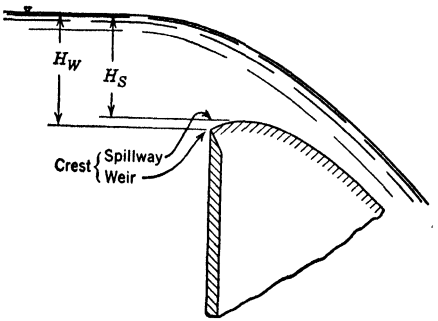


FIG. 187.

$$C_w \tfrac{2}{3} b \sqrt{2g}\, H_w^{\frac{3}{2}} = C_s \tfrac{2}{3} b \sqrt{2g}\, H_s^{\frac{3}{2}}$$

giving

$$C_s = C_w \left(\frac{H_w}{H_s}\right)^{\frac{3}{2}}$$

72. Current-Meter Measurements. The construction of a weir for measuring the flow in large canals, streams, or rivers is impractical for many obvious reasons; but existing spillways whose coefficients are known may frequently serve as measuring devices. However, the standard method of river-flow measurement is to measure the velocity by means of a current meter (Art. 62) and integrate the results as for Pitot-tube measurements in a pipe line (Art. 68).

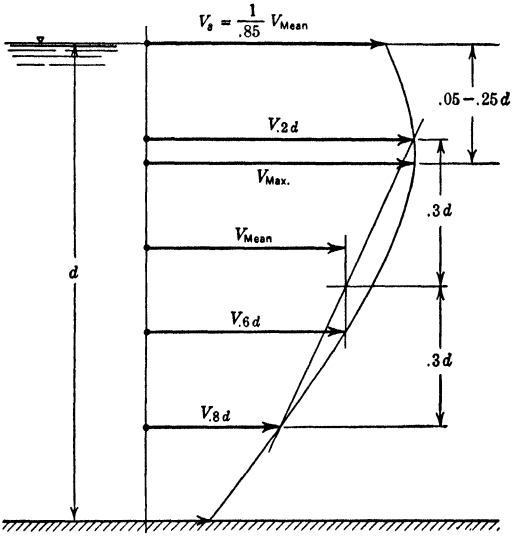


FIG. 188. Average Velocity Distribution in a Vertical in Open Flow.

Fundamental to the use of a current meter is a knowledge of the properties of velocity distribution in open flow. As in pipes, the velocities are reduced at the banks and bed of the channel, but it must be realized that in open flow the roughnesses and turbulences are of such great and irregular magnitudes that the velocity-distribution problem cannot be placed on the precise basis which it enjoys in pipe flow. However, from long experience and thousands of measurements, the United States Geological Survey has established certain average characteristics of velocity distribution in streams and rivers which serve as a basis for current-meter measurements. These characteristics of velocity distribution in a vertical are shown in Fig. 188 and may be

amplified by the following statements: (1) the curve may be assumed parabolic; (2) the location of the maximum velocity is from 0.05 d to 0.25 d below the water surface; (3) the average velocity occurs at approximately 0.6 d below the water surface; (4) the average velocity is approximately 85 per cent of the surface velocity; (5) a more accurate and reliable means of obtaining the average velocity is by taking a numerical mean of the velocities at 0.2 d and 0.8 d below the water surface. The above average values will naturally not apply perfectly to a particular stream or river, but numerous measurements with the current meter will tend toward accurate results since deviations from the above average values will tend to compensate, thus giving a greater accuracy than can be obtained in individual measurements.

Numerous current-meter measurements, always required in the calculation of the flow in a stream or river, are usually taken in the following manner. A reach of river is selected having a fairly regular

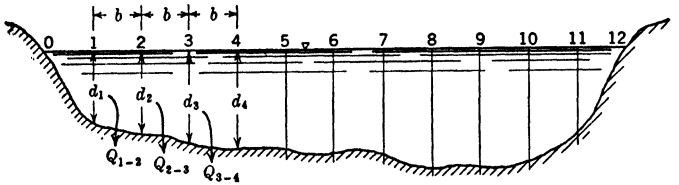


FIG. 189. Division of River Cross Section for Current Meter Measurements.

cross section. This cross section is measured accurately by soundings. It is then divided into vertical strips of equal width (Fig. 189), the current meter is suspended, and velocities are measured at the two-tenths and eight-tenths points in each vertical (1, 2, 3, etc., Fig. 189). From these measurements the average velocities (V_1, V_2, V_3, etc.) in each vertical may be calculated. The average velocity through each vertical strip is taken as the mean of the average velocities in the two verticals which bound the strip, and thus the rates of flow (Q_{1-2}, Q_{2-3}, etc.) through the strips may be calculated from

$$Q_{1-2} = b\left(\frac{d_1 + d_2}{2}\right)\left(\frac{V_1 + V_2}{2}\right)$$

$$Q_{2-3} = b\left(\frac{d_2 + d_3}{2}\right)\left(\frac{V_2 + V_3}{2}\right)$$

and the total flow in the stream may be calculated by totaling the rates of flow through the various strips.

73. Float Measurements. The velocities of surface floats may sometimes be used under satisfactory flow conditions to obtain rough measurements of river flow, but floats of this type are subject to the vagaries of winds and to local surface currents which may drive them far off their courses. The reach of river selected for float measurements should be straight and uniform and should have a minimum of surface disturbances; measurements should be taken on a windless day. The time for the floats to travel a certain distance may be measured easily, and from this the surface velocities may be computed and the average velocities approximated by using the relationships of Fig. 188. It should not be inferred, however, that even under ideal conditions the accuracy of float measurements is high. This is due to the above-mentioned general difficulties and to the fact that the ratio of mean velocity to surface velocity, although having an average value of 0.85, may be as low as 0.80 or as high as 0.95 and quite unpredictable for a given reach of river.

BIBLIOGRAPHY

Density Measurement

A.S.M.E. Power Test Codes, Series 1929, Part 16.

Viscosity Measurement

A.S.M.E. Power Test Codes, Series 1929, Part 17.

R. A. Dodge and M. J. Thompson, *Fluid Mechanics*, McGraw-Hill Book Co., 1937.

E. C. Bingham, *Fluidity and Plasticity*, McGraw-Hill Book Co., 1922.

Measurement of Pressure, Velocity, and Rate of Flow

Handbuch der experimental Physik, Band IV, Teil 1. Akademische Verlagsgesellschaft, Leipzig, 1932.

Measurement of Pressure and Velocity

L. Prandtl and O. G. Tietjens. *Applied Hydro- and Aerodynamics*, McGraw-Hill Book Co., 1934.

C. M. Allen and L. J. Hooper, "Piezometer Investigation," *Trans.* A.S.M.E., Vol. 54, 1932.

K. H. Beij, "Aircraft Speed Instruments," *N.A.C.A. Rept.* 420, 1932.

Measurement of Rate of Flow

Fluid Meters, Their Theory and Application, A.S.M.E., 1937.

H. Diederichs and W. C. Andrae, *Experimental Mechanical Engineering*, Vol. I, John Wiley & Sons, 1930.

Venturi Meter

C. Herschel, "The Venturi Water Meter," *Trans. A.S.C.E.*, Vol. 17, 1887, p. 228.

Weirs

H. Rouse, *Fluid Mechanics for Hydraulic Engineers*, McGraw-Hill Book Co., 1938.
J. G. Woodburn, "Tests of Broad Crested Weirs," *Trans. A.S.C.E.*, Vol. 96, 1932, p. 387.

Current-Meter Measurements

W. A. Liddell, *Stream Gaging*, McGraw-Hill Book Co., 1927.

PROBLEMS

405. A pycnometer weighs 100 grams when empty and 420 grams when filled with liquid. If its volume is 200 cc, calculate the specific gravity of the liquid.

406. A plummet weighs 400 grams in air and 300 grams in a liquid. If the volume of liquid displaced by the plummet is 120 cc, what is the specific gravity of the liquid?

407. A crude hydrometer consists of a cylinder of $\frac{1}{2}$-in. diameter and 2-in. length surmounted by a cylindrical tube $\frac{1}{8}$-in. in diameter and 8 in. long. Lead shot in the cylinder brings the hydrometer's total weight to 0.3 oz. What range of specific gravities may be measured with this hydrometer?

408. To what depth will the bottom of the hydrometer of the preceding problem sink in a liquid of specific gravity 1.10?

409. Mercury is placed in an open U-tube and liquid is poured into one of the legs. A liquid column 10-in. high balances a mercury column 1.5-in. high. What is the specific gravity of the liquid?

410. Water is placed in an open U-tube and oil (sp. gr. < 1) is poured into each leg. The water column is 6-in. high, one oil column 3-in., and the other 10-in. What is the specific gravity of the oil?

411. A Stormer type viscometer consists of two cylinders, one of 3.0-in. outside diameter, the other of 3.1-in. inside diameter, both 10-in. high. A 1-lb weight falls 5 ft in 10 sec, its supporting wire unwinding from a spool of 2-in. diameter on the main shaft of the viscometer. If the space between the cylinders is filled with oil to a depth of 8 in., calculate the viscosity of the oil, neglecting the force on the bottom of the cylinder.

412. Using the result of problem 29, recalculate problem 411 including the torque on the bottom of the cylinder, assuming a clearance of 0.05 in. between cylinder bottoms.

413. A steel sphere ($S = 7.8$) $\frac{1}{2}$ in. in diameter falls at a constant velocity of 0.3 ft/sec through an oil ($S = 0.90$). Calculate the viscosity of the oil.

414. What constant speed will be attained by a lead ($S = 11.4$) sphere 1 in. in diameter falling freely through an oil of kinematic viscosity, 0.12 ft^2/sec and specific gravity 0.95?

415. A Saybolt universal viscometer has tube diameter and length of 0.0693 in. and 0.482 in., respectively. The internal diameter of the cylindrical reservoir is 1.17 in., and the height from tube outlet to rim of reservoir is 4.92 in. Assuming as a rough approximation that the loss of head may be taken as the average of the total heads on the tube outlet at the beginning and end of the run, calculate the relationship between ν (ft^2/sec) and t (Saybolt seconds), and compare with the correct equation relating these quantities.

416. It takes 80 sec for 60 cc of an oil of specific gravity 0.95 to escape from a Saybolt viscometer during a routine viscosity test. What is the viscosity of this oil?

417. The disk of Fig. 137 and a Pitot tube are placed in an air stream aligned properly with the flow and connected to a U-tube containing water. If the difference of water elevation in the legs of the manometer is 4 in., calculate the air velocity, assuming $w = 0.0763$ lb/ft^3.

418. A Pitot-static tube on an airplane is connected to a differential manometer which reads 3 in. of water when flight occurs through still air (14.7 lb/in.^{2} and 60° F). Calculate the speed of the airplane in miles per hour.

419. If the Pitot tube of the preceding problem is connected to a sensitive differential-pressure gage which reads 0.08 lb/in.^{2}, calculate the speed of the airplane.

420. An airplane is designed to have a top speed of 250 mph when flying through still air of specific weight 0.0763 lb/ft^3. What will be the largest pressure difference recorded between the stagnation and static pressure openings of its Pitot tube?

421. A $1\frac{1}{2}$-in. smooth nozzle is connected to a horizontal 3-in. pipe in which the pressure is 60 lb/in.^{2} Calculate the stagnation pressure in the pipe and in the nozzle stream.

422. A Pitometer ($C_I = 0.85$) is placed at a point in a water line. If the attached differential manometer containing mercury and water shows a reading of 5 in., what is the velocity at the point?

423. A Pitot tube is placed at the center of a 6-in. pipe in which carbon tetrachloride flows at 68° F. The attached differential manometer containing mercury and carbon tetrachloride shows a difference of 3 in. What flow exists in the line?

424. The pipe-line Pitot tube of Fig. 147 is installed on the center of a 12-in. water line and connected to one end of a U-tube manometer containing carbon tetrachloride. The other end of the manometer is connected to the pipe wall. If water fills the manometer tubes above the CCl_4 and the manometer reads 10 in., what is the velocity at the center of the pipe?

425. A Venturi tube of $d_1 = 1\frac{1}{2}$ in., $d_2 = \frac{3}{4}$ in., and $C = 0.95$ is installed on the airplane of problem 420. Calculate the pressure difference $p_0 - p_2$. Calculate the pressure difference $p_s - p_2$ created by a Pitot-Venturi installed on this airplane. Compare answers.

426. A Venturi tube having $C = 0.95$ and $A_1/A_2 = 3$ has an open-ended water manometer connected to section 2. If the manometer reads 12 in. and the open end is at atmospheric pressure, what is the velocity of the tube through still air of specific weight 0.0763 lb/ft^3?

427. The gasometer of Fig. 158 is used to measure the flow of hydrogen at 65° F. The internal diameter of the cover is 5 ft, and it rises 1.87 ft in 34.6 sec. The manometer reads 16 in. of water, and the barometric pressure is 14.66 lb/in.^{2} Calculate the weight rate of flow. If the counterweight weighs 600 lb, what is the weight of the cover?

428. A 12 in. by 6 in. Venturi meter is installed in a horizontal water line. The pressure gages read 30 lb/in.^{2} and 10 lb/in.^{2} Calculate the flow, assuming $C_v = 0.97$. Calculate the loss of head between base and throat of the meter.

429. If the meter of the preceding problem is in a vertical pipe line with throat 2 ft below the base, calculate the rate of flow.

430. Oil ($S = 0.90$) flows through a 12 in. by 6 in. horizontal Venturi meter. The attached differential manometer contains mercury (and oil to the mercury

surfaces) and shows a difference of 10 in. Calculate the rate of flow if $C_v = 0.97$. Calculate the loss of head between base and throat of meter. If the cone angle of the diffusor tube is 7°, calculate the total lost head through the meter.

431. If the meter of the preceding problem is in a vertical pipe line with throat 2 ft below the base, calculate the rate of flow.

432. Linseed oil flows through a horizontal 6 in. by 3 in. Venturi meter. What is the difference in pressure head between base and throat of the meter when 120 gpm flow at (*a*) 80° F, (*b*) 120° F? What is the head loss for these two cases?

433. The maximum flow expected through an 18 in. by 9 in. Venturi meter installed in an 18-in. line is 15 cfs of water at 80° F. How long a manometer is necessary for this installation if the manometer is to contain mercury?

434. Calculate the weight flow of air through a 4 in. by 2 in. Venturi meter when the gage pressures at base and throat of meter are 40 lb/in.^{2} and 30 lb/in.^{2} The barometer reads 29.5 in. of mercury, the temperature of the air as it enters the meter is 100° F, and $C_v = 0.985$.

435. Carbon dioxide flows through a 6 in. by 2 in. Venturi meter. Gages at base and throat read 20 lb/in.^{2} and 14 lb/in.^{2}, and temperature at the base of the meter is 80° F. Calculate the weight flow, assuming standard barometer and $C_v = 0.99$.

436. Calculate the weight flow in the preceding problem when the throat pressure gage reads (*a*) 10 lb/in.^{2}, (*b*) 2 lb/in.^{2}

437. A 3-in. A.S.M.E. long-radius flow nozzle is installed in a 6-in. water line. The attached manometer contains mercury and registers a difference of 15 in. Calculate the flow through the nozzle. Calculate the head lost by the nozzle installation.

438. A 2-in. A.S.M.E. long-radius flow nozzle is installed in a 5-in. pipe line where linseed oil is flowing. The attached differential manometer, containing mercury, registers a difference of 8 in. Calculate the flow through the nozzle and the lost head caused by the nozzle installation.

439. If air flows through the pipe and nozzle of the preceding problem, open mercury manometers at points 1 and 2 show positive gage pressures of 30 in. and 20 in., and the temperature at point 1 is 60° F, calculate the weight rate of flow, assuming standard barometric pressure.

440. A 1-in. fire nozzle has $C_v = 0.98$ and $C_c = 1.00$, and is attached to a 3-in. hose. What flow will occur through the nozzle when the pressure in the hose is 60 lb/in.^{2} What is the velocity of the nozzle stream? What head is lost through the nozzle? To what height will this stream go, neglecting air friction?

441. Assuming an I.S.A. flow nozzle, calculate the rates of flow in: (*a*) problem 437; (*b*) problem 438; (*c*) problem 439.

442. A 2-in. nozzle having $C_v = 0.98$ and $C_c = 0.90$ is attached to a 6-in. pipe line and delivers water to an impulse turbine. The pipe line is 1000 ft long, leaving a reservoir of surface elevation 450 at elevation 420. The nozzle is at elevation 25. Assuming a sharp pipe entrance and a friction factor of 0.02, calculate: (*a*) the flow through the pipe and nozzle; (*b*) the horsepower of the nozzle stream; (*c*) the horsepower lost in line and nozzle.

443. Calculate the flow through a 3-in. I.S.A. orifice installed in a 6-in. water line when the attached manometer containing mercury shows a difference of 12 in.

444. Air flows through a 2-in. I.S.A. orifice installed in a 6-in. pipe line. A pressure gage upstream from the orifice reads 30 lb/in.^{2}, and a differential manometer connected between points 1 and 2 shows a difference of 15 in. of mercury. If the tem-

perature of the air upstream from the orifice is 70° F and the barometer reads 14.3 lb/in.^{2}, calculate the weight rate of flow.

445. Air flows through a 1-in. rounded orifice ($C_v = 0.99$) installed in a 6-in. pipe line. Pressure gages upstream and downstream from the orifice read 70 and 20 lb/in.^{2} Calculate the weight flow if the barometer is 14.3 lb/in.^{2} and temperature upstream from the orifice is 100° F.

446. Steam flows through a $\frac{1}{2}$-in. rounded orifice, having $C_v = 0.99$, installed in a 3-in. pipe line, the barometer is 14.5 lb/in.^{2}, and the temperature upstream from the orifice is 400° F. Pressure gages above and below the orifice read 60 and 20 lb/in.^{2} Calculate the weight rate of flow, taking $(p_2/p_1)_c = 0.55$.

447. Water discharges into the atmosphere from a 1.5-in. sharp-edged orifice under a 5-ft head. Calculate the rate of flow, diameter of the jet at the contracted section, and velocity at this point.

448. Under a 4.42 ft head, 0.056 cfs of water discharges from a 1-in. sharp-edged orifice in a vertical plane; 3.30 ft outward horizontally from the contracted section the jet has dropped 0.65 ft below the centerline of the orifice. Calculate C, C_v, and C_c.

449. Water flows from one tank to an adjacent one through a 3-in.-diameter sharp-edged orifice. The head of water on one side of the orifice is 6 ft and on the other 2 ft. Taking $C_c = 0.62$ and $C_v = 0.95$, calculate the rate of flow.

450. A 3-in. sharp-edged orifice discharges vertically upward. At a point 10 ft above the contracted section, the diameter of the jet is 3 in. Under what head is the orifice discharging?

451. A Pitot tube is placed in the contracted section of a jet from a 2-in. orifice operating under a 6-ft head. The Pitot tube is connected to a piezometer column in which water stands at a level 1.50 in. below that in the tank. Calculate C_v for the orifice.

452. A sluice gate 4 ft wide is open 3 ft and discharges onto a horizontal surface. If the coefficient of contraction is 0.80 and the coefficient of velocity 0.90, calculate the rate of flow if the upstream water surface is 15 ft above the top of the gate opening.

453. Calculate the rate of flow in the preceding problem if tailwater stands 10 ft deep over the top of the gate opening.

454. An open vertical cylindrical tank 20 ft high and 5 ft in diameter contains a valve in the bottom which is connected to a short piece of vertical 3-in. pipe which discharges into the atmosphere at a point 4 ft below the bottom of the tank. If the tank is full of water and the valve opened, how much time is required to reduce the water depth to 8 ft? Treat the pipe and valve as a 3-in. orifice having $C_c = 1.00$ and $C_v = 0.65$.

455. A cylindrical tank contains a 1-in. orifice 4 in. above the bottom. If the tank is 2 ft in diameter and it requires 65 sec for the water depth to drop from 4 ft to 3 ft, calculate the discharge coefficient of the orifice.

456. How much time is required to drain a full conical water tank (apex down) 10 ft high and having a base diameter of 4 ft through a 2-in. orifice ($C_c = 0.80$ and $C_v = 0.98$) in the apex?

457. Solve the preceding problem assuming a square pyramid with base having 4-ft sides.

458. A V-shaped tank is 10 ft long, 5 ft deep, and 4 ft wide at the top. A slot at the point of the V is 1 in. wide and runs the full length of the tank. How much time is required to drain the tank from the full condition, assuming that $C_c = 0.85$ and $C_v = 0.98$ for the slot.

459. A flow bend consisting of a 4-in. flanged elbow has a coefficient C_k of 1.50. What flow of water occurs through this bend when the attached manometer (Fig. 171) contains mercury and shows a difference of 10 in.?

460. A Pitometer ($C_I = 0.85$) is installed in a 6-in. water line. A manometer containing CCl_4 and water, connected to the Pitometer, shows the following readings when the tip of the instrument is placed at the points specified for the numerical average method for calculating rate of flow.

Pitometer location...	1	2	3	*C*	4	5	6
Manometer readings, In.	1.20	2.04	2.83	3.03	2.89	2.10	1.26

Calculate the rate of flow, pipe coefficient, and the distance from pipe centerline to station 2.

461. A Pitot tube is placed at various points along a diameter of a 20-in. pipe in which water is flowing. The pressure difference is measured on a manometer containing mercury and water. If the following manometer readings are taken, calculate the rate of flow and pipe coefficient by the graphical method.

Distance from Pitot tube location to pipe centerline, in.....	0	2	4	6	8	9	9.5
Manometer reading, in.	6	5.95	5.64	5.07	4.12	3.25	2.45

462. The apparatus of Fig. 174 is installed in an insulated 6-in. pipe line in which air is flowing. A potential of 110 volts is maintained across the 30-ohm resistance, and the thermometers read 100 and 105° F. The gage pressure in the pipe is 50 lb/in.^{2} If the specific heat of the air is 0.24 Btu/lb/° F, what weight flow exists in the line?

463. The flow in a brook is measured by the salt-dilution method; 0.20 gpm of salt solution having a concentration of 20 lb salt/gal are introduced and mix with the flow. A sample extracted below the mixing point shows a concentration of 0.00008 lb/gal. Calculate the flow in the brook.

464. The salt-velocity method is to be used on a 24-in. pipe line, and electrodes are installed 100 ft apart. The time between deflection of the ammeter needles is 12.0 sec. Calculate the flow in the line.

465. Calculate the flow over a rectangular sharp-crested suppressed weir 4 ft long and 3 ft high when the head thereon is 4 in., using the coefficients of (*a*) Bazin, (*b*) Rehbock, (*c*) Swiss Society, (*d*) Frese. What is the velocity of approach in (*a*)? (Use $P/H = \infty$ in finding *C*.)

466. If the weir of the preceding problem is only 4 in. high, calculate the flows and velocity of approach.

467. What depth of water must exist behind a rectangular sharp-crested suppressed weir 5 ft long and 4 ft high when a flow of 10 cfs passes over it? What is the velocity of approach? Use Rehbock *C*.

468. A rectangular channel 18 ft wide carries a flow of 50 cfs. A rectangular suppressed weir is to be installed near the end of the channel to create a depth of 3 ft upstream from the weir. Taking $C = 0.62$, calculate the necessary weir height.

469. A sharp-crested rectangular contracted weir 6 ft long measures the outflow from a small pond. If $C = 0.623$, what is the flow over the weir when the head is 0.816 ft?

470. A rectangular contracted weir is to be used to maintain a depth of 4 ft in a channel 15 ft wide where the flow is 12 cfs. Taking a coefficient of 0.62, what length and height of weir crest are required?

471. Derive the theoretical flow equation for the triangular weir.

472. Calculate the flow over a smooth sharp-crested triangular weir of 90° notch angle when operating under a head of 7 in. according to (*a*) Thomson, (*b*) Barr.

473. A triangular weir of 90° notch angle is to be used for measuring flows up to 1.5 cfs. What is the minimum depth of notch which will pass this flow?

474. A triangular weir has a 60° notch angle. What is the flow over this weir under a 9-in. head if the coefficient is 0.57?

475. What length of Cipoletti weir is required for a flow up to 20 cfs if the maximum head is limited to 8 in.?

476. Calculate the flow over a Cipoletti weir 12 ft long when the head thereon is 0.783 ft.

477. If a proportional weir is to be designed for a maximum flow of 5 cfs under a head of 3 ft, what is the width of its notch 1.5 ft above the crest, taking $C = 0.60$?

478. A proportional weir is 3 in. wide at a height of 2 ft above the crest. What rate of flow will occur under a head of 4 ft if C is taken as 0.62?

479. What flow will occur over a spillway of 500-ft length when the head thereon is 4 ft if the coefficient of the spillway is 0.72?

480. A spillway 1000 ft long is found by model experiments to have a coefficient of 0.68. It has a crest elevation of 100.00. When a flood flow of 50,000 cfs passes over the spillway what is the elevation of the water surface just upstream from the crest?

481. A broad-crested weir has a flat crest and a coefficient of 0.55. If this weir is 20 ft long and the head on it is 1.5 ft, what flow will occur over it? What is the maximum flow that could be expected if flow were frictionless?

482. A rectangular channel 20 ft wide carries 100 cfs at a depth of 3 ft. What height of broad-crested suppressed weir must be installed to double the depth? $C = 0.56$.

483. The following data are collected in a current-meter measurement at the river cross section of Fig. 189 which is 60 ft wide at the water surface. Assume $V = 2.22 \times$ (rps), and calculate the flow in the river.

Station....	0	1	2	3	4	5	6	7	8	9	10	11	12
Depth, ft..	0.0	3.0	3.2	3.5	3.6	3.7	3.9	4.0	4.4	4.4	4.2	3.5	0.0
						Rpm of rotating element							
0.2 *d*.....	...	40.0	53.5	58.6	63.0	66.7	61.5	56.3	54.0	52.6	50.0	45.0	....
0.8 *d*.....	...	30.7	42.8	50.0	54.2	58.8	53.3	49.4	46.5	43.2	40.1	32.5	....

CHAPTER IX

FLOW ABOUT IMMERSED OBJECTS

Problems involving the forces exerted on a solid body when fluid flows by it no longer belong exclusively to the aeronautical engineer. In the design of ship hulls, automobile bodies, and trains, minimizing fluid resistance or drag has become of increasing importance; in the design of ship propellers, turbines, and centrifugal pumps, the principles of lift are being applied with increasing success. As these principles find increasingly wide application, it becomes necessary for all engineers to be familiar with the fundamental mechanics of these principles. The origins of drag have been discussed briefly in Art. 28, and it is the purpose of this chapter to expand the treatment of the subject and to outline the elementary principles of lift as well.

74. Fundamentals and Definitions. In general when fluid flow occurs about an object which is either unsymmetrical or whose axis is not aligned with the flow, the velocities on either side of the object have different magnitudes. From the streamline picture about the foil of Fig. 190*a*, it is obvious at once that the velocity is higher on the upper side of the foil than on the lower, and hence from the Bernoulli principle the pressure on the upper side is less than on the lower side. Further examination of the flow picture indicates the pressure on the upper side of the foil to be less than, and that on the lower side greater than, the pressure, p_o, in the undisturbed fluid stream; in other words, there is a pressure reduction, or "suction," on the upper side of the foil and in increase of pressure on the lower side. Designating the suction by arrows drawn away from the foil and pressure increase by arrows drawn toward the foil, the distribution of pressure over the surface of the foil becomes as shown in Fig. 190*b*.[1]

Along with these pressures which are exerted everywhere normal to the surface of the foil, there are, of course, tangential shear stresses τ_o as well, acting on the foil in a downstream direction and resulting

[1] Note that the larger pressure diagram on the top of the foil indicates that the larger part of the force on the foil is contributed by pressure reduction on the upper side.

from the frictional effects which exist when fluids flow over solid boundaries (Art. 26).

The resultant force, F, exerted by fluid on foil by the normal (pressure) and tangential (frictional) stresses will have a direction as shown in Fig. 190*c* and may be resolved into components parallel and perpendicular to the direction of the undisturbed velocity,[2] V. The

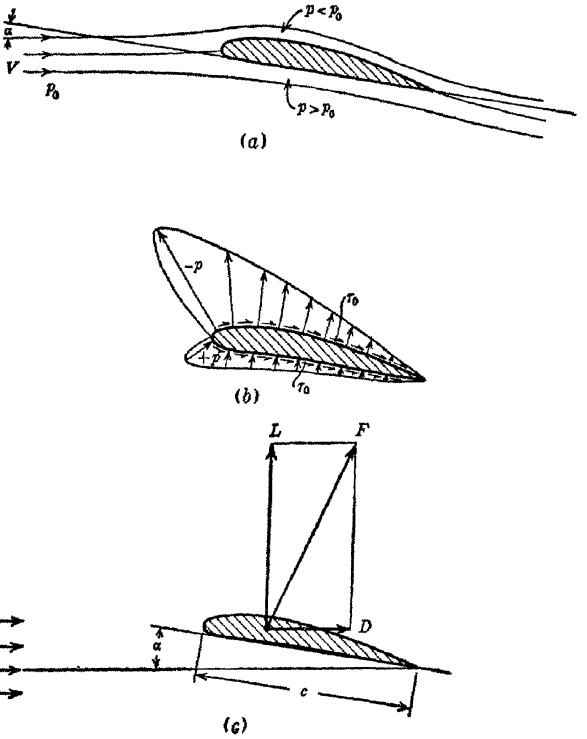


FIG. 190.

former component, D, is termed the "drag" (force) and the latter one, L, the "lift" (force) on the foil. Obviously, both these force components embody the effects of both normal and tangential stresses exerted by fluid on foil. The effect of normal and tangential stresses on drag has been discussed in Art. 28 and resulted in the definition of "profile" and "frictional" drag. The effect of tangential stresses upon the lift force may, however, be safely neglected because the

[2] Or, stating this in another way, parallel and perpendicular to the direction of motion of the foil through still fluid.

tangential stresses τ_o not only are small but also act in a direction roughly normal to that of the lift force and thus contribute little to it; thus the lift force exerted on the foil may be safely considered to result from pressure variation alone.

The width of the foil, c, is called the "chord;" its length, b, perpendicular to the plane of the paper, the "span;" and the angle α between chord and direction of the undisturbed velocity, V, the "angle of attack."

The lift and drag are calculated by

$$L = C_L A \frac{\rho V^2}{2} \tag{93}$$

and

$$D = C_D A \frac{\rho V^2}{2} \tag{94}$$

in which C_L and C_D are the (dimensionless) lift coefficient and drag coefficient of the foil, and A the area of the projection of the airfoil on the plane of the chord.[3] The coefficients of lift and drag may be found experimentally by wind-tunnel or flight tests; their magnitudes obviously depend upon the shape of the foil and (among other variables) upon the angle of attack.

Illustrative Problem

The lift and drag coefficients of a rectangular airfoil of 50-ft span and 7-ft chord are 0.6 and 0.05, respectively, when at an angle of attack of 7°. Calculate the horsepower required to drive this airfoil through still air ($w = 0.0763$ lb/ft^3) at 150 mph. What lift is obtained when this horsepower is expended?

$$\rho = \frac{0.0763}{32.2} = 0.00237 \text{ slugs/ft}^3$$

$$V = \frac{150 \times 5280}{3600} = 220 \text{ ft/sec}$$

$$D = C_D A \frac{\rho V^2}{2} = 0.05 \times (50 \times 7) \frac{0.00237 \times \overline{220^2}}{2} = 1006 \text{ lb}$$

$$\text{H.P.} = \frac{1006 \times 220}{550} = 402.5 \text{ hp}$$

$$L = 0.6 \times (50 \times 7) \frac{0.00237 \times \overline{220^2}}{2} = 12{,}080 \text{ lb}$$

[3] If the plan form of the foil is rectangular, $A = b \times c$.

75. Dimensional Analysis of the Drag Problem. The general aspects of fluid resistance on immersed bodies and the properties of the drag coefficient may be examined to advantage by dimensional analysis, before considering the physical details of the problem.

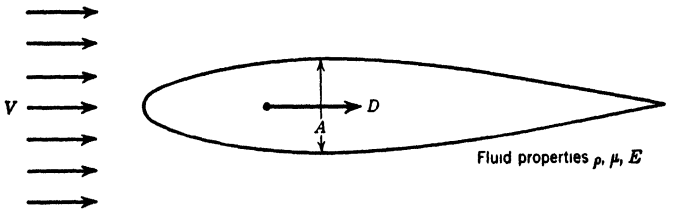


FIG. 191.

The smooth body of Fig. 191, having area [4] A, moves through a fluid of density ρ, viscosity μ, and modulus of elasticity E, with a velocity V. If the drag on the body is D,

$$D = f(A, \rho, \mu, V, E)$$

and because of dimensional homogeneity,

$$D = CA^a\rho^b\mu^c V^d E^e$$

Writing the equations dimensionally

$$\frac{ML}{T^2} = (L^2)^a \left(\frac{M}{L^3}\right)^b \left(\frac{M}{LT}\right)^c \left(\frac{L}{T}\right)^d \left(\frac{M}{LT^2}\right)^e$$

the equations of exponents of M, L, and T becomes

$$M: \quad 1 = b + c + e$$

$$L: \quad 1 = 2a - 3b - c + d - e$$

$$T: \quad -2 = -c - d - 2e$$

Solving for b, d, and a in terms of c and e,

$$b = 1 - c - e$$

$$d = 2 - c - 2e$$

$$a = 1 - \frac{c}{2}$$

[4] Any convenient significant area may be used.

Resubstituting these above

$$D = CA^{1-\frac{c}{2}} \rho^{1-c-e} \mu^c V^{2-c-2e} E^e$$

and rearranging

$$D = C\left(\frac{\mu}{A^{\frac{1}{2}} \rho V}\right)^c \left(\frac{E}{V^2 \rho}\right)^e A\rho V^2$$

But, referring to Art. 30,

$$\frac{A^{\frac{1}{2}} \rho V}{\mu} = N_R \quad \text{and} \quad \frac{V^2 \rho}{E} = N_C$$

but (Art. 4)

$$\frac{E}{\rho} = c^2$$

Therefore $N_c = V^2/c^2$, in which V/c is known as N_M, the Mach number. Substituting these values above, the drag equation may be written

$$D = f(N_R, N_M) \frac{A\rho V^2}{2}$$

and by comparison with equation 94

$$C_D = f(N_R, N_M) \tag{95}$$

This equation indicates: (1) that bodies of the same shape and having the same alignment with the flow possess the same drag coefficients if their Reynolds numbers and Mach numbers are the same; or (2) that the drag coefficient of bodies of given shape and alignment depend upon their Reynolds and Mach numbers. Thus, dimensional analysis has, as in previous problems (ship resistance and pipe friction), opened the way to a comprehensive treatment of the resistance of immersed bodies by indicating the dimensionless combinations of variables upon which the drag coefficient depends.

Although the drag coefficient is theoretically dependent upon both the Reynolds and Mach numbers simultaneously, this is seldom true in actual practice because the Reynolds number (containing the effect of viscosity) affects the size of the drag coefficient only at relatively low speeds where the Mach number is small and compression of fluid by body usually negligible; on the other hand, when velocities approach or exceed that of sound (N_M approaching or greater than unity), compression of fluid by body contributes the major part of the drag

force whereas here the contribution of viscosity is very small. This reasoning divides the study of drag force into two separate physical problems, one involving velocities well below the acoustic velocity, and the other velocities near to or exceeding this velocity. In the first, the variation in fluid density may be neglected and laminar or turbulent flow conditions and drag coefficients are governed by the Reynolds number; this is the field of present-day aerodynamics where the velocities involved are usually well below the acoustic velocity. The second case embraces the field of high-velocity motion in which flow is highly turbulent, but in which the Mach number governs flow patterns and drag coefficients since these result primarily from fluid compression and not from viscous action. The motion of bullets and projectiles through air and the motion of airplane propeller tips at high speeds are governed by compressibility and the Mach number.

A complete treatment of drag includes "drag at low velocities" and "drag at high velocities." For the first, frictional and pressure forces must both be considered; they have been seen to result in frictional drag and profile drag respectively. For drag at high velocities, frictional forces are neglected and a study of the topic is one of pressure effects, which leaves only profile drag to be considered. These three subjects will be treated in detail in the above order in the succeeding articles.

Illustrative Problem

An airfoil of 6-ft chord moves at 300 mph through still air (14.7 lb/in.^{2} abs and 60° F). Calculate the Reynolds and Mach numbers.

$$V = \frac{300 \times 5280}{3600} = 440 \text{ ft/sec}$$

$$\rho = \frac{0.0763}{32.2} = 0.00237 \text{ slugs/ft}^3$$

$$\mu = 0.000000375 \text{ lb sec/ft}^2$$

$$N_R = \frac{440 \times 6 \times 0.00237}{0.000000375} = 16{,}700{,}000$$

$$c = \sqrt{\frac{kp}{\rho}} = \sqrt{\frac{1.4 \times 14.7 \times 144}{0.00237}} = 1120 \text{ ft/sec}$$

$$N_M = \frac{440}{1120} = 0.393$$

76. Frictional Drag.[5] To discover the essential properties of frictional drag, consider the drag force exerted on one side of a smooth flat plate aligned with the flow; such a surface eliminates geometrical complexities and possesses no profile drag.

As fluid flow occurs over the flat plate of Fig. 192, the viscosity causes the velocity to be zero at every point on the surface of the plate whereas the velocity at a very small distance δ from this surface is the undisturbed velocity V. Thus, a very thin layer of fluid, the boundary layer, containing a velocity gradient, forms over the surface of the plate; since shear stress in fluids depends upon the existence of a velocity gradient, it is immediately apparent that resistance effects are confined to the boundary layer and must, therefore, be dependent upon the characteristics of this layer.

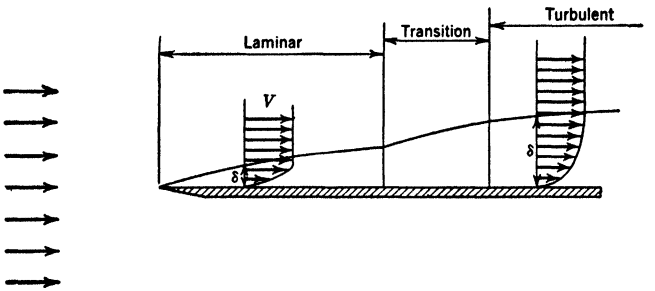


FIG. 192. Boundary Layers on a Flat Plate.

The layer must start from no thickness at the leading edge of the plate where viscous action begins and must increase its thickness in a downstream direction as the increasing viscous action exerted by increasing plate area extends into the flow and reduces the velocity of more and more fluid. Near the leading edge of the plate where the boundary layer is thin and contains small quantities of fluid subject to high viscous influence, the flow within the layer will be laminar, but, as the layer becomes thicker and includes more fluid mass, instability results and flow within the layer becomes turbulent. The change from a laminar to a turbulent boundary layer is not, however, an abrupt one, but occurs through a transition region in which both viscous and turbulent action are present; viscosity effects in the transition region are finally replaced by those of turbulence, and a wholly turbulent boundary layer results (Fig. 192).

[5] The student should restudy Art. 28.

Now consider, for simplicity, the laminar boundary layer (Fig. 193) having a thickness δ at a distance x from the leading edge of a plate of unit width, and apply the impulse-momentum law to an element of this layer of length, dx. The net applied (drag) force, dD, is given by

$$dD = \tau_o dx$$

The flow dQ drawn into the boundary layer in distance dx is of the order $Vd\delta$, and the reduction ΔV of its velocity is proportional to V. Thus

$$\frac{dQw}{g}\Delta V \sim Vd\delta\rho V$$

or

$$\frac{dQw}{g}\Delta V = \alpha Vd\delta\rho V$$

in which α is the factor necessary to make an equality of the above approximate relations and will be a constant if the velocity profiles

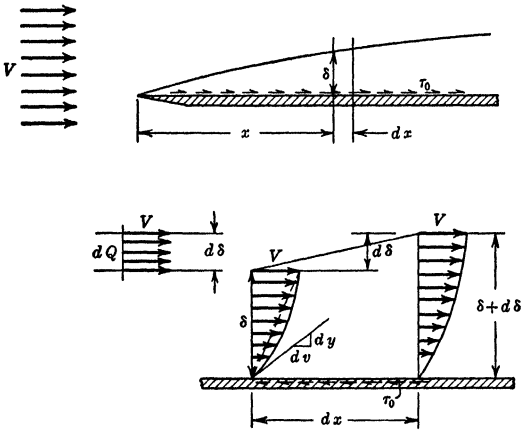


FIG. 193. Laminar Boundary Layer.

throughout the laminar boundary layer are of similar shape. Equating net force dD and change of momentum per unit time,

$$dD = \frac{dQw}{g}\Delta V$$

and substituting the above values

$$\tau_o dx = \alpha\rho V^2 d\delta \qquad (96)$$

Now, since the flow is laminar, the shear stress τ_o is given by

$$\tau_o = \mu \left(\frac{dv}{dy}\right)_{\text{surface}}$$

But if the velocity profiles are all of similar shape $(dv/dy)_{\text{surface}}$ will be a fixed proportion, β, of a linear velocity gradient V/δ. Therefore,

$$\tau_o = \beta\mu \frac{V}{\delta}$$

which may be substituted in equation 96 to give

$$\beta\mu \frac{V}{\delta} dx = \alpha\rho V^2 d\delta$$

which may be rearranged and integrated

$$\int_o^x dx = \frac{\alpha\rho V}{\mu\beta} \int_o^\delta \delta d\delta$$

giving the relation between x and δ

$$x = \left(\frac{\alpha\rho V}{2\beta\mu}\right) \delta^2 \tag{97}$$

thus showing the contour of the laminar boundary layer to be parabolic in shape. This equation may be rearranged and put in dimensionless form by solving it for δ/x, giving

$$\frac{\delta}{x} = \frac{\left(\frac{2\beta}{\alpha}\right)}{\left(\frac{V\delta\rho}{\mu}\right)} \tag{98}$$

and indicating this ratio to be inversely proportional to the Reynolds number $(N_R)_\delta$ calculated with δ as the length parameter. Blasius [6] has shown theoretically and experimentally that $2\beta/\alpha = 27.0$, and thus the above equation becomes

$$\frac{\delta}{x} = \frac{27.0}{(N_R)_\delta}$$

[6] H. Blasius, "Grenzschichten in Flüssigkeiten mit kleiner Reibung," *Zeit. f. Math. u. Physik*, Vol. 56, 1908, p. 1.

However, this equation is obviously not convenient for calculation of δ for a certain numerical value of x, because δ occurs on both sides of the equation; it may be placed in more usable form by substituting for δ, in the Reynolds number, its value obtained in terms of x from equation 97. This is

$$\delta = \sqrt{\frac{2\beta}{\alpha}}\sqrt{\frac{\mu x}{\rho V}}$$

and substituting in equation 98

$$\frac{\delta}{x} = \frac{\frac{2\beta}{\alpha}}{\sqrt{\frac{2\beta}{\alpha}}\sqrt{\frac{\mu x}{\rho V}}\frac{V\rho}{\mu}} = \frac{\sqrt{\frac{2\beta}{\alpha}}}{\sqrt{\frac{Vx\rho}{\mu}}}$$

and since

$$\sqrt{\frac{2\beta}{\alpha}} = \sqrt{27.0} = 5.20, \text{ and letting } \frac{Vx\rho}{\mu} = N_R$$

$$\frac{\delta}{x} = \frac{5.20}{\sqrt{N_R}} \tag{99}$$

which shows that the shape of the laminar boundary layer—an inertia viscosity phenomenon—is dependent, as might have been expected, only on a Reynolds number.

The drag coefficient and total drag of this flat plate now remain to be calculated. Expressing the differential drag force dD on the element of plate of length dx in the conventional way (equation 94),

$$\tau_o dx = dD = c_f\, dx \frac{\rho V^2}{2}$$

giving

$$c_f = \frac{2\tau_o}{\rho V^2} \tag{100}$$

in which c_f is the (frictional) drag coefficient for the element of plate dx. Since τ_o can be shown to decrease with increasing x, c_f varies with x in the same way. However, a drag coefficient which differs for every element of plate is obviously inconvenient, so a more practical average frictional drag coefficient C_f will be derived for the plate length x, so that the total drag D for the length x will be given by

$$D = C_f\, x \frac{\rho V^2}{2}$$

But total drag for the plate length x is also given by

$$D = \int_o^D dD = \int_o^x c_f \, dx \frac{\rho V^2}{2}$$

Equating the above two expressions for D

$$C_f = \frac{\int_o^x c_f \, dx}{x} \tag{101}$$

and with this equation C_f may be easily derived after an expression for c_f is found. If

$$\tau_o = \beta\mu \frac{V}{\delta}$$

is substituted in equation 100

$$c_f = \frac{2\beta\mu}{\rho V \delta}$$

and substituting

$$\delta = \sqrt{\frac{2\beta\mu x}{\alpha\rho V}}$$

gives

$$c_f = \frac{2\beta\mu}{\rho V}\sqrt{\frac{\alpha\rho V}{2\beta\mu x}} = \frac{\sqrt{2\alpha\beta}}{\sqrt{\frac{Vx\rho}{\mu}}}$$

in which $\sqrt{2\alpha\beta}$ has been shown by Blasius to have the value 0.664. Thus

$$c_f = \frac{0.664}{\sqrt{N_R}}$$

and substituting this expression in equation 101

$$C_f = \frac{\int_o^x \frac{0.664}{\sqrt{\frac{Vx\rho}{\mu}}} dx}{x} = \frac{1.328}{\sqrt{\frac{Vx\rho}{\mu}}} = \frac{1.328}{\sqrt{N_R}}$$

This equation allows the frictional drag on flat plates of length x to be calculated when the plates are placed in a flow of velocity V, density ρ, and viscosity μ, *provided that the boundary layer remains in laminar condition.* It should be noted that the results of the above physical treatment of drag confirm and amplify those of dimensional analysis which showed that drag coefficients of smooth bodies at low velocities depend only upon Reynolds numbers (equation 95).

A flat plate with a turbulent boundary layer may be analyzed physically by methods similar to those above, but the concepts and mathematics involved are too advanced for inclusion in an elementary textbook. Prandtl [7] has shown that the equation

$$C_f = \frac{0.455}{(\log N_R)^{2.58}}$$

gives the relation between C_f and N_R for a flat plate with turbulent boundary layer and has also shown that the approximate thickness of such a turbulent layer is given by

$$\frac{\delta}{x} = \frac{0.37}{N_R^{0.2}}$$

A plot of C_f against N_R for smooth flat plates (Fig. 194) with laminar and turbulent boundary layers bears a striking resemblance to that of friction factor against Reynolds number for circular pipes (Fig. 86). However, the critical Reynolds number at which the laminar boundary layer changes to a turbulent one is not so well defined as its counterpart in pipe flow, because of flow conditions which are not so well controlled. With increased initial turbulence in the approaching fluid flow, earlier breakdown of the laminar boundary layer occurs, thus reducing the critical Reynolds number; roughening the leading edge of the plate has also been found to decrease the critical Reynolds number by decreasing the flow stability and causing earlier breakdown of the laminar layer. A typical equation which satisfies experimental results in the transition region and which determines the critical Reynolds number is that suggested by Prandtl from Gebers' tests on a smooth flat plate. This equation is

$$C_f = \frac{0.455}{(\log N_R)^{2.58}} - \frac{1700}{N_R}$$

[7] L. Prandtl, *Ergebnisse der aerodynamischen Versuchsanstalt zu Göttingen*, IV, 1932, p. 27, R. Oldenbourg.

giving a critical Reynolds number of 530,000. This figure, however, should be taken only as a typical value; the range of experimentally determined critical Reynolds numbers is approximately from 100,000 to 1,000,000.

From the above statements, and from the plot of Fig. 194, there is obviously great uncertainty in the selection of values of C_f for Reynolds numbers of less than 10,000,000. Above this figure there is ample experimental confirmation of Prandtl's equation.

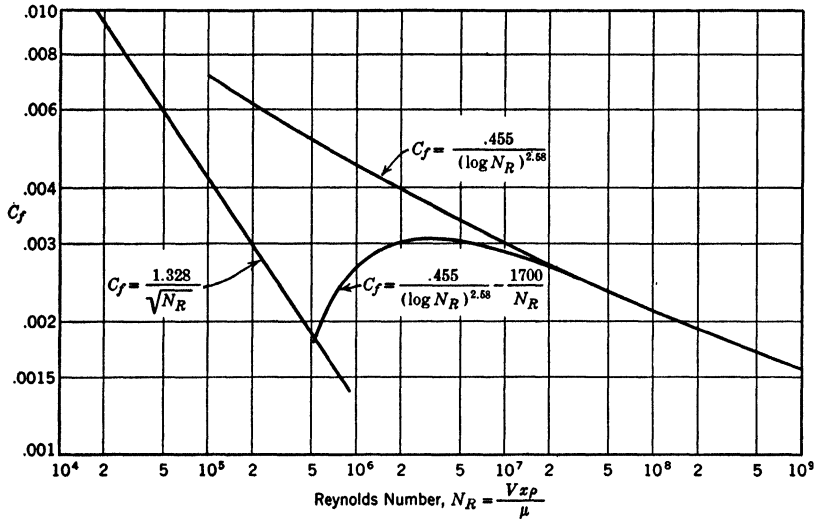


FIG. 194. Drag Coefficients for Smooth Flat Plates.

ILLUSTRATIVE PROBLEM

A smooth rectangular plate 3 ft wide and 100 ft long moves in the direction of its length through water (68° F) at 30 ft/sec. Calculate the drag force on the plate and the thickness of the boundary layer at the trailing edge of the plate.

$$N_R = \frac{Vx\rho}{\mu} = \frac{30 \times 100 \times 1.935}{0.000021} = 276{,}500{,}000$$

$$C_f = \frac{0.455}{(\log 276{,}500{,}000)^{2.58}} = 0.00186$$

Total drag (2 sides of plate) $= 2C_f A \frac{\rho V^2}{2}$

$$D = 2 \times 0.00186 \times (100 \times 3) \frac{1.935 \times \overline{30^2}}{2} = 972 \text{ lb}$$

$$\frac{\delta}{100} = \frac{0.37}{(276{,}500{,}000)^{0.2}} = 0.0076, \quad \delta = 0.76 \text{ ft}$$

77. Profile Drag.[8] Profile drag has been shown to be that part of total drag resulting from pressures over the surface of an object and to be dependent on the formation of a wake behind the object. In general, when wakes are large profile drag is large, and when wakes are reduced by streamlining profile drag is reduced also.

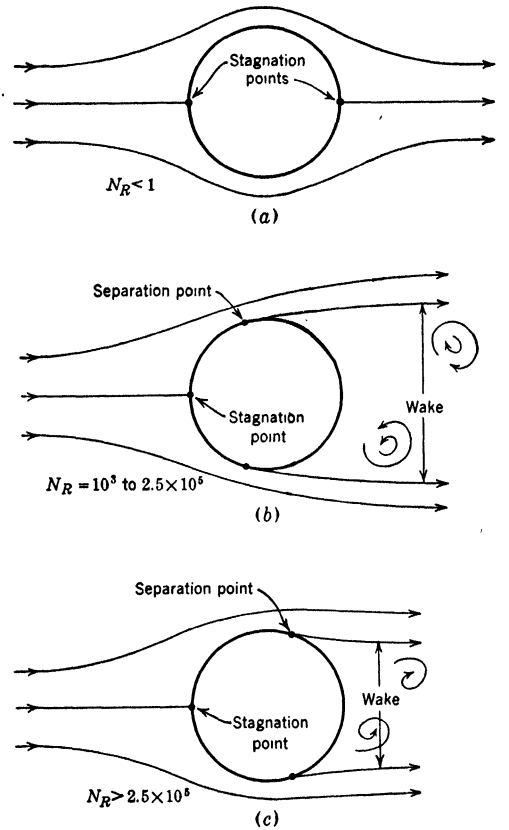


FIG. 195. Flow about a Sphere at Various Reynolds Numbers.

The properties of profile drag can best be obtained by examining the details of flow about a blunt object such as a sphere which has an appreciable and variable wake width, but on which the frictional drag may be neglected because of the small surface area on which frictional effects can act.

[8] The student should restudy Art. 28.

Even for a blunt object, however, profile drag is not always predominant or frictional drag negligible since flow at very low Reynolds numbers about a blunt object will close behind the object and no wake will form (Fig. 195*a*). Under these conditions total drag is composed primarily of frictional drag. Stokes[9] has shown that, in laminar flow at very low Reynolds numbers, where inertia forces may be neglected and those of viscosity alone considered, the drag of a sphere of diameter d, moving at a velocity V through a fluid of viscosity μ, is given theoretically by

$$D = 3\pi\mu Vd$$

and this equation has been confirmed by many experiments. The drag coefficient C_D for the sphere under these conditions may be found by equating the above expression to equation 94

$$C_D A \frac{\rho V^2}{2} = 3\pi\mu Vd$$

Taking A as the cross-sectional area of the sphere at the center,

$$A = \frac{\pi d^2}{4}$$

and substituting this above,

$$C_D \frac{\pi d^2}{4} \frac{\rho V^2}{2} = 3\pi\mu Vd$$

whence

$$C_D = \frac{24}{\frac{Vd\rho}{\mu}} = \frac{24}{N_R}$$

Thus the drag coefficients of spheres at low velocities are dependent only on the Reynolds number, again confirming the results of the dimensional analysis of Art. 75.

As the Reynolds number increases, the drag coefficients of spheres continue to depend only upon the size of this number, and a plot of experimental results over a large range of Reynolds numbers for spheres of many sizes, tested in many fluids, gives the single curve of Fig. 196.

[9] G. G. Stokes, *Mathematical and Physical Papers*, Vol. III, p. 55, Cambridge University Press, 1901.

Up to a Reynolds number of unity, the Stokes equation holds and the drag coefficient results from frictional effects. As the Reynolds number is increased to about 1, separation and weak eddies begin to form, enlarging into a fully developed wake near a Reynolds number of 1000; in this range the drag coefficient results from a combination of profile and frictional drag, the latter being of negligible size as a Reynolds number of 1000 is reached. Above this figure the effects of friction may be neglected and the drag problem becomes one of profile drag alone.

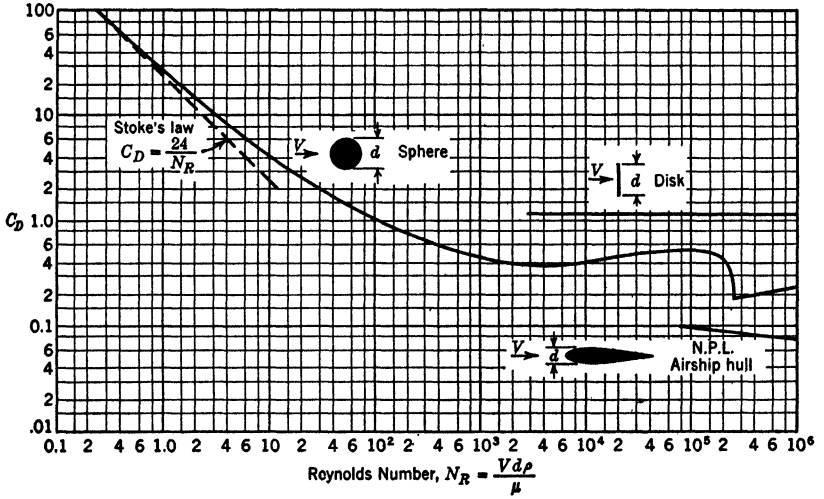


FIG. 196. Drag Coefficients for Sphere, Disk, and Streamlined Body.[10]

The profile-drag coefficient of the sphere is roughly constant from $N_R \sim 1000$ to $N_R \sim 250{,}000$ at which point it suddenly drops about 50 per cent and stays practically constant for further increase in the Reynolds number. In the above range of Reynolds numbers, experiments have shown the separation point to be upstream from the midpoint of the sphere, resulting in a relatively wide turbulent wake; the boundary layer on the surface of the sphere from stagnation point to separation point has been found to be laminar up to $N_R \sim 250{,}000$. At this point, the boundary layer becomes turbulent and the separa-

[10] Data from L. Prandtl, "Ergebnisse der aerodynamischen Versuchsanstalt zu Göttingen," Vol. II, R. Oldenbourg, 1923, p. 29, and G. J. Higgins, "Tests of the N. P. L. Airship Models in the Variable Density Wind Tunnel," *N.A.C.A. Tech. Note* No. 264, 1927.

tion point moves to a point downstream from the center of the sphere, causing a decrease in the width of the wake and consequently a decrease in the drag coefficient.

The sudden shift of the separation point and decrease in the profile-drag coefficient as the boundary layer changes from laminar to turbulent are characteristic of all blunt bodies and may be explained by examination of the energy properties of the laminar and turbulent boundary layers of Fig. 197. For comparison let these layers be of the same thickness and have the same undisturbed velocity V. It is evident from the velocity profiles that the turbulent layer possesses greater kinetic energy than the laminar one; this kinetic energy allows the flow to continue further around the sphere before friction destroys this energy, bringing the fluid to rest and causing separation. The increased energy of the turbulent boundary layer thus brings about the

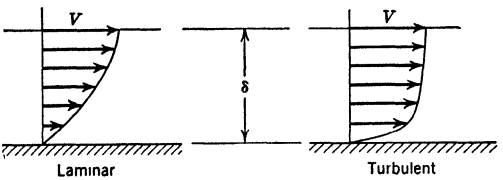


FIG. 197. Velocity Profiles in Boundary Layers.

shift in separation point, the decrease in the width of the wake, and consequent decrease in drag coefficient.

The change from laminar to turbulent boundary layer on a flat plate has been seen (Art. 76) to occur at a critical Reynolds number dependent upon the turbulence of the approaching fluid. This also occurs with a sphere, and with increased turbulence in the approaching flow the sudden drop in the drag coefficient curve occurs at a lower Reynolds number. Thus, a sphere may be used as a relative measure of turbulence by noting the Reynolds number at which a drag coefficient of 0.30 (see Fig. 196) is obtained.

The change from laminar to turbulent boundary layer has also been seen (Art. 76) to occur (for the same initial turbulence) at a fixed distance from the leading edge of a flat plate (or after a fixed length of boundary layer) for given flow conditions (V, ρ, and μ). Applying this fact in a qualitative way to elongated bodies (e.g., ellipsoids with the major axes in the direction of flow), it may be concluded that breakdown of the laminar boundary layer will occur at a lower Reynolds number than 300,000, and conversely that ellipsoids with the major axis normal to the flow will have breakdown of the laminar layer

and decrease of the drag coefficient at Reynolds numbers greater than 300,000. This trend is borne out by experiments but cannot be carried to extremes. The limit of ellipsoids with major axis normal to the flow is one of zero minor axis, i.e., a thin circular disk. The drag coefficient of such a disk shows practically no variation with the Reynolds number since the separation point is fixed at the edge of the disk and cannot shift from this point, regardless of the condition of the boundary layer. Thus, the width of the wake remains constant, as does the drag coefficient also. This thought may be usefully generalized and applied to all brusque or very rough objects in a fluid flow; experiment indicates that such objects have drag coefficients which vary little with the Reynolds number.[11]

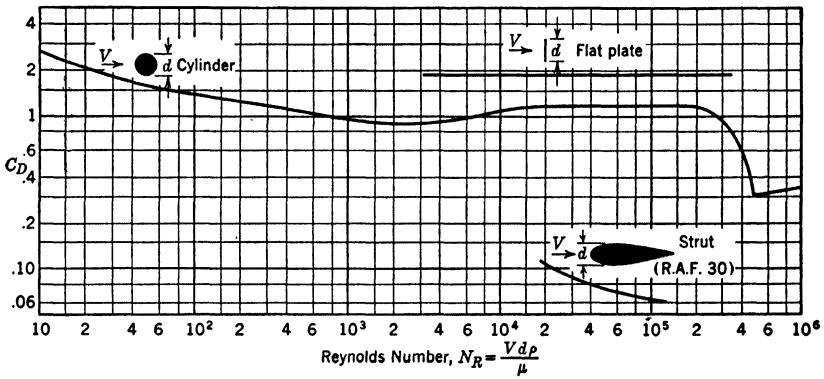


FIG. 198. Drag Coefficients for Circular Cylinders, Flat Plates, and Streamlined Struts of Infinite Length.[12]

The drag coefficients of circular cylinders placed normal to the flow show characteristics similar to those of spheres. The coefficients shown in Fig. 198 are for infinitely long cylinders. The drag coefficients of streamlined struts [13] and flat plates of infinite length are also shown for comparison. The total drags of the flat plate and cylinder contain negligible frictional drag at ordinary velocities, whereas the streamlined strut, because of its small turbulent wake, possesses little

[11] Cf. relation of friction factor, f, and N_R for rough pipes, Fig. 85, and the fact that the minor loss coefficients of pipe flow show little variation with the Reynolds number.

[12] Data from L. Prandtl, "Ergebnisse der aerodynamischen Versuchsanstalt zu Göttingen," Vol. II, R. Oldenbourg, 1923, p. 24, and B. A. Bakhmeteff, "Mechanics of Fluids," Part II, Columbia University Press, 1933, p. 44.

[13] The area to be used in the drag equation is the projection of the body on a plane normal to the direction of flow.

profile drag. The curves are typical of those resulting from tests of brusque, blunt, and streamlined objects.

ILLUSTRATIVE PROBLEM

What is the drag force on a 6-in.-diameter smooth sphere when placed in an airstream (60° F, 14.7 lb in.^{2}) having a velocity of 30 mph?

$$V = \frac{30 \times 5280}{3600} = 36.65 \text{ ft/sec}$$

$$N_R = \frac{36.65 \times \frac{6}{12} \times 0.00237}{0.000000375} = 116{,}000$$

From the plot of Fig. 196,

$$C_D = 0.49$$

$$D = 0.49 \times \frac{\pi(\frac{6}{12})^2}{4} \times \frac{0.00237 \times \overline{36.65}^2}{2} = 0.153 \text{ lb}$$

78. Drag at High Velocities. As objects move at increasing speeds through compressible fluid the assumption of constant density is less valid, since higher velocities bring about greater variations of pressure over the object, these pressures in turn causing changes in the density of the fluid. At points of low and high pressure on the surface of the object the fluid is respectively rarefied and compressed. At the stagnation point on the nose of the object, the increased pressure compresses the fluid, creating a zone of dense fluid ahead of the object; the nose of the body thus moves through a fluid of increased density and, of course, encounters increased resistance because of this.

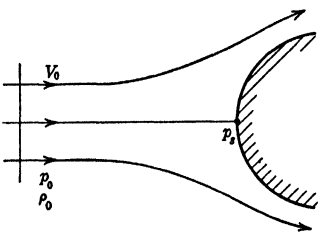


FIG. 199.

An understanding of the effect of high velocity on pressure variation may be gained by calculating the stagnation pressure on the nose of an object placed in a high-velocity flow of compressible fluid (Fig. 199). Applying the Euler equation

$$\frac{dp}{\rho} + VdV = 0$$

and integrating between point 0 in the undisturbed flow and the stagnation point, S.

$$\int_{p_0}^{p_s} \frac{dp}{\rho} = \int_{V_s}^{V_0} VdV$$

At the stagnation point there is no velocity and $V_s = 0$; and if adiabatic compression of the fluid is assumed

$$\frac{p}{\rho^k} = \frac{p_o}{\rho_o^k} \quad \text{or} \quad \rho = \rho_o \left(\frac{p}{p_o}\right)^{\frac{1}{k}}$$

Substituting these values above,

$$\frac{p_o^{\frac{1}{k}}}{\rho_o} \int_{p_o}^{p_s} \frac{dp}{p^{\frac{1}{k}}} = \int_0^{V_o} V dV$$

and integrating,

$$\frac{p_o}{\rho_o} \frac{k}{k-1} \left[\left(\frac{p_s}{p_o}\right)^{\frac{k-1}{k}} - 1 \right] = \frac{V_o^2}{2}$$

Solving for p_s,

$$p_s = p_o \left[1 + \frac{k-1}{p_o k} \frac{\rho_o V_o^2}{2} \right]^{\frac{k}{k-1}}$$

but (Art. 4)

$$c^2 = \frac{k p_o}{\rho_o}$$

and therefore

$$p_s = p_o \left[1 + \frac{k-1}{2} \frac{V_o^2}{c^2} \right]^{\frac{k}{k-1}}$$

Expanding this expression by the binomial theorem and substituting c for $\sqrt{k p_o/\rho_o}$ gives (using the first three terms)

$$p_s = p_o + \tfrac{1}{2}\rho_o V_o^2 \left[1 + \frac{1}{4}\left(\frac{V_o}{c}\right)^2 + \cdots \right]$$

which indicates that the stagnation pressure is always greater than that of an incompressible fluid and depends not only upon p_o, V_o, and ρ_o but also upon the ratio of undisturbed velocity to acoustic velocity, the Mach number, N_M. Thus

$$p_s = p_o + \tfrac{1}{2}\rho_o V_o^2 [1 + \tfrac{1}{4}(N_M)^2 + \cdots]$$

and once again the importance of the Mach number in compressible fluid flow calculations is observed.

The increase in stagnation pressure due to compression of the fluid leads directly to one of the principles of minimizing drag at high

velocities. Obviously, increased pressure on the nose of the object contributes directly to profile drag, and to minimize this contribution the area on which such high pressures act must be reduced to a minimum, resulting in pointed rather than blunt noses for high-speed bodies. At low velocities it has been seen that the shape of the *tail* of the body, in determining the size of the wake, was of primary importance in determining profile drag, whereas the shape of the nose had little effect. At higher velocities, where wakes are fully developed, drag depends little upon the tail of the body and much upon the shape of the nose. The shapes of the airship form and projectile of Fig. 200 are striking examples of the application of these principles.

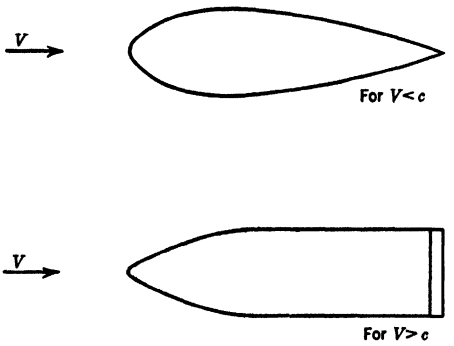


FIG. 200.

The effect of shape upon the drag coefficients of various projectiles at high velocities is shown on Fig. 201. In this velocity range, viscosity has little effect on drag and coefficients will vary primarily with Mach number as was indicated by the dimensional analysis of Art. 75. On the plot may be clearly seen (1) the increased effect of shape of nose on the drag coefficient as the Mach number increases, and (2) the abrupt increase in the coefficient near $N_M = 1$, where the velocity equals the acoustic velocity. Here the effects of compressibility become pronounced and the nature of the flow changes radically. For a typical air foil, used as a wing or propeller blade element, the sudden increase of drag coefficient occurs before $N_M = 1$; i.e., the effects of compressibility are felt before the foil reaches the acoustic velocity. This condition arises from the fact that local velocities at certain points on an airfoil are always greater than the velocity of the foil, and acoustic velocities and serious compressibility effects occur at these points before the foil itself attains the acoustic velocity.

When bodies travel through a fluid at supersonic ($V > c$) speeds a new physical condition arises, which completely changes the nature of the flow. To investigate this condition briefly, consider the projectile of Fig. 202, moving at a supersonic speed, V, and let it occupy the positions 1, 2, 3, and 4, at times t_1, t_2, t_3, and t_4. At time t_1 the nose of the projectile disturbs the fluid at point 1, and this disturbance

progresses through the fluid as a spherical wave with a celerity of propagation, c. After a time $(t_4 - t_1)$ has elapsed, the radius of the spherical wave is $c(t_4 - t_1)$. In this same time, however, the projectile has moved to point 4; therefore

$$t_4 - t_1 = \frac{l_1}{V}$$

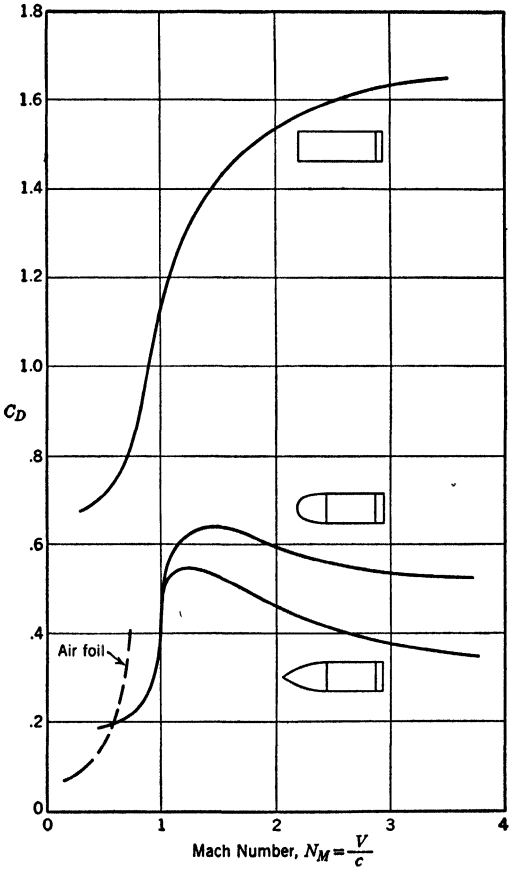


FIG. 201. Drag Coefficients for Artillery Projectiles.[14]

and the radius of the sphere (by substitution) is cl_1/V. Similarly the disturbances which started at points 2 and 3 have (when the projectile reaches point 4) radii of cl_2/V and cl_1/V, respectively. Obviously a

[14] F. R. W. Hunt, in *The Mechanical Properties of Fluids*, p. 341, Blackie and Sons, 1925.

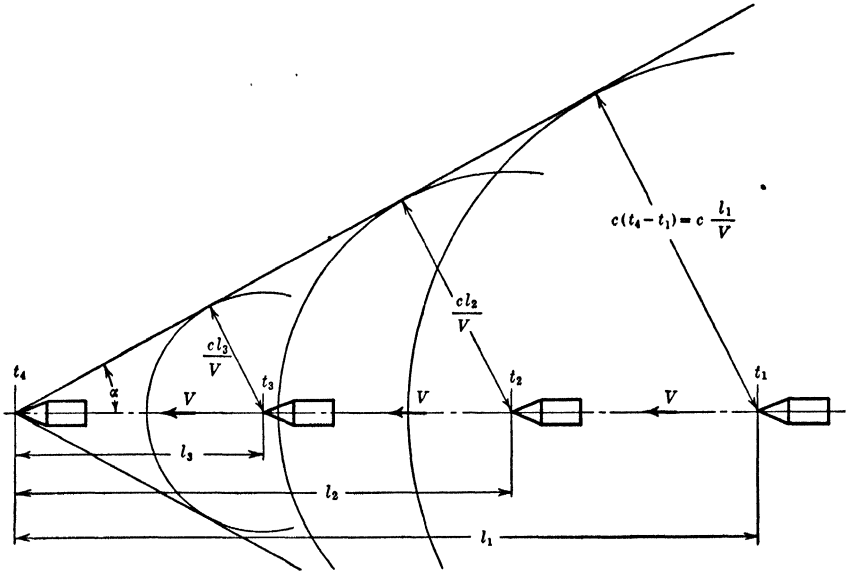
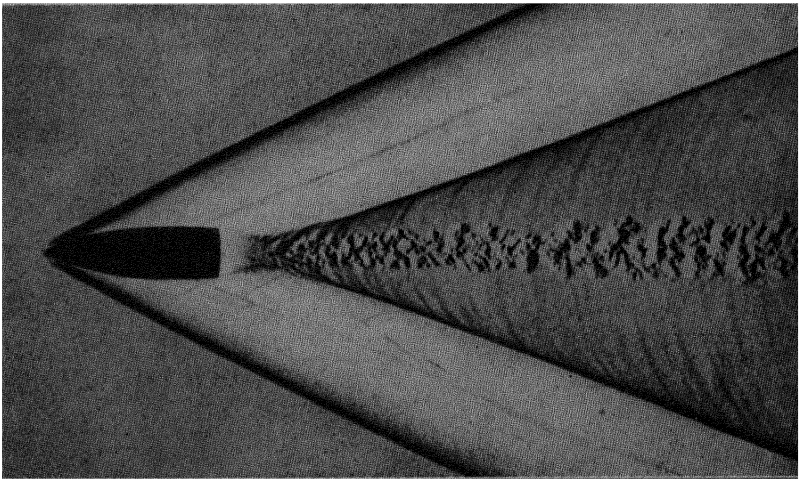


FIG. 202.



C. Cranz

FIG. 203. Small Bore Bullet in Flight.[15]

[15] From C. Cranz, *Lehrbuch der Ballistik*, Vol. I, B. G. Teubner, Leipzig, 1917.

surface tangent to these spherical waves is a conical one with its apex at the nose of the projectile, and such a surface represents the line of advance of the aggregation of pressure disturbances; it is a wave front, or a "shock wave." The "Mach angle," α, may be seen from the figure to be given by

$$\alpha = \sin^{-1} \frac{c}{V}$$

Since this angle depends only on c and V, the velocity of projectiles may be obtained from photographs of the wave front by measuring the Mach angle. A typical photograph of the wave front caused by a rifle bullet is shown in Fig. 203.

79. Lift by Change of Momentum. The lift force on an unsymmetrical body has been seen to arise from pressure differences caused by velocity variations over the surface of the body, but this force may also be associated with the change of fluid momentum caused by the body. If about the foil of Fig. 204 a rectangle is drawn in such a way

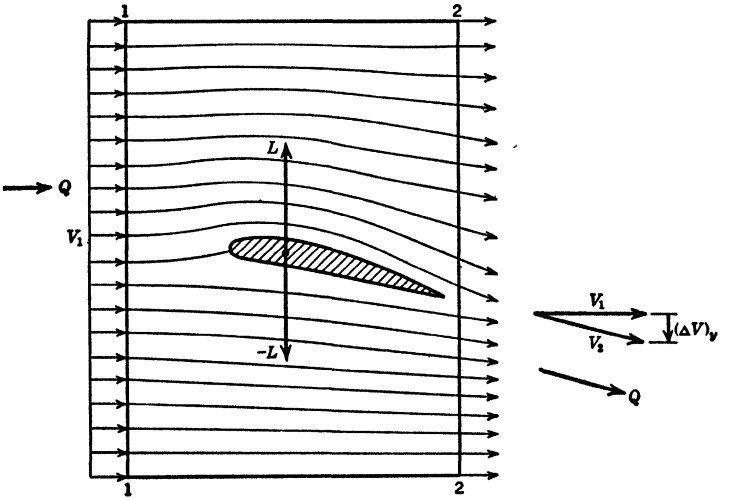


FIG. 204.

that the velocity, V_1, entering the left-hand side of the rectangle is horizontal and the upper and lower boundaries are streamlines, it is evident at once that the flow Q which enters the rectangle horizontally at the left is deflected downward, leaving the rectangle with an average velocity V_2. Since there is a continual change in the vertical momentum of the fluid within the rectangle, a force must be continually

exerted vertically downward upon this fluid to bring about this change. This force cannot come from the pressure difference between top and bottom of the rectangle since this difference is canceled by the difference in elevation of these boundaries. The force must, therefore, be that exerted vertically downward by the foil on the fluid, the equal and opposite of the lift force. From the impulse-momentum law

$$-L = \frac{Qw}{g}(\Delta V)_y$$

or

$$L = \frac{Qw}{g}(-\Delta V)_y$$

thus giving a physical picture of the relation of momentum change to lift force.

Such an equation is of some interest in the light of previous applications of the impulse-momentum law and may serve as an exposition of principles, but to use it for lift calculations is obviously impossible; the size of the rectangle is unknown, thus preventing the calculation of Q, and, with unknown magnitudes and directions of velocities at section 2, ΔV is also incalculable.

80. Circulation Theory of Lift. Although the foregoing studies of pressure variation and momentum change have contributed to an understanding of lift phenomena, a more comprehensive knowledge may be had by applying the principles of circulation.[16] This was first done by Kutta (1902) and Joukowski (1906), whose equations were written for the forces on a body of any shape and whose results were, therefore, entirely general. Because of the mathematical ability required to follow their analysis it will not be included here, but the physical significance of the (Kutta-Joukowski) theorem may be seen by a simple application suggested by Professor Bakhmeteff.[17]

The foil of Fig. 205 is a flat plate of chord c and infinite length from which a section of 1-ft length is to be considered. When the plate is placed in a rectilinear flow (Fig. 205*a*) of velocity V with its axis aligned with the flow, there is obviously no lift force since the velocities and pressures are the same on both sides of the plate.

[16] The student should restudy Art. 24.

[17] B. A. Bakhmeteff, *Mechanics of Fluids*, Part II, p. 70, Columbia University Press, 1933.

Now about the plate assume a clockwise circulatory flow (Fig. 205*b*) having a circulation Γ given by

$$2cv$$

Traversing a closed curve *adjacent to the plate* in a clockwise direction, the length of curve is $2c$ so that the average velocity along the curve must be v, if the product of these quantities is to give the above circulation. This means that with the circulatory flow there is a velocity v to the right along the top of the plate and the same velocity v to the

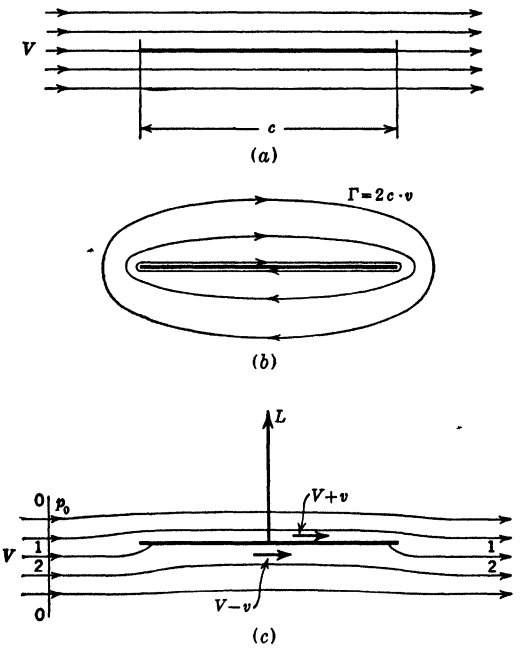


FIG. 205.

left along the bottom. Since there is no velocity difference there can be no pressure difference, and hence no lift force is exerted on the plate.

Now, superpose the two flows, and the flow picture of Fig. 205*c* results. The circulatory flow has bent the rectilinear flow upward at the leading edge of the plate and downward at the trailing edge, yet the effect on the rectilinear flow at a distance from the plate is negligible because of the small velocities induced by a vortex at great distances from its center. The circulatory motion has the same direction as the rectilinear motion on the top of the plate, but opposes it along the bottom. Thus, when the two flows are superposed the

average velocity along the top of the plate becomes $(V + v)$ and that along the bottom $(V - v)$. Now, applying the Bernoulli equation along streamtube 1–1 between O and the top of the plate and along streamtube 2–2 between O and the bottom of the plate, letting p_T and p_B be the average pressures over the top and bottom respectively.

$$p_o + \tfrac{1}{2}\rho V^2 = p_T + \tfrac{1}{2}\rho(V + v)^2$$

$$p_o + \tfrac{1}{2}\rho V^2 = p_B + \tfrac{1}{2}\rho(V - v)^2$$

Equating these,

$$p_B - p_T = \tfrac{1}{2}\rho[(V + v)^2 - (V - v)^2]$$

Simplifying,

$$p_B - p_T = \tfrac{1}{2}\rho[4Vv]$$

But the lift, L, on a section of 1-ft length is given by

$$L = (p_B - p_T)\, c$$

Therefore

$$L = \tfrac{1}{2}\rho(4Vv)c = (2vc)\rho V$$

But

$$\Gamma = 2vc$$

and therefore

$$L \text{ (per foot of span)} = \Gamma\rho V$$

which is the Kutta-Joukowski result in its simplest form and indicates clearly that the *combination of velocity and circulation* is essential to the existence of a lift force—if either one of these terms is zero there can be no lift.

Although the foregoing proof is not rigorous owing to the use of certain average velocities and pressures it nevertheless indicates the physical essence of the problem; and in view of the Kutta-Joukowski general treatment it may be applied to airfoils, cylinders, spheres, or bodies of any shape. The result serves to explain certain familiar phenomena in which bodies rotating in a viscous fluid create their own circulation and when exposed to a rectilinear flow are acted upon by a transverse force. Some examples are the force exerted on the rotating cylinders of a "rotorship" and the transverse force which causes a pitched baseball to curve.

81. Origin of Circulation. Although it is not difficult to imagine a rotating body in a viscous fluid inducing its own circulation, to explain the origin of circulation about an airfoil, or an element of a propeller or turbine blade requires knowledge of other principles.

Consider the flow conditions about a typical airfoil as it starts to move. Before motion begins the circulation about the foil is obviously zero (Fig. 206*a*). As motion occurs, the circulation about the foil tends to remain zero and the "potential" flow of Fig. 206*b* tends to be

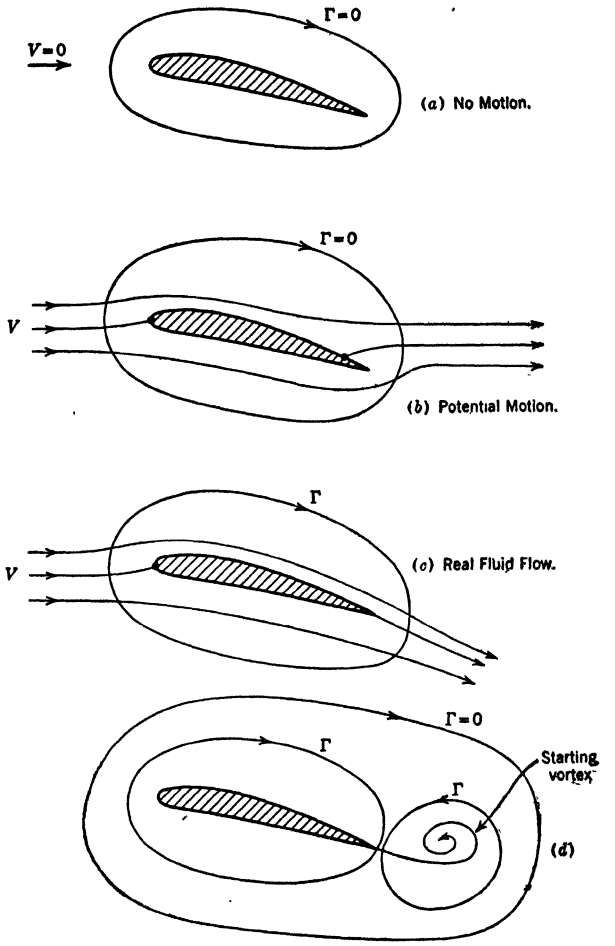


FIG. 206. Development of Circulation about an Airfoil.

set up, but such a flow, which includes a stagnation point near the rear of the foil and flow around its sharp trailing edge, cannot be maintained in a real fluid, because of separation caused by viscosity. This potential flow gives way immediately to the flow of Fig. 206*c*, and in the process a circulation, Γ, develops about the foil, and a vortex, the

"starting vortex" (Fig. 206*d*), is shed from the foil. During the creation of this vortex, however, the circulation around a closed curve including and at some distance from the foil is not changed and must remain zero; thus, from the properties of circulation, the circulation about, or the strength of, the starting vortex must be equal and opposite to that about the foil. The existence of circulation about a foil is, therefore, dependent upon the creation of the starting vortex; since the vortex in turn is dependent upon separation and the viscosity of the fluid it may be observed that *circulation and, therefore, lift result from the existence of fluid viscosity.*

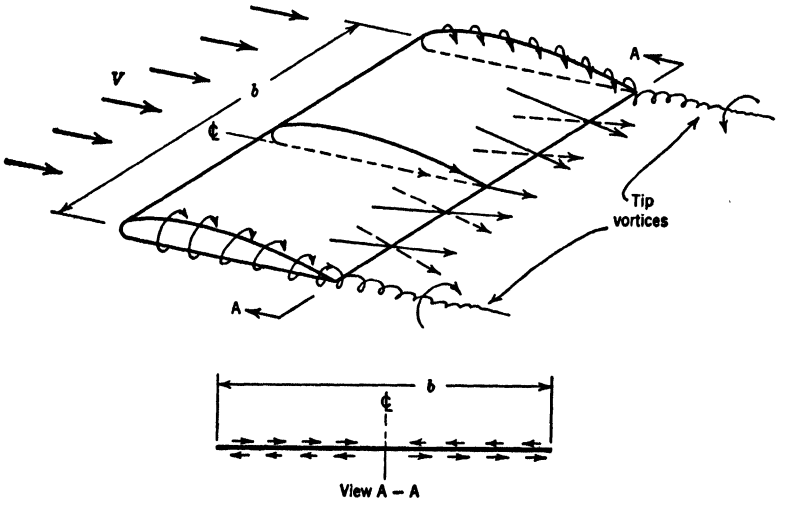


FIG. 207. Airfoil of Finite Length.

82. Foils of Finite Length. When fluid flows about foils of finite length, flow phenomena result which affect both lift and drag of the foil; these phenomena may be understood by further investigation and application of the foregoing circulation theory of lift.

Since pressure on the bottom of an airfoil is greater than that on the top, flow will escape from below the foil at the end and flow toward the top, thus distorting the general flow about the foil, causing fluid to move inward over the top of the foil and outward over the bottom (Fig. 207). As the fluid merges at the trailing edge of the wing, a surface of discontinuity is set up, and flows above and below this surface have components of velocity inward and outward as shown. The tendency for vortices to form from these velocity components is obvious and in fact this surface of discontinuity is a "sheet of vortices."

However, such a vortex sheet is unstable and the rotary motions contained therein combine to form two large vortices trailing from the tips of the foil (Fig. 207); these are called tip vortices and are often visible when an airfoil passes through dust-laden air.

Since the pressure difference between top and bottom of an airfoil must reduce to zero at the tips, it is evident that the lift per unit length of span varies over the span (Fig. 208), being maximum at the center and reducing to zero at the tips. The total lift of the foil is, of course, the total force resulting from this lift diagram. Since lift per unit length of span varies directly with circulation ($L = \Gamma \rho V$), a diagram showing distribution of circulation over the span has the same shape as that of a diagram of lift distribution. The variation of

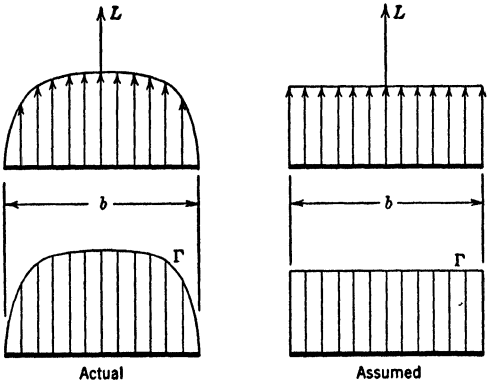


FIG. 208. Distribution of Lift and Circulation over an Airfoil of Finite Length.

lift and circulation over the span of an airfoil cannot, of course, be disregarded in a rigorous treatment of the subject, but such treatment leads to mathematical and physical complexities which are beyond the scope of this volume. A simple physical picture may be obtained, however, from the following analysis in which lift and circulation will be assumed to be distributed uniformly over the span (Fig. 208).

One of the properties of vortices is that their axes can end only at solid boundaries. Since there is no solid boundary at the end of the airfoil, the circulation Γ cannot stop here, but must continue to exist about the axes of the tip vortices (Fig. 209). The axes of the tip vortices extend rearward to the axis of the starting vortex; thus, according to the theory, the axis of the vortex having circulation Γ does not end, but is a closed curve composed of the axes of the airfoil, tip vortices, and starting vortex. In the real fluid the circulation

persists only about the foil and portions of the tip vortices close to the foil; the starting vortex and remainder of the tip vortices are quickly extinguished by viscosity.

The circulations about the tip vortices induce a downward motion in the fluid passing over a foil of finite length and in so doing affect

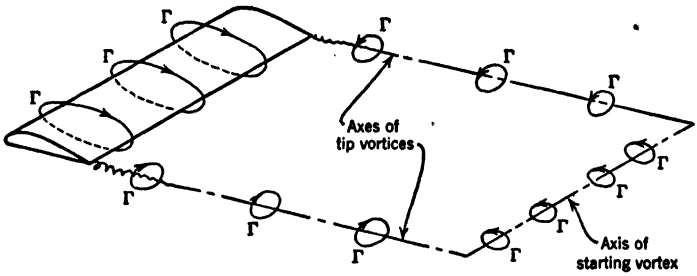


FIG. 209. Circulation about an Airfoil of Finite Length.

both lift and drag by changing the effective angle of attack. The strength of this induced motion will obviously depend upon the proximity of the tip vortices and thus upon the span of the foil or upon the ratio of span to chord, b/c, called the aspect ratio of the foil.

An airfoil of finite span is shown at angle of attack α in the horizontal flow of Fig. 210. The downward (downwash) velocity induced

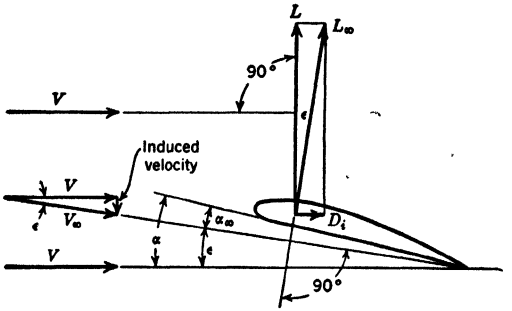


FIG. 210.

near the wing by the tip vortices decreases the angle of attack by a small angle of downwash, ϵ, making the effective angle of attack $(\alpha - \epsilon)$. This effective angle of attack is that for no induced downward velocity or, in other words, it is the angle of attack which would be obtained if the foil had infinite span and aspect ratio. Calling this angle of attack α_∞

$$\alpha_\infty = \alpha - \epsilon \tag{102}$$

Now treating the foil as one of infinite span at an angle of attack α_∞, the lift L_∞ exerted on such a foil is by definition normal to the direction of flow in which it is placed; therefore L_∞ is normal to the effective velocity V_∞, and at an angle ϵ with the vertical. The lift, L, on the foil of finite span is normal to the approaching horizontal velocity V and is the vertical component of L_∞. But L_∞ also has a component in the direction of the original velocity V, a drag force, D_i, called the induced drag because its existence depends upon the downward velocity induced by the tip vortices. Thus, an additional drag force, D_i, must be added to profile and frictional drag in computing the total drag of a body of finite length about which a circulation exists. Calling the sum of frictional and profile drag D_∞, since it is the drag of a foil of infinite span (which has no induced drag), the total drag D of a foil of finite length is given by

$$D = D_\infty + D_i \tag{103}$$

which, by dividing by $A\rho V^2/2$, may be expressed in terms of dimensionless drag coefficients as

$$C_D = C_{D_\infty} + C_{Di} \tag{104}$$

Thus the drag coefficient, C_D, of a body of finite length with circulation is the sum of the profile-frictional drag coefficient C_{D_∞} and the induced drag coefficient, C_{D_i}.

From the foregoing statements and Fig. 210, it is evident that induced drag D_i is related to lift L, angle α, and aspect ratio b/c; the equations relating these variables are of great practical importance. Since ϵ is small

$$L = L_\infty, \quad V = V_\infty, \quad D_i = L\epsilon$$

If the distribution of lift over a wing of finite span is taken [18] to be a half ellipse (see Fig. 208), it may be shown that

$$\epsilon = \frac{C_L}{\left(\frac{b}{c}\right)\pi} \tag{105}$$

and substituting this value and $L = C_L A(\rho V^2/2)$ in the equation for D_i

$$D_i = L\epsilon = \frac{C_L \rho A V^2}{2\left(\frac{b}{c}\right)\pi} \tag{106}$$

[18] An assumption which gives minimum induced drag and conforms well with fact.

Now, expressing D_i in terms of the induced drag coefficient C_{Di},

$$D_i = C_{Di} A \frac{\rho V^2}{2}$$

and substituting this value in equation 106 there results

$$C_{Di} = \frac{C_L^2}{\left(\frac{b}{c}\right)\pi} \qquad (107)$$

which relates lift and induced drag through their dimensionless coefficients and shows that induced drag is inversely proportional to aspect ratio, becoming zero at infinite aspect ratio (infinite span) and increasing as aspect ratio and span decrease—thus offering mathematical proof of the foregoing statements on the effect of span, aspect ratio, and proximity of tip vortices on induced downward velocity and induced drag.

When the foregoing expressions for ϵ and C_{Di} are substituted in equations 102 and 104, respectively, there result

$$\alpha = \alpha_\infty + \frac{C_L}{\left(\frac{b}{c}\right)\pi} \qquad (108)$$

and

$$C_D = C_{D_\infty} + \frac{C_L^2}{\left(\frac{b}{c}\right)\pi} \qquad (109)$$

With these equations airfoil data obtained at one aspect ratio may be converted into corresponding conditions at infinite aspect ratio, and these data in turn reconverted to foils of any aspect ratio; thus, extensive testing of the same airfoil at various aspect ratios becomes unnecessary.

Illustrated Problem

A rectangular airfoil of 6-ft chord and 36-ft span has a drag coefficient of 0.0543 and lift coefficient of 0.960 at an angle of attack of 7.2°. What are the corresponding lift and drag coefficients and angle of attack for a similar wing of aspect ratio 8?

For aspect ratio 8: $C_L = 0.960$ (No change in lift coefficient.)

Assuming semi-elliptical lift distribution,

$$C_{Di} = \frac{(0.960)^2}{\pi\left(\frac{36}{6}\right)} = 0.0489$$

$$C_{D_\infty} = 0.0543 - 0.0489 = 0.0054$$

For aspect ratio 8:

$$C_D = 0.0054 + \frac{(0.960)^2}{\pi \times 8} = 0.0421$$

$$\epsilon = \frac{0.960}{\pi(\frac{3}{8})} = 0.0509 \text{ radian} = 2.9°$$

$$\alpha_\infty = 7.2 - 2.9 = 4.3°$$

For aspect ratio 8:

$$\alpha = 4.3 + \frac{0.960}{\pi \times 8}\left(\frac{360}{2\pi}\right) = 6.5°$$

83. Lift and Drag Diagrams. The relation between lift and induced drag coefficients suggests plotting lift coefficient against drag

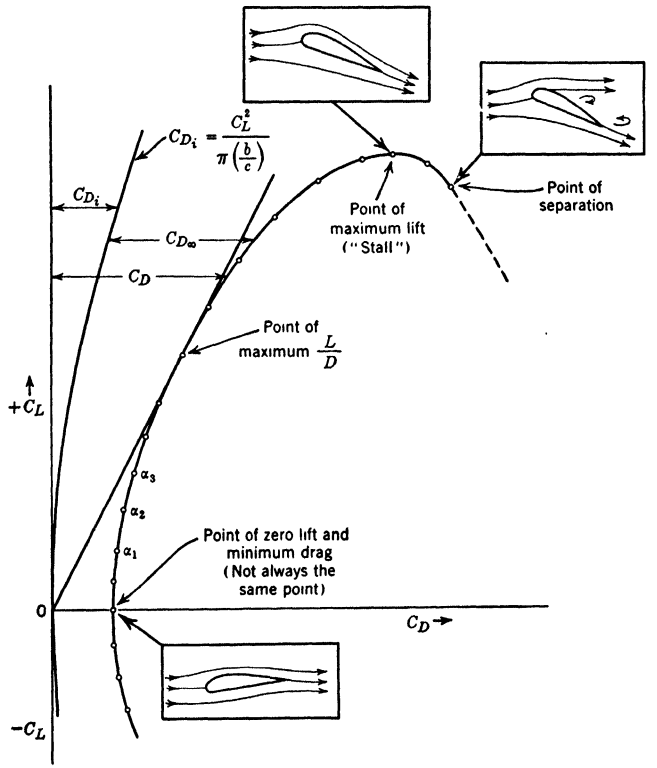
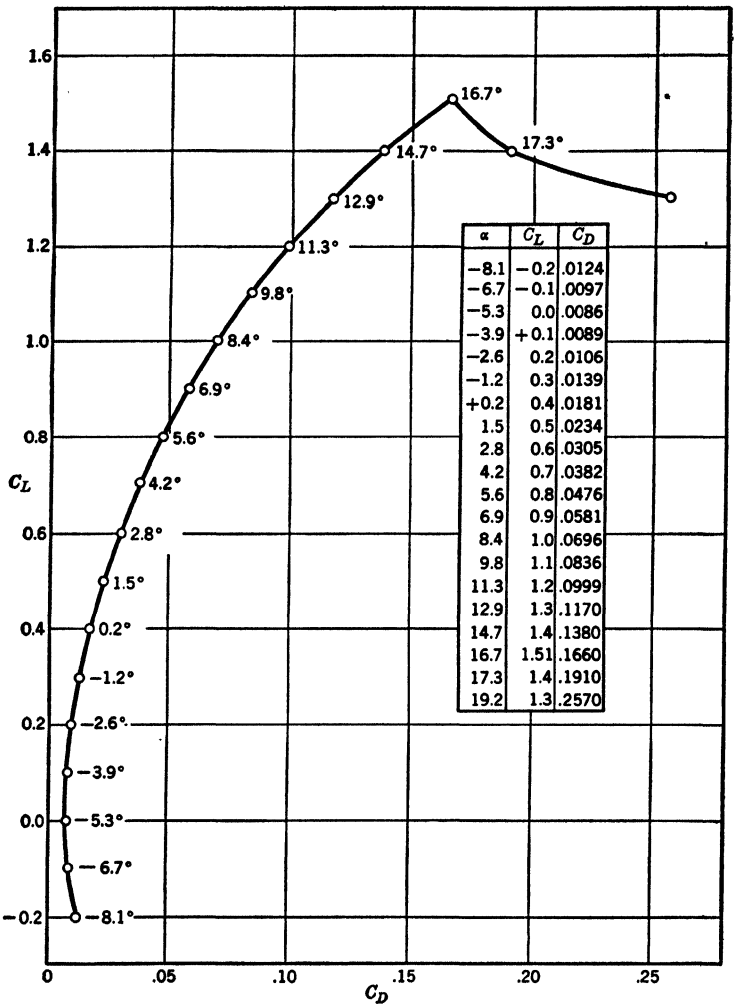


FIG. 211. Polar Diagram for a Typical Airfoil.

coefficient and gives the so-called polar diagram of Fig. 211, which is used extensively in airplane design. On this diagram equation 107 is a parabola passing through the origin and symmetrical about the

C_D axis, the slope of the parabola depending on the aspect ratio. Since the two curves are for foils of the same aspect ratio, the horizontal distance between them is the profile-frictional drag coefficient,



α	C_L	C_D
−8.1	−0.2	.0124
−6.7	−0.1	.0097
−5.3	0.0	.0086
−3.9	+0.1	.0089
−2.6	0.2	.0106
−1.2	0.3	.0139
+0.2	0.4	.0181
1.5	0.5	.0234
2.8	0.6	.0305
4.2	0.7	.0382
5.6	0.8	.0476
6.9	0.9	.0581
8.4	1.0	.0696
9.8	1.1	.0836
11.3	1.2	.0999
12.9	1.3	.1170
14.7	1.4	.1380
16.7	1.51	.1660
17.3	1.4	.1910
19.2	1.3	.2570

FIG. 212. Polar Diagram for 48 ft by 8 ft Clark-Y Airfoil.[19] ($N_R \backsim 6{,}000{,}000$.)

C_{D_∞}; in this way, the polar diagram gives graphical significance to equation 109. But the diagram does much more than this alone:

[19] A. Silverstein, "Scale Effect on Clark-Y Airfoil Characteristics from N.A.C.A. Full-Scale Wind-tunnel Tests," N.A.C.A. Report 502, 1934.

The important ratio of lift to drag is the slope of a straight line drawn between origin and the point for which this ratio is to be found; the maximum value of this ratio is the slope of a straight line tangent to

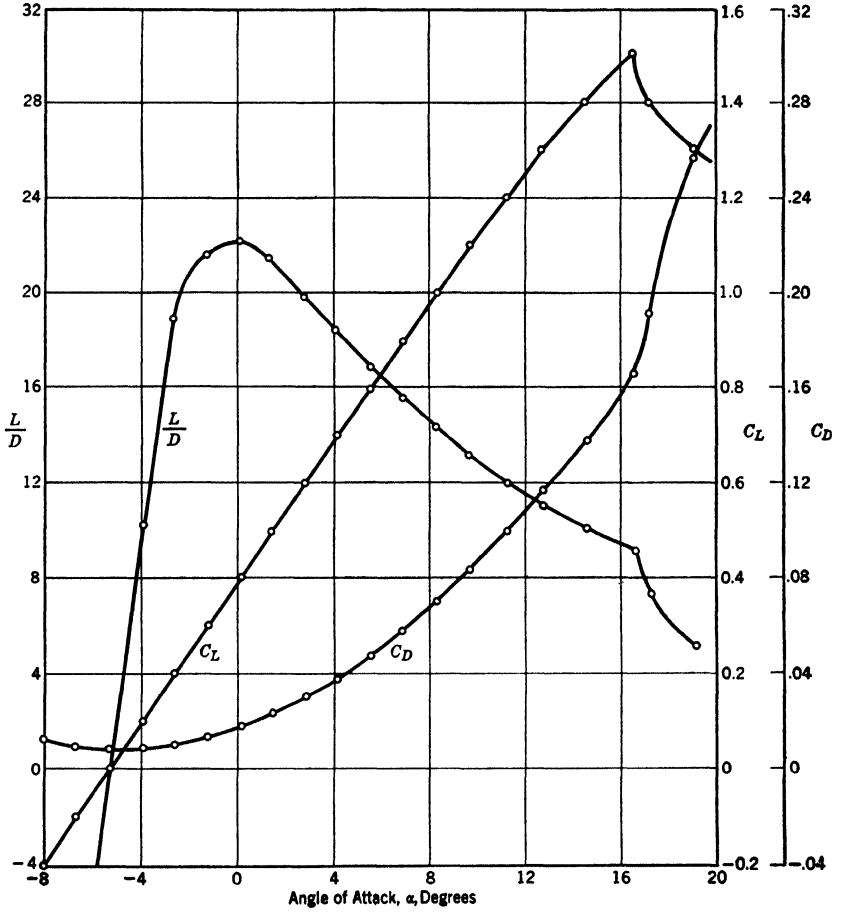


FIG. 213. Lift and Drag Coefficients and L/D Ratio for 48 ft by 8 ft Clark-Y Airfoil.[19] ($N_R \backsim 6{,}000{,}000$).

the curve and passing through the origin; on the diagram are easily seen also the points of zero lift, minimum drag, and the point of maximum lift or "stall," which determines "stalling angle" above which lift no longer continues to increase with angle of attack; the end

[19] See footnote on p. 328.

of the upper solid portion of the curve is the point at which the flow separates from the upper side of the wing, forming a turbulent wake which increases the profile drag and therefore the drag coefficient, accompanied by a large drop in lift and lift coefficient because of increased pressure on the upper side of the wing.

A polar diagram for a Clark-Y airfoil obtained in the N.A.C.A. full-scale wind tunnel is shown in Fig. 212, and another way of presenting the same data in Fig. 213. Because of the *assumption* of semi-elliptical lift distribution made in deriving equations 108 and 109 it is to be expected that these equations must be modified for use in actual practice.

These equations are now written

$$\alpha = \alpha_\infty + \frac{C_L}{\left(\frac{b}{c}\right)\pi}(1 + \tau)$$

and

$$C_D = C_{D_\infty} + \frac{C_L^2}{\left(\frac{b}{c}\right)\pi}(1 + \sigma)$$

in which the τ and σ are correction factors. Since lift distribution varies increasingly from the semi-elliptical one with increasing aspect ratio these correction factors vary with aspect ratio and increase with this ratio. Some typical values for τ and σ for the Clark-Y airfoil are [19]

b/c	4	6	8
τ	0.030	0.051	0.070
σ	0.118	0.176	0.212

The data of Figs. 212 and 213 were obtained at a Reynolds number of about 6,000,000, and from many foregoing statements it should be expected that the data will change with changing Reynolds number. The following trends, which are confirmed by experiment, are of some interest in the light of foregoing principles. With increasing Reynolds number the drag coefficient at zero lift decreases; here the drag coefficient contains predominantly frictional effects and its variation with Reynolds number is similar to that of the flat plate (Fig. 194). With increased turbulence, due either to increased initial turbulence or

[19] See footnote on p. 328.

increased Reynolds number, the maximum lift coefficient increases; in other words, higher angles of attack can be attained without causing separation. Here the energy of the turbulent boundary layer (Fig. 197) delays separation, allowing high-velocity flow to cling to the upper side of the foil, causing lower pressures and greater lift.

BIBLIOGRAPHY

L. PRANDTL and O. G. TIETJENS, *Fundamentals of Hydro- and Aeromechanics*, McGraw-Hill Book Co., 1934.

Applied Hydro- and Aeromechanics, McGraw-Hill Book Co., 1934.

L. PRANDTL, *The Physics of Solids and Fluids*, Part II, Second Edition, Blackie & Son, 1936.

H. GLAUERT, *Aerofoil and Airscrew Theory*, Cambridge University Press, 1930.

E. G. REID, *Applied Wing Theory*, McGraw-Hill Book Co., 1932.

E. A. STALKER, *Principles of Flight*, Roland Press, 1931.

W. F. DURAND, *Aerodynamic Theory*, Julius Springer, Berlin, 1934. Six volumes.

C. V. DRYSDALE and Others, *The Mechanical Properties of Fluids*, Blackie & Son, 1925.

S. GOLDSTEIN, *Modern Developments in Fluid Dynamics*, Vols. I and II, Oxford University Press, 1938.

Reports, Technical Memoranda, and Technical Notes of the National Advisory Committee for Aeronautics (N.A.C.A.).

PROBLEMS

484. A rectangular airfoil of 40-ft span and 6-ft chord has lift and drag coefficients of 0.5 and 0.04, respectively, when at an angle of attack of 6°. Calculate the drag and horsepower necessary to drive this airfoil at 50, 100, and 150 mph through still air (40° F and 13.5 lb/in.^{2} abs). What lifts are obtained at these speeds?

485. A rectangular airfoil of 30-ft span and 6-ft chord moves at a certain angle of attack through still air at 150 mph. Calculate the lift and drag, and the horsepower necessary to drive the airfoil at this speed through air of (*a*) 14.7 lb/in.^{2} and 60° F and (*b*) 11.5 lb/in.^{2} and 0° F. $C_D = 0.035$, $C_L = 0.46$.

486. Calculate the speed and horsepower required for condition (*b*) of the previous problem to obtain the lift of condition (*a*).

487. The drag coefficient of a circular disk when placed normal to the flow is 1.12. Calculate the force and horsepower necessary to drive a 12-in. disk through (*a*) air ($w = 0.0763$ lb/ft^3) and (*b*) water at 30 mph.

488. The drag coefficient of an airship is 0.04 when the area used in the drag formula is the $\frac{2}{3}$ power of the volume. Calculate the drag of an airship of this type having a volume of 500,000 ft^3 when moving at 60 mph through still air ($w = 0.0763$ lb/ft^3).

489. A wing model of 5-in. chord and 2.5-ft span is tested at a certain angle of attack in a wind tunnel at 60 mph using air at 14.5 lb/in.^{2} abs and 70° F. The lift and drag are found to be 6.0 lb and 0.4 lb, respectively. Calculate the lift and drag coefficient for the wing at this angle of attack.

490. An airplane and an artillery projectile move through still air (14.0 lb/in.^{2}, 40° F), the former at 350 mph, the latter at 1500 ft/sec. Calculate their Mach numbers.

491. A cylindrical body of 6-in. diameter moves through still air (14.7 lb/in.^{2} abs and 60° F) at 500 mph. At what velocity must a geometrically similar body move through still air (13.0 lb/in.^{2} and 0° F) if the two flows are to be completely similar dynamically? What must be the diameter of this body?

492. A smooth plate 10 ft long and 3 ft wide moves through still air (60° F, 14.7 lb/in.^{2} abs) at 5 ft/sec. Assuming the boundary layer to be laminar, calculate (*a*) the thickness of the layer at 2, 4, 6, 8, and 10 ft from the leading edge of the plate; (*b*) the constants α and β; (*c*) the stress, τ_o at the above points; (*d*) the coefficient c_f at the above points; (*e*) the total drag force on one side of the plate.

493. What is the drag on one side of the plate of the preceding problem if the boundary layer is turbulent?

494. A flat-bottomed scow having a 150 ft by 20 ft bottom is towed through still water (60° F) at 10 mph. What is the frictional drag force exerted by the water on the bottom of the scow? How long is the laminar portion of the boundary layer, using the critical N_R of Fig. 194? What is the thickness of this layer at the point at which it becomes turbulent? What is the thickness of the boundary layer at the rear end of the bottom of the scow?

495. A streamlined train 400 ft long is to travel at 90 mph. Treating the sides and top of the train as a smooth flat plate 30 ft wide, calculate the total drag on these surfaces when the train moves through air at 60° F and 14.7 lb/in.^{2} Calculate the length of the laminar boundary layer and the thickness of this layer where it becomes turbulent. What is the thickness of the boundary layer at the rear end of the train? What horsepower must be expended to overcome this resistance?

496. Calculate the drag of a smooth sphere of 12-in. diameter in a stream of standard air at Reynolds numbers of 1, 10, 100, and 1000.

497. Calculate the drag of a smooth sphere of 20-in. diameter when placed in an airstream (60° F, 14.7 lb/in.^{2} abs) if the velocity is (*a*) 20 ft/sec, (*b*) 28 ft/sec.

498. At what velocity will the sphere of the preceding problem attain the same drag which it had at a velocity of 20 ft/sec?

499. Estimate the drag on a model of an N.P.L. airship hull of 6-in. diameter which is to be tested in a wind tunnel (14.7 lb/in.^{2}, 60° F) at 60 mph.

500. A sphere of 10-in. diameter is tested in a wind tunnel (14.7 lb/in.^{2}, 60° F) at 80 mph. At what speed must a 2-in. sphere be towed in water (68° F) for these spheres to have the same drag coefficients? What are the drag forces on these two spheres?

501. A sphere 1 ft in diameter is towed through water (68° F) at 5 mph. What size sphere has the same drag coefficient in an airstream (60° F, 14.7 lb/in.^{2}) having a velocity of 60 mph? Calculate the drags of these spheres.

502. What is the stagnation (gage) pressure of an air stream (14.70 lb/in.^{2} abs, 60° F) of velocity 200, 400, and 600 mph considering and neglecting compressibility?

503. At what velocity of air (14.7 lb/in.^{2}, 60° F) will an error of 1 per cent be caused in the dynamic pressure by neglecting compressibility?

504. If the pointed artillery projectile of Fig. 201 is 12 in. in diameter and is to travel at 2000 ft/sec through air (60° F, 14.7 lb/in.^{2}), what force is necessary to propel it?

505. What is the drag of the blunt-nosed projectile of Fig. 201 (if its diameter is 3 in.) when it travels at (*a*) 700 mph, (*b*) 800 mph through air at 60° F and 14.7 lb/in.^{2}?

506. Calculate the Mach angle for a bullet moving at 2000 ft/sec through air of 14.5 lb/in.^{2} and 100° F.

507. If the Mach angle of the photograph of Fig. 203 is 30° and the bullet is moving through air at 14.0 lb/in.^{2} and 50° F, calculate the speed of the bullet.

508. An airfoil of 5-ft chord and 30-ft span develops a lift of 3000 lb when moving through air of specific weight 0.0763 lb/ft^3 at a velocity of 100 mph. What is the average circulation about the wing?

509. The circulation about a wing of 40-ft span and 6-ft chord when moving at 150 mph is 700 ft^2/sec. Calculate the lift on the wing if it moves through still air at 14.7 lb/in.^{2} and 60° F.

510. Derive a general expression for lift coefficient in terms of circulation.

511. If Γ is the average circulation about a wing per foot of span, calculate the circulation about the wing at midpoint and quarter-points of the span, assuming a semi-elliptical lift distribution.

512. A model wing of 5-in. chord and 3-ft span is tested in a wind tunnel (60° F, 14.5 lb/in.^{2}) at 60 mph, and the lift and drag are found to be 9.00 and 0.460 lb, respectively, at an angle of attack of 6.7°. Assuming a semi-elliptical lift distribution, calculate: (*a*) the lift and drag coefficients; (*b*) C_{D_i}; (*c*) C_{D_∞}; (*d*) the corresponding angle of attack for an airfoil of infinite span; (*e*) the corresponding angle of attack for a foil of this type with aspect ratio 5; (*f*) the lift and drag coefficients at this aspect ratio.

513. An airfoil of infinite span has lift and drag coefficients of 1.31 and 0.062, respectively, at an angle of attack of 7.3°. Assuming semi-elliptical lift distribution, what will be the corresponding coefficients for a foil of the same cross section but aspect ratio 6? What will be the corresponding angle of attack?

514. From Fig. 212, calculate the lift and drag coefficients for a Clark-Y airfoil of aspect ratio 8, and plot the polar diagram for this airfoil.

515. The Clark-Y airfoil of Figs. 212 and 213 is to move at 180 mph through air at 60° F and 14.7 lb/in.^{2} Determine the minimum drag, drag at optimum L/D, and drag at point of maximum lift. Calculate the lift at these points and the horsepower that must be expended to obtain these lifts.

APPENDIX I

DESCRIPTION AND DIMENSIONS OF SYMBOLS

SYMBOL	DESCRIPTION	FT-LB-SEC DIMENSIONS
A, a	Area	ft^2
a	Linear acceleration	ft/sec^2
b	Breadths; lengths normal to flow; span of an airfoil; length of weir; width of open channel, etc.	ft
C, C_c, C_D, C_f, C_I, C_k, C_L, C_v	Various dimensionless coefficients	
C	Chezy coefficient	$ft^{\frac{1}{2}}/sec$
c	Acoustic velocity	ft/sec
c	Chord of an airfoil	ft
D, D_P, D_f, D_i	Drag forces	lb
d	Diameter; depth of flow in open channels	ft
d_c	Critical depth	ft
E	Modulus of elasticity	lb/ft^2
E	Various unit energies	ft lb/lb
E_H	Unit heat energy	Btu/lb
e	Height of roughness	ft
F	Force	lb
f	Darcy friction factor	
G	Weight (rate of) flow	lb/sec
g	Acceleration due to gravity	ft/sec^2
H	Enthalpy	Btu/lb
H	Head on weirs	ft
h	Vertical distance, head	ft
h_L	Lost head	ft
I	Moment of inertia	ft^4
I	Unit internal energy	ft lb/lb
K	Various dimensional coefficients	
K_L	Various dimensionless loss coefficients	
k	Adiabatic constant	
L	Lift force	lb
l	Length; distance along flow; mixing length	ft
M	Mass	lb sec^2/ft
M	Expression for graphical solution of hydraulic jump	ft^2
m	Molecular weight	
N	Revolutionary speed	rps

DESCRIPTION AND DIMENSIONS OF SYMBOLS—*Continued*

SYMBOL	DESCRIPTION	FT-LB-SEC DIMENSIONS
N_C, N_F, N_M, N_N, N_R, N_W	Various dimensionless numbers (force ratios)	
n	Distance normal to direction of flow	ft
P	Power	ft lb/sec
P	Weir height	ft
p	Intensity of pressure	lb/ft^2
Q	Rate of flow	ft^3/sec
q	Rate of flow per foot width (in rectangular channels)	ft^2/sec
R	Engineering gas constant	ft/° F. abs
R	Pipe radius; hydraulic radius	ft
r	Radius	ft
S	Specific gravity	
S	Slope	
s_t	Tension stress	lb/ft^2
T	Absolute temperature	°F. abs
T	Surface tension	lb/ft
T	Torque	ft lb
t	Time	sec
t	Thickness	ft
t	Temperature	°F.
u	Velocity relative to a moving body	ft/sec
V	Volume	ft^3
V	Average velocity, Q/A	ft/sec
v	Specific volume	ft^3/lb
v	Velocity	ft/sec
W	Weight	lb
w	Specific weight; weight density	lb/ft^3
Y	Expansion factor	
Z	A gas constant (equation 24)	(°F. abs)$^{\frac{1}{2}}$/sec
z	Height above datum	ft
α	Angle of attack of an airfoil; various other angles	radians
Γ	Circulation	ft^2/sec
δ	Thickness of laminar film; thickness of boundary layer	ft
η	Efficiency	radians
μ	Coefficient of viscosity	lb sec/ft^2
ν	Kinematic viscosity	ft^2/sec
ρ	Mass density	lb sec^2/ft^4
τ	Shear stress	lb/ft^2
ω	Angular velocity	radians/sec

APPENDIX II

Specific Weight and Density of Water[1]

Temperature, °F	Specific weight,[2] w, lb/ft^3	Density, slugs/ft^3 or lb sec^2/ft^4
32	62.42	1.940
39.2	62.45 (max.)	1.941 (max.)
50	62.42	1.940
68	62.32	1.937
86	62.16	1.932
104	61.96	1.926
122	61.71	1.918
140	61.39	1.908
158	61.07	1.898
176	60.68	1.886
194	60.26	1.873
212	59.84	1.860

[1] *Handbook of Engineering Fundamentals.*

[2] Taking acceleration due to gravity to be 32.174 ft/sec^2.

APPENDIX III

VELOCITY OF A PRESSURE WAVE THROUGH A FLUID

Consider fluid at rest in a rigid pipe fitted with a piston at one end (Fig. 214). This piston is suddenly advanced at a velocity v for a time dt and sends a pressure disturbance along the pipe at a velocity c.

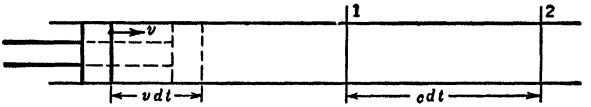


FIG. 214.

While the piston moves a distance vdt the pressure wave will cover a distance cdt. Through any time dt, since no mass has been destroyed, the fluid displaced by the piston must be equal to the gain in the mass of fluid between sections 1 and 2 due to increased density. Therefore

$$A\rho vdt = cdtAd\rho$$

whence

$$c = v\frac{\rho}{d\rho} \tag{1}$$

But, according to the law of impulse and momentum, the force exerted on the mass multiplied by the time the force acts is equal to the change of momentum accomplished:

Force $= Adp$

Time $= dt$

Mass $= cdtA\rho$

Velocity change $= v$

thus

$$Adpdt = cdtA\rho v$$

or

$$c = \frac{dp}{\rho v} \tag{2}$$

Multiplying equations 1 and 2,

$$c^2 = \frac{dp}{d\rho} \tag{3}$$

But

$$E = -\frac{dp}{\frac{dV}{V}} = \frac{dp}{\frac{d\rho}{\rho}}$$

Therefore

$$\frac{dp}{d\rho} = \frac{E}{\rho}$$

and substituting in equation 3 and solving for c,

$$c = \sqrt{\frac{E}{\rho}}$$

APPENDIX IV[1]

Viscosity of Liquids

($\mu \times 10^5$ lb sec/ft^2)

Temperature °F	Water	Carbon Tetrachloride	Benzene	Linseed Oil	Ethyl Alcohol	Turpentine
32	3.75	2.825	1.892	.....	3.71	4.70
50	2.73	2.38	1.594	.....	3.06	3.73
68	2.10	2.035	1.367	.....	2.51	3.11
86	1.667	1.772	1.185	69.2	2.10	2.68
104	1.372	1.56	1.040	.....	1.744	2.24
122	1.148	1.384	0.928	36.8	1.468	1.935
140	0.980	.....	.....	.....	1.238	.....
158	0.850	1.116	0.750	.....	1.053	1.52
176	0.746	.....	.....	.....	.....	.....
194	0.662	.....	.....	14.84	.....	.....
212	0.593	.....	.....	.....	.....	.....

Temperature °F	Mercury	Castor Oil	Glycerine	Olive Oil
32	3.475	....	....	.....
37.0	.....	....	8830	.....
41	.....	7860	....	.....
50	.....	5060	....	288.3
57.7	.....	....	2900	.....
59	.....	3166	....	224.5
68	3.235	2060	....	175.5
68.5	.....	....	1735	.....
77	.....	1362	....	.....
79.7	.....	....	1032	.....
86	.....	943	....	112.8
93.2	3.083	....	....	.....
95	.....	661	....	.....
104	.....	483	....	75.9
122	.....	....	....	54.0
158	.....	....	....	25.9
208.4	2.64	....	....	.....

[1] All physical data from *Smithsonian Physical Tables*, Eighth Edition, Smithsonian Insitution, 1933.

Viscosity of Gases[2]

($\mu \times 10^5$ in lb sec/ft^2)

Temperature, °F	Hydrogen	Oxygen	Air	Nitrogen	Carbon Dioxide
0	0.01726	0.0372	0.0342	0.0328	0.02775
100	.01982	.04385	.0402	.0383	.0336
200	.0222	.0500	.0457	.0435	.0392
300	.02435	.0555	.0506	.04805	.0443
400	.0264	.0608	.0554	.0524	.04915
500	.0282	.0656	.0598	.0565	.05385

[2] Calculated from Sutherland's formula.

$$\mu = \mu_o \left(\frac{273 + C}{T + C}\right) \left(\frac{T}{273}\right)^{\frac{3}{2}}$$

in which μ_o = viscosity at 0° C.
T = absolute temperature ° C.
C = a constant.

	Hydrogen	Oxygen	Air	Nitrogen	Carbon Dioxide
μ_o	0.01812	0.0395	0.0362	0.0347	0.0297
C	72	131	124	110	240

APPENDIX V

CAVITATION

The phenomenon of cavitation has assumed increased importance in the design and operation of high-speed hydraulic machinery such as turbines, pumps, and ship propellers. Briefly, it is characterized by local reduction of pressure to the vapor pressure, formation of a cavity within the flowing fluid, rapid pitting, and destruction of the

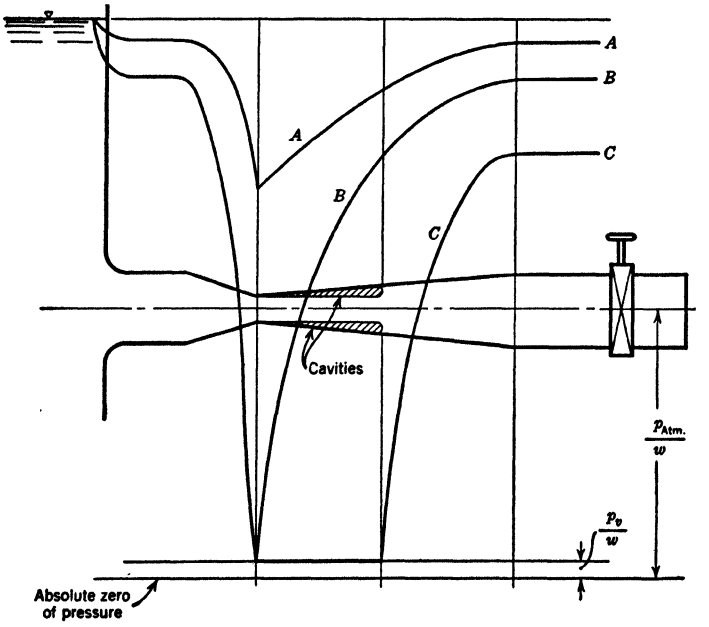


FIG. 215.

parts of the machine in contact with the flowing fluid, losses in the efficiency of the machine, and serious vibration problems.

The fundamentals of cavitation may be easily observed by a study of flow through a constriction in the pipe line of Fig. 215. With the valve partially open, the variation of pressure head through pipe and

constriction is given by curve A, the point of lowest pressure occurring at the point of minimum area, where the velocity is highest. Increased valve opening produces a condition B, at which the pressure at the constriction has fallen to the vapor pressure of the liquid. Further opening of the valve leads to a pressure-head variation C, lowering the

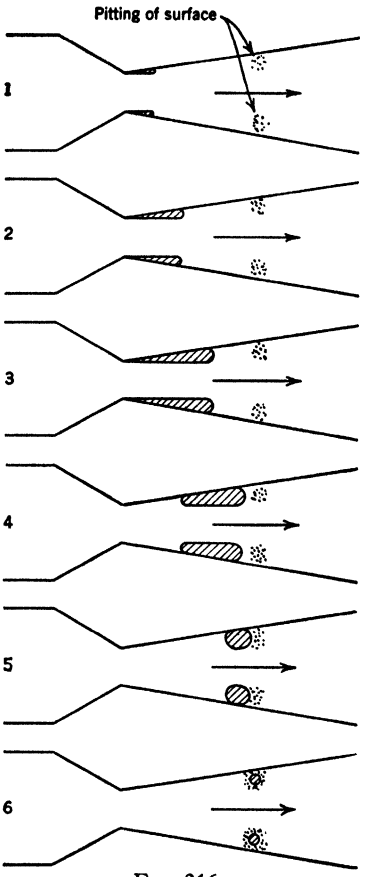
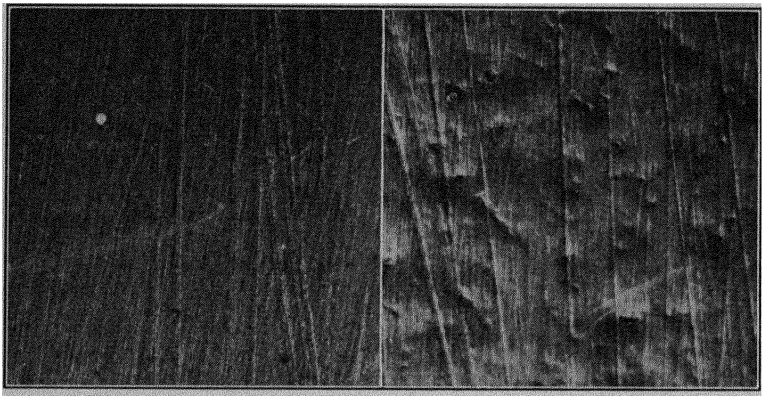


FIG. 216.

pressure downstream from the constriction but not changing the pressure within the constriction. Thus the increased valve opening cannot increase the velocity and rate of flow through the pipe since at two points in the flow (in the reservoir and in the constriction) the pressures are fixed. For pressure variation C a considerable region downstream from the constriction possesses only the vapor pressure

of the liquid. Here a cavity forms as shown, the live stream no longer following the boundary walls of the passage. The cavity contains a swirling mass of droplets and vapor and, although appearing steady to the naked eye, actually forms and reforms many times a second. The formation and disappearance of a single cavity are shown schematically in Fig. 216, and the disappearance of the cavity is the clue to the destructive action caused by cavitation. The low-pressure cavity is swept swiftly downstream into a region of high pressure where it collapses suddenly, the surrounding liquid rushing in to fill the void. At the point of disappearance of the cavity the inrushing liquid comes together, momentarily raising the pressure at a point within the liquid



M. I. T.

Before. After

FIG. 217. Pitting of Brass Plate after 5 Hours' Exposure to Cavitation (Magnification 10×).

to a very high value. If the point of collapse of the cavity is in contact with the boundary wall, the wall receives a blow (Fig. 217) as from a tiny hammer and its surface is stressed locally beyond its elastic limit, resulting eventually in fatigue and destruction of the wall material.

The guiding principles of cavitation prevention obviously are to maintain pressures relatively high and to provide surfaces having curvatures gentle enough to prevent separation of the live stream from them. However, to apply such principles, particularly the latter one, to problems of design inevitably involves uncertainties because of the generally complex nature of the flows.

BIBLIOGRAPHY

W. SPANNHAKE, "Cavitation and Its Influence on Hydraulic Turbine Design," *N.E.L.A., Pub.* 222, June, 1932.

L. P. SMITH, "Cavitation on Marine Propellers," *Trans. A.S.M.E.*, July, 1935.

S. L. KERR, "Determination of the Relative Resistance to Cavitation Erosion by the Vibratory Method," *Trans. A.S.M.E.*, July, 1937.

E. ENGLESSON, "Pitting in Water Turbines," *The Engineer*, October 17, 1930.

J. M. MOUSSON, "Pitting Resistance of Metals under Cavitation Conditions," *Trans. A.S.M.E.*, July, 1937.

INDEX

Absolute pressure, 25–26
Absolute temperature, 6
Acceleration, centrifugal, 44
  convective, 57
  horizontal linear, 42
  local, 57
  total, 57
  vertical linear, 41
Acoustic velocity, 10, 73–74, 298, 312–316, 338
Adiabatic constant, 9
  for various gases, 9
Adiabatic process, 8
Alternate depths, 211
Anemometer, cup type, 247
  hot-wire, 248
  vane type, 247
Angle of attack, 296
  effective, 324
Archimedes' principle, 38
Aspect ratio of a foil, 325
Atmospheric pressure, 24, 26

Barometer, 28
Bernoulli's equation, 60
  for compressible fluids, 68
  for incompressible fluids, 61
Best hydraulic cross section, 204
Borda orifice, 264
Boundaries, 111
  flow over, 110–111
Boundary layer, 116, 300
  kinetic energy of, 310
  on flat plates
    laminar, 301–304
    turbulent, 305
Bourdon pressure gage, 25
Boyle's Law, 6, 8
Branching pipes, 185–188
Buoyancy, 38

Capillarity, 17, 30
Cauchy number, 127
Cavitation, 63, 184, 342
  pitting due to, 63, 344
Center of buoyancy, 39
Center of pressure, 32–36
Charles' law, 6
Chezy coefficient, 200–203
Chezy equation, 199
Chord of a foil, 296
Circulation, 94
  about a foil, 324
  origin of, 320
  theory of lift, 318
Coefficient of discharge, for nozzles, 258
  for orifices under static head, 264
  for pipe-line orifices, 260
Cole Pitometer, 243, 268
Compressibility, 8
Compressible fluid, flow about immersed objects, 312–316
  flow through a constriction in a stream-tube, 70–75
  flow through nozzles, 257–258
  flow through orifices, 260–262
  flow through Venturis, 253–254
  flow with friction in pipes, 160–163
  stagnation pressure in, 313
Conjugate depths, 222
Continuity, equation of, 58
Contraction, coefficient of, 260, 264
Controls, 217
Critical depth, 211–213
  occurrence of, 214–217
Critical pressure ratio, 72
Critical Reynolds number, 108
Current meter, 247
  measurement of river flow with, 285
Curvilinear flow, 92
Cylinders, drag coefficients of, 311

D'Alembert paradox, 1, 121
Density, 4
  measurement of, 229–231
  of water, 337

Dilution methods of flow measurement, 270
Dimensional analysis, 131–137
  of drag of floating objects, 136
  of drag of immersed objects, 297
  of pipe friction, 147
Dimensions of symbols, 133, 335–336
Discontinuity, surface of, 117, 122, 168, 307
Disks, drag coefficients of, 309
Drag, 116
  at high velocities, 299, 312–317
  frictional, 119, 295, 300
  induced, 325
  profile, 119, 295, 307
Dynamic similarity, *see* Similarity

Eddy formation, 117–118
Eddying turbulence, 118, 122, 168
Elasticity, 8
  force, 127
  modulus of, 8
Energy, heat, 66
  internal, 66
  kinetic, 66
  loss, *see* Loss of head
  mechanical, 66
  potential, 66
  pressure, 66
Energy equations, 65, 139
Energy line, 61, 141, 209, 218
Enthalpy, 67
Euler's equation, 59
Expansion factor, 254

Float gage, 239
Float measurements, 287
Floating objects, 38
  dimensional analysis of drag of, 136
  similarity applied to drag of, 130
Flow bends, 267
Fluid mechanics, development of, 1
Fluid properties, 4–19
  measurement of, 229–236
Fluid state, characteristics of, 3
Foils, angle of attack of, 296, 324
  aspect ratio of, 325
  chord of, 296
  circulation about, 318
Foils, drag on, 324–331
  lift on, 317–331
  span of, 296
Free overfall, 215
Free surface, measurement of, 238–240
Friction factor, 149
  in laminar flow, 150
  in turbulent flow, 151
  plotted against Reynolds number, 150, 153.
Frictional drag, *see* Drag
Froude number, 127
  relation to drag of floating objects, 130, 136

Gage pressure, 26
Gases, equation of state of, 6
  gas constants for, 6–7
  modulus of elasticity for, 9–10
Gasometer, 249
Gravity force, 127

Hagen-Poiseuille law, 146
Hazen-Williams formula, 166–167
Head loss, *see* Loss of head
Heat energy, 66
Hook gage, 239
Hooke's law, 8
Horsepower of fluid machines, 69
Hydraulic grade line, 141, 179–184
Hydraulic jump, 219–224
  location of, 223
  solution by M-curve, 222
Hydraulic radius, 164, 200
Hydraulics, 2
Hydrodynamics, 2
Hydrometer, 229, 231

Ideal fluid, 55
Immersed objects, flow about, 116–121, 128, 294–331
Impulse-momentum law, 77–80
Impulse turbine, 82
Induced drag, *see* Drag
Inertia force, 127
Internal energy, 66
Isothermal process, 8

Jet, 63

Kinematic viscosity, 14
Kinetic energy, 66
Kutta-Joukowski theorem, 320

Laminar film, 111, 152, 158
Laminar flow, 106
  about spheres, 308
  between parallel plates, 115
  in boundary layers, 116, 301–304
  in pipes, 107, 143–146
  similarity for, 129
Lift, 295, 317–331
  by change of momentum, 317
  by circulation theory, 318
  coefficient of, 296
Loss of head, 139, 141
  in circular pipes due to pipe friction,
    for compressible fluids, 160–163
    for incompressible fluids, 141–153, 166
  in constrictions, 252
  in hydraulic jump, 223
  in non-circular pipes, 164–167
  in nozzles, 259
  in open channels, 199, 209, 218
  in pipes, due to bends, 177
    due to contractions, 174–175
    due to enlargements, 170–173
    due to entrances, 175–176
    due to exits, 172
    due to pipe fittings, 178

Mach angle, 317
Mach number, 298, 313–315
Manometers, 27–30
Mechanical energy, 66
Mild slope, 211
Minor losses in pipes, 167–178
  See also Loss of head
Models, *see* Similarity
Modulus of elasticity, 8
Momentum, 77–80
  lift by change of, 317

Nozzles, 255–259

Open-channel flow, 196–224
  Chezy coefficient, 200–203
  Chezy equation. 199
Open-channel flow, critical depth, 211, 213–217
  hydraulic jump in, 219–224
  rapid flow, 211, 212, 215, 223
  specific energy, 209–211
  tranquil flow, 211, 212, 215
  uniform flow, 199–208
  varied flow, 197, 217–219
  velocity distribution, 209, 285
Orifices, coefficients for, 264
  in pipe lines, 259–262
  loss of head at, 252
  under falling head, 266
  under static head, 63, 263–265

Perfect fluid, 55
Piezometer, 24
  opening, 237
  ring, 238
Pipe coefficient, 154
  relation to friction factor, 156
Pipes, branching, 185–188
  flow of compressible fluids in, 160–163
  head losses in (*see* Loss of head)
  laminar film in, 158–159
  laminar flow in 106–108, 143–146
  non-circular, 164–167
  pressure grade line for, 179–188
  Reynolds number for fluid flow in, 107
  stress in walls, 40
  turbulent flow in, 106–108, 150–154
Pitometer, 243, 268
Pitot (Pitot-static) tube, 241–245, 268
Pitot-Venturi, 246
Plates, drag of, 300–306, 311
  flow between, 113–115
Point gage, 239
Polar diagram, 327
Potential energy, 66
Potential head, 61
Potential pressure, 62
Pressure, measurement of, by gage, 25–27
    by manometer, 27–31
    by piezometer column, 24
    in a flowing fluid, 236
Pressure energy, 66
Pressure force, 127
  on submerged curved areas, 35–38
  on submerged plane areas, 31–35

Pressure grade line, 141, 179–184
Pressure head, 24, 61
Pressure wave, velocity of propagation of, 338–339
Profile drag, *see* Drag
Projectiles, drag coefficients of, 315
Propeller, 88
Pycnometer, 229

Rapid flow, 211
Reaction turbine, 90
Resistance of immersed objects, *see* Drag
Reynolds' experiment, 106
Reynolds number, 107, 127–129, 130, 136
Roughness, 112
  in open channels, 200–204
  in pipes, 150–153
  relative, 149

Salt-velocity method, 272
Secondary flows, 121
Separation, 116–117, 122, 307
Sewer diagram, 208
Shearing stress, 11, 115
  in laminar flow, 108, 146
  in pipe flow, 141
  in turbulent flow, 109–110
  on immersed objects, 119, 294
Short tube, 264
Similarity, applied to, drag of floating objects, 130
  drag of immersed objects, 128, 298
  pipe flow, 129, 150
  dynamic, 126
  geometric, 125
  kinematic, 126
Siphon, 184
Skin friction, *see* Drag
Sluice gate, 265
Span of a foil, 296
Specific energy, 209
Specific gravity, 4
  of various liquids, 5
Specific volume, 4
Specific weight, 4
  of water, 337
Spheres, drag of, 307–309
Spillway, 284
Stagnation point, 64, 307
Stagnation pressure, in compressible fluids, 313
  in incompressible fluids, 64, 240
Static tube, 237
Steady flow, 55
Steep slope, 211
Streamline, 56
  absolute, 57
  instantaneous, 56
  picture, 56
Streamlined form, 120–121
Streamtube, 57
Struts, drag coefficients of, 311
Submerged areas, forces on, 31–38
Surface tension, 14
  force, 127

Tanks, stress in walls, 40
Torricelli's theorem, 63
Total heat content, 67
Tranquil flow, 211
Transition from laminar to turbulent flow, about spheres, 309
  in boundary layers, 116, 300
  in pipes, 106–108
Turbulence, eddying, 118
  normal, 107, 118
Turbulent flow, 106–110
  in boundary layers, 116, 305–306
  in open channels, 197
  in pipes, 107, 150–154

Uniform flow, 198–199
Unsteady flow, 55
  orifice under falling head, 266

Vacuum, 26
Vapor flow, 67
  through an orifice, 262
  through constriction in a streamtube, 76
Vapor pressure, 18
  effect on cavitation, 342
  effect on siphon, 184
  in barometer tubes, 29
  in various liquids, 19
  of water, 19
Varied flow, 198, 217

Velocity, coefficient of, 251–252
energy, 66
gradient, 108
head, 61
pressure, 62
Velocity distribution, effect on velocity head, 157
in boundary layers, 116, 300–301
in open flow, 285
in pipes, 154
pipe coefficient, 154
Venturi meter, 249
Venturi tube, 245
double venturi, 246
Viscometers, Bingham, Ostwald, 234
Engler, Redwood, Saybolt, 234
Falling sphere, 234
MacMichael, Stormer, 232
Viscosity, absolute, 11
force, 127
Viscosity, kinematic, 14
measurement of, 231–236
of gases, 12, 341
of liquids, 13, 340
Vortex, compound, 98
forced, 94
free, 96
starting, 321
tip, 323

Wake, formation of, 116–117, 307
Weber number, 127
Weir, broad-crested, 216–283
sharp-crested, proportional, 282
rectangular contracted, 279
rectangular suppressed, 273–278
trapezoidal, 281
triangular, 280
spillway, 284
Westphal balance, 229–230